frontiers | Research Topics

Advances in thyroid surgery and ablation therapy - treatment considerations in the era of quality of life

Edited by
Tzu-Yen Huang, I-Cheng Lu and Gianlorenzo Dionigi

Published in
Frontiers in Endocrinology

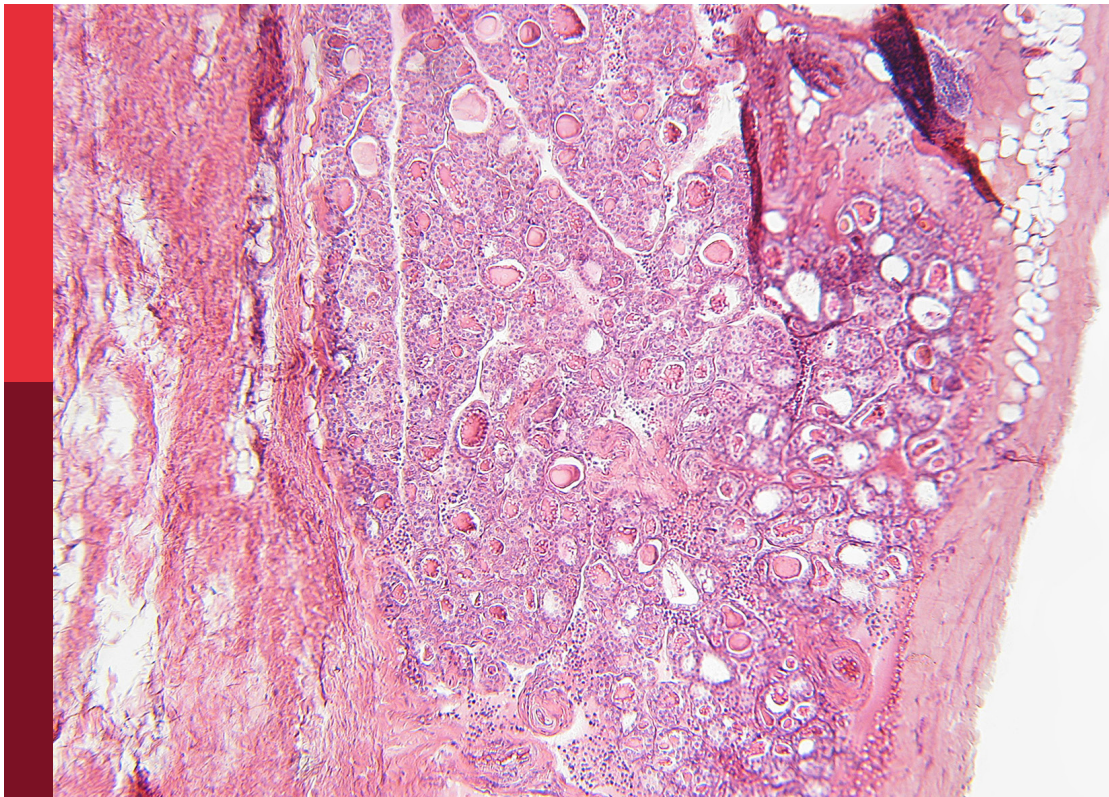

ISSN 1664-8714
ISBN 978-2-8325-6132-4
DOI 10.3389/978-2-8325-6132-4

Generative AI statement
Any alternative text (Alt text) provided alongside figures in the articles in this ebook has been generated by Frontiers with the support of artificial intelligence and reasonable efforts have been made to ensure accuracy, including review by the authors wherever possible. If you identify any issues, please contact us.

About Frontiers

Frontiers is more than just an open access publisher of scholarly articles: it is a pioneering approach to the world of academia, radically improving the way scholarly research is managed. The grand vision of Frontiers is a world where all people have an equal opportunity to seek, share and generate knowledge. Frontiers provides immediate and permanent online open access to all its publications, but this alone is not enough to realize our grand goals.

Frontiers journal series

The Frontiers journal series is a multi-tier and interdisciplinary set of open-access, online journals, promising a paradigm shift from the current review, selection and dissemination processes in academic publishing. All Frontiers journals are driven by researchers for researchers; therefore, they constitute a service to the scholarly community. At the same time, the *Frontiers journal series* operates on a revolutionary invention, the tiered publishing system, initially addressing specific communities of scholars, and gradually climbing up to broader public understanding, thus serving the interests of the lay society, too.

Dedication to quality

Each Frontiers article is a landmark of the highest quality, thanks to genuinely collaborative interactions between authors and review editors, who include some of the world's best academicians. Research must be certified by peers before entering a stream of knowledge that may eventually reach the public - and shape society; therefore, Frontiers only applies the most rigorous and unbiased reviews. Frontiers revolutionizes research publishing by freely delivering the most outstanding research, evaluated with no bias from both the academic and social point of view. By applying the most advanced information technologies, Frontiers is catapulting scholarly publishing into a new generation.

What are Frontiers Research Topics?

Frontiers Research Topics are very popular trademarks of the *Frontiers journals series*: they are collections of at least ten articles, all centered on a particular subject. With their unique mix of varied contributions from Original Research to Review Articles, Frontiers Research Topics unify the most influential researchers, the latest key findings and historical advances in a hot research area.

Find out more on how to host your own Frontiers Research Topic or contribute to one as an author by contacting the Frontiers editorial office: frontiersin.org/about/contact

Advances in thyroid surgery and ablation therapy - treatment considerations in the era of quality of life

Topic editors
Tzu-Yen Huang — Kaohsiung Medical University, Taiwan
I-Cheng Lu — Kaohsiung Medical University, Taiwan
Gianlorenzo Dionigi — University of Milan, Italy

Citation
Huang, T.-Y., Lu, I.-C., Dionigi, G., eds. (2025). *Advances in thyroid surgery and ablation therapy - treatment considerations in the era of quality of life*. Lausanne: Frontiers Media SA. doi: 10.3389/978-2-8325-6132-4

Table of contents

frontiers | Frontiers in Endocrinology

TYPE Editorial
PUBLISHED 03 March 2025
DOI 10.3389/fendo.2025.1576425

OPEN ACCESS

EDITED AND REVIEWED BY
Terry Francis Davies,
Icahn School of Medicine at Mount Sinai,
United States

*CORRESPONDENCE
I-Cheng Lu
u9251112@gmail.com
Gianlorenzo Dionigi
gianlorenzo.dionigi@unimi.it

RECEIVED 13 February 2025
ACCEPTED 19 February 2025
PUBLISHED 03 March 2025

CITATION
Huang T-Y, Lu I-C and Dionigi G (2025) Editorial: Advances in thyroid surgery and ablation therapy - treatment considerations in the era of quality of life.
Front. Endocrinol. 16:1576425.
doi: 10.3389/fendo.2025.1576425

Editorial: Advances in thyroid surgery and ablation therapy - treatment considerations in the era of quality of life

Tzu-Yen Huang[1,2,3], I-Cheng Lu[4]* and Gianlorenzo Dionigi[5,6]*

[1]Department of Otorhinolaryngology-Head and Neck Surgery, Kaohsiung Medical University Hospital, Kaohsiung Medical University, Kaohsiung, Taiwan, [2]Department of Otorhinolaryngology, School of Post-Baccalaureate Medicine and School of Medicine, College of Medicine, Kaohsiung Medical University, Kaohsiung, Taiwan, [3]Department of Otolaryngology-Head and Neck Surgery, Kaohsiung Medical University Gangshan Hospital, Kaohsiung Medical University, Kaohsiung, Taiwan, [4]Department of Anesthesiology, Kaohsiung Medical University Hospital, Kaohsiung Medical University, Kaohsiung, Taiwan, [5]Division of General Surgery, Endocrine Surgery Section, Istituto Auxologico Italiano IRCCS (Istituto di Ricovero e Cura a Carattere Scientifico), Milan, Italy, [6]Department of Pathophysiology and Transplantation, University of Milan, Milan, Italy

KEYWORDS

thyroid surgery, thyroid ablation therapy, quality of life, patient safety, personalized treatment

Editorial on the Research Topic

Advances in thyroid surgery and ablation therapy - treatment considerations in the era of quality of life

In recent years, remarkable advances in thyroid surgery and ablation therapy have transformed the management of thyroid disease. These developments reflect a growing emphasis on precision, safety, and personalized care, as well as an increasing focus on optimizing patients' quality of life (QoL). This Research Topic, "*Advances in Thyroid Surgery and Ablation Therapy - Treatment Considerations in the Era of Quality of Life*," compiles 11 outstanding papers that address key aspects of this evolving field, including innovative surgical techniques, advanced technologies, and patient-centered treatment approaches.

A cornerstone of modern thyroid surgery is the ability to preserve critical anatomical structures while minimizing complications. Parathyroid gland preservation remains a major challenge, especially during reoperations for recurrent benign multinodular goiter. The study by Wang et al. highlights the use of carbon nanoparticles to enhance parathyroid gland identification and protection during reoperations, demonstrating a significant reduction in transient and permanent hypoparathyroidism. These findings underscore the potential of carbon nanoparticles to improve surgical outcomes in complex cases.

In addition to surgery, thyroid ablation treatments, such as radiofrequency ablation (RFA), are gaining traction as effective alternatives to traditional surgery for certain conditions. Kong et al. conducted a meta-analysis comparing RFA to surgery for papillary thyroid microcarcinoma and reported that RFA offers comparable oncologic outcomes with fewer complications, faster recovery, and better QoL. This shift toward minimally invasive options highlights the importance of patient-centered treatment paradigms.

Another significant advancement in thyroid surgery is the use of intraoperative neuromonitoring (IONM) to protect the recurrent laryngeal nerve (RLN) and external branch of the superior laryngeal nerve (EBSLN). Chiang et al. investigated the efficacy of transthyroid cartilage recording methods, emphasizing the superior electromyographic (EMG) signal quality obtained from contralateral electrode placements. Aygun et al. introduced cricothyroid muscle EMG to improve EBSLN monitoring, providing a complementary method to improve surgical precision and reduce the risk of nerve injury.

Technological innovations also play a pivotal role in refining surgical techniques and improving outcomes. Near-infrared autofluorescence (NIRAF) imaging, as described by Richard and Rizo, offers a promising solution for intraoperative parathyroid gland identification and viability assessment. The feasibility of combining autofluorescence and indocyanine green fluorescence angiography to assess parathyroid function is another notable development that bridges technology and patient safety.

Beyond intraoperative advances, preoperative and postoperative considerations are equally critical. The predictive models and nomograms developed by Liu et al. for lateral cervical lymph node metastasis in papillary thyroid carcinoma (PTC) exemplify the integration of diagnostic accuracy into clinical decision making. In addition, the findings in Zhang et al. provide insight into diagnostic accuracy for lateral cervical lymph node metastasis in PTC through nomograms, which facilitate personalized surgical planning. These tools facilitate personalized surgical planning, reducing unnecessary interventions and optimizing outcomes.

Pediatric thyroid surgery, a less common but highly specialized field, is addressed by Sosnowska-Sienkiewicz et al., who analyzed a decade of experience in the management of thyroid disease in children. Their findings emphasize the importance of multidisciplinary collaboration and surgeon expertise in achieving safe and effective outcomes for young patients.

Moreover, the study by Chen et al. on Delphian lymph node metastasis in PTC provides valuable insights into its prognostic implications and surgical management. This work contributes to a better understanding of central and lateral lymph node metastasis patterns, guiding individualized treatment strategies.

As the incidence of thyroid cancer continues to rise, the ability to predict and manage surgical risk remains paramount. Li et al. evaluated the utility of various EBSLN classification systems and concluded that Friedman's classification provides superior predictive accuracy for EBSLN injury. These findings highlight the importance of adopting standardized classification systems in clinical practice.

Patient-centered outcomes such as voice and swallowing function are increasingly recognized as essential components of QoL. Zhao et al. examined subjective and objective analyses of these functions, providing critical data to inform treatment planning and postoperative care. The findings reinforce the need for a multidisciplinary approach to optimize functional outcomes.

This Research Topic highlights the significance of integrating advanced technologies, precision diagnostics, and patient-centered care into thyroid surgery and ablation therapy. The collective insights from these articles pave the way for safer, more effective, and QoL-focused thyroid care. We hope this compilation inspires continued innovation and collaboration among thyroid specialists, ultimately benefiting patients worldwide.

Author contributions

T-YH: Writing – original draft, Writing – review & editing. I-CL: Writing – original draft, Writing – review & editing. GD: Writing – original draft, Writing – review & editing.

Conflict of interest

The authors declare that the research was conducted in the absence of any commercial or financial relationships that could be construed as a potential conflict of interest.

Generative AI statement

The author(s) declare that no Generative AI was used in the creation of this manuscript.

Publisher's note

frontiers | Frontiers in Endocrinology

TYPE Original Research
PUBLISHED 03 November 2023
DOI 10.3389/fendo.2023.1248449

OPEN ACCESS

EDITED BY
I-Cheng Lu,
Kaohsiung Medical University, Taiwan

REVIEWED BY
Claudio Casella,
University of Brescia, Italy
Brendan Stack,
Southern Illinois University Carbondale, United States
Mohamed Rahouma,
NewYork-Presbyterian, United States

*CORRESPONDENCE
Marieke Richard
marieke.richard@getinge.com

RECEIVED 27 June 2023
ACCEPTED 13 September 2023
PUBLISHED 03 November 2023

CITATION
Richard M and Rizo P (2023) Feasibility of parathyroid gland autofluorescence imaging after indocyanine green fluorescence angiography.
Front. Endocrinol. 14:1248449.
doi: 10.3389/fendo.2023.1248449

Feasibility of parathyroid gland autofluorescence imaging after indocyanine green fluorescence angiography

Marieke Richard* and Philippe Rizo

Fluoptics SAS, Grenoble, France

Background: In thyroid surgery, autofluorescence allows the parathyroid glands (PTGs) to be located very early to protect them. Moreover, indocyanine green (ICG) fluorescence angiography (ICG-FA) allows for assessing the viability of the PTGs and identifying blood vessels to preserve them. The main limitation of using ICG-FA is that once ICG has been injected, it is no longer possible to observe PTG autofluorescence using existing devices. This study aimed to describe an approach that allows for visualization of the PTGs by autofluorescence, even after ICG injection.

Methods: We redesigned the FLUOBEAM® LX system to excite fluorescence at 685 nm and detect fluorescence between 700 and 900 nm. This device had short-pass filters at 775 nm that helped to split the contributions of the PTG autofluorescence and ICG fluorescence. Tests were performed on extemporaneous PTG preparations placed next to ICG droplets to assess for rejection of the ICG signal.

Results: A low-pass filter at 775 nm detected 60% of the autofluorescence signals and 10% of the ICG signals.

Conclusion: These findings support the possibility of visualizing PTG autofluorescence despite multiple ICG injections and measuring the balance between ICG and autofluorescence signals.

KEYWORDS

parathyroid autofluorescence, ICG fluorescence angiography, NIR intraoperative fluorescence imaging, thyroid Surgery, hypocalcemia, hypoparathyroidism

Introduction

The preservation of the parathyroid glands (PTGs) and their vascularization is crucial during thyroidectomy because damage to the PTG can result in postoperative hypoparathyroidism and hypocalcemia, which can significantly increase cardiovascular and renal morbidity and patient mortality (1, 2).

Autofluorescence has recently been introduced in thyroid surgery to facilitate the detection of PTGs (3–6). Initially, surgeons relied only on their experience and training to detect the parathyroid glands and decide which blood vessels to preserve to protect gland vascularization during thyroidectomies. Depending on the surgeon, in 30–60% of cases, autofluorescence imaging allows for the detection of the PTGs before the surgeon sees them. Although, in some cases, autofluorescence allows for better preservation of the PTG (4), it does not provide any information regarding the vascularization pathway of the glands. Identifying the blood vessels feeding the PTGs is critical because the vascularization of the PTG is unpredictable (7). Recently, fluorescence angiography using indocyanine green (ICG) during thyroidectomy has demonstrated the possibility of identifying critical blood vessels needing preservation (8). 0.1mg/kg of ICG is usually intravenously injected as a bolus. 10 to 30 seconds after injection, ICG reaches the thyroid gland and fluorescence signal can be detected by the imaging device and displayed on a screen.

The main limitation of ICG fluorescence angiography, used for detection in the range of 800–900 nm, is that once ICG has been injected, even at 0.1mg/kg, it would no longer be possible to visualize the autofluorescence of the PTGs. ICG Angiography is performed to visualize small blood vessels. Therefore, injected dose leads to high levels of fluorescence that overwrite parathyroid autofluorescence. ICG fluorescence is at least one order of magnitude brighter than PTG autofluorescence in the range of 800–900 nm. Currently, available systems use fluorescence excitation wavelengths longer than 740 nm and detect in the range 800-900nm (9). Thus, once ICG is present in the field, the PTG autofluorescence signal becomes negligible compared with the ICG signal.

Thyroidectomies are usually performed in two phases (one lobectomy per side), and the surgeon must preserve the PTGs independently on each side. If the surgeon wants to use autofluorescence on both sides of the thyroid, then ICG can only be used on the second operated side. Consequently, during total thyroidectomy using existing devices, ICG fluorescence angiography can be combined with autofluorescence on only one side of the patient.

With classical devices based on excitation wavelengths longer than 740 nm, a waiting time of about 1 hour is required between the last ICG injection and the next autofluorescence measurement. However, despite this delay, several areas remain marked by ICG because it is injected into the dissected tissue, which degrades the readability of the autofluorescence images by registering many ICG-related false positives.

Furthermore, the inability to use perfusion imaging on the two operative sides leads to (i) a potentially greater risk of damaging the vascularization of the PTGs of the first lobe and (ii) not knowing if the PTGs left in place on the first lobe are functional. This has a significant implication on how the second lobe should be dissected, especially if the PTGs on the second lobe are poorly localized. Therefore, it is crucial to visualize the autofluorescence of the PTGs *in situ* even after ICG injection. Here, we described an approach that allows for visualization of the PTGs by autofluorescence, even after ICG injection.

Materials and methods

ICG (25 mg) was purchased from Diagnostic Green (Indocyanine Green for Injection Kit, 25 mg). Bovine Serum Albumin was purchased from Sigma Aldrich (Bovine Serum Albumin, 5%; reference A4628-20ML). We performed fluorescence spectrometry measurements of ICG diluted with albumin at an excitation wavelength of 685 nm. We observed that the fluorescence yield was 30–50% lower than that measured at an excitation wavelength of 750 nm. The detection was performed on a larger bandwidth of 700–900 nm. The maximum fluorescence of ICG excited at a wavelength of 685 nm was observed near 820 nm.

Next, a comparison of the emission spectra of PTG autofluorescence for excitation at 650 nm, as provided by Serra (10), with that of ICG (Figure 1) showed that their peak maxima were well separated. We assumed that the autofluorescence spectra for wavelengths longer than 700 nm were similar, with excitation wavelengths of 650 and 685 nm.

To alternatively visualize PTG autofluorescence and the ICG signal on the same system, we modified a FLUOBEAM® LX device (FLUOPTICS© France) by replacing the 750 nm excitation laser with a 685 nm laser and also fit detection filters with a range of 700–900 nm. This system will hereafter be referred to as the LX700. The excitation power at the area of interest was 4.6 mW/cm^2 at a distance of 10 cm from the optical head, and we ensured that the device was operating in laser class 1 (11).

To separate the PTG autofluorescence signal from the ICG fluorescence signal using this device, we tested a retractable low-pass filter with a cut-off wavelength of 775 nm in front of the camera sensor. This led to two spectral detection windows: 700–900 nm without the filter and 700–775 nm with the filter. The experimental setup is shown in Figure 2.

To perform the tests, we used (i) five different dilutions of ICG, i.e., from 0.05 to 1 μM (0.05 μM, 0.1 μM, 0.25 μM, 0.5 μM, and 1 μM) in a solution containing 5% of albumin described earlier, which were arranged as drops of 10 μL, and (ii) freshly resected anatomical specimens of PTGs obtained during a parathyroidectomy. Six series of ICG droplets and resected PTGs were examined. The sample setup and areas of interest for each series are shown in Figures 3–8.

We measured the fluorescence signal using three possible system configurations, namely, FLUOBEAM® LX, LX700, and

Abbreviations: PTGs, parathyroid glands; ICG, indocyanine green; ROI, region of interest; SNR, signal-to-noise ratio; CMOS, Complementary Metal Oxide Semiconductor; CCD, Charge Coupled Device.

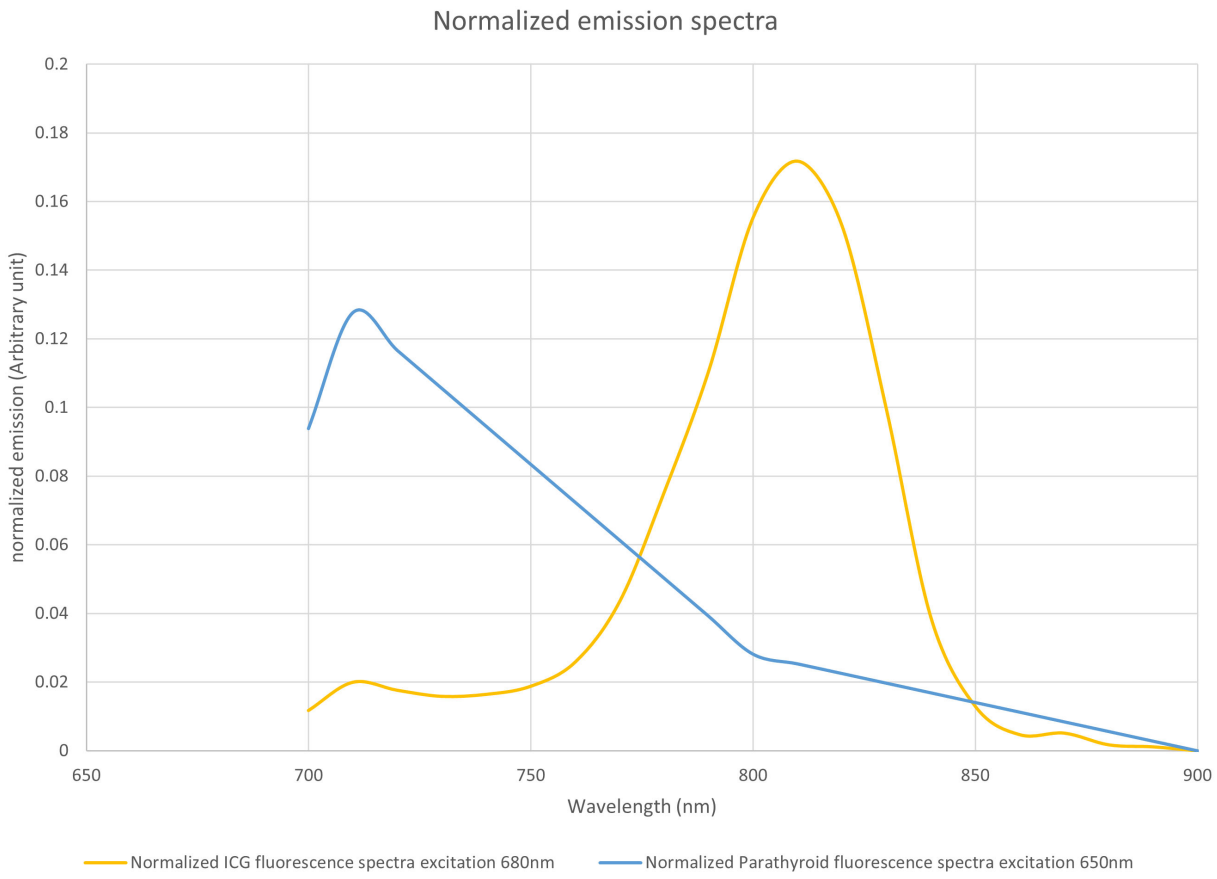

FIGURE 1
Normalized emission spectra of indocyanine green (ICG) when excited at 685 nm and parathyroid gland (PTG) autofluorescence when excited at 650 nm. Both spectra were plotted with an arbitrary unit such that the area under the curve equaled 1. The fluorescence units are, therefore, different between ICG and PTG autofluorescence. However, the maximum emission peaks were adequately separated. The data for the PTG spectrum was derived from the study by Serra et al. (10), while that for the ICG was measured on a Perkin Elmer LS50B system. ICG (25 mg) was solubilized in sterile water (10 mL). Further, the stock solution was diluted with bovine serum albumin to obtain a 1 μM solution. This diluted solution was placed in a Polymethyl Methacrylate cuvette, and the ICG emission spectrum was measured with 685 nm excitation. We assumed that the autofluorescence spectra for wavelengths longer than 700 nm were similar, with an excitation wavelength at 650 nm and 685 nm, respectively.

10.3389/fendo.2023.1248449

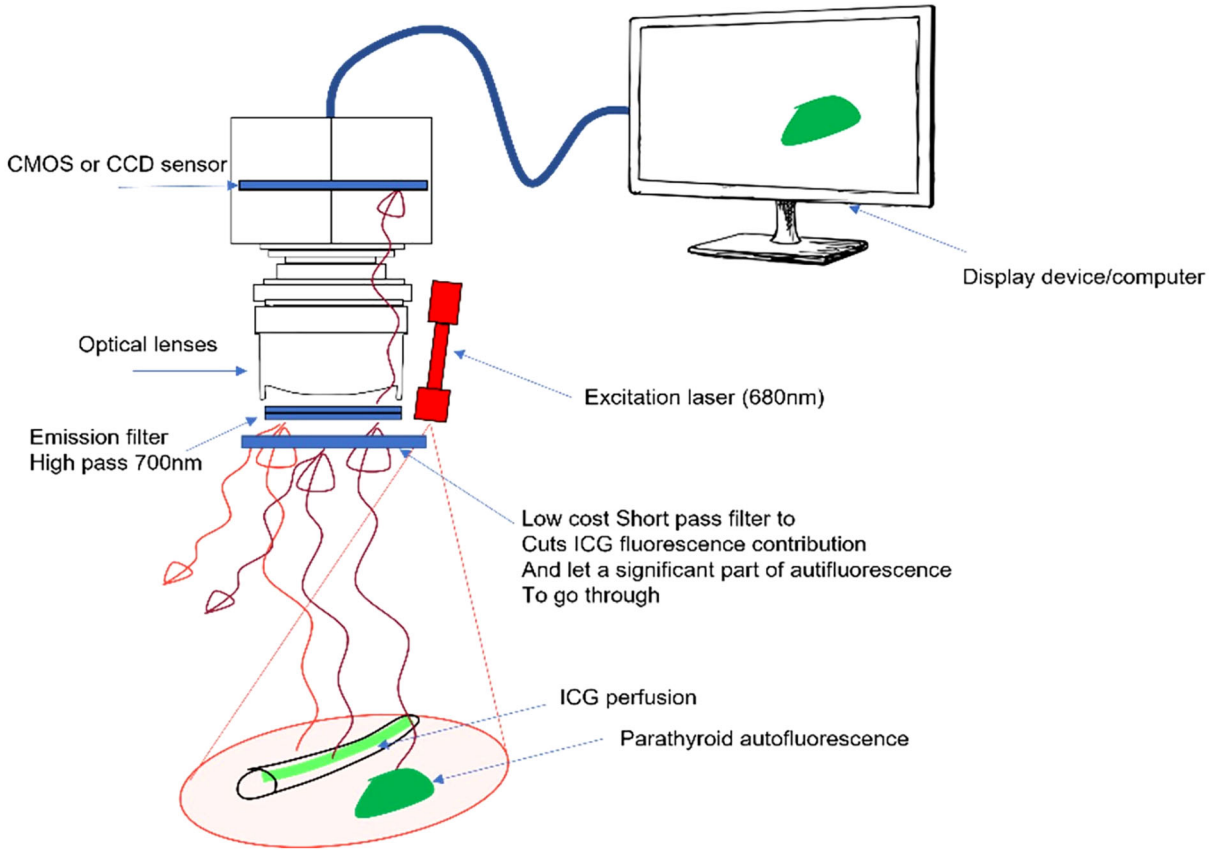

FIGURE 2
Proposed approach with a removable low-pass filter. The device excites autofluorescence of the parathyroid gland (PTG) and indocyanine green (ICG) fluorescence at 685 nm and reads the signal between 700 and 900 nm. A removable low-pass filter is placed in front of the camera sensor to narrow the detection window between 700 and 775 nm, the goal being to manage the ratio between the ICG and PTG signals.

10.3389/fendo.2023.1248449

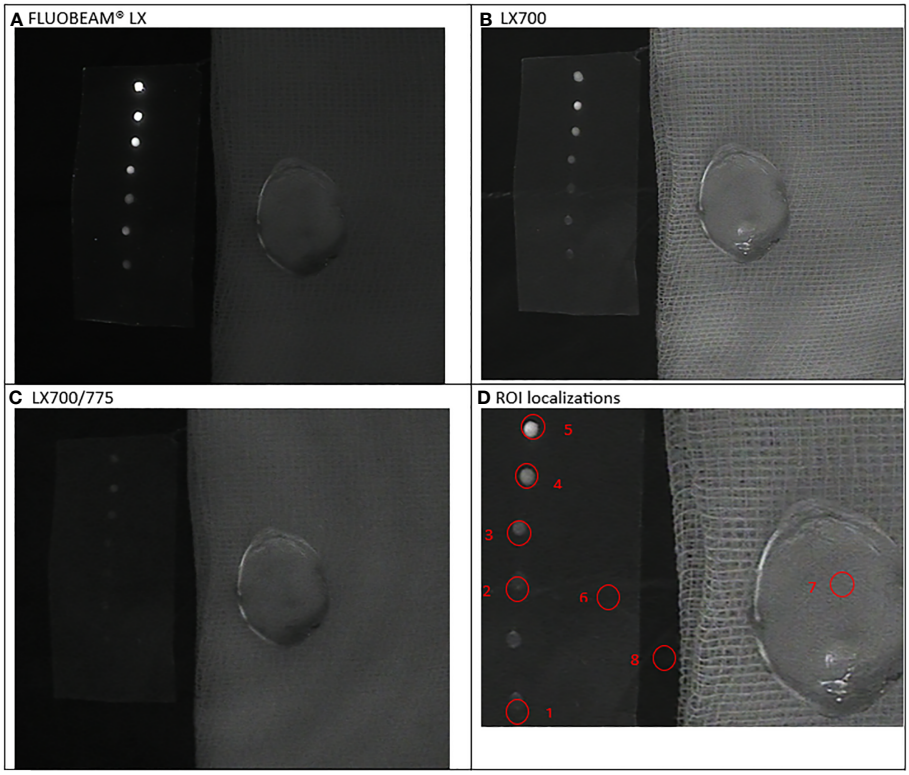

FIGURE 3
First experimental setup: Parathyroid adenoma. **(A)**. image captured with FLUOBEAM® LX, **(B)**. Image captured with LX700, **(C)**. Image taken with LX700/775, **(D)** Region of interest (ROI) for the signal measurements based on the structure of the examined sample with the concentration and location of the indocyanine green (ICG) droplets and location of the parathyroid gland. 1, 0.05 µM ICG droplet; 2, 0.1 µM ICG droplet; 3, 0.25 µM ICG droplet; 4, 0.5 µM ICG droplet; 5, 1 µM ICG droplet; 6, Background for ICG droplets; 7, Parathyroid specimen; 8, Background for parathyroid specimen.

LX700 with a low-pass filter at 775 nm, referred to as the LX700/775.

All acquisitions were performed under typical detection conditions for the PTGs with the FLUOBEAM® LX, LX700, and LX700/775. The measurement distance was 10 cm, and the integration time was 40ms. Different camera amplification factors were used depending on the system configuration to provide useful, unsaturated images.

All results were scaled to a 40 ms/8.7 dB gain before computation. When the signal was saturated, the gain was reduced to obtain unsaturated data. Decreasing the camera gain does not impact the SNR.

Data analyses

Data were extracted from digital images captured by the camera without any processing. Data extraction was performed using an image analysis software (ImageJ 1.53e). A region of interest (ROI) was designed for each droplet, and the mean values and standard deviations were computed for each ROI. Since the main variation of signal at pixel level was linked to camera amplification and smoothly varying fluorescence or autofluorescence levels in the ROIs, the signal distributions were almost symmetrical without outliers and could be characterized by means and standard deviations. An area without any samples was used as the background level reference. Signal distribution on these background areas was symmetrical without outliers because this signal is the reflectance of the remaining parasitic light by a uniform non fluorescent support. The following readings were obtained based on these formulas:

1) Signal measurement, S:

$$S = mean_{ROI} - mean_{background},$$

where $mean_{ROI}$ is the average value of the pixels of the ROI and $mean_{background}$ is the average value of the pixels in the area used as the background

2) Signal-to-noise ratio, SNR:

$$SNR = 10 * log_{10}\left(S/\sqrt{std_{ROI}^2 - std_{background}^2}\right)$$

where std_{ROI} is the standard deviation of the value of the pixels of the ROI and $std_{background}$ is the standard deviation of the value of the pixels in the area used as the background. The SNR was plotted using a logarithmic scale.

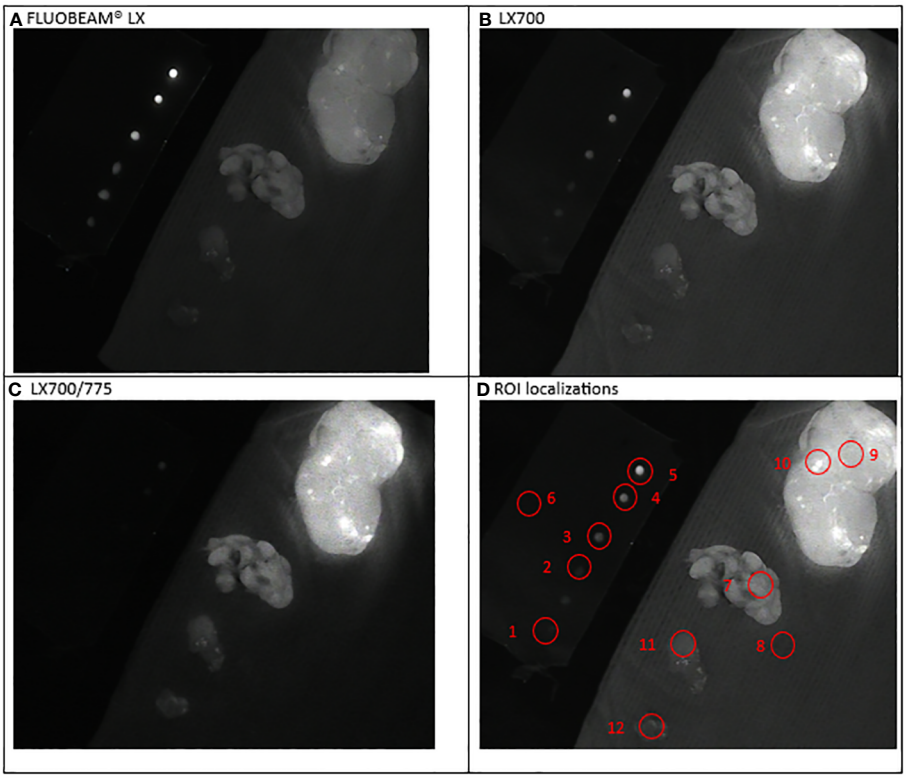

FIGURE 4
Second experimental setup: Parathyroid ablation. Simultaneous observation of the ICG droplets (top left corner) and specimen of neck tissues: extrathyroidal nodule with fluorescent grains (top right), parathyroid; nodule; brown fat (bottom left corner). **(A)** Image captured with FLUOBEAM® LX, **(B)** Image captured with LX700, **(C)** Image taken with LX700/775, **(D)** Region of interest (ROI) for the signal measurements based on the structure of the examined sample with the concentration and location of the indocyanine green (ICG) droplets and location of the parathyroid gland. 1, 0.05 µM ICG droplet; 2, 0.1 µM ICG droplet; 3, 0.25 µM ICG droplet; 4, 0.5 µM ICG droplet; 5, 1 µM ICG droplet; 6, Background for ICG droplets; 7, Parathyroid specimen; 8, Background for parathyroid specimen; For information only: 9, Thyroid nodule; 10, Thyroid nodule-fluorescent grain; 11, Nodule; 12, Brown fat.

Results

Assessment of the PTG specimens and ICG droplets

The signals in the raw images provided by the LX700 were very similar to those acquired using the FLUOBEAM® LX regarding their ability to detect ICG and autofluorescence. These raw images also showed that the LX700/775, with a short-pass filter at 775 nm, could visualize autofluorescence alone, even in the presence of high concentrations of ICG in the field.

To estimate the equivalence between the LX700 and FLUOBEAM® LX, we compared the signal levels based on ICG and those regarding autofluorescence of the PTGs. Figure 9 shows that the LX700 was more sensitive to PTG autofluorescence than FLUOBEAM® LX. In contrast, the FLUOBEAM® LX was more sensitive to ICG, which intrinsically produced very high signals.

To analyze the ability of these two systems to measure and discriminate signal variations, we compared the SNR of the two systems on the same samples. Figure 10 shows that the SNR from the LX700 and FLUOBEAM® LX were comparable for PTG signals and for the different concentrations of ICG. Even for low concentrations of ICG the SNR with the LX700 remained higher than 5dB ensuring unambiguous detectability.

For fluorescence angiography using ICG, we compared these two devices with the LX700/775. Images were acquired with FLUOBEAM® LX, LX700, and LX700/775. Figure 11 shows the average ratio of the ICG signal (average signal value minus the background; the background was defined as an area with no ICG or PTG signal) and PTG signal for the five ICG concentrations listed in Table 1. Our results demonstrated that an additional 775 nm low-pass filter reduced the detected ICG fluorescence signal. Although the autofluorescence signal simultaneously decreased, the drop in the signal was limited; that is, for the highest ICG concentration (1.0 µM), the parathyroid signal was 7 times higher than the ICG signal (Figure 11). Therefore, it was possible to detect PTG autofluorescence in the presence of ICG using LX700/775 at ICG concentrations as high as 1.0 µM.

To demonstrate that this type of approach does not worsen the detection quality of the autofluorescence of PTGs, we analyzed the SNR of the different configurations of the systems (FLUOBEAM® LX, LX700, LX700/775) on the same sample (Table 2). For all configurations tested, the average SNR for

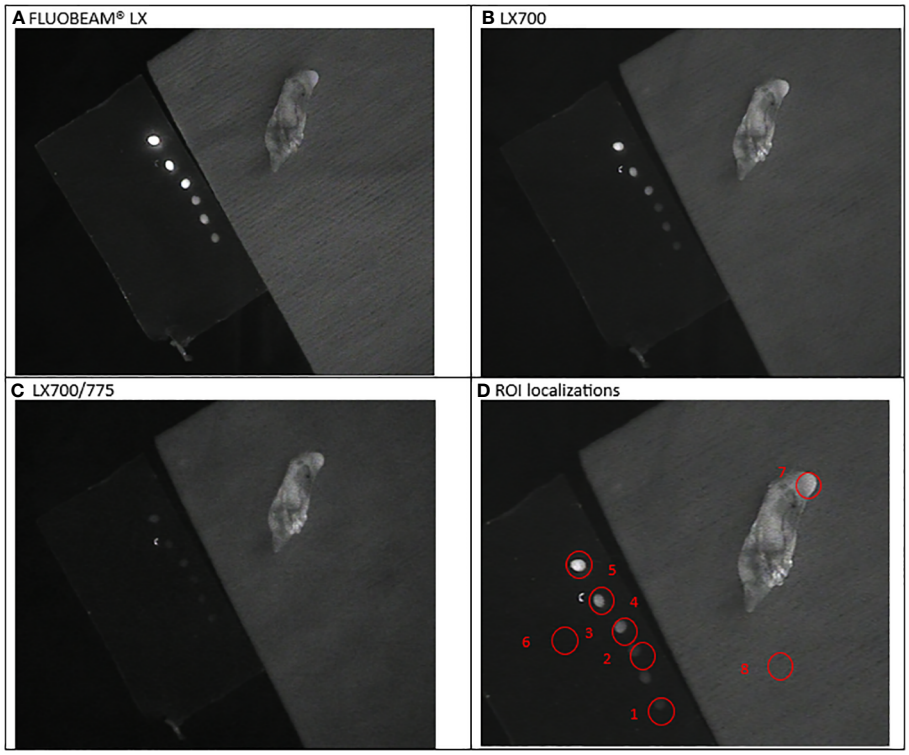

FIGURE 5
Third experimental setup: Parathyroid adenoma **(A)** image captured with FLUOBEAM® LX, **(B)** Image captured with LX700, **(C)** Image taken with LX700/775, **(D)** Region of interest (ROI) for the signal measurements based on the structure of the examined sample with the concentration and location of the indocyanine green (ICG) droplets and location of the parathyroid gland. 1, 0.05 µM ICG droplet; 2, 0.1 µM ICG droplet; 3, 0.25 µM ICG droplet; 4, 0.5 µM ICG droplet; 5, 1 µM ICG droplet; 6, Background for ICG droplets; 7, Parathyroid specimen; 8, Background for parathyroid specimen

the PTGs was close to 10, indicating that even with a reduced detection bandwidth of 700–775 nm (corresponding to the LX700/775 detection bandwidth), PTG autofluorescence could be unambiguously detected. Figures 11, 12 and Table 2 show that the decrease in the SNR of the ICG droplets linked to the additional low-pass filter enabled the detection of PTG autofluorescence in the presence of ICG.

From the spectra in Figure 1, we calculated the measured signal for a low-pass filter with a specified cut-off length. This value correspond to the area below the curve in Figure 1, limited by the 700nm wavelength on one side and by the cut off wavelength on the other side. The proportion of the fluorescence signal, as a function of the cut-off wavelength, is shown in Figure 13.

The difference between the two curves allowed us to locate the maximum difference between the ICG and the autofluorescence signals near 775 nm. We observed that, with a low-pass filter at 775 nm, 60% of the autofluorescence signal and 10% of the ICG signal were detected. With a 750 nm filter, we detected 34% of the autofluorescence signal and 3% of the ICG signal.

Other possible data that were processed using the two detections windows

An LX700 with a retractable low-pass filter at 775 nm can provide two images of the same sample containing different proportions of ICG and autofluorescence signals. The unfiltered image (LX700) was dominated by ICG, and the filtered image (LX700/775) was dominated by autofluorescence (Figure 14).

To be able to analyze the data provided by the device, we acquired two sets of two images. With the low-pass filter on (LX700/775), we acquired one image with the excitation laser off and one image with the excitation laser on. With the low-pass filter off (LX700), we acquired one image with the excitation laser off and another with the excitation laser on. For each position of the low pass filter, the difference between the measure with the laser on and off provided the actual contribution of the autofluorescence signal plus the ICG signal on the corresponding detection waveband.

Referring to the autofluorescence signal of the tissues emitted between 700 nm and 900 nm as *AFsignal* and the ICG signal emitted between 700 nm and 900 nm as *ICGsignal*, we can define α and β, two

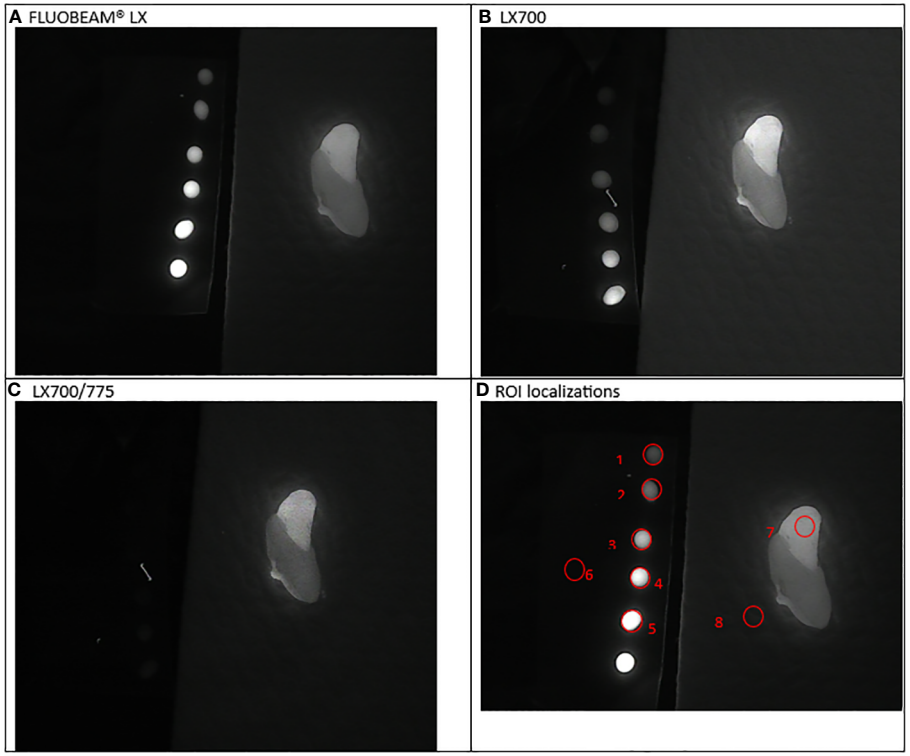

FIGURE 6
Fourth experimental setup: Parathyroid presenting a parathyroid nodule. **(A)** Image captured with FLUOBEAM® LX, **(B)** Image captured with LX700, **(C)** Image taken with LX700/775, **(D)** Region of interest (ROI) for the signal measurements based on the structure of the examined sample with the concentration and location of the indocyanine green (ICG) droplets and location of the parathyroid gland. 1, 0.05 μM ICG droplet; 2, 0.1 μM ICG droplet; 3, 0.25 μM ICG droplet; 4, 0.5 μM ICG droplet; 5, 1 μM ICG droplet; 6, Background for ICG droplets; 7, Parathyroid specimen; 8, Background for parathyroid specimen.

10.3389/fendo.2023.1248449

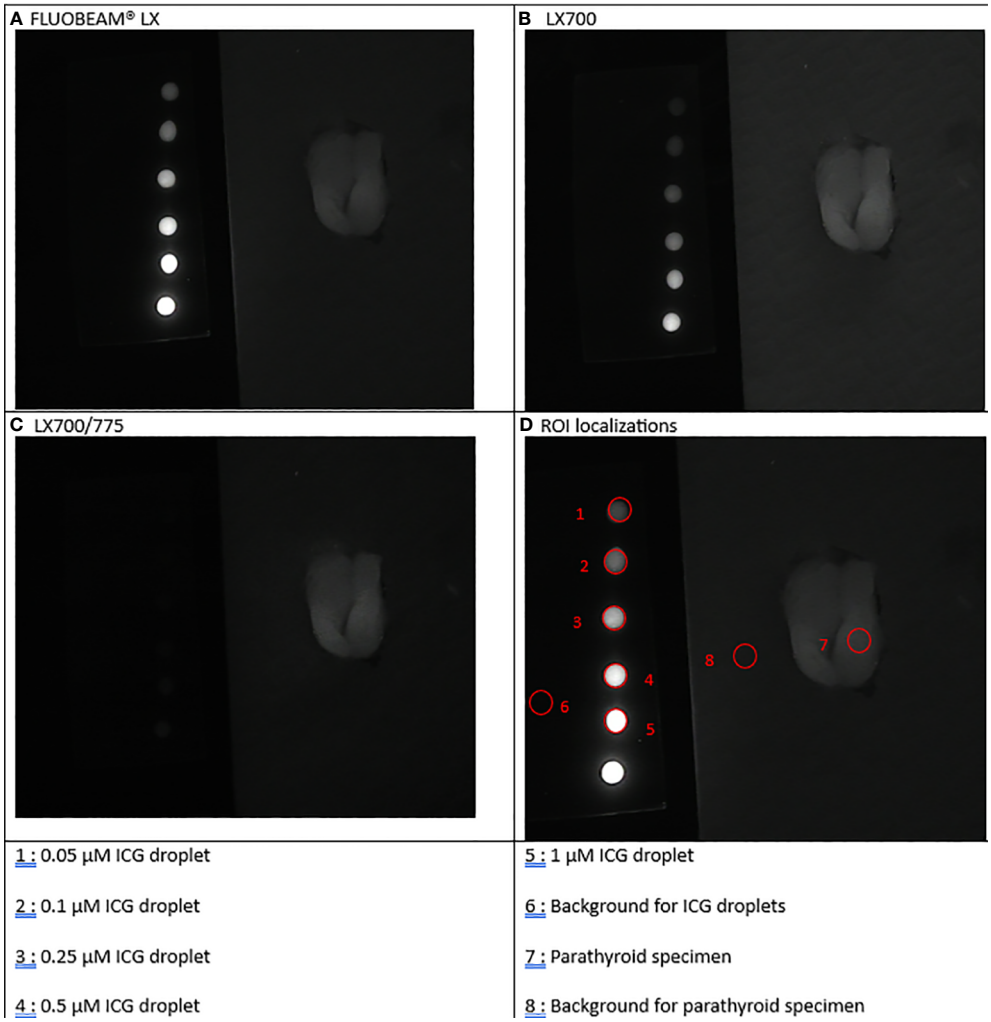

FIGURE 7
Fifth experimental setup: Parathyroid (split in two parts by the surgeon). **(A)** Image captured with FLUOBEAM® LX, **(B)** Image captured with LX700, **(C)** Image taken with LX700/775, **(D)** Region of interest (ROI) for the signal measurements based on the structure of the examined sample with the concentration and location of the indocyanine green (ICG) droplets and location of the parathyroid gland.

numbers between 0 and 1, such that $\alpha * AFsignal$ is the autofluorescence signal of tissues emitted between 700 nm and 775 nm and $\beta * ICGsignal$ is the ICG signal emitted between 700 nm and 775 nm.

Then we can write that

$$\text{Image with the filter off} = AFsignal + ICG\ \ signal$$

$$\text{Image with the filter on} = \alpha * AFsignal + \beta * ICG\ \ signal$$

If α and β have been measured in independent samples, we can easily produce images of ICG or autofluorescence alone.

We measured α on the set of thyroid and parathyroid specimens presented earlier and β on ICG droplets. We observed α=0.3 (for thyroid and parathyroids) and β=0.025.

In the first approach, assuming that the contribution of ICG represented by β*ICG is negligible when the low-pass filter is on, contributions of ICG and autofluorescence can be split to increase the accuracy of the provided information.

Once processed by subtracting the background signal, these images lead to one image containing only the ICG contribution (Figure 15). Although the ICG image is noisier than the image with the filter off, it is not ambiguous in the perfused area, and small vessels can easily be discriminated.

Discussion

Until recently, it was commonly accepted that the maximum autofluorescence of the PTGs is observed between 800 and 900 nm and that this autofluorescence is reduced significantly below 800 nm (3, 9, 12, 13). Thus, PTG autofluorescence used to be measured between

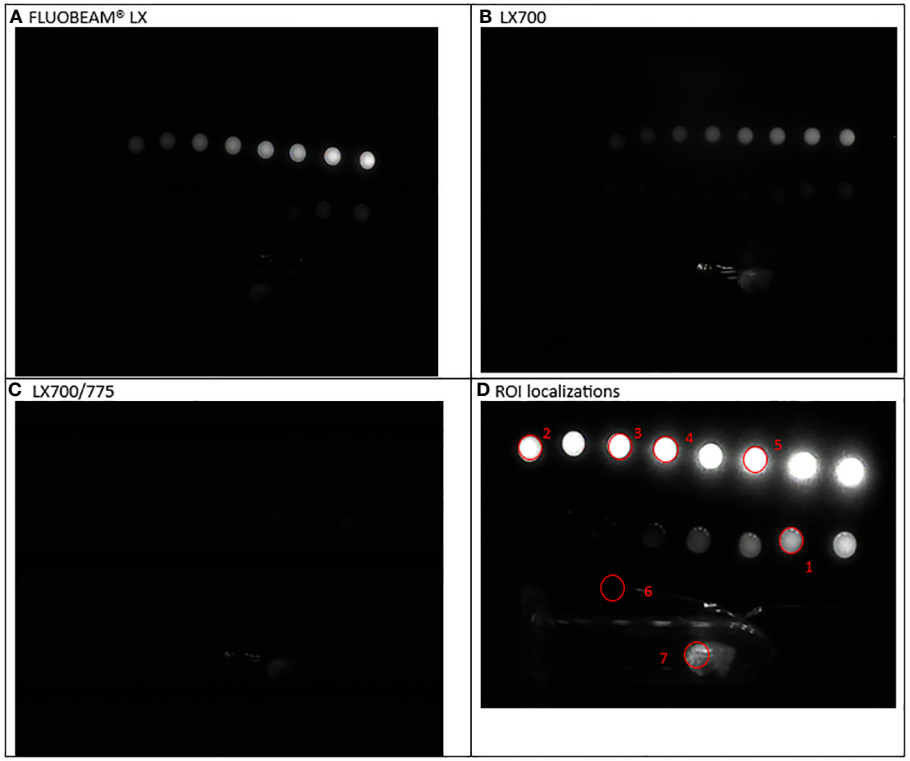

FIGURE 8
Sixth experimental setup: Parathyroid adenoma **(A)** Image captured with FLUOBEAM® LX, **(B)** Image captured with LX700, **(C)** Image taken with LX700/775, **(D)** Region of interest (ROI) for the signal measurements based on the structure of the examined sample with the concentration and location of the indocyanine green (ICG) droplets and location of the parathyroid gland. 1, 0.05 μM ICG droplet; 2, 0.1 μM ICG droplet; 3, 0.25 μM ICG droplet; 4, 0.5 μM ICG droplet; 5, 1 μM ICG droplet; 6, Background for ICG droplets and parathyroid specimen; 7, Parathyroid specimen.

10.3389/fendo.2023.1248449

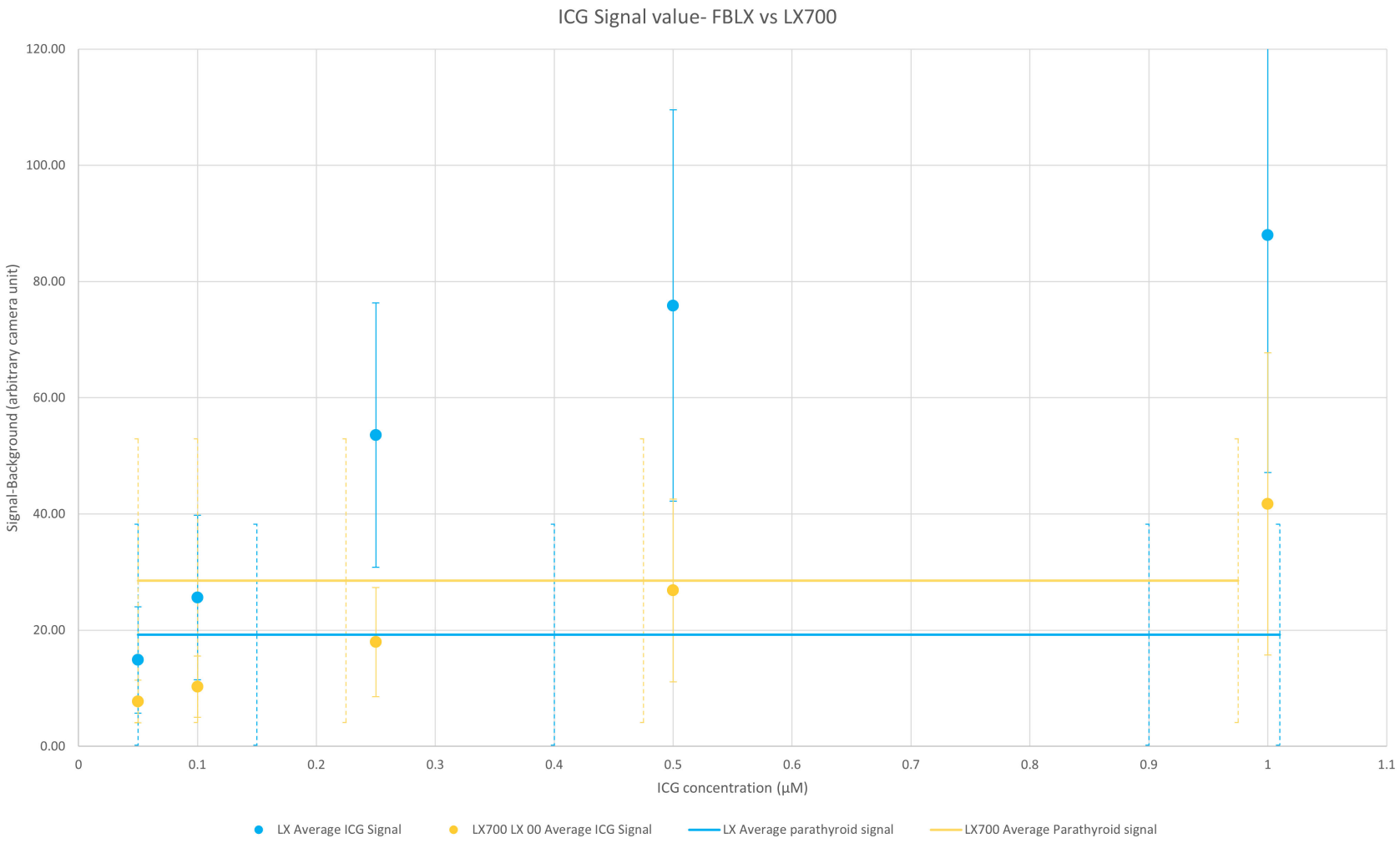

FIGURE 9
Comparison of the average value over the six setups of measured signals between the FLUOBEAM® LX and LX700 for the parathyroid gland (PTG) and indocyanine green (ICG) signals. For each data point, the subtracted background value was measured on the same dark area (an area where there was no sample). The range of the measured signal for the autofluorescence of the PTGs with FLUOBEAM® LX and LX700 is also indicated. This indicates that the same concentration of ICG could be easily detected by the two devices. The LX700 provides a signal almost 20% higher for the autofluorescence of the PTGs than the FLUOBEAM® LX.

10.3389/fendo.2023.1248449

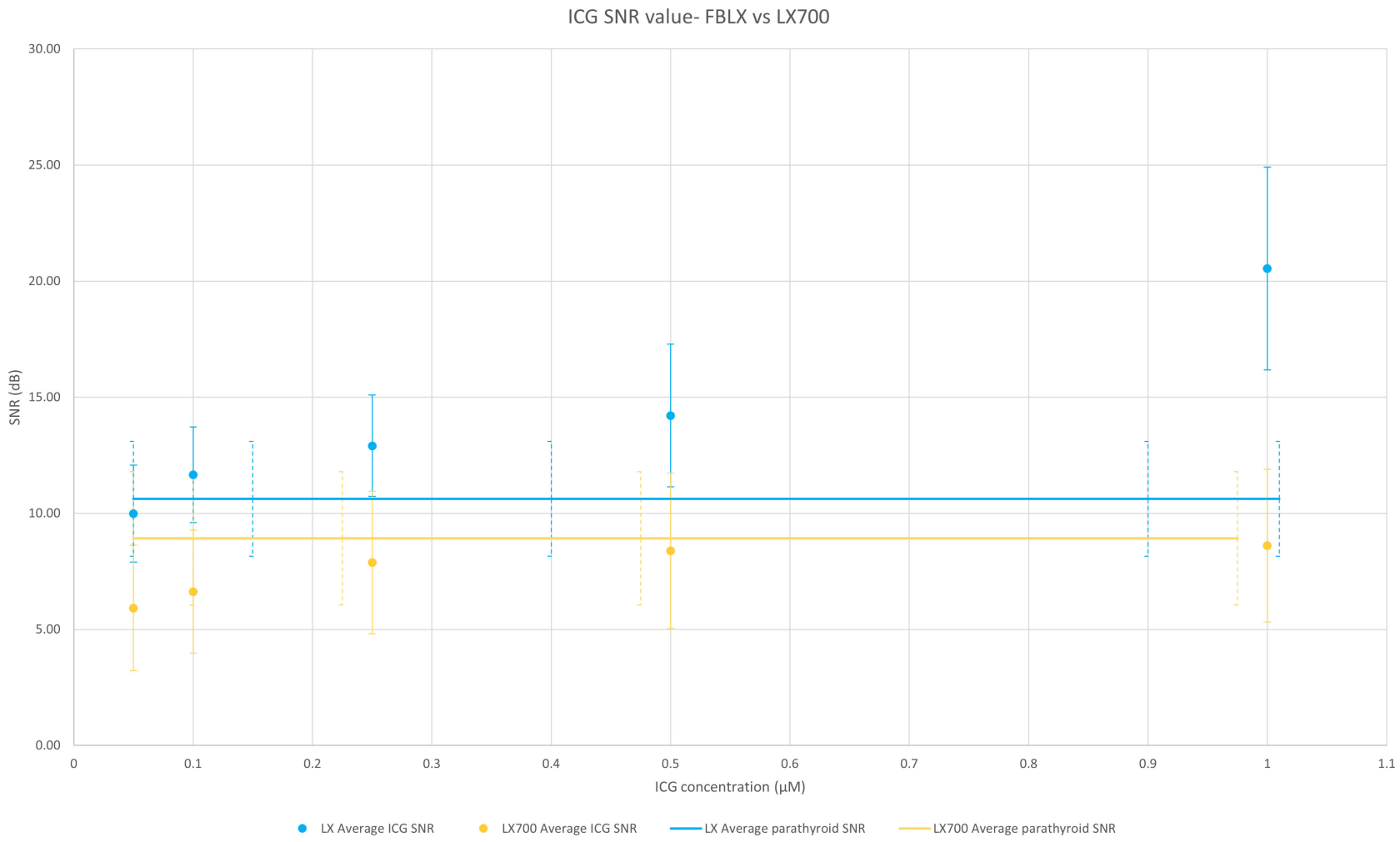

FIGURE 10
Comparison of the average value over the 6 setups of SNRs of the FLUOBEAM® LX and LX700 for a range of indocyanine green (ICG) concentrations. The two devices (FLUOBEAM® LX and LX700) could discriminate the same concentrations of ICG and were equivalent in terms of PTG detection. Even though the SNR was higher regarding ICG at low concentrations using the FLUOBEAM® LX, the SNR obtained using the LX700 stayed higher than 5 even for the lowest concentrations ensuring an unambiguous detectability.

10.3389/fendo.2023.1248449

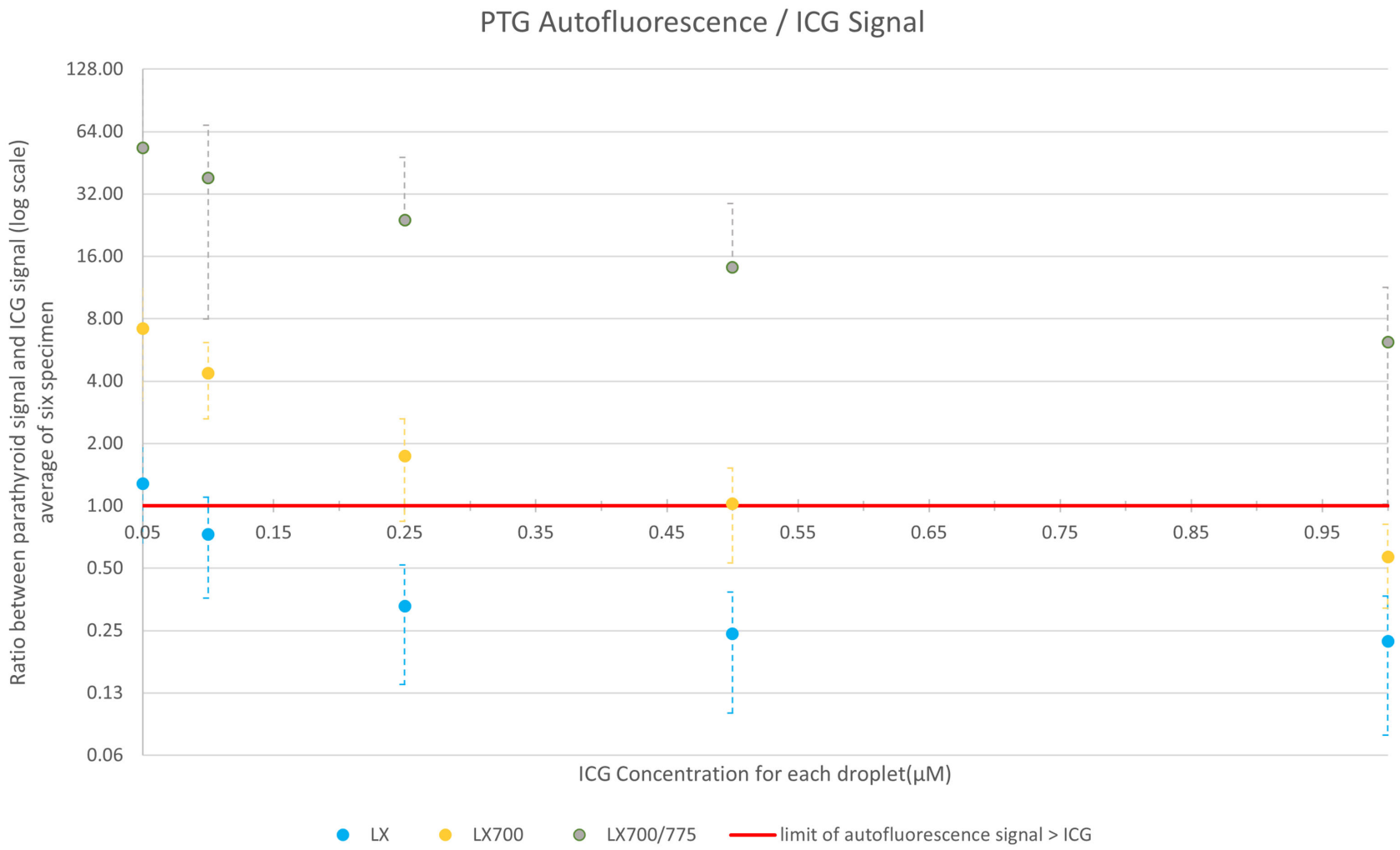

FIGURE 11
Comparison of the average value over the six setups of the ratio between ICG and parathyroid signals for the 3 systems: FLUOBEAM® LX, LX700 (unfiltered), and LX700/775 (low pass filtered; cut-off wavelength, 775 nm). The data used for this figure are presented in Table 2. Reducing the detection bandwidth with a low-pass filter decreased the overall sensitivity of the LX700/775 device. However, it increased its ability to discriminate parathyroid gland (PTG) autofluorescence in the presence of ICG by a factor of at least 60.

10.3389/fendo.2023.1248449

TABLE 1 Datasets regarding the three systems used in this study.

TABLE 1.1 FLUOBEAM® LX dataset.

	System	FLUOBEAM®LX					
	Set up #	1	2	3	4	5	6
	Initial gain	24.6	24.6	32.7	16.8	16.8	8.7
0.05 µM	Mean	10.93	8.04	11.60	31.98	31.06	14.20
	Stdev	1.25	0.88	0.96	1.70	1.20	1.47
0.1 µM	Mean	17.38	13.45	16.12	48.94	47.71	28.59
	Stdev	1.50	1.14	1.43	1.84	1.52	1.50
0.25 µM	Mean	38.55	36.26	31.05*	88.00	85.39	60.69
	Stdev	4.24	2.59	0.75	2.67	3.02	3.25
0.5 µM	Mean	55.99*	52.45	31.52*	119.63	117.65	96.42
	Stdev	4.54	4.12	0.17	2.46	2.86	5.44
1 µM	Mean	61.99*	62.03*	31.72*	123.76*	123.67*	143.16
	Stdev	0.60	0.41	0.10	0.25	0.21	7.91
Background for the ICG drops	Mean	3.50	2.02	3.09	4.40	3.54	1.99
	Stdev	0.20	0.14	0.35	0.27	0.26	0.11
Parathyroid	Mean	11.19	17.97	16.39	71.33	25.21	11.51
	Stdev	0.45	0.98	1.28	2.14	1.39	1.37
Background for the parathyroid	Mean	2.16	6.01	8.66	10.00	9.64	1.99
	Stdev	0.12	0.43	0.72	0.51	0.47	0.11

TABLE 1.2 LX700 dataset.

	System	LX700					
	Set up # #	1	2	3	4	5	6
	Initial gain	24.6	24.6	28.5	18.6	16.8	8.7
0.05 µM	Mean	11.37	7.30	6.87	9.46	11.93	10.82
	Stdev	0.98	0.65	0.54	0.47	0.56	1.35
0.1 µM	Mean	11.46	8.83	7.80	15.80	17.30	17.34
	Stdev	0.57	0.44	0.79	1.34	0.87	1.58
0.25 µM	Mean	17.99	15.96	16.79	27.33	31.23	36.98
	Stdev	1.58	1.08	1.25	1.29	1.86	2.31
0.5 µM	Mean	26.61	24.18	22.34	44.38	49.27	56.90
	Stdev	2.01	2.43	1.81	1.70	1.93	4.02
1 µM	Mean	43.08	41.37	37.17	80.80	79.39	83.66
	Stdev	4.77	3.31	3.23	3.51	2.83	6.58
Background for the ICG drops	Mean	7.82	5.11	4.41	3.83	4.73	2.17
	Stdev	0.68	0.32	0.30	0.28	0.36	0.38
Parathyroid	Mean	23.16	34.44	27.03	99.32	37.16	43.38

(Continued)

TABLE 1.2 Continued

	System	LX700					
	Set up # #	1	2	3	4	5	6
	Stdev	1.78	1.96	2.49	2.62	1.76	2.55
Background for the parathyroid	Mean	5.66	13.28	12.34	16.01	15.47	2.17
	Stdev	0.34	0.59	0.69	1.04	0.89	0.38

TABLE 1.3 LX700/775 dataset.

	System	LX700					
	Set up # #	1	2	3	4	5	6
	Initial gain	24.6	24.6	28.5	18.6	16.8	8.7
0.05 µM	Mean	11.37	7.30	6.87	9.46	11.93	10.82
	Stdev	0.98	0.65	0.54	0.47	0.56	1.35
0.1 µM	Mean	11.46	8.83	7.80	15.80	17.30	17.34
	Stdev	0.57	0.44	0.79	1.34	0.87	1.58
0.25 µM	Mean	17.99	15.96	16.79	27.33	31.23	36.98
	Stdev	1.58	1.08	1.25	1.29	1.86	2.31
0.5 µM	Mean	26.61	24.18	22.34	44.38	49.27	56.90
	Stdev	2.01	2.43	1.81	1.70	1.93	4.02
1 µM	Mean	43.08	41.37	37.17	80.80	79.39	83.66
	Stdev	4.77	3.31	3.23	3.51	2.83	6.58
Background for the ICG drops	Mean	7.82	5.11	4.41	3.83	4.73	2.17
	Stdev	0.68	0.32	0.30	0.28	0.36	0.38
Parathyroid	Mean	23.16	34.44	27.03	99.32	37.16	43.38
	Stdev	1.78	1.96	2.49	2.62	1.76	2.55
Background for the parathyroid	Mean	5.66	13.28	12.34	16.01	15.47	2.17
	Stdev	0.34	0.59	0.69	1.04	0.89	0.38

*Saturated signal

Tables 1.1, 1.2, and 1.3 show the measured values obtained from the analysis. ImageJ (software developed by NIH) was used to extract data on digitized fluorescence 8-bit images provided by the camera. For each droplet and each parathyroid gland region of interest, the averages (Mean) and standard deviations (Stdev) were computed with the following different acquisition configurations: FLUOBEAM® LX, LX700, and LX700 with 775 nm low-pass filter (referred to as the LX700/775). Different camera amplification factors were used depending on the system configuration to provide useful, unsaturated images. All results were normalized to a 40ms/8.7dB gain before computation.

800 and 900 nm. Furthermore, as the excitation wavelength is between 740 and 805 nm in most commercially available systems, fluorescence is usually detected between 800 and 900 nm in these systems, e.g., PTeye (Medtronic), FLUOBEAM LX (Fluoptics), EleVision IR platform (Medtronic), and PDE (Hamamatsu). Balasubramanian et al. (14), using the FLUOBEAM® 700, indicated that PTG autofluorescence is visible with an excitation wavelength of 685 nm and an emission window between 700 and 900 nm. This autofluorescence allowed for the pre-localization of the PTGs during thyroidectomy. More recently, Serra et al. (10), using fluorescence spectrometry and excitation at 650 nm, confirmed that the PTGs emitted autofluorescence at least at 700 nm and that maximum autofluorescence was observed close to 711 nm.

TABLE 2 SNR of Parathyroid glands with the three devices.

	LX	LX700	LX700/775
SNR (dB)	10,623	10,781	9,985
Stdev	2,476	2,190	1,695

The averaged SNR has been computed from the data of Table 1. Variation of the parathyroid gland (PTG) autofluorescence according to the filtering. The SNR was slightly lower with the LX700 filtered at 775 nm because only about 60% of the emitted spectra were detected. The SNR with the FLUOBEAM® LX was comparable to that with the LX 700 because although only about 40% of the emitted autofluorescence signal was detected, the detection window was at a higher wavelength. Therefore, it was much less sensitive to background signals such as parasitic lights.

In order to avoid using two excitation wavelengths, we examined a single excitation that rebalanced the measured signal levels between ICG and PTG autofluorescence. Exciting at a wavelength of 685 nm reduces the ICG contribution and

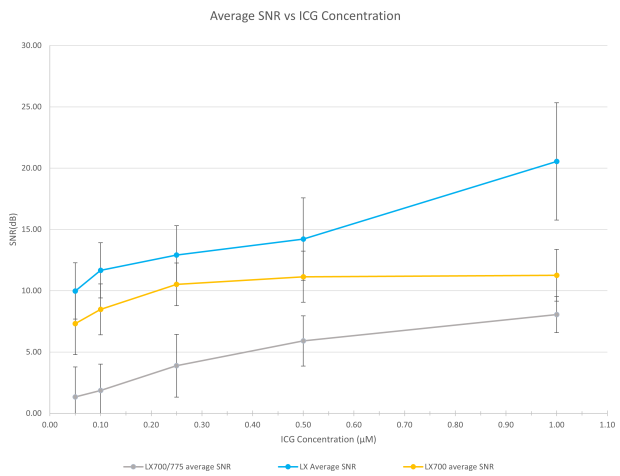

FIGURE 12
Comparison of the measured SNRs for the 3 systems (FLUOBEAM® LX, LX700, LX700/775). The low-pass filtering decreased the signal level by detecting on a narrower bandwidth. However, as the detection was performed on a narrower bandwidth, the background noise was significantly reduced.

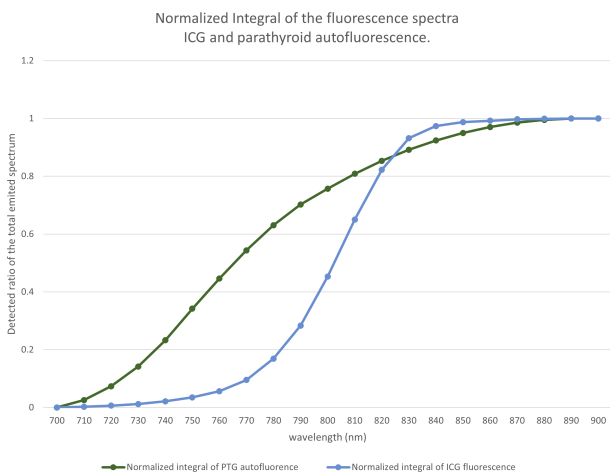

FIGURE 13
Proportion of the fluorescence signal as a function of the cut-off wavelength. Based on the spectra of Figure 1, for each wavelength between 700 and 900 nm, for indocyanine green (ICG) and the parathyroid gland (PTG), we computed the ratio of the spectra that would be detected by a device using a low-pass filter at a particular wavelength.

increases the autofluorescence signal. Nevertheless, the contribution of PTG autofluorescence over a detection window ranging from 700 to 900 nm is negligible compared to that of ICG. Narrowing the detection window between 700 and 775 nm will reduce the contribution of ICG more than that of the PTG.

In our study, we observed that PTG autofluorescence could be visualized with a good SNR ratio upon excitation at 685 nm. Moreover, the autofluorescence signal was substantial between 700 and 800 nm.

We also demonstrated that the SNR of the autofluorescence signal obtained with an excitation at 685 nm and a detection between 700 and 775nm is similar to that obtained with the FLUOBEAM® LX (about 10 dB). This imaging approach opens new opportunities for the possibility of i) using autofluorescence alone even after injection of ICG and ii) combining images with different detection windows (700–900 nm and 700–775 nm) to split the contribution of ICG and autofluorescence.

By considering the possibility of renewing the ICG injections if necessary while observing the parathyroids by autofluorescence, the technical improvement described here removes the current main obstacle of intraoperative evaluation of the PTGs by fluorescence imaging at the end of the dissection of each lobe. Once the ICG has been injected, it would not be possible to observe the autofluorescence because the signal is dominated by ICG. However, identification by autofluorescence is crucial because it aids in PTG identification, which positively impacts the quality and function of the preserved glands (4).

By contrast, the injection, sometimes repeated, of ICG helps improve the dissection and/or intraoperative decision by helping to create a vascular mapping of the PTGs before thyroid dissection (8). It can also help improve the dissection by helping to evaluate the parathyroid perfusion at the end of the lobectomy, which would allow for the adaptation of the radicality of the thyroid resection on the second lobe in cases of total thyroidectomy (15). Both modalities are greatly facilitated by the possibility of easy and accurate visualization of the PTG with autofluorescent imaging during ICG injection.

Without the innovation described in this study, to be able to use autofluorescence on the four PTGs without endangering the recurrent nerve in case of loss of signal requiring a stop of the procedure and re-intervention in an already dissected area, the surgeon has to reserve mapping angiographies and perfusion assessment to one side only (the second) during total thyroidectomies.

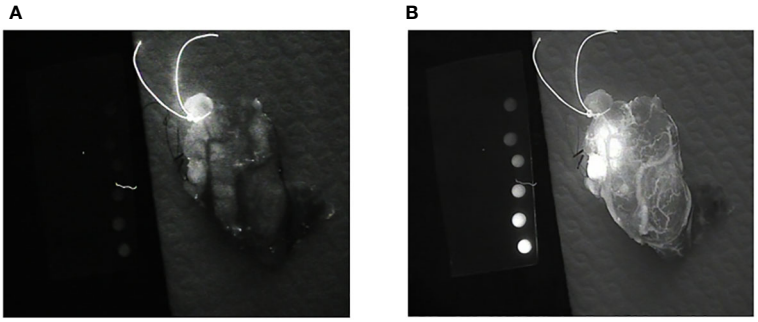

FIGURE 14
Images of the same thyroid lobe after excision. This lobe was removed after the injection of indocyanine green (ICG) to identify the blood vessels feeding the parathyroid glands. **(A)** Image obtained using a low-pass filter with a cut-off wavelength of 775 nm (LX700/775). **(B)** Image obtained with a nonfiltered device (LX700), in which the ICG contribution was clearly predominant.

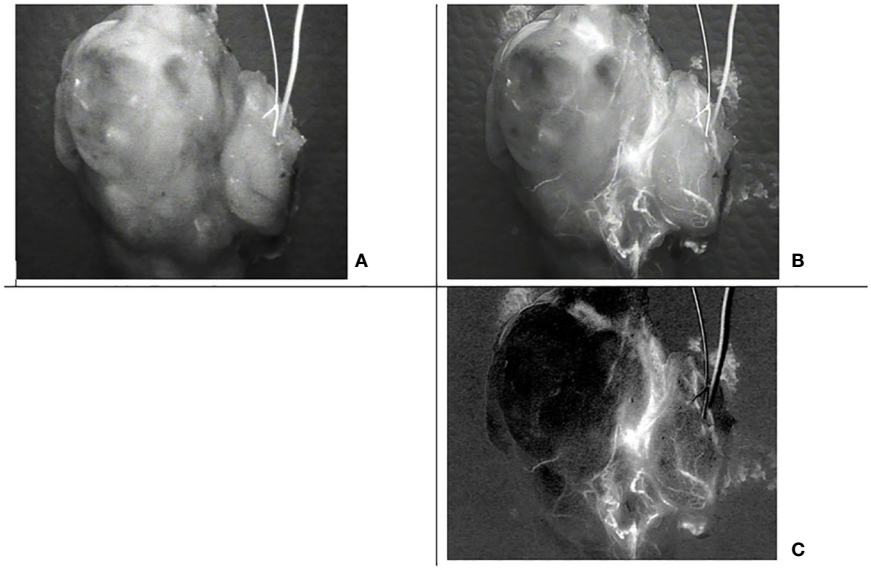

FIGURE 15
Images of the same thyroid lobe after excision. This lobe was removed after the injection of indocyanine green (ICG) to identify the blood vessels feeding the parathyroid glands **(A)** Image with the low pass filter on, **(B)** Image with the low pass filter off, **(C)** Indocyanine green (ICG) image computed from the four acquisitions assuming that alpha= 0.3 and beta =0.025.

In conclusion, this study demonstrates that PTG autofluorescence can be detected in the presence of ICG, in concentrations as high as 1.0 μM, with a fluorescence imaging device performing excitation at 685 nm and with detection between 700 and 775 nm. It also demonstrates that ICG can be detected at concentrations as low as 0.05 μM with the same excitation at 685 nm and a detection window between 700 and 900 nm.

The expected clinical benefits versus drawbacks (added time, expense, etc.) from using fluorescence-based parathyroid imaging combined with ICG angiography compared to either technique alone or other imaging methods must be evaluated because the potential for this combination is the key advance offered by changing the excitation and emission settings.

This feasibility study needs to be complemented by an extensive clinical assessment to evaluate the clinical benefits of using a device with excitation at 685 nm and a removable low-pass filter for different pathologies leading to thyroid and/or parathyroid surgery.

Data availability statement

The original contributions presented in the study are included in the article/supplementary material. Further inquiries can be directed to the corresponding author.

Author contributions

MR and PR contributed equally to the conception, design, and data analysis of the study. All authors contributed to the article and approved the submitted version.

Funding

This work was internally funded by the FLUOPTICS© part of GETINGE.

Acknowledgments

The authors would like to express their gratitude towards Dr Fares Benmiloud for his valuable participation in this work. Dr Benmiloud performed all the surgeries and analyzed the surgical impact of the technology.

Conflict of interest

PR and MR are both FLUOPTICS© SAS employees.

Publisher's note

All claims expressed in this article are solely those of the authors and do not necessarily represent those of their affiliated organizations, or those of the publisher, the editors and the reviewers. Any product that may be evaluated in this article, or claim that may be made by its manufacturer, is not guaranteed or endorsed by the publisher.

References

1. Almquist M, Ivarsson K, Nordenström E, Bergenfelz A. Mortality in patients with permanent hypoparathyroidism after total thyroidectomy. *Br J Surg* (2018) 105:1313–8. doi: 10.1002/bjs.10843

2. Bergenfelz A, Nordenström E, Almquist M. Morbidity in patients with permanent hypoparathyroidism after total thyroidectomy. *Surgery* (2020) 167:124–8. doi: 10.1016/j.surg.2019.06.056

3. Paras C, Keller M, White L, Phay J, Mahadevan-Jansen A. Near-infrared autofluorescence for the detection of parathyroid glands. *J BioMed Opt* (2011) 16:067012. doi: 10.1117/1.3583571

4. Benmiloud F, Rebaudet S, Varoquaux A, Penaranda G, Bannier M, Denizot A. Impact of autofluorescence-based identification of parathyroids during total thyroidectomy on postoperative hypocalcemia: a before and after controlled study. *Surgery* (2018) 163:23–30. doi: 10.1016/j.surg.2017.06.022

5. Kahramangil B, Dip F, Benmiloud F, Falco J, de la Fuente M, Verna S, et al. Detection of parathyroid autofluorescence using near-infrared imaging: a multicenter analysis of concordance between different surgeons. *Ann Surg Oncol* (2018) 25:957–62. doi: 10.1245/s10434-018-6364-2

6. Hartl D, Obongo R, Guerlain J, Breuskin I, Abbaci M, Laplace-Builhé C. Intraoperative parathyroid gland identification using autofluorescence: pearls and pitfalls. *World J Surg Surg Res* (2019) 2:1166.

7. Delattre JF, Flament JB, Palot JP, Pluot M. Variations in the parathyroid glands. Number, situation and arterial vascularization. Anatomical study and surgical application. *J Chir (Paris)* (1982) 119:633–41.

8. Benmiloud F, Penaranda G, Chiche L, Rebaudet S. Intraoperative mapping angiograms of the parathyroid glands using indocyanine green during thyroid surgery: results of the fluogreen study. *World J Surg* (2022) 46:416–24. doi: 10.1007/s00268-021-06353-4

9. Solórzano CC, Thomas G, Berber E, Wang TS, Randolph GW, Duh QY, et al. Current state of intraoperative use of near infrared fluorescence for parathyroid identification and preservation. *Surgery* (2021) 169:868–78. doi: 10.1016/j.surg.2020.09.014

10. Serra C, Serra J, Ferreira MaChado IL, Vieira Ferreira LF. Spectroscopic analysis of parathyroid and thyroid tissues by ground-state diffuse reflectance and laser induced luminescence: a preliminary report. *J Fluoresc* (2021) 31:1235–9. doi: 10.1007/s10895-021-02783-4

11. *European standards: IEC 60825-1* (2014). Available at: https://www.en-standard.eu/iec-60825-1-2014-safety-of-laser-products-part-1-equipment-classification-and-requirements (Accessed March 15, 2023).

12. Mahadevan-Jansen A, White L, Phay J, Paras CA, Bartz EK, Keller MD, et al. United States patent US2012010483 (2012). Available at: https://worldwide.espacenet.com.

13. Mahadevan-Jansen A, White L, Phay J, Paras CA, Bartz EK, Keller MD, et al. United States patent US 10258275 (2019).

14. Hillary SL, Guillermet S, Brown NJ, Balasubramanian SP. Use of methylene blue and near-infrared fluorescence in thyroid and parathyroid surgery. *Langenbecks Arch Surg* (2018) 403:111–8. doi: 10.1007/s00423-017-1641-2

15. Vidal Fortuny J, Sadowski SM, Belfontali V, Guigard S, Poncet A, Ris F, et al. Randomized clinical trial of intraoperative parathyroid gland angiography with indocyanine green fluorescence predicting parathyroid function after thyroid surgery. *Br J Surg* (2018) 105:350–7. doi: 10.1002/bjs.10783

frontiers | Frontiers in Endocrinology

TYPE Original Research
PUBLISHED 13 November 2023
DOI 10.3389/fendo.2023.1235354

OPEN ACCESS

EDITED BY
I-Cheng Lu,
Kaohsiung Medical University, Taiwan

REVIEWED BY
Hanqing Lin,
First Affiliated Hospital of Fujian Medical University, China
Ludovico Docimo,
University of Campania Luigi Vanvitelli, Italy

*CORRESPONDENCE
Shuai Xue
xueshuai@jlu.edu.cn

RECEIVED 06 June 2023
ACCEPTED 27 October 2023
PUBLISHED 13 November 2023

CITATION
Zhang C, Fu S, Liu H and Xue S (2023) Risk prediction for <1 cm lateral lymph node metastasis in papillary thyroid microcarcinoma.
Front. Endocrinol. 14:1235354.
doi: 10.3389/fendo.2023.1235354

Risk prediction for <1 cm lateral lymph node metastasis in papillary thyroid microcarcinoma

Chengxin Zhang[1], Siqi Fu[1], He Liu[1] and Shuai Xue[2]*

[1]Business College, Guilin University Of Electronic Technology, Guilin, Guangxi, China, [2]General Surgery Center, Department of Thyroid Surgery, The 1st Hospital of Jilin University, Changchun, Jilin, China

Background: Because the diameter of the suspicious lymph nodes is less than 1 cm and adjacent to important structures in the neck, the diagnosis of small LLNM is important but difficult without the help of fine needle aspiration (FNA). There are no relevant reports of risk factors that predict the risk of suspicious <1 cm LLNM.

Methods: A total of 159 PTMC patients with suspicious <1 cm LLNM were included in the study. Multivariate logistic regression analysis was used to identify ultrasound independent predictors of LLNM. A predictive model was developed according to multivariate logistic regression and evaluated by Hosmer-Lemeshow fit test.

Results: Age ≤ 38 years old, the largest PTMC was located in the upper part, and the presence of liquefaction or microcalcification in suspicious lymph nodes were independent risk factors for LLNM (univariate analysis P = 0.00, 0.00, 0.00; multivariate analysis P = 0.00, 0.02, 0.00. OR = 4.66 [CI: 1.78-12.21], 3.04 [CI: 1.24-7.46], 6.39 [CI: 1.85-22.00]). The predictive model for the diagnosis of suspicious <1 cm lymph nodes was established as: $P = e^X/(1 + e^X)$. X = -1.29 + (1.11 × whether the largest tumor is located in the upper part) + (1.54 × whether the age is ≤ 38 years) + (1.85 × whether the suspicious lymph nodes have liquefaction/microcalcification). The Hosmer-Lemeshow fit test was used to test the predicted ability, and it found that the predictive model had a good fit and prediction accuracy ($X^2 = 6.214$, P = 0.623 > 0.05). Chi squared trend analysis showed that the increase in the number of risk factors gradually increased the malignancy possibility of suspicious <1 cm lymph nodes (chi squared trend test, P = 0.00).

Conclusions: Age ≤ 38 years old, the largest PTMC located in the upper part, and the presence of liquefaction or microcalcification in suspicious lymph nodes were independent risk factors for suspicious <1 cm LLNM in PTMC patients. Our result show that it is feasible to evaluate the malignant possibility of these lymph nodes using the number of risk factors.

KEYWORDS

risk factor, predictive model, lateral lymph node metastasis, papillary thyroid microcarcinoma, lateral lymph node dissection

1 Introduction

The worldwide increasing incidence of thyroid cancer is primarily attributed to the rapid rise of papillary thyroid microcarcinoma (PTMC) (1). Most patients with PTMC were diagnosed using routine physical examination and had no clinical symptoms. The development and popularization of high-frequency ultrasound (US) and fine needle aspiration (FNA) in recent years have increased the diagnosis of PTMC (2, 3). Most PTMC are low-risk with a 1-5% of recurrence rate and a 0.3% 10-year mortality rate. Therefore, the use of a more conservative treatment strategy for low-risk PTMC is the current consensus. However, increasing studies reported that lateral lymph node metastasis (LLNM) was associated with locoregional recurrence, distant metastases and worse prognosis for PTMC (4, 5). The revised American Thyroid Association (ATA) guidelines in 2015 also considered that approximately 20% of PTC patients with LLNM would have structural recurrence in the future (6).

Approximately 20-50% of differentiated thyroid cancer patients found LLNM before surgery. The incidence of LLNM is less than 10% in PTMC. However, LLNM is a risk factor of high recurrence rate and poor prognosis in PTMC patients. Thyroid cancer guidelines suggest that only LLNM with definite preoperative or intraoperative diagnosis should be treated with therapeutic lateral lymph node dissection (LLND). Therefore, the diagnosis of LLNM is particularly important. Common preoperative examinations include US, Computed Tomography (CT), FNA and thyroglobulin (TG)-FNA. ATA guidelines recommend FNA only for ≥1 cm suspicious lateral lymph nodes (6). However, the diameter of suspicious lateral lymph nodes from many PTMC patients are less than 1 cm in the clinic. Because the diameter of the suspicious lymph nodes is small and adjacent to important structures of the neck, it is very difficult to diagnose using preoperative FNA. The diagnosis of small lymph nodes is only made from frozen sections during surgery. However, the frozen section diagnosis of lymph nodes during surgery may produce false-positive and false-negative results (7, 8). If it is misdiagnosed as negative, the patients must undergo re-operation after the corrected pathological diagnosis, which causes physical and psychological burden for the patients. If it is misdiagnosed as positive, the patient receives LLND, which may lead to more complications. Therefore, whether there are risk factors that predict the risk of suspicious <1 cm LLNM is not known.

We included patients who received LLND because of suspicious <1 cm lymph nodes, analyzed the clinical data and US characteristics, established a predictive diagnosis model, and evaluated its diagnostic ability. The present study improved the diagnosis of suspicious <1 cm lymph nodes in the lateral neck.

2 Materials and methods

2.1 Patient selection

The data of PTMC patients who underwent thyroid surgery in the First Hospital of Jilin University from January 2009 to July 2019 were analyzed retrospectively. The inclusion criteria of patients were complete information of patients in the hospital database, PTMC confirmed in postoperative pathology, suspicious <1 cm LLNM indicated on preoperative US, and suspicious lymph nodes were resected and confirmed by pathology. The exclusion criteria were age < 18 years old, neck radiotherapy history, and previous thyroid surgery history. A total of 159 PTMC patients with suspicious <1 cm LLNM were included in the study.

2.2 Diagnosis and treatment

Most patients with PTMC were diagnosed using US, which was performed by a trained radiologist, and re-evaluated by surgeons for thyroid tumors and cervical lymph nodes before surgery. It was suggested that FNA be performed preoperatively for the diagnosis of suspicious thyroid nodules. The ultrasonic manifestations of malignant lymph nodes are microcalcification, liquefaction, peripheral blood flow signal, hyperechoic, and round. If the largest diameter of suspicious lymph nodes in the neck was greater than 1.0 cm, then FNA was recommended. If the maximum diameter of the suspicious lymph nodes in the neck was smaller than 1.0 cm, then selective LLND was performed during the surgery, and frozen sectioning was performed to determine whether the suspicious lymph nodes were metastatic and whether modified radical LLND (at least II - IV area) should be performed.

2.3 Ultrasonic examination

Experienced US doctors in our department performed US examinations of thyroid nodules and lateral cervical lymph nodes before surgery. Thyroid nodules were primarily evaluated for its location, size, echo, texture, boundary, shape, blood flow and other characteristics. Most studies reported that the location of PTMC was a risk factor for LLNM, and we recorded the location of PTMC in detail. The size, location, shape, echo, calcification, blood flow and other characteristics of the lateral cervical lymph nodes were evaluated. We recorded this related information. Before the surgery, the clinician checked the accuracy of the US information again. If there was any inconformity, an experienced radiologist and surgeon were consulted.

2.4 Statistical analysis

Nominal variables are described as frequency and proportion, and continuous variables are described as means and standard deviation. To determine differences between specific variable groups, Pearson's chi squared test was used for nominal variables, and Mann-Whitney U test was used for continuous variables. The risk factors were determined via univariate analysis and multivariate logistic regression analysis. The optimal cutoff value of continuous variable was determined using a receiver operating characteristic curve (ROC) and transformed into binary variables to better explain the results of risk factors. The prediction model of LLNM was

10.3389/fendo.2023.1235354

calculated using the β coefficient provided by the multivariate logistic regression analysis. The ROC curve was used to evaluate the predictive ability of the predictive model. The Hosmer-Lemeshow fit test was used to test the predictive ability compared to the pathological results. Nonnormally distributed continuous variables were compared using the Kruskal Wallis test. The chi squared trend test was used to evaluate the correlation between the number of risk factors and the malignancy possibility of lateral cervical lymph nodes. P value < 0.05 was considered statistically significant. The 22nd edition SPSS software (SPSS Inc, Chicago, IL, USA) was used for all statistical analyses.

3 Results

3.1 General clinicopathological characteristics

Table 1 summarizes the general clinicopathological characteristics of 159 PTMC patients with suspicious <1 cm lateral lymph nodes. One hundred and nineteen patients were female (74.8%) with an average age of 42.0 years. Most of the patients had the largest tumor in the upper part (57.9%). The shape of suspicious lymph nodes in the lateral neck of 49 patients (30.8%) was round or irregular. In 130 cases (81.8%) of the suspicious small lateral lymph nodes, no clear hilar structure was found. In 70 cases (44.0%), the suspicious lymph nodes were liquefied or microcalcified. Preoperative US diagnosis was correct in 121 cases, and the correct rate was 76.1%.

TABLE 1 Clinicopathological features of PTMC with suspicious <1cm lateral lymph nodes.

Variables	N=159 (%)
Sex	
Female	119 (74.8)
Male	40 (25.2)
Age, years	42.0±10.9
Location of largest tumor	
Upper	92 (57.9)
Non-upper	67 (42.1)
Shape	
Circle or irregular	49 (30.8)
Oval	110 (69.2)
Disappearance of lymphatic hilum	
Yes	130 (81.8)
No	29 (18.2)
Liquefaction or microcalfication	
Yes	70 (44.0)
No	89 (56.0)
Correct US diagnosis	
Yes	121 (76.1)
No	38 (23.9)

Categorical variables are presented as number (%, percentage). Continuous variables are presented as the average±standard deviation. PTMC, papillary thyroid microcarcinoma; US, ultrasound.

3.2 Univariate and multivariate analyses of risk factors

To examine the risk factors of LLNM in PTMC patients with suspicious <1 cm lateral lymph nodes, binary multivariate logistic regression analysis was performed. The continuous variable of age was converted into nominal variables using the cutoff value calculated in the ROC analysis (Table 2). As shown in Tables 3 and 4, univariate and multivariate analyses showed that age ≤ 38 years old, the largest PTMC located in the upper part, the presence of liquefaction or microcalcification in suspicious lymph nodes were independent risk factors for LLNM (univariate analysis P = 0.00, 0.00, 0.00; multivariate analysis P = 0.00, 0.02, 0.00. OR = 4.66 [CI: 1.78-12.21], 3.04 [CI: 1.24-7.46], 6.39 [CI: 1.85-22.00]).

3.3 Establishment and evaluation of prediction model

The predictive model for the diagnosis of suspicious <1 cm lymph nodes was established as: $P = e^x/(1 + e^x)$. X = -1.29 + (1.11 × whether the largest tumor is located in the upper part) + (1.54 × whether the age is ≤ 38 years) + (1.85 × whether the suspicious lymph nodes have liquefaction/microcalcification). P is the probability of malignant prediction, e is the natural logarithm, yes = 1, and no = 0. This group of data established the prediction model and calculated the value of malignant probability. An ROC curve was drawn according to the pathological results, as shown in Figure 1. The area under the curve was 0.832 ± 0.03, and the 95% confidence interval was 0.77-0.89. When the best cross-section value was 0.64, the sensitivity was 65.29%, and the specificity was 86.84%. The Hosmer-Lemeshow fit test was used to test the predictive ability and found that the predictive model had a good fit and prediction accuracy ($X^2 = 6.214$, P = 0.623 > 0.05).

3.4 Relationship between the number of risk factors and the probability of malignancy prediction

The number of risk factors was used as the abscissa, and the ordinate and box chart were created according to the malignant

TABLE 2 ROC analysis for optimal cutoff of continuous variables.

Variables	AUC (95% CI)	P value	Youden Index	Cutoff
Age	0.70 (0.63-0.77)	0.00	0.33	≤38

ROC, receiver operating characteristic curve; AUC, area under curve.

10.3389/fendo.2023.1235354

TABLE 3 Univariate analysis for risk factors of suspicious <1cm lateral lymph nodes in PTMC.

Variables	LLNM (N=159)		Univariate analysis
	Present, n=121	Absent, n=38	*P*
Sex			
Female	87 (71.9)	32 (84.2)	
Male	34 (28.1)	6 (15.8)	0.41
Age			
≤38 yr	65 (53.7)	8 (21.1)	
>38yr	56 (46.3)	30 (78.9)	0.00
Location of largest tumor			
Upper	79 (65.3)	13 (34.2)	
Non-upper	42 (34.7)	25 (65.8)	0.00
Shape			
Circle or irregular	46 (38.0)	3 (7.9)	
Oval	75 (62.0)	35 (92.1)	0.00
Disappearance of lymphatic hilum			
Yes	105 (86.8)	25 (65.8)	
No	16 (13.2)	13 (34.2)	0.00
Liquefaction or microcalfication			
Yes	66 (41.5)	4 (10.5)	
No	55 (58.5)	34 (89.5)	0.00

PTMC, papillary thyroid microcarcinoma; OR, odd ratio; LLNM, lateral lymph node metastasis.

TABLE 4 Multivariate analysis for risk factors of suspicious <1cm lateral lymph nodes in PTMC.

Variables	Multivariate analysis		
	β	OR (95% CI)	*P*
Sex			
Female		1 (reference)	
Male	0.64	1.89 (0.72-4.96)	0.20
Age			
≤38 yr		4.66 (1.78-12.21)	
>38yr	1.54	1 (reference)	0.00
Location of largest tumor			
Upper		3.04 (1.24-7.46)	
Non-upper	1.11	1 (reference)	0.02
Shape			
Circle or irregular		3.5 (0.57-22.03)	
Oval	0.87	1 (reference)	0.23
Disappearance of lymphatic hilum			
Yes		1.81 (0.65-5.03)	
No	0.59	1 (reference)	0.25
Liquefaction or microcalfication			
Yes		6.39 (1.85-22.00)	
No	1.85	1 (reference)	0.00
Constant	-1.29	1 (reference)	0.02

prediction probability calculated by the prediction model. There was a significant difference in malignant possibility between subgroups with different numbers of risk factors (Kruskal Wallis test, P = 0.00). The chi squared trend analysis showed that the malignancy possibility of suspicious <1 cm lymph nodes increased gradually with the increase of the number of risk factors (chi squared trend test, P = 0.00) (Figure 2).

4 Discussion

The diagnosis of suspicious <1 cm lateral lymph nodes is always difficult in clinical work. Because of the small size of the suspicious lymph nodes and adjacency to the important vessels, FNA before surgery is very difficult. The present study showed that 76.1% of the suspicious <1 cm lateral lymph nodes were diagnosed. However, 23.9% of the PTMC patients received radical LLND due to misdiagnosis, which caused physical and mental injury to these patients. Therefore, we determined some risk factors and established a prediction model to improve the accuracy of the diagnosis of suspicious <1 cm lateral lymph nodes.

Univariate and multivariate analyses found that age ≤ 38 years old, the largest tumor located in the upper part, and the presence of liquefaction or microcalcification in the suspicious lymph nodes were risk factors for suspicious <1 cm lateral lymph nodes. A large number of studies showed that age was a risk factor of LLNM in

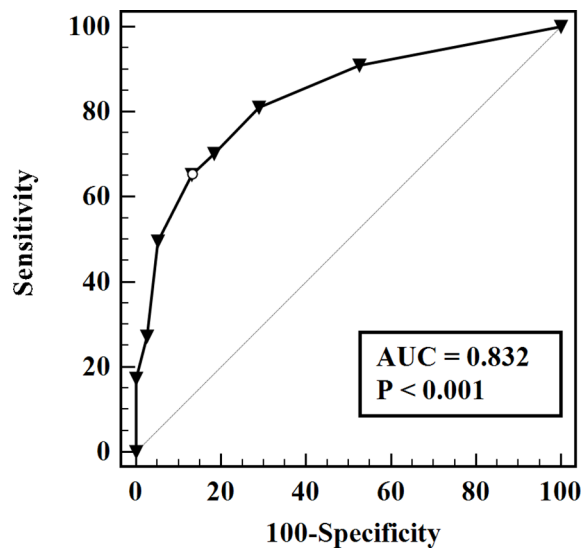

FIGURE 1
ROC evaluation for the prediction model.

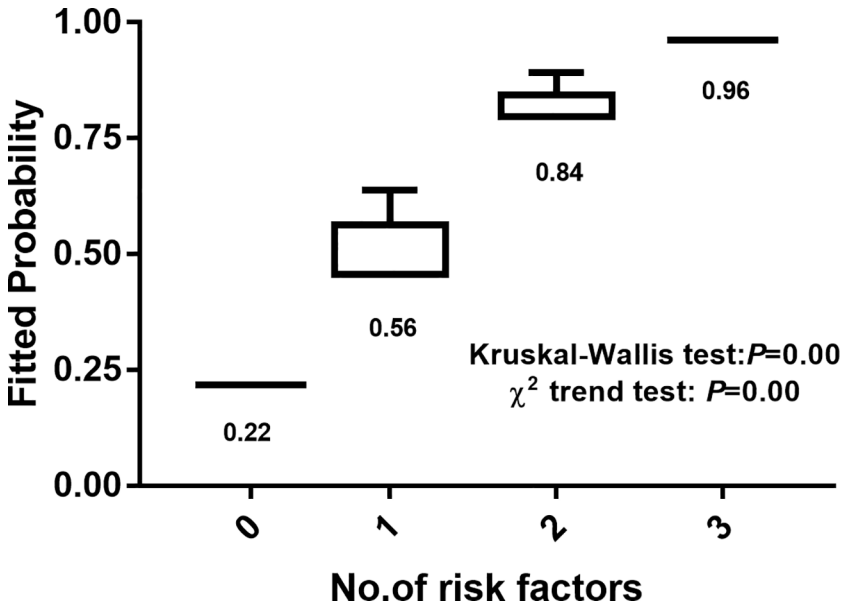

FIGURE 2
Relationship between number of risk factors and malignant prediction probability.

PTMC patients (9, 10). One active surveillance cohort study also found that young patients were more likely to have lymph node metastasis. Among ≤20 year-old PTMC patients under active surveillance, the possibility of LLNM during observation was as high as 11% (11). The specific mechanism of age-dependent tumorigenesis and development was not clear. The monitoring effect of the immune system on tumors changes with age, which may be the reason for the difference between young and old cancer patients (12, 13). Tumors located in the upper part were also closely related to LLNM of PTMC, especially with skip metastasis of PTMC (14–18). The reason may be that the lymph in the upper part of the thyroid gland flows into the lateral neck alone. Tumor in the upper part may not pass through the central neck region, and the tumor cells may be directly metastasized to the lateral neck, which may explain why thyroid cancer patients with tumors in the upper part have more LLNM (16). There are many malignant features of lymph nodes, such as round, irregular shape, high echo, uneven internal echo, unclear structure of lymphatics, liquefaction or microcalcification, and peripheral blood flow signal. Among these features, liquefaction and microcalcification have the highest specificity for the diagnosis of LLNM, which reaches 93-100% (6, 19, 20). Our study also found that liquefaction or microcalcification of the suspicious <1 cm lateral lymph nodes was very important for the diagnosis of LLNM.

There was no prediction model or grading system for the diagnosis of lateral cervical lymph nodes primarily due to the following reasons. 1) The sensitivity and specificity of US in the diagnosis of LLNM are high, at 62% - 100% and 68% - 98% respectively. 2) Preoperative CT combined with US further improved the diagnosis rate of metastatic lymph nodes in the lateral neck. 3) FNA may be used to directly diagnose a few suspicious lymph nodes. Therefore, many researchers believed that it was not necessary to risk-stratify LLNM. However, for suspicious <1 cm lateral lymph nodes, the diagnostic rate of US and CT is reduced. Because the lymph nodes are small and adjacent to important structures in the neck, FNA also has higher technical requirements for doctors. Therefore, it is very necessary to determine preoperative risk factors and examine a prediction model for suspicious <1 cm lateral lymph nodes.

Multivariate logistic regression analysis examined the prediction equation of malignant probability and verified its prediction efficiency. We found that this prediction model reliably predicted the benign and malignancy of suspicious <1 cm lateral lymph nodes. We also found that the number of risk factors positively correlated with the predicted malignant probability (chi squared trend test p = 0.00). Compared with the US grading system of thyroid nodules, the risk factors included were only the US characteristics of thyroid nodules. However, the prediction equation proposed in this experiment included a patient factor (age ≤ 38 years), a thyroid tumor factor (located in the upper part) and a US factor (liquefaction or microcalcification) of suspicious lymph nodes. Whether there is LLNM in PTMC patients is closely related to the predisposing factors of patients and the characteristics of thyroid cancer. Therefore, the incorporation of these factors may improve the prediction efficiency of the prediction model for suspicious lateral neck lymph nodes.

However, there are some limitations in this study. First, the number of patients included is too small, and there may be some bias in the multivariate analysis. The inclusion of more cases would improve the stability of the prediction model. Second, the prediction model obtained using calculation should be verified in another independent sample. However, due to the small number of PTMC with suspicious < 1 cm lymph nodes in the lateral neck, it was impossible to provide an independent case group to verify the correctness of the model. Finally, there is no strong evidence that <1 cm LLNM is closely related to a worse prognosis of PTMC patients, and whether the

LLND for these lymph nodes less than 1 cm is beneficial to patients require verification in prospective randomized controlled trials.

5 Conclusion

Age ≤ 38 years old (18-38 years), the largest PTMC located in the upper part, and the presence of liquefaction or microcalcification in suspicious lymph nodes were independent risk factors for suspicious <1 cm LLNM in PTMC patients. The predictive model had better sensitivity and specificity for the diagnosis of suspicious <1 cm LLNM, and the diagnostic accuracy was high. The increase in the number of risk factors gradually increased the malignant possibility of the suspicious <1 cm lateral lymph nodes. It is feasible to evaluate the malignant possibility of the lymph nodes using the number of risk factors. However, independent case groups are needed to verify the accuracy and stability of the prediction model.

Data availability statement

The raw data supporting the conclusions of this article will be made available by the authors, without undue reservation.

Ethics statement

This study was approved by the Institutional Ethics Committee of First Hospital of Jilin University. Informed consent were gave to all these patients in the study.

Author contributions

All authors contributed to the article and approved the submitted version.

Funding

The author(s) declare financial support was received for the research, authorship, and/or publication of this article. This research was supported by the Natural Science Funding of Jilin Province [YDZJ202201ZYTS109;YDZJ202301ZYTS458]; and the Interdiscipline Subject Foundation of the First Hospital of Jilin University [04033990001].

Conflict of interest

The authors declare that the research was conducted in the absence of any commercial or financial relationships that could be construed as a potential conflict of interest.

Publisher's note

All claims expressed in this article are solely those of the authors and do not necessarily represent those of their affiliated organizations, or those of the publisher, the editors and the reviewers. Any product that may be evaluated in this article, or claim that may be made by its manufacturer, is not guaranteed or endorsed by the publisher.

References

1. Dralle H, Machens A. Surgical management of the lateral neck compartment for metastatic thyroid cancer. *Curr Opin Oncol* (2013) 25(1):20–6. doi: 10.1097/CCO.0b013e328359ff1f

2. Wiltshire JJ, Drake TM, Uttley L, Balasubramanian SP. Systematic review of trends in the incidence rates of thyroid cancer. *Thyroid Off J Am Thyroid Assoc* (2016) 26(11):1541–52. doi: 10.1089/thy.2016.0100

3. Lee KL, Chen TJ, Won GS, Chou YH, Chiou HJ, Wang HK, et al. The use of fine needle aspiration and trends in incidence of thyroid cancer in taiwan. *J Chin Med Assoc JCMA* (2018) 81(2):164–9. doi: 10.1016/j.jcma.2017.09.008

4. Cracchiolo JR, Wong RJ. Management of the lateral neck in well differentiated thyroid cancer. *Eur J Surg Oncol J Eur Soc Surg Oncol Br Assoc Surg Oncol* (2018) 44 (3):332–7. doi: 10.1016/j.ejso.2017.06.004

5. Nixon IJ, Shaha AR. Management of regional nodes in thyroid cancer. *Oral Oncol* (2013) 49(7):671–5. doi: 10.1016/j.oraloncology.2013.03.441

6. Haugen BR, Alexander EK, Bible KC, Doherty GM, Mandel SJ, Nikiforov YE, et al. American thyroid association management guidelines for adult patients with thyroid nodules and differentiated thyroid cancer: The american thyroid association guidelines task force on thyroid nodules and differentiated thyroid cancer. *Thyroid Off J Am Thyroid Assoc* (20152016) 26(1):1–133. doi: 10.1089/thy.2015.0020

7. Kim SM, Kim HK, Kim KJ, Chang HJ, Kim BW, Lee YS, et al. Thyroidectomy without lateral neck dissection for papillary thyroid carcinoma with lateral neck lymph node metastases and negative intraoperative frozen section. *Head Neck* (2016) 38 (2):285–9. doi: 10.1002/hed.23893

8. Qiao G, Cong Y, Zou H, Lin J, Wang X, Li X, et al. False-negative frozen section of sentinel lymph node biopsy in a chinese population with breast cancer. *Anticancer Res* (2016) 36(3):1331–7.

9. Sheng L, Shi J, Han B, Lv B, Li L, Chen B, et al. Predicting factors for central or lateral lymph node metastasis in conventional papillary thyroid microcarcinoma. *Am J Surg* (2020) 220(2):334–40. doi: 10.1016/j.amjsurg.2019.11.032

10. Lin DZ, Qu N, Shi RL, Lu ZW, Ji QH, Wu WL. Risk prediction and clinical model building for lymph node metastasis in papillary thyroid microcarcinoma. *OncoTargets Ther* (2016) 9:5307–16. doi: 10.2147/ott.S107913

11. Ito Y, Miyauchi A, Kihara M, Higashiyama T, Kobayashi K, Miya A. Patient age is significantly related to the progression of papillary microcarcinoma of the thyroid under observation. *Thyroid Off J Am Thyroid Assoc* (2014) 24(1):27–34. doi: 10.1089/thy.2013.0367

12. Pawelec G. Age and immunity: What is "immunosenescence"? *Exp Gerontology* (2018) 105:4–9. doi: 10.1016/j.exger.2017.10.024

13. Taniguchi K, Karin M. NF-κB, inflammation, immunity and cancer: coming of age. *Nat Rev Immunol* (2018) 18(5):309–24. doi: 10.1038/nri.2017.142

14. So YK, Kim MJ, Kim S, Son YI. Lateral lymph node metastasis in papillary thyroid carcinoma: A systematic review and meta-analysis for prevalence, risk factors, and location. *Int J Surg (London England)* (2018) 50:94–103. doi: 10.1016/j.ijsu.2017.12.029

15. Jeon MJ, Chung MS, Kwon H, Kim M, Park S, Baek JH, et al. Features of papillary thyroid microcarcinoma associated with lateral cervical lymph node metastasis. *Clin Endocrinol* (2017) 86(6):845–51. doi: 10.1111/cen.13322

16. Zhang TT, Qi XZ, Chen JP, Shi RL, Wen SS, Wang YL, et al. The association between tumor's location and cervical lymph nodes metastasis in papillary thyroid cancer. *Gland Surg* (2019) 8(5):557–68. doi: 10.21037/gs.2019.10.02

17. Zhang L, Wei WJ, Ji QH, Zhu YX, Wang ZY, Wang Y, et al. Risk factors for neck nodal metastasis in papillary thyroid microcarcinoma: a study of 1066 patients. *J Clin Endocrinol Metab* (2012) 97(4):1250–7. doi: 10.1210/jc.2011-1546

18. Liu Z, Lei J, Liu Y, Fan Y, Wang X, Lu X. Preoperative predictors of lateral neck lymph node metastasis in papillary thyroid microcarcinoma. *Medicine* (2017) 96(10): e6240. doi: 10.1097/md.0000000000006240

19. Kwak JY, Kim EK, Kim MJ, Son EJ, Chung WY, Park CS, et al. Papillary microcarcinoma of the thyroid: predicting factors of lateral neck node metastasis. *Ann Surg Oncol* (2009) 16(5):1348–55. doi: 10.1245/s10434-009-0384-x

20. Landry CS, Grubbs EG, Busaidy NL, Monroe BJ, Staerkel GA, Perrier ND, et al. Cystic lymph nodes in the lateral neck as indicators of metastatic papillary thyroid cancer. *Endocrine Pract Off J Am Coll Endocrinol Am Assoc Clin Endocrinologists* (2011) 17(2):240–4. doi: 10.4158/ep10134.Or

frontiers | Frontiers in Endocrinology

TYPE Original Research
PUBLISHED 22 November 2023
DOI 10.3389/fendo.2023.1301838

OPEN ACCESS

EDITED BY
Mehmet Uludag,
Şişli Hamidiye Etfal Education and Research Hospital, Türkiye

REVIEWED BY
Adnan Işgör,
Memorial Sisli Hospital, Türkiye
Marcin Barczynski,
Jagiellonian University Medical College, Poland

*CORRESPONDENCE
Hui Sun
s_h@jlu.edu.cn

†These authors have contributed equally to this work and share first authorship

RECEIVED 25 September 2023
ACCEPTED 30 October 2023
PUBLISHED 22 November 2023

CITATION
Li C, Zhang J, Dionigi G and Sun H (2023) Assessment of different classification systems for predicting the risk of superior laryngeal nerve injury during thyroid surgery: a prospective cohort study. *Front. Endocrinol.* 14:1301838. doi: 10.3389/fendo.2023.1301838

Assessment of different classification systems for predicting the risk of superior laryngeal nerve injury during thyroid surgery: a prospective cohort study

Changlin Li[1†], Jiao Zhang[1†], Gianlorenzo Dionigi[2,3] and Hui Sun[1*]

[1]Division of Thyroid Surgery, China-Japan Union Hospital of Jilin University, Jilin Provincial Key Laboratory of Surgical Translational Medicine, Jilin Provincial Engineering Laboratory of Thyroid Disease Prevention and Control, Changchun, Jilin, China, [2]Division of Surgery, Istituto Auxologico Italiano Istituto di Ricovero e Cura a Carattere Scientifco (IRCCS), Milan, Italy, [3]Department of Medical Biotechnology and Translational Medicine, University of Milan, Milan, Italy

Background: A multitude of anatomical variations have been noted in the external branch of the superior laryngeal nerve (EBSLN). In this study, intraoperative neuromonitoring (IONM) was used to assess the potential value of the different classical EBSLN classifications for predicting the risk of EBSLN injury.

Methods: In total, 136 patients with thyroid nodules were included in this prospective cohort study, covering 242 nerves at risk (NAR). The EBSLN was identified by observing the cricothyroid muscle twitch and/or typical electromyography (EMG) biphasic waveform. The EBSLNs were classified by Cernea classification, Kierner classification, and Friedman classification, respectively. The EMG parameters and outcomes of vocal acoustic assessment were recorded.

Results: The distribution of Cernea, Kiernea, and Friedman subtypes were, respectively, Cernea 1 (40.9%), Cernea 2A (45.5%), Cernea 2B (10.7%), Kierner 1 (40.9%), Kierner 2 (45.5%), Kierner 3 (10.7%), Kierner 4 (2.9%) and Friedman 1 (15.7%), Friedman 2 (33.9%), Friedman 3 (50.4%). The amplitudes of EBSLN decreased significantly after superior thyroid pole operation, respectively, in Cernea 2A (193.7 vs. 226.6μV, P=0.019), Cernea 2B (185.8 vs. 221.3μV, P=0.039), Kierner 2 (193.7vs. 226.6μV, P=0.019), Kierner 3 (185.8 vs. 221.3μV, P=0.039), Kierner 4 (126.8vs. 226.0μV, P=0.015) and Friedman type 2 (184.8 vs. 221.6μV, P=0.030). There were significant differences in F_{max} and F_{range} for Cernea 2A (P=0.001, P=0.001), 2B (P=0.001, P=0.038), Kierner 2 (P=0.001), Kierner 3 (P=0.001, P=0.038), and Friedman 2 (P=0.004, P=0.014). In the predictive efficacy of EBSLN injury, the Friedman classification showed higher accuracy (69.8% vs. 44.3% vs. 45.0%), sensitivity (19.5% vs. 11.0% vs. 14.0%), and specificity (95.6% vs. 89.9% vs. 89.9%) than the Cernea and Kierner classifications. However, the false negative rate of Friedman classification was significantly higher than other subtypes (19.5% vs. 11.0% vs. 14.0%).

Conclusion: Cernea 2A and 2B; Kierner 2, 3, and 4; and Friedman 2 were defined as the high-risk subtypes of EBSLN. The risk prediction ability of the Friedman classification was found to be superior compared to other classifications.

KEYWORDS

Cernea classification, Kierner classification, Friedman classification, the external branch of the superior laryngeal nerve, intraoperative nerve monitoring

Introduction

Intraoperative neural monitoring (IONM) is applied to explore the effects of vocal cord (VC) movement, voice quality, and swallowing during thyroid surgery. Quality of voice, breathing, and swallowing represent the final asset of the vagal nerve (VN), recurrent laryngeal nerve (RLN), and external branch of the superior laryngeal nerve (EBSLN) system. The intact RLN function is the prerequisite of intact VC function. However, intraoperative assessment of VN and RLN function may not be identical to VC movement and quality of voice. For this reason, there is an increasing consideration of the potential role of EBSLN identification, monitoring, functional preservation, and evaluation (1, 2).

EBSLN damage mainly leads to cricothyroid muscle (CTM) paralysis, and its clinical symptoms and signs are mild, which can be easily misdiagnosed as laryngeal edema, vocal cord edema, and pharyngolaryngitis. In unilateral EBSLN damage, the vocal cord tension is weakened. When vocalizing, there may be a decrease in pitch, narrowing of the range, low voice, shortening of phonation time, inability to speak loudly, and other phonological changes. When bilateral EBSLN is damaged, the change in tone and sound quality is more obvious, and the symptoms of reduced pitch and monotonous tone can occur. EBSLN injury is more likely to be overlooked when combined with RLN damage (1–3). In fact, unlike RLN injuries, the symptoms of EBSLN injuries are mostly manifested during applications, such as singers and announcers. The first detection of symptoms of EBSLN injuries was seen in a soprano singer (1–3). Because these voice changes are peculiar and variable, the diagnosis of EBSLN dysfunction is difficult to confirm based solely on clinical or endoscopic findings (3, 4). The EBSLN is anatomically categorized on the basis of its association with surrounding adjacent organs, including the superior thyroid vasculature (STV), hypopharyngeal constrictor, CTM, and thyroid cartilage. According to EBSLN closeness, different classifications have been proposed (Table 1) (5–7). The Cernea, Kierner, and Friedman schemes have been widely applied in clinical and research practice with the intention of identifying a risk condition.

In this prospective clinical study, IONM was used to evaluate the value of the different EBSLN classifications for predicting EMG alterations and the risk of EBSLN injury.

Materials and methods

Patients

The protocol was approved by the Institutional Review Board of the China-Japan Union Hospital of Jilin University, Division of Thyroid Surgery, Changchun, China. Patients signed an informed consent form before surgery. The technical details of the protocol were explained to them because it is difficult to understand. Those with the presence of preoperative vocal cord fixation/weakening, history of neck surgery, preoperative presence of tumor invasion of nerves, refusal of a neuromonitoring catheter, and preoperative presence of altered tone were excluded from enrollment.

IONM standards

IONM was offered in the intermitted mode of application (1, 9, 10). Endotracheal tube-based surface electrodes were applied (Trivantage EMG tube, Medtronic, Jacksonville, Florida, USA) connected to both audio and visual IONM systems (NIM-Response 3.0, Medtronic, Jacksonville, Florida, USA).

TABLE 1 The classifications of EBSLN applied in the study.

Classification	Classification criteria			
Cernea (5) (Cadaver)	Type 1(60%):crossing STV more than 1 cm above the STP	Type 2A(17%):crossing STV less than 1 cm above the STP	Type 2B(20%):crossing STV below the STP	unidentified(3%)
Kierner (6) (Cadaver)	Type 1(42%):crossing STV more than 1 cm above the STP	Type 2(30%): crossing STV less than 1 cm above the STP	Type 3(14%):crossing STV below the STP	Type 4(14%);running dorsally to the STP
Friedman (7, 8) (Living and cadaver)	Type 1 (20%):running superficially to the ICM	Type 2(67%):partly running the superficial of ICM	Type 3(13%):running deep to the ICM	

STV, superior thyroid vessels; ICM, inferior constrictor muscle; STP, superior thyroid pole.

EBSLNs were stimulated using a single-use, incrementing prass stimulating probe, monopolar, standard flexible tip (product n.8225490, Medtronic, Jacksonville, Florida, USA), 100ms impulse duration, and 4Hz frequency. Since the maximum amplitude of the EBSLN is usually low, the EMG of the EBSLN is monitored by lowering the event threshold to 50μV. Peak-to-peak amplitudes of evoked EMG activities were read directly on the monitor screen and stored.

EMG amplitude profile may vary during intraoperative nerve monitoring because of variations in several variables unrelated to nerve status. For this reason, the following issues were continuously verified and standardized: (a) the type of induction or maintenance of anesthesia was the same for each patient; (b) endotracheal tube position was continuously verified with video laryngoscopy; (c) efforts to choose an EMG internal diameter (ID) tube with ideal contact with the VC; (d) no manipulation of the trachea and surrounding tissues during stimulation and monitoring; (e) efforts to maintain precise stimulation probe-nerve contact and invariable site of incitement; (f) dry surgical field and nerve ensheathed by fascia); and (g) no electrical cautery was used with bleeding vessels around the nerve.

IONM technique

In the current study, the EBSLN was identified and monitored using the following scheme of Chinese guidelines of intraoperative neural monitoring during thyroid and parathyroid surgery (2023 edition) (1, 9, 10):

Definitions

True positive EBSLN signal

CTM twitch and EMG response were references for EBSLN identification and STV dissection. This response serves as a true positive stimulation.

True negative

Stimulation of the upper pedicle that can be divided without cricothyroid twitch and EMG response. This response serves as a true negative stimulation. EBSLN was named differently according to different anatomical markers (Table 1). Under the guidance of IONM, dissection and functional identification were performed on potentially damaged nerves at risk (NAR). S1 was defined as the EBSLN stimulation at initial identification. S2 was the EBSLN stimulation after Superior thyroid artery (STA) ligation.

Loss of signal

LOS of the EBSLN was defined as an absence of CTM twitch combined with the previously obtained EMG signal and biphasic waveform.

EBSLN outcomes measured

Parameters recorded for each NAR were: EBSLN (S1, S2), RLN (R1, R2), and VN (V1, V2) amplitudes and latency determinations; pre- and post-operative stroboscopy evaluation (L1, L2) (at 24 hours before surgery and on the first postoperative day); Pre-, intra- and postoperative needle EMG of the CTM were not performed.

Vocal folds mucosal wave

In contrast to recurrent laryngeal nerve injury, when the EBSLN is injured, the overall movement of the vocal cords tends to remain unchanged. However, it should be noted that the vibrational characteristics of the vocal fold mucous membrane do undergo alterations, resulting in changes in timbre and vocal range. The unaffected cricothyroid muscle tension on the healthy side causes the anterior joint to shift towards the affected side, leading to an asymmetric mucosal wave. This change in wave propagation and mucosal wave pattern primarily manifests in the affected folds. In order to assess this phenomenon, we utilized the Japanese PENTAX VNL-1070STK 3.3mm electronic stroboscopic video laryngoscope system to evaluate specific vocal cord mucosal wave parameters. These parameters include maximum vibration frequency (F_{max}), minimum frequency (F_{min}), frequency range (F_{range}), and maximum frequency duration ($F_{duration}$). Acoustic evaluation of the vocal cords was conducted both pre-surgery (within 24 hours before the procedure) and post-surgery (on the first day following the operation).

Statistical analysis

All patient data were collected prospectively in a Microsoft Office EXCEL spreadsheet. All data are expressed as mean and standard deviation (Mean ± SD) unless otherwise stated. Statistical analysis was performed using SPSS, 20.0 for Windows (SPSS Inc, Chicago-Ill, USA). The chi-square test was used for dichotomous or hierarchical data. A t-test was used for normally distributed measures and $p < 0.05$ was the level of significance.

Results

Patients

From July 2022 to August 2022, 26 patients were excluded because of missing data (16), loss to follow-up (8), or a refusal to participate (2).

In total, 136 patients with thyroid benign/malignant nodules were included in this prospective cohort study. There were 31

(22.2%) men and 105 (77.8%) women, their ages ranged from 21 to 66 years, with a mean age of 43.4 years. In all, there were 25 cases in which unilateral thyroid lobectomy was performed, and 111 cases in which bilateral thyroidectomy was performed, covering 242 NAR. Of these tumors, 127 (93.4%) were papillary thyroid cancer (PTC), 1 (0.7%) was a follicular tumor, 1 was (0.7%) medullary, 1 (0.7%) was coexisting PTC and MTC, and 6 (4.4%) were nodular goiter. Five NARs were not identified and 242 EBSLNs were analyzed (Figure 1).

EBSLN monitoring

In total, 221 (91.3%) EBSLNs were identified by simultaneous twitch combined with EMG response and 21 (8.7%) EBSLNs were found by CTM twitch without clear EMG response. The mean initial amplitude (S1) of response for the EBSLNs was 224.5 ± 162.0 (62-932) μV.

The mean final amplitude (S2) was 193.4 ± 128.1 (53-754) μV. Two S2 determinations resulted in CTM twitch and EMG signal loss intraoperatively. Their S1 determinations were, respectively, 131 and 91 μV.

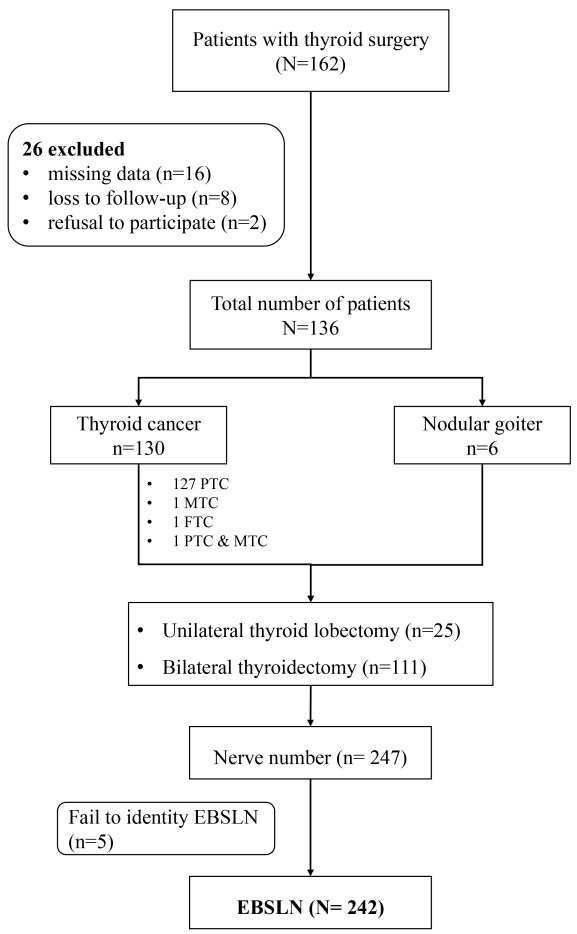

FIGURE 1
Flow chart of this study. EBSLN, the external branch of the superior laryngeal nerve.

Distribution of subtypes

The distribution of Cernea subtypes were 99(40.9%), 110 (45.5%), 26(10.7%), respectively for type 1, type 2A, and 2B; Friedman were 138(15.7%), 82(33.9%), and 122(50.4%) for type 1, type 2, and type 3; and Kierner were 99(40.9%), 110(45.5%), 26 (10.8%), and 7(2.9%) for type 1, type 2, type 3, and type 4 (Table 2).

Amplitudes profiles

The amplitude values changed significantly from S1 to S2 for Cernea 2A and 2B (193.7 vs. 226.6μV, P=0.019; 185.8 vs. 221.3μV, P=0.039); Kierner 2, 3, and 4 (193.7 vs. 226.6μV, P=0.019; 185.8 vs. 221.3μV, P=0.039; 126.8 vs. 226.0μV, P=0.015); and Friedman 2 (184.8 vs.221.6μV, P=0.030) (Table 3). S1 and S2 amplitudes were similar for Cernea 1 (P=0.070), Kierner 1 (P=0.070), and Friedman 2 and 3 (P=0.078, P=0.072). The number of EBSLN with a decrease of amplitude exceeding 25% is significantly higher in Cernea 2B than in Cernea 1 and Cernea 2A (53.8% vs. 19.2% vs. 19.1%, P<0.001). In the Friedman classification, the number of EBSLN with a decrease exceeding 25% in Friedman 2 is significantly higher than in other subtypes (34.1% vs. 18.4% vs. 11.5%, P=0.035). Kierner 4 is revealed as the subtype with the highest proportion of decrease (71.4% vs. 53.8% vs. 19.2% vs. 19.1%, P<0.001). Similar trends are observed in subgroups with an amplitude decrease exceeding 50% (Table 3).

Two S2 determinations resulted in CTM twitch and EMG signal loss intraoperatively, each of which belongs to high-risk subtypes of EBSLN (Cernea 2B and Friedman 2).

Stroboscopy

Two nerves were confirmed EBSLN injuries by stroboscopy. The vibration of bilateral vocal cords was asymmetrical, irregular, and non-periodic, and the injured side was slightly bent, the length was shortened, and the tension was reduced.

Vocal acoustic assessment

There were significant differences in F_{max} and F_{ange} for the Cernea 2A (P=0.001, P=0.001), Cernea 2B (P=0.001, P=0.038), Kierner 2 (P=0.001, P=0.001), Kierner 3 (P=0.001, P=0.038), Friedman 1 (P=0.015, P=0.030), and Friedman 2 (P=0.004, P=0.014) schemes (Table 4). There were no significant differences in F_{max}, F_{range}, and $F_{duration}$ for Kierner subtype 4.

Horizontal comparison

The predictive efficacy of three types of classification for EBSLN injury was compared. There was no significant difference in the predictive ability of the Cernea and Kierner classifications for the

TABLE 2 The distribution of EBSLN subtypes.

Cernea classification		Kierner classification		Friedman classification	
n (n/N %)		n (n/N %)		n (n/N %)	
Type 1	99 (40.9%)	*Type 1*	99 (40.9%)	*Type 1*	38 (15.7%)
Type 2A	110 (45.5%)	*Type 2*	110 (45.5%)	*Type 2*	82 (33.9%)
Type 2B	26 (10.7%)	*Type 3*	26 (10.7%)	*Type 3*	122 (50.4%)
Unidentified (running dorsally to the STP)	7 (2.9%)	*Type 4*	7 (2.9%)		

STP, superior thyroid pole.

risk of EBSLN injury, including accuracy (44.3% vs. 45.0%), sensitivity (11.0% vs. 14.0%), and specificity (89.9% vs. 89.9%) (Table 5). However, there was a significant difference in predicting the risk of EBSLN injury between the Friedman classification and the Cernea and/or Kierner classifications. The Friedman classification showed higher diagnostic accuracy (69.8% vs. 44.3% vs. 45.0%), sensitivity (19.5% vs. 11.0% vs. 14.0%), and specificity (95.6% vs. 89.9% vs. 89.9%). Moreover, the positive predictive value (69.6% vs. 60.0% vs. 66.7%) and negative predictive value (69.9% vs. 42.4% vs. 42.0%) of the Friedman classification were superior to other classifications (Table 5). However, the false negative rate of Friedman classification was significantly higher than other subtypes (19.5% vs. 11.0% vs. 14.0%).

Discussion

IONM with its EMG values obtained during surgery is similar to a new language that has to be learned: i.e., changes in amplitude, latency and waveforms, and postoperative assessments. Monitoring does not differ from other biological systems (1–3). Table 1 describes the distribution of the Cernea, Kierner, and Friedman subtypes. In the Cernea classification reported in a cadaver study in 1992, type 1 (60%) was the most common subtype. The prevalent subtype in the Kierner classification was type 1 (42%) reported in 1998 in cadavers, and type 2 (67%) was the most frequent in the Friedman classification (5–7). In our clinical study, Cernea 2A (45.5%), Kierner 2 (45.5%), and Friedman 3 (50.4%) were more prevalent than other subtypes. The reason for these differences may be related to race, type of dissection, surgeon technique, cadaver use, underlying thyroid pathology, and the use of IONM.

Historically, the high-risk categories of EBSLN have been classified through clinical experience. Surgeons with their clinical experience thought that the EBSLN crossing the STV < 1 cm above the upper edge of the thyroid superior pole (Cernea 2A and 2B), or the nerve running in the pharyngeal muscle surface (Friedman 1), were at higher risk than other nerves.

Subsequently, surgeons defined the high-risk subtypes according to subjective indicators, such as the VHI-10 score and

TABLE 3 Longitudinal comparison of the amplitude profiles.

Classification	S1 (μV) Mean ± SD	S2 (μV) Mean ± SD	S2 25% decrease (N, %)	S2 50% decrease (N, %)	No CTM and LOS (N, %)
Cernea					
Type 1	226.4±164.9	200.3±135.1^{NS}	19 (19.2%)	10 (10.1%)	0
Type 2A	226.6±165.6	193.7±123.5*	21 (19.1%)	12 (10.9%)	0
Type 2B	221.3±128.7	185.8±94.8*	14 (53.8%)**	3 (11.5%)^{NS}	2 (7.7%)
Kierner					
Type 1	226.4±164.9	200.3±135.1 ^{NS}	19 (19.2%)	10 (10.1%)	0
Type 2	226.6±165.6	193.7±123.5*	21 (19.1%)	12 (10.9%)	0
Type 3	221.3±128.7	185.8±94.8*	14 (53.8%)	3 (11.5%)	2 (7.7%)
Type 4	226.0±54.3	126.8±45.7*	5 (71.4%)**	5 (71.4%)*	0
Friedman					
Type 1	247.7±242.4	214.3±197.2 ^{NS}	7 (18.4%)	0(0%)	0
Type 2	221.6±145.2	184.8±128.1*	28 (34.1%)	16 (19.5%)	2 (2.4%)
Type 3	217.1±166.6	192.9±123.4 ^{NS}	14 (11.5%)*	7 (5.7%)*	0

Not indicated indicates no correlation.
^{NS} no significance.
*indicates significant correlation at level 0.05.
** Significant correlation at 0.01 level.

10.3389/fendo.2023.1301838

TABLE 4 Longitudinal comparison of the vocal acoustic assessment.

Classification	Pre-operative Mean ± SD			Post-operative Mean ± SD		
	F_{max} (HZ)	F_{range} (HZ)	$F_{duration}$ (s)	F_{max} (HZ)	F_{range} (HZ)	$F_{duration}$ (s)
Cernea						
Type 1	294.8 ± 39.0	119.6 ± 39.9	10.3 ± 6.4	275.8 ± 50.1*	119.8 ± 48.8	10.8 ± 5.5
Type 2A	294.4 ± 61.4	127.4 ± 47.8	9.2 ± 6.9	224.5 ± 42.1***	69.4 ± 26.5***	7.9 ± 4.4
Type 2B	325.2 ± 43.9	144 ± 39.1	6.3 ± 3.6	244.8 ± 22.1**	85.3 ± 30.8*	9.4 ± 2.2**
Kierner						
Type 1	294.8 ± 39.0	119.6 ± 39.9	10.3 ± 6.4	275.8 ± 50.1*	119.8 ± 48.8	10.8 ± 5.5
Type 2	294.4 ± 61.4	127.4 ± 47.8	9.2 ± 6.9	224.5 ± 42.1***	69.4 ± 26.5***	7.9 ± 4.4
Type 3	325.2 ± 43.9	144 ± 39.1	6.3 ± 3.6	244.8 ± 22.1**	85.3 ± 30.8*	9.4 ± 2.2**
Type 4	303 ± 60.8	93 ± 18.4	9.8 ± 5.6	248.5 ± 46.0	58 ± 9.9	11.1 ± 2.9
Friedman						
Type 1	320 ± 27.1	110.4 ± 45.8	10.0 ± 9.8	234.4 ± 55.5*	61.4 ± 33.1*	8.8 ± 6.9
Type 2	294.5 ± 63.3	125.6 ± 50.7	11.6 ± 6.5	242.3 ± 46.4**	88.1 ± 39.4*	10.3 ± 4.4
Type 3	300.3 ± 41.1	128.6 ± 30.8	6.8 ± 4.9	266.8 ± 48.2**	100.9 ± 42.8	8.0 ± 3.9

Not indicated indicates no correlation.
*indicates significant correlation at level 0.05.
** Significant correlation at 0.01 level.
*** Significant correlation at 0.001 level.
F_{max}, the maximum frequency; F_{range}, range of frequency; $F_{duration}$, maximum frequency duration.

TABLE 5 Prediction effectiveness of EBSLN risk.

	EBSLN Classification		
	Cernea	Kierner	Friedman
Accuracy (%)	44.3%	45.0%	69.8%*
Sensitivity (%)	11.0%	14.0%	19.5%*
Specificity (%)	89.9%	89.9%	95.6%*
FPR (%)	10.1%	10.1%	4.4%*
FNR (%)	11.0%	14.0%	19.5%*
PPV (%)	60.0%	66.7%	69.6%*
NPV (%)	42.4%	42.0%	69.9%*

FPR, false positive rate; FNR, false negative rate; PPV, positive predictive value; NPV, negative predictive value.

VII-5 score (11, 12). As we investigated in a previous article, the value of Cernea subtypes was assumed by EMG parameters for risk stratification (13). In the current study, we evaluated the risk of each EBSLN pattern by means of two objective indicators, both EMG parameters and vocal acoustic assessment.

By correlating the S1 amplitude with the S2 amplitude of different subtypes, amplitudes changed significantly from S1 to S2, respectively, in Cernea type 2A and 2B; Kierner type 2, type 3, and type 4; and Friedman type 2 (Table 3), which indicated that the above subtypes have a greater risk of EBSLN injury and were defined as the high-risk subtypes of EBSLNs. By examining the pre- and postoperative outcomes of vocal acoustic assessment, including F_{max}, F_{range}, and $F_{duration}$, we observed different degrees of changes in particular high-risk subtypes (Table 4).

In clinical practice, when the EBSLN crosses the STV less than 1 cm above the upper edge of the thyroid superior pole (Cernea 2A and 2B), the nerve is at higher risk of injury than other subtypes of Cernea classification. When the nerve runs into the pharyngeal muscle surface (Friedman 1), it is not an indicator of a high-risk condition. However, Friedman subtype 2 is more likely to have a higher risk of EBSLN injury (Table 3). Compared to other subtypes, Kierner 4 is a rare type with a high risk of injury.

Moreover, this is the first research that has analyzed which EBSLN classification is the most useful for predicting high-risk conditions. We found the risk prediction of the Friedman scheme was greater than Cernea and Kierner. Surgeons should pay more attention to the relationship between the EBSLN and STV. The STV should not be blindly ligated before confirming the relationship with the nerve.

Furthermore, the assessment of EBSLN by CTM twitch was higher than the EMG response. In our study, the identification by CTM twitch was 100%, but the EMG response was 91.2%. Related research pointed out that the identification by CTM twitch was 100%, and the EMG response was 74-100% (1, 14–19). The variability may be due to a) the presence of the human communicating nerve (20, 21), b) EMG tube position, c) the limited area of muscle activity induced, and d) intrinsic EBSLN low amplitude and short latency profiles. Therefore, we recommend that the EBSLN is identified by CTM twitch response. EMG is only for reference and not the standard for identifying EBSLN.

During the study, we faced two LOS of EBSLN, in S2 determination. The EBSLN guidelines (1) were published in 2013, but the LOS of EBSLN has not been defined, due to the EBSLN amplitude being lower and individual variation being larger than RLN. In our study, the difference among the Cernea subtypes was found to be significant by comparing the amplitude of EBSLNs and vocal acoustic assessment (Table 3).

This might result in the definition of EBSLN LOS. Unlike RLN, the amplitude of EBSLN is lower and with larger individual variation. In this study, the EBSLN amplitude was 225 ± 162μV, Dionigi et al. (13) concluded from 400 EBSLNs that the mean amplitude was 259 ± 67 (180-421), 321 ± 79 (192-391), 371 ± 38 (200-551)μV, respectively, for type 1, 2A, 2B of Cernea classification. Barczynski et al. (14) found the mean EBSLN amplitude was equal to 249 ± 144μV. Randolph et al. (22) concluded from 73 EBSLN studies that the EBSLN amplitude was 269 ± 176μV. Thus, the cut-off value of EBSLN may be lower than that of RLN (50%).

Finally, EBSLN damage rates are different with distinct diagnostic criteria, from 0.45% to 58% (23–29) (Table 6). In this study, high-risk subtypes showed significant differences in the maximum frequency, range of frequency, and maximum frequency duration, which may indicate the existence of dysfunction. However, the postoperative symptoms of EBSLN injury are similar to symptoms of laryngeal and vocal cord edema caused by intubation technology and too long surgery time. It may be useful to evaluate the EBSLN injury rate through both intraoperative EMG parameters combined with vocal acoustic assessment and stroboscopy (30).

A limitation of this study is the absence of incorporating CTM electromyography as a reference for evaluating the incidence of EBSLN injury. Additionally, there was a lack of assessment of other potential risk factors for recurrent laryngeal nerve injury, such as thyroid volume, neck length, and distance of the tumor from the upper pole of the thyroid. These variables could potentially influence the risk of nerve injury and should be considered in future research. Acknowledging these limitations, we aim to address these factors in future studies.

TABLE 6 EBSLN injury rates and diagnostic criteria.

Author	The rate of EBSLN injury (%)	Diagnostic criteria
EI-Guindy (24)	2.4%	Vocal acoustic assessment
Hunt (25)	0.45%	Laryngoscope
Dener (26)	0.9%	Not reported
Kark (27)	18%	Voice handicap index
Lennquist (28)	2.0%	Laryngoscope
Jansson (23)	58%	EMG
Aluffi (29)	14%	EMG

Data availability statement

The raw data supporting the conclusions of this article will be made available by the authors, without undue reservation.

Ethics statement

The studies involving humans were approved by the Institutional Review Board of the China-Japan Union Hospital of Jilin University. The studies were conducted in accordance with the local legislation and institutional requirements. Written informed consent for participation was not required from the participants or the participants' legal guardians/next of kin in accordance with the national legislation and institutional requirements. Patients signed an informed consent before surgery.

Author contributions

CL: Writing – original draft. JZ: Writing – review & editing. GD: Writing – review & editing. HS: Funding acquisition, Supervision, Writing – review & editing.

Funding

The author(s) declare financial support was received for the research, authorship, and/or publication of this article. This study was sponsored by the Project of Jilin Provincial Finance Department [2022SCZ38].

Conflict of interest

The authors declare that the research was conducted in the absence of any commercial or financial relationships that could be construed as a potential conflict of interest.

Publisher's note

References

1. Barczyński M, Randolph GW, Cernea CR, Dralle H, Dionigi G, Alesina PF, et al. External branch of the superior laryngeal nerve monitoring during thyroid and parathyroid surgery: International neural monitoring study group standards guideline statement. *Laryngoscope* (2013) 123(Suppl 4):S1–S14. doi: 10.1002/lary.24301

2. Randolph GW, Dralle H, International Intraoperative Monitoring Study Group, Abdullah H, Barczynski M, Bellantone R, et al. Electrophysiologic recurrent laryngeal nerve monitoring during thyroid and parathyroid surgery: international standards guideline statement. *Laryngoscope* (2011) 121(Suppl 1):S1–S16. doi: 10.1002/lary.21119

3. Sulica L. The superior laryngeal nerve: function and dysfunction. *Otolaryngologic Clin North Am* (2004) 37(1):183–201. doi: 10.1016/S0030-6665(03)00175-0

4. Teitelbaum BJ, Wenig BL. Superior laryngeal nerve injury from thyroid surgery. *Head Neck* (1995) 17(1):36–40. doi: 10.1002/hed.2880170108

5. Cernea CR, Ferraz AR, Furlani J, Monteiro S, Nishio S, Hojaij FC, et al. Identification of the external branch of the superior laryngeal nerve during thyroidectomy. *Am J Surg* (1992) 164(6):634–9. doi: 10.1016/s0002-9610(05)80723-8

6. Kierner AC, Aigner M, Burian M. The external branch of the superior laryngeal nerve: its topographical anatomy as related to surgery of the neck. *Arch Otolaryngol–Head Neck Surg* (1998) 124(3):301–3. doi: 10.1001/archotol.124.3.301

7. Friedman M, LoSavio P, Ibrahim H. Superior laryngeal nerve identification and preservation in thyroidectomy. *Arch Otolaryngol–Head Neck Surg* (2002) 128(3):296–303. doi: 10.1001/archotol.128.3.296

8. Ozlugedik S, Acar HI, Apaydin N, Tekdemir I, Elhan A, Comert A. Surgical anatomy of the external branch of the superior laryngeal nerve. *Clin Anat (New York NY)* (2007) 20(4):387–91. doi: 10.1002/ca.20399

9. Sywak M, Cornford L, Roach P, Stalberg P, Sidhu S, Delbridge L. Routine ipsilateral level VI lymphadenectomy reduces postoperative thyroglobulin levels in papillary thyroid cancer. *Surgery* (2006) 140(6):1000–7. doi: 10.1016/j.surg.2006.08.001

10. Sun H, Tian W. Chinese guidelines of intraoperative neural monitoring during thyroid and parathyroid surgery (2023 edition). *Chin J Of Pract Surg* (2023) 43(1):11. doi: 10.19538/j.cjps.issn1005-2208.2023.01.04

11. Rosen CA, Lee AS, Osborne J, Zullo T, Murry T. Development and validation of the voice handicap index-10. *Laryngoscope* (2004) 114(9):1549–56. doi: 10.1097/00005537-200409000-00009

12. Masuoka H, Miyauchi A, Higashiyama T, Yabuta T, Fukushima M, Ito Y, et al. Prospective randomized study on injury of the external branch of the superior laryngeal nerve during thyroidectomy comparing intraoperative nerve monitoring and a conventional technique. *Head Neck* (2015) 37(10):1456–60. doi: 10.1002/hed.23778

13. Dionigi G, Kim HY, Randolph GW, Wu CW, Sun H, Liu X, et al. Prospective validation study of cernea classification for predicting EMG alterations of the external branch of the superior laryngeal nerve. *Surg Today* (2016) 46(7):785–91. doi: 10.1007/s00595-015-1245-9

14. Barczyński M, Konturek A, Stopa M, Honowska A, Nowak W. Randomized controlled trial of visualization versus neuromonitoring of the external branch of the superior laryngeal nerve during thyroidectomy. *World J Surg* (2012) 36(6):1340–7. doi: 10.1007/s00268-012-1547-7

15. Selvan B, Babu S, Paul MJ, Abraham D, Samuel P, Nair A. Mapping the compound muscle action potentials of cricothyroid muscle using electromyography in thyroid operations: a novel method to clinically type the external branch of the superior laryngeal nerve. *Ann Surg* (2009) 250(2):293–300. doi: 10.1097/SLA.0b013e3181b17342

16. Dionigi G, Boni L, Rovera F, Bacuzzi A, Dionigi R. Neuromonitoring and video-assisted thyroidectomy: a prospective, randomized case-control evaluation. *Surg Endoscopy* (2009) 23(5):996–1003. doi: 10.1007/s00464-008-0098-3

17. Inabnet WB, Murry T, Dhiman S, Aviv J, Lifante JC. Neuromonitoring of the external branch of the superior laryngeal nerve during minimally invasive thyroid surgery under local anesthesia: a prospective study of 10 patients. *Laryngoscope* (2009) 119(3):597–601. doi: 10.1002/lary.20071

18. Lifante JC, McGill J, Murry T, Aviv JE, Inabnet WB 3rd. A prospective, randomized trial of nerve monitoring of the external branch of the superior laryngeal nerve during thyroidectomy under local/regional anesthesia and IV sedation. *Surgery* (2009) 146(6):1167–73. doi: 10.1016/j.surg.2009.09.023

19. Aina EN, Hisham AN. External laryngeal nerve in thyroid surgery: recognition and surgical implications. *ANZ J Surg* (2001) 71(4):212–4. doi: 10.1046/j.1440-1622.2001.02078.x

20. Kochilas X, Bibas A, Xenellis J, Anagnostopoulou S. Surgical anatomy of the external branch of the superior laryngeal nerve and its clinical significance in head and neck surgery. *Clin Anat (New York NY)* (2008) 21(2):99–105. doi: 10.1002/ca.20604

21. Morton RP, Whitfield P, Al-Ali S. Anatomical and surgical considerations of the external branch of the superior laryngeal nerve: a systematic review. *Clin Otolaryngol Off J ENT-UK; Off J Netherlands Soc Oto-Rhino-Laryngol Cervico-Facial Surg* (2006) 31(5):368–74. doi: 10.1111/j.1749-4486.2006.01266.x

22. Potenza AS, Phelan EA, Cernea CR, Slough CM, Kamani DV, Darr A, et al. Normative intra-operative electrophysiologic waveform analysis of superior laryngeal nerve external branch and recurrent laryngeal nerve in patients undergoing thyroid surgery. *World J Surg* (2013) 37(10):2336–42. doi: 10.1007/s00268-013-2148-9

23. Jansson S, Tisell LE, Hagne I, Sanner E, Stenborg R, Svensson P. Partial superior laryngeal nerve (SLN) lesions before and after thyroid surgery. *World J Surg* (1988) 12(4):522–7. doi: 10.1007/BF01655439

24. el-Guindy A, Abdel-Aziz M. Superior laryngeal nerve preservation in peri-apical surgery by mobilization of the viscerovertebral angle. *J Laryngol Otol* (2000) 114(4):268–73. doi: 10.1258/0022215001905535

25. Hunt CJ. The superior and inferior laryngeal nerve as related to thvroid surgery. *Am Surgeon* (1961) 27:548–52.

26. Dener C. Complication rates after operations for benign thyroid disease. *Acta Oto-Laryngologica* (2002) 122(6):679–83. doi: 10.1080/000164802320396394

27. Kark AE, Kissin MW, Auerbach R, Meikle M. Voice changes after thyroidectomy: role of the external laryngeal nerve. *Br Med J (Clinical Res Ed)* (1984) 289(6456):1412–5. doi: 10.1136/bmj.289.6456.1412

28. Lennquist S, Cahlin C, Smeds S. The superior laryngeal nerve in thyroid surgery. *Surgery* (1987) 102(6):999–1008.

29. Aluffi P, Policarpo M, Cherovac C, Olina M, Dosdegani R, Pia F. Post-thyroidectomy superior laryngeal nerve injury. *Eur Arch Oto-Rhino-Laryngology Off J Eur Fed Oto-Rhino-Laryngological Societies (EUFOS) Affiliated German Soc Oto-Rhino-Laryngol-Head Neck Surg* (2001) 258(9):451–4. doi: 10.1007/s004050100382

30. Dackiw AP, Rotstein LE, Clark OH. Computer-assisted evoked electromyography with stimulating surgical instruments for recurrent/external laryngeal nerve identification and preservation in thyroid and parathyroid operation. *Surgery* (2002) 132(6):1100–8. doi: 10.1067/msy.2002.128483

frontiers | Frontiers in Endocrinology

TYPE Original Research
PUBLISHED 28 November 2023
DOI 10.3389/fendo.2023.1242061

OPEN ACCESS

EDITED BY
Tzu-Yen Huang,
Kaohsiung Medical University, Taiwan

REVIEWED BY
Yutian Zou,
Sun Yat-sen University Cancer Center (SYSUCC), China
Mehmet Haciyanli,
Izmir Katip Celebi University, Türkiye
Cheng-Hsun Chuang,
Kaohsiung Medical University Hospital, Taiwan

*CORRESPONDENCE
Wei Xing
suzhxingwei@suda.edu.cn
Feng Qian
13861222790@163.com

†These authors have contributed equally to this work

RECEIVED 18 June 2023
ACCEPTED 17 October 2023
PUBLISHED 28 November 2023

CITATION
Liu S-Q, Feng J-W, Yan Z-T, Xing X-X, Jiang W-Y, Jiang Y, Qian F and Xing W (2023) Constructing a nomogram based on the distribution of thyroid nodules and suspicious lateral cervical lymph nodes in fine-needle aspiration biopsies to predict metastasis in papillary thyroid carcinoma. *Front. Endocrinol.* 14:1242061. doi: 10.3389/fendo.2023.1242061

Constructing a nomogram based on the distribution of thyroid nodules and suspicious lateral cervical lymph nodes in fine-needle aspiration biopsies to predict metastasis in papillary thyroid carcinoma

Shui-Qing Liu[1†], Jia-Wei Feng[2†], Zhan-Tao Yan[3], Xiao-Xiao Xing[1], Wen-Yin Jiang[4], Yong Jiang[2], Feng Qian[1*] and Wei Xing[5*]

[1]Department of Ultrasound, The Third Affiliated Hospital of Soochow University, Changzhou First People's Hospital, Changzhou, Jiangsu, China, [2]Department of Thyroid Surgery, The Third Affiliated Hospital of Soochow University, Changzhou First People's Hospital, Changzhou, China, [3]Department of Pathology, The Third Affiliated Hospital of Soochow University, Changzhou First People's Hospital, Changzhou, Jiangsu, China, [4]Department of Breast Surgery, The Third Affiliated Hospital of Soochow University, Changzhou First People's Hospital, Changzhou, Jiangsu, China, [5]Department of Medical Imaging, The Third Affiliated Hospital of Suzhou University, Changzhou First People's Hospital, Changzhou, Jiangsu, China

Purpose: Elevated concentrations of thyroglobulin eluent is a risk factor for lateral cervical lymph node metastasis (LLNM) in patients with papillary thyroid cancer (PTC). We aimed to develop a practical nomogram based on the distribution of thyroid nodules and the presence of suspicious lateral cervical lymph nodes in fine-needle aspiration biopsies (LN-FNABs), including the cytopathology and the suspicious lateral cervical lymph node (LLN) thyroglobulin eluent (Tg), to predict the possibility of LLNM preoperatively in patients with PTC.

Methods: The clinical data of PTC patients who were admitted to the Third Affiliated Hospital of Soochow University from January 2022 to May 2023 to undergo fine-needle aspiration biopsy (FNAB) were included in this study. A total of 208 patients in 2022 served as the training set (70%), and 89 patients in 2023 served as the validation set (30%). The clinical characteristics and LN-FNAB results were collected to determine the risk factors of LLNM. A preoperative nomogram was developed for predicting LLNM based on the results of the univariate and multivariate analyses. Internal calibration, external calibration, and decision curve analysis (DCA) were performed for these models.

Results: The multivariate logistic regression analysis showed that the maximum thyroid nodule diameter (Odds Ratio (OR) 2.323, 95% CI 1.383 to 3.904; p = 0.001), Tg level (OR 1.007, 95% CI 1.005 to 1.009; p = 0.000), Tg divided by serum thyroglobulin, (Tg/sTg) [odds ratio (OR) 1.005, 95% CI 1.001 to 1.008; p = 0.009],

and cytopathology (OR 9.738, 95% CI 3.678 to 25.783; p = 0.000) (all $p <$ 0.05) had a significant impact on the LLNM of patients with suspicious LLNs. The nomogram showed a better predictive value in both the training cohort [area under the curve, (AUC) 0.937, 95% CI 0.895 to 0.966] and the validation cohort (AUC 0.957, 95% CI 0.892 to 0.989). The nomogram also showed excellent internal and external calibration in predicting LLNM. According to the DCA, the diagnostic performance of this model was dependent on the following variables: maximum thyroid nodule diameter, Tg level, Tg/sTg, and cytopathology.

Conclusion: Based on the aforementioned risk factors, we believe that it is necessary to establish a personalized LLNM model for patients with PTC. Using this practical nomogram, which combines clinical and Tg risk factors, surgeons could accurately predict the possibility of LLNM preoperatively. The nomogram will also help surgeons to establish personalized treatment plans before surgery.

KEYWORDS

thyroglobulin in fine-needle aspiration, lateral lymph node metastasis, lateral neck dissection, nomogram, papillary thyroid carcinoma

Introduction

Papillary thyroid carcinoma (PTC) is endocrinology's most common malignant tumor (1). Although PTC has an indolent nature and a good prognosis, it is also associated with an incidence of 10% to 30% in lateral lymph node metastasis (LLNM) (2, 3). Lateral cervical lymph node dissection (LND) is the main method for treating LLNM. Compared with central neck dissection, LND has some severe complications, such as nerve injury, hyperparathyroidism, chyle leakage, and neck and shoulder pain (4). Therefore, the evaluation of preoperative LLNM needs to be carried out with great caution. The cytopathology of suspicious lateral cervical lymph nodes (LLNs) in fine-needle aspiration biopsies (FNABs) can be used to clarify the status of lymph nodes (5), but the false-negative rate of cytopathology is up to 20% (6). Therefore, some scholars (7) recommend combining cytopathology with thyroglobulin to reduce this false-negative rate.

Not only the malignancy of thyroid nodules but also the distribution of thyroid nodules were related to the occurrence of LLNM in PTC. Some studies suggest that nodules located at the upper pole of the thyroid gland are more prone to LLNM (8).

In order to improve the true-positive rate and enable surgeons to have more confidence in formulating surgical plans, we developed a nomogram based on the distribution of thyroid nodules and the LN-FNAB.

Materials and methods

Patients

A retrospective study was conducted at the Third Affiliated Hospital of Soochow University between January 2022 and May 2023. The Institutional Review Board of Changzhou First People's Hospital approved this study. Our study collected data from 387 patients admitted to our hospital's thyroid surgery department, who were confirmed to have PTC through pathology and who underwent LND. All patients with suspicious lymph nodes were randomly split into the training dataset and the validation dataset (2: 1). Subsequently, based on the pathology of LND, those in the training dataset (208 patients) were divided into the LLNM group and the non-LLNM group. These patients underwent preoperative ultrasound (US) examination of the thyroid and suspicious lateral cervical lymph nodes, as well as fine-needle aspiration biopsy (LN-FNAB) for suspected lymph nodes. This retrospective study was approved by the Institutional Review Board of Changzhou First People's Hospital, and the informed consent was waived.

All study patients had undergone clinical examination, preoperative ultrasound, and the measurement of thyroglobulin in FNAB. The inclusion criteria were as follows: (1) patients with pathology-confirmed PTC who had underwent LND; (2) suspicious LLNs with preoperative LN-FNAB, including cytopathology and thyroglobulin; (3) complete clinical data; and (4) patients with a postoperative follow-up period of at least 6 months. The exclusion criteria were as follows: (1) patients who did not undergo LND; (2) LLNs without preoperative LN-FNABs; (3) subtypes other than classic PTC; (4) incomplete clinical data; (5) missing follow-up data; and (6) patients who had received treatment for head and neck cancer previously, or with a history of neck radiation history or a family history of thyroid carcinoma (TC). Finally, 208 patients with suspected LLNs with LND in 2022 were enrolled in this study as the training group, and 89 consecutive suspicious LLNs in 2023 were enrolled in this study as the validation group. In the training group, according to the pathological results of the LND, patients were divided into the LLNM group (n = 79) and the non-LLNM group

(n = 129). Figure 1 shows the flow chart of the patients enrolled in our study.

Preoperative examination of thyroid nodules

The clinical and ultrasound parameters included the patients' sex and age, the aspect ratio of the thyroid nodule (A/T), chronic lymphocytic thyroiditis (CLT), thyroid nodule site (upper pole, middle-upper third of the thyroid gland, middle pole, middle-lower third of the thyroid gland, and lower pole). If there were multiple nodules in the thyroid gland, we selected the largest or most typical nodule.

Preoperative examination of suspicious lateral cervical lymph node thyroglobulin eluent in fine-needle aspiration biopsies

The clinical parameters included the cytopathology of the suspicious LLNs in FNABs, Tg level, and Tg/sTg. The suspicious LLNs may have one of the following ultrasound (US) characteristics, such as an A/T > 1, a globular hyperechoic mass, loss of the fatty hilum, microcalcification, and necrosis. The positive aspect of a suspicious LLN cytopathology was inherent to the detection of thyroid cells among the lymphocytes. The negative aspect of the suspicious LLN cytopathology was inherent to the fact that no thyroid cells appeared among the lymphocytes and that no suspicious LLNs were found even after 6 months of follow-up. The normal level of serum Tg ranged from 3.5 ng/mL to 77 ng/mL. Before our study, considering that the cutoff values of Tg had not been standardized, the surgeon performed LND on the basis of standard serum Tg levels. The experienced radiologists performed all the preoperative US and FNABs under ultrasound guidance. The decision of whether or not to perform LND depends on the LN-FNAB results, Tg range, doctor's experience, and individual patient conditions. (1) When the cytopathology revealed definite malignant cells in the suspicious LLNs and the Tg level exceeded 77 ng/mL, the surgeon performed LND; (2) when indefinite malignant cells were found in the cytopathology or the Tg level ranged from 3.5 ng/mL to 77 ng/mL, LND was carefully considered; (3) if both the cytopathology or the Tg less than 3.5ng/mL, surgeons would carry out preventive lateral neck LND based on their own experience and individual circumstances; and (4) if both the cytopathology and the Tg were negative, and there were no surgical indications based on the experience of the physician and the individual condition of the patient, then LND was avoided, but it was suggested that patients were followed up at least every 3 months. Considering the fact that some patients have a high level of serum Tg, which could have been an indication of nodular goiter or subacute thyroiditis, some studies (9) suggested incorporating Tg/sTg into the study.

Surgery and pathology

As suspicious lateral cervical lymph nodes were discovered in patients with thyroid nodules, a detailed preoperative examination including FNAB and clinical characteristics were carried out. We determined the status of suspicious LLNs based on the results of cytopathology and the level of Tg before

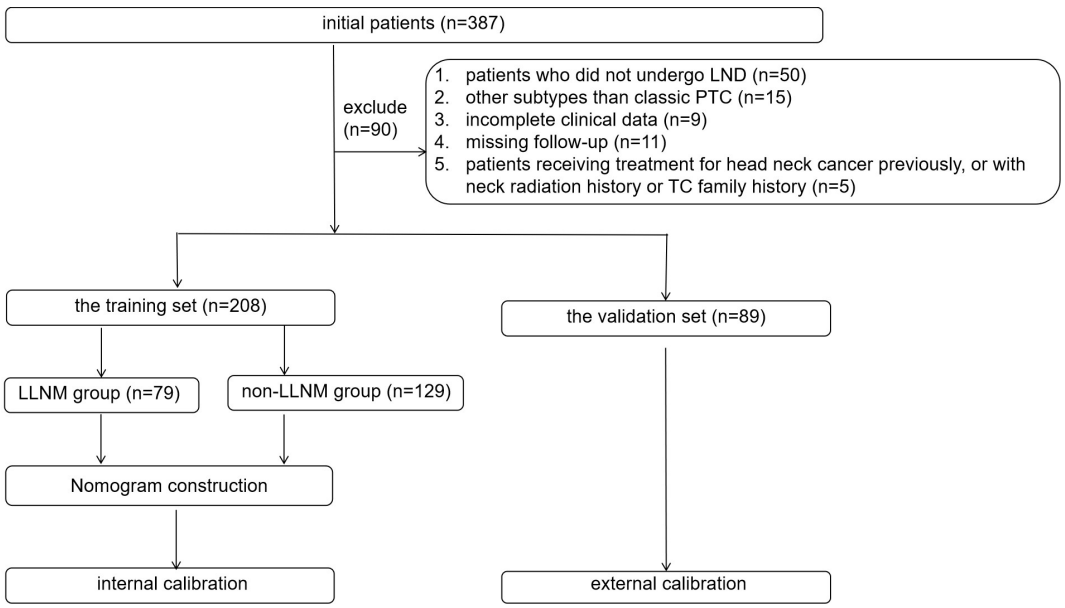

FIGURE 1
shows the flow chart of the patients enrolled in our study.

surgery. The LND was performed for patients with a positive FNAB. The resected thyroid and LLN specimens were processed for pathological examination (including evaluating for the existence of chronic lymphocytic thyroiditis, maximum size of the thyroid nodule, and the neck level of the metastatic nodes). The pathological results pertaining to the thyroid nodules and LLNs were used as the gold standard.

Pathological examination

Two or more experienced pathologists, who were blinded to the clinical characteristics and ultrasonographic findings, reviewed all the surgical specimens. The gold standard of this study was the pathological diagnosis. Every patient who needed to undergo LND was marked on the skin under preoperative ultrasound guidance and injected with tissue glue around the suspected lymph nodes. During the surgery, the surgeon would first remove the marked lymph nodes and send them to the pathology department separately. Subsequently, the lymph nodes around the suspected lymph nodes that are visible or palpable to the naked eye were also removed. Each cervical lymph node was fixed in 20% buffered formalin, embedded in paraffin, sectioned, and stained with hematoxylin and eosin. The pathologists investigated the lymph nodes with suspected cancer through immunohistochemical staining. All the pathological specimens were reviewed and cross-checked by two or more experienced pathologists microscopically.

Statistical analyses

The statistical analysis was performed using IBM SPSS Statistics version 26.0 software (IBM Corporation, Armonk, NY, USA), MedCalc (version 15.6; MedCalc software, Mariakerke, Belgium), and R software version 3.5.3 (The R Foundation for Statistical Computing, Vienna, Austria). Normally distributed variables were expressed as means ± standard deviations (SDs), and skew-distributed variables were reported as numbers and percentages. An independent *t*-test, a Pearson's chi-squared test, or a Fisher's exact test was used for the univariable analysis. The variables with statistical differences ($p < 0.05$) in the univariate analysis were included in the multivariate binary logistic regression analysis to determine the independent risk factors affecting lateral cervical lymph node metastasis. These independent predictors were used to construct the nomogram in R software for predicting the risk of LLNM. We used the receiver operating characteristic (ROC) curve in MedCalc to test our established prediction model's discriminative power and consensus. The performance of the nomogram was further evaluated using the calibration chart, which plotted the predicted probability of the nomogram against the observed probability. In the nomogram, each variable was estimated into scores, and the scores of each variable were then added for each patient to determine the probability of LLNM based on their total score. The internal calibration curve, external calibration curve, decision curve analysis (DCA), and ROC were used to evaluate the discrimination and calibration ability of the training set and the validation set. The statistical significance was set at a *p*-value < 0.05.

Results

Patient characteristics

Table 1 shows the comparison of the clinical baseline data of the training set and the validation set. A total of 208 patients in 2022 entered the training set (70%), and 89 patients from January to May 2023 entered the validation set (30%). There were no significant differences between the training set and the validation set ($p > 0.05$ for all comparisons).

In our study, 387 patients with 387 suspicious LLNs underwent LLN FNAB between January 2022 and December 2022. Finally, 208 patients who underwent LND were enrolled in this study. The postoperative pathology revealed the presence of LLNM in 79 patients with suspicious LLNs (Figure 1).

Distribution of suspicious lateral cervical lymph nodes in the lateral neck

As summarized in Table 2, of the 208 PTC patients with 208 suspicious LLNs, 67 men (32.2%) and 141 women (67.7%) underwent LND in our study, with an average age of 43.3 years ± 11.9 years (range from 18 years to 78 years), a maximum thyroid nodule diameter of 1.25 cm ± 0.9 cm (range from 0.22 cm to 6.0 cm), and an A/T of 0.8 ± 0.1 (range from 0.37 to 1.2). The suspicious LLNs in the right neck were detected in 104 (50%) patients, and tumors in the left neck were detected in 104 (50%) patients (Table 1).

Risk factors for lateral cervical lymph node metastasis in papillary thyroid carcinoma patients

LLNM had a significant association with the maximum thyroid nodule diameter, tumor site, neck level of the metastatic nodes, cytopathology, Tg level, and Tg/sTg in the univariate analysis (all $p < 0.05$). A binary logistic regression equation of lateral cervical lymph node metastasis was constructed based on the variables used in the univariate analysis. The multivariate analysis showed that the maximum thyroid nodules diameter [odds ratio (OR) 2.323, 95% CI 1.383 to 3.904; $p = 0.001$], Tg level (OR 1.007, 95% CI 1.005 to 1.009; $p = 0.000$), Tg/sTg (OR 1.005, 95% CI 1.001 to 1.008; $p = 0.009$), and cytopathology (OR 9.738, 95% CI 3.678 to 25.783; $p = 0.000$) remained independent predictors for LLNM in PTC patients with suspicious LLNs (Tables 2–4).

10.3389/fendo.2023.1242061

TABLE 1 Clinical characteristics of the training set and the validation set.

Characteristics	Training set (n=208)		Validation set (n = 89)	*P* value
	LLNM- (n=129)	LLNM+ (n=79)		
Gender				
female	84	57	60	
male	45	22	29	0.950
Age(y)				
>36	92	41	55	
<=36	37	38	34	0.948
CLT				
absence	108	62	71	
presence	21	17	18	0.694
A/T				
<=0.71	22	23	19	
>0.71	107	56	70	0.676
Maximum tumer size (cm)				
<1.1	96	25	46	
>1.1	33	54	43	0.506
Location of thyroid nodules 1				
left lobe	69	30	50	
right lobe	56	47	35	
bilateral	4	1	1	
isthmus	0	1	3	0.244
Location of thyroid nodules 2				
upper pole	31	28	21	
middle upper one-third of the thyroid gland	18	21	15	
middle pole	43	21	32	
middle lower one-third of the thyroid gland	20	4	11	
lower pole	17	5	10	0.373
Location of thyroid nodules 3				
ventral side	28	7	14	
dorsal side	19	10	17	
inside	5	3	2	
outside	9	6	5	
penetrating	51	40	39	
central	17	13	12	0.813
Location of lymph nodes				
left	72	32	50	
right	57	47	39	0.330

(Continued)

10.3389/fendo.2023.1242061

TABLE 1 Continued

Characteristics	Training set (n=208)		Validation set (n = 89)	*P* value
	LLNM- (n=129)	LLNM+ (n=79)		
Level of lymph nodes				
2	12	0	7	
3	56	32	34	
4	58	38	41	
5	0	2	1	0.771
Cytopathology				
Negative	116	21	56	
Positive	13	58	33	0.627
Tg				
<61.6	107	10	52	
>61.6	22	69	37	0.605
Tg/s-tg				
<2.91	104	7	51	
>2.91	25	72	38	0.543

LLNM, lateral cervical lymph node metastasis; CLT, chronic lymphocytic thyroiditis; A/T, aspect ratio (height divided by width on transverse views); Tg, thyroglobulin in fine-needle aspiration, 61.6 is the cutoff value obtained from this study; Tg/s-tg, Tg divided by serum thyroglobulin, 2.91 is the cutoff value obtained from this study.
If there are multiple nodules in the thyroid gland, we selected the largest or most typical nodule.
The positive of cytopathology refers to the detection of thyroid cells in the background of lymphocytes. The negative of cytopathology means no thyroid cells appeared in the background of lymphocytes and no suspicious LLNs were founded after at least six months of follow-up.
P value < 0.05 indicates a significant difference between the training set and the validation set.

Validation of the nomogram

The risk factors, including maximum thyroid nodule diameter, Tg level, Tg/sTg, and cytopathology, identified through multivariate analysis were included in the nomogram for predicting LLNM. The nomogram showed that the maximum thyroid nodule diameter and cytopathology had the greatest effects on the score (Figure 2). Thereafter, this prediction model was used to develop the ROC analysis. The area under the curve (AUC) of the training model was 0.937 (95% CI 0.895 to 0.966), the sensitivity was 0.88, and the specificity was 0.89 (Figure 3). The AUC of the validation model was 0.957 (95% CI 0.892 to 0.989), the sensitivity was 0.96, and the specificity was 0.92 (Figure 3B). In addition, we developed the internal and external validation of the LLNM model. In the nomogram, the solid line represents the true LLNM, whereas the dotted line represents the virtual incidence rate based on the prediction model. The higher the matching degree between the dashed and solid lines, the higher the accuracy of the prediction model. Our prediction model showed that the risk of LLNM was consistent with the actual results. Furthermore, we conducted the external calibration for the established model. The AUC of the training cohort and validation cohort were in good agreement (Figures 4A, B). The decision curve analysis (DCA) was also frequently used to evaluate the practical value of these models (Figure 5). The abscissa of this graph represents the threshold probability. The vertical axis is the net benefit (NB) after subtracting the pros and cons. The solid black line (none line) and the solid grey line (all line) represent two extreme situations, respectively. The first extreme situation is represented by the solid black line. At this point, it was assumed that the patient did not have LLNM and had not undergone LND, and the NB was zero. The second extreme situation is represented by the solid grey line. At this point, it was assumed that all patients had LLNM and had undergone LND. The NB is a backslash line. The solid blue line is the result of our nomogram. The solid blue line performed significantly better than the solid grey line at most of the threshold points.

Discussion

The presence of LLNM in PTC patients often indicates poor prognosis and local recurrence; therefore, the preoperative evaluation of LLNM was the focus of this study. According to the American Thyroid Association (ATA) guidelines, LND is necessary for PTC patients with LLNM (8). Prophylactic ipsilateral cervical LND is still a controversial topic. Its supporters have pointed out that preventive ipsilateral cervical LND could eliminate the

10.3389/fendo.2023.1242061

TABLE 2 Clinical characteristics of suspicious LLNs.

Characteristics		value
Gender	female	141
	male	67
Age(y)	range	18-78
	mean+SD	43.3±11.9
CLT	absence	170
	presence	38
A/T	range	0.37 - 1.2
	Mean+SD	0.8±0.1
Maximum tumer size (cm)	range	0.22 - 6.0
	Mean+SD	1.25±0.9
Location of thyroid nodules 1	left lobe	99
	right lobe	103
	bilateral	1
	isthmus	5
Location of thyroid nodules 2	upper pole	59
	middle upper one-third of the thyroid gland	39
	middle pole	64
	middle lower one-third of the thyroid gland	24
	lower pole	22
Location of thyroid nodules 3	ventral side	35
	dorsal side	29
	inside	8
	outside	15
	penetrating	91
	central	30
Location of lymph nodes	left	104
	right	104
Level of lymph nodes	2	12
	3	88
	4	96
	5	2
	6	10
Cytopathology	Negative	137
	Positive	71
Tg	median	19.44
	IQR	10.55-500
Tg/s-tg	median	2.45
	IQR	0.08-29.11

LLNM, lateral cervical lymph node metastasis; CLT, chronic lymphocytic thyroiditis; A/T, aspect ratio (height divided by width on transverse views); Tg, thyroglobulin in fine-needle aspiration, 61.6 is the cutoff value obtained from this study; Tg/s-tg, Tg divided by serum thyroglobulin, 2.91 is the cutoff value obtained from this study.
If there are multiple nodules in the thyroid gland, we selected the largest or most typical nodule.
The positive of cytopathology refers to the detection of thyroid cells in the background of lymphocytes. The negative of cytopathology means no thyroid cells appeared in the background of lymphocytes and no suspicious LLNs were founded after at least six months of follow-up.
P value < 0.05 indicates a significant difference between the training set and the validation set.

possibility of local recurrence (6), but its opponents believe that prophylactic ipsilateral LND could increase the probability of some potential complications such as permanent hypoparathyroidism (10). At present, compared with prophylactic LND, therapeutic CND is more widely recognized by many surgeons (11, 12). Many studies have focused on evaluating the accuracy of surgery in PTC while ignoring the distribution of thyroid nodules within the thyroid gland. Many scholars have reported that the incidence of LLNM varied from 10% to 30%. However, the frequency of LLNM was 37.9% (i.e., in 79 out of 208 patients) in our study. This difference could be due to the selection bias, because the samples included in our study were those of patients with PTC.

Many clinical factors related to LLNM have been previously reported, including sex, age, CLT, and tumor size (13, 14). In addition to the clinical features mentioned above, we also added some parameters of preoperative evaluation. According to our findings, the maximum thyroid nodule diameter, tumor location, cytopathology, Tg level, and Tg/sTg were risk factors in the univariate analysis. However, in the multivariate analysis, the maximum thyroid nodule diameter, cytopathology, Tg level, and Tg/sTg were independent risk factors for LND.

All of the above factors can be used to create individual possibilities for clinical events and ultimately help clinicians in decision-making. These clinical parameters were incorporated into the nomogram as risk factors for LLNM.

As some investigators have reported, a malignant tumor has the characteristic of unlimited proliferation (15). In our study population, the cutoff value for the maximum diameter of a thyroid nodule was greater than 1.1 cm. As the maximum thyroid nodule diameter of thyroid nodules increases, the probability of LLNM also increases (16, 17). One of the influencing factors is the distribution of thyroid nodules within the thyroid gland. There are five distribution modes, namely the upper pole, middle-upper third of the thyroid gland, middle pole, middle-lower third of the thyroid gland, and the lower pole. Many studies have focused on analyzing the possibility of LLNM from the morphology of thyroid nodules (18), but have overlooked the relationship between the distribution of thyroid nodules and LLNM. Due to the special location and lymphatic drainage

10.3389/fendo.2023.1242061

TABLE 3 Univariate analysis of factors associated with LLNM.

Characteristics	Univariate analysis		
	LLNM group (n = 79)	non-LLNM group (n = 129)	*P* value
Gender(n)			0.359
female	57	84	
male	22	45	
Age(y)			0.468
>36	41	92	
<=36	38	37	
CLT			0.360
negative	62	108	
positive	17	21	
A/T			0.054
>=1	3	14	
<1	76	115	
Maximum tumer size (cm)	1.62±0.926	1.03±0.8	
Location of thyroid nodules 1			0.061
left lobe	30	69	
right lobe	47	56	
bilateral	1	0	
isthmus	1	4	
Location of thyroid nodules 2			0.007
upper pole	28	31	
middle upper one-third of the thyroid gland	21	18	
middle pole	21	43	
middle lower one-third of the thyroid gland	4	20	
lower pole	5	17	
Location of thyroid nodules 3			0.242
ventral side	7	28	
dorsal side	10	19	
inside	3	5	
outside	6	9	
penetrating	40	51	
central	13	17	
Location of lymph nodes 1			0.045
left	32	72	
right	47	57	
Level of lymph nodes			0.004
2	0	12	
3	32	56	
4	38	58	
5	2	0	
6	7	3	
Tg			0.000
Median (IQR)	500 (176.3-500)	2.46 (0.49-22.84)	
Tg/s-tg			0.000
Median (IQR)	34.04 (6.16-155.76)	0.25 (0.04-2.45)	
Cytopathology			0.000
Negative	21	116	
Positive	58	13	

(Continued)

TABLE 3 Continued

LLNM, lateral cervical lymph node metastasis; CLT, chronic lymphocytic thyroiditis; A/T, aspect ratio (height divided by width on transverse views); Tg, thyroglobulin in fine-needle aspiration, 61.6 is the cutoff value obtained from this study; Tg/s-tg, Tg divided by serum thyroglobulin, 2.91 is the cutoff value obtained from this study.
If there are multiple nodules in the thyroid gland, we selected the largest or most typical nodule.
The positive of cytopathology refers to the detection of thyroid cells in the background of lymphocytes. The negative of cytopathology means no thyroid cells appeared in the background of lymphocytes and no suspicious LLNs were founded after at least six months of follow-up.
P value < 0.05 indicates a significant difference between the training set and the validation set.

characteristics of the isthmus of the thyroid gland, the lymphatic vessels in the isthmus drain into the anterior larynx and anterior trachea lymph nodes, leading to a higher incidence of CLNM (9). Gong Y and Ito Y's research (19, 20) shows that, compared with the nodules located at the middle pole of the thyroid gland, nodules at the upper pole and middle-upper third of the thyroid gland are extremely prone to LLNM. This is mainly because the lymphatic drainage system of the thyroid gland is similar to the venous drainage system (21). In our study, the prevalence of LLNM was 63.2% (i.e., in 50 out of 79 patients) in the upper pole or the upper part of the high plane of the isthmus of the thyroid gland, which was higher than the thyroid nodules in middle pole and isthmus (22.7%). Moreover, we evaluated the distribution of LLNM in the different levels of the neck. We found that the incidence of LLNM was highest in level 4 of the lateral neck (71.4%), followed by level 3 and level 5 (25% and 3.5%, respectively). The main reason for this might be related to the lymphatic drainage, which collects lymph from the upper and middle poles of the thyroid gland. Therefore, we suggest that during the preoperative evaluation, the thyroid nodules located at the upper or middle poles should be carefully evaluated for the condition of the lateral neck lymph nodes, especially those in level 4.

10.3389/fendo.2023.1242061

TABLE 4 Multivariate analysis of factors associated with LLNM.

Characteristics	multivariate analysis	
	Adjusted OR (95% CI)	*P* value
Maximum tumer size (cm)	2.364 (1.985-2.810)	0.047
Location of thyroid nodules 2		
upper pole	ref	
middle upper one-third of the thyroid gland	0.408 (0.100-1.676)	0.214
middle pole	0.366 (0.112-1.194)	0.096
middle lower one-third of the thyroid gland	0.185 (0.028-1.219)	0.079
lower pole	0.146 (0.025-0.840)	0.051
Location of lymph nodes 1		
left	ref	
right	2.157 (0.859-5.420)	0.102
Tg	1.005 (1.003-1.007)	0.000
Tg/s-tg	1.005 (1.001-1.009)	0.009
Cytopathology	9.738 (3.678-25.783)	0.000

LLNM, lateral cervical lymph node metastasis; CLT, chronic lymphocytic thyroiditis; A/T, aspect ratio (height divided by width on transverse views); Tg, thyroglobulin in fine-needle aspiration, 61.6 is the cutoff value obtained from this study; Tg/s-tg, Tg divided by serum thyroglobulin, 2.91 is the cutoff value obtained from this study.

If there are multiple nodules in the thyroid gland, we selected the largest or most typical nodule.

The positive of cytopathology refers to the detection of thyroid cells in the background of lymphocytes. The negative of cytopathology means no thyroid cells appeared in the background of lymphocytes and no suspicious LLNs were founded after at least six months of follow-up.

P value < 0.05 indicates a significant difference between the training set and the validation set.

Another important influencing factor is the measurement of Tg concentration (22). As we all know, thyroid follicular epithelial cells secrete thyroglobulin (23, 24). ATA (25) and the European Thyroid Association (26) recommended that measuring the concentration of thyroglobulin in lymph nodes increases the accuracy of the diagnosis of LLNM (9). The key factors included the amount of Tg remaining in the needle tip and any volume of diluent. The ideal diluent should have the following characteristics (27). The first point is that it should have less influence on the conformation of proteins. Another point is that the diluent needs to be readily available. Currently, the available diluents include normal saline and Tg-free solution (28). Normal saline is more widely used than Tg-free solution, and it is reported that normal saline is a more economical option and exerts a smaller matrix effect (29, 30). Our study adopted 1 mL of normal saline as the diluent. The cutoff value of Tg has been controversial. Some scholars (31) set the cutoff value to 1 ng/mL, whereas Kim et al. (32) set the cutoff value to 10 ng/mL. The fluctuation range of this cutoff value is too extensive, leading to many false-positive and false-negative cases. In our study, the cutoff values of Tg and Tg/sTg were 61.6 ng/mL and 2.91 ng/mL (without a log conversion), and the associated sensitivity and specificity were 87.3% vs. 82.9% and 91.1% vs. 81.4%, respectively.

In the debate about prophylactic ipsilateral cervical LND with PTC, our model provides a reference for the development of surgical methods through personalized preoperative evaluation. Meanwhile, based on the model, we stratified the risk level of PTC patients based on their preoperative evaluation results. The patients at the different risk levels were treated using different strategies. In our nomogram, the low risk level refers to PTC patients with a relatively low level (< 30%) of ipsilateral LLNM, for whom prophylactic ipsilateral LND should be avoided. The moderate risk level refers to PTC patients with a moderate level

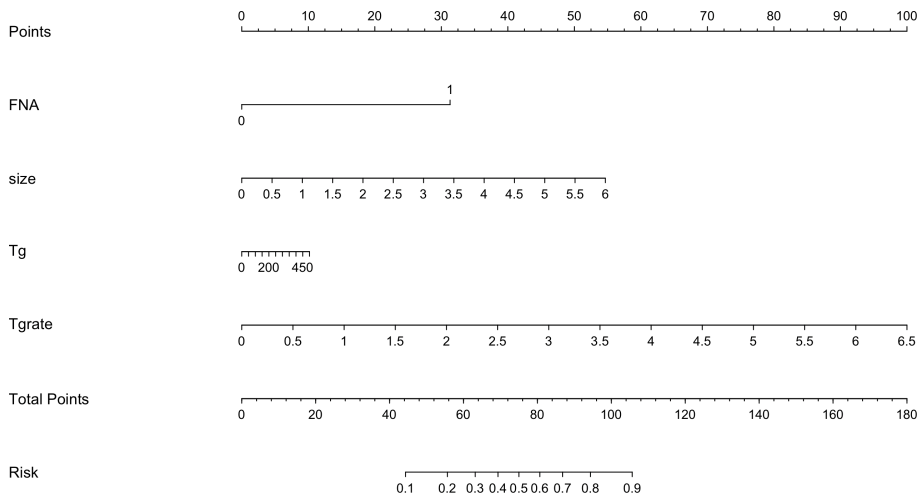

FIGURE 2
Nomogram for predicting LLNM in patients with PTC.

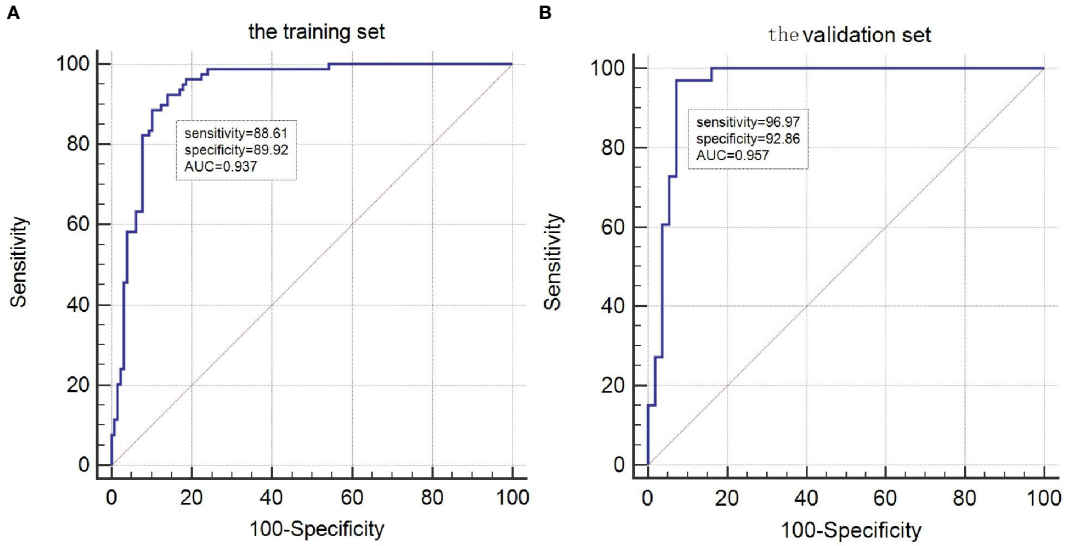

FIGURE 3
ROC curves for the LLNM model. **(A)** The ROC of the training group (AUC =0.937); **(B)** The ROC of the validation group (AUC =0.957).

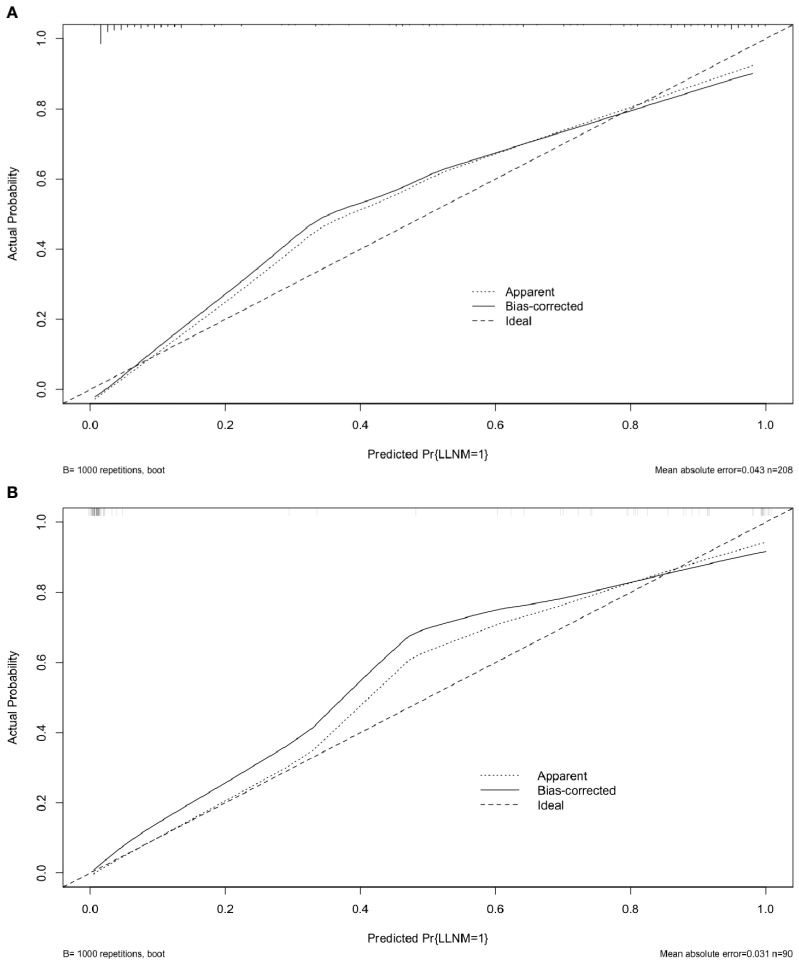

FIGURE 4
Calibration curves for the LLNM model. These are calibration curves of nomograms for predicting LLNM. The diagonal dashed line represents the ideal prediction made using the perfect nomogram; the solid line represents the calibration estimate from the internally validated model; and the dotted line indicates the apparent predictive accuracy. **(A)** The calibration curves of the training group; **(B)** The calibration curves of the validation group. The closer the solid line is to the dotted line, then the stronger the LLNM model's predictive ability.

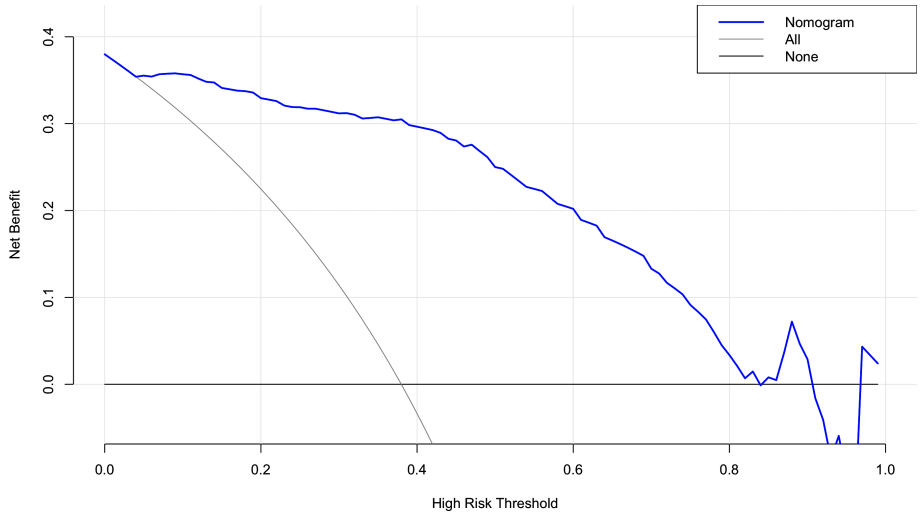

FIGURE 5
DCA for the LLNM model.

(30%–70%) of ipsilateral LLNM, for whom whether or not LND should be performed needs to be carefully evaluated. The specific process was to locate the suspicious LLNs first, then remove them and send it for rapid pathology, and finally to determine whether or not to perform LND based on the results of the rapid pathology. The high risk level is PTC patients with a high level (> 70%) of ipsilateral LLNM, for whom ipsilateral LND is recommended. Therefore, our nomogram could be used carefully, and to guide surgeons in their assessment of the suspected LLN status and to enable them to avoid unnecessary LND. The nomogram usage method is as follows. First, the scores corresponding to each indicator of the patient should be recorded, and then, these scores should be added together to correspond to the risk level on the horizontal axis. Finally, the surgical method can be determined based on the risk level (14).

Although this study provides a more appropriate evaluation method, it still has some limitations. In our study, 13 patients had a positive cytopathology, but negative histopathology. We speculate that the reasons may be as follows: (1) although we provided preoperative localization, the suspected lymph nodes were small in size, concealed in location, and were difficult for surgeons to detect; (2) the puncture area of the lymph nodes was contaminated, resulting in the presence of false positives; (3) last but not least, this may have been related to the ectopic thyroid tissue, which cannot be clearly distinguished under US. Therefore, during the puncture process, fine needles were inserted into the ectopic thyroid tissue, resulting in false-positive results. Frasoldati et al. (33) believed that there was only a weak correlation between sTgAb and FNAB Tg, but Baskin et al. (34) and Boi et al. (35) believed that the correlation between them were worth discussing. In the future, we will first perform FNAB on suspected lymph nodes, and then focus on thyroid nodules. Meanwhile, during the puncture process, the puncture needle should be directly inserted into the suspected lymph nodes to avoid interference from ectopic thyroid as much as possible. Compared with other multicenter prospective studies, the patients in our study were retrospectively selected and came from only one medical center. Hence, the selective bias of the sample was inevitable. In addition, different sonographers performed the preoperative evaluation of suspicious LLNs. Due to the limited sample size, this study included only the training group and not the validation group, which will be the next work plan of this study.

In conclusion, our nomogram showed that LLNM was independently associated with the maximum of thyroid nodules, cytopathology, Tg level and Tg/sTg. It was possible to obtain the individual incidence probability for each PTC patient with suspected LLNs using the nomogram, which provides a critical reference for the clinical preparation of a surgical plan.

Data availability statement

The original contributions presented in the study are included in the article/supplementary material. Further inquiries can be directed to the corresponding authors.

Ethics statement

The studies involving humans were approved by The Institutional Review Board of Changzhou First People's Hospital. The studies were conducted in accordance with the local legislation and institutional requirements. Written informed consent for participation in this study was provided by the participants' legal guardians/next of kin.

Author contributions

S-QL and J-WF: writing—original draft, software, and data curation. Z-TY and X-XX: validation, formal analysis, and data curation. W-YJ: conceptualization. YJ: validation and investigation. WX and FQ: writing—review and editing, visualization, and supervision. All authors contributed to the article and approved the submitted version.

Funding

The author(s) declare that no financial support was received for the research, authorship, and/or publication of this article.

Conflict of interest

The authors declare that the research was conducted in the absence of any commercial or financial relationships that could be construed as a potential conflict of interest.

Publisher's note

All claims expressed in this article are solely those of the authors and do not necessarily represent those of their affiliated organizations, or those of the publisher, the editors and the reviewers. Any product that may be evaluated in this article, or claim that may be made by its manufacturer, is not guaranteed or endorsed by the publisher.

References

1. Grani G, Zatelli MC, Alfò M, Montesano T, Torlontano M, Morelli S, et al. Real-world performance of the American thyroid association risk estimates in predicting 1-year differentiated thyroid cancer outcomes: A prospective multicenter study of 2000 patients. *Thyroid* (2021) 31(2):264–71. doi: 10.1089/thy.2020.0272

2. Liu Y, Huang J, Zhang Z, Huang Y, Du J, Wang S, et al. Ultrasonic characteristics improve prediction of central lymph node metastasis in cN0 unifocal papillary thyroid cancer. *Front Endocrinol (Lausanne)* (2022) 13:870813. doi: 10.3389/fendo.2022.870813

3. Heng Y, Yang Z, Zhou L, Lin J, Cai W, Tao L. Risk stratification for lateral involvement in papillary thyroid carcinoma patients with central lymph node metastasis. *Endocrine* (2020) 68(2):320–8. doi: 10.1007/s12020-020-02194-8

4. Siddiqui S, White MG, Antic T, Grogan RH, Angelos P, Kaplan EL, et al. Clinical and pathologic predictors of lymph node metastasis and recurrence in papillary thyroid microcarcinoma. *Thyroid* (2016) 26(6):807115. doi: 10.1089/thy.2015.0429

5. Jia Xi, Wang Y, Liu Y, Wang X, Yao X, Tao R, et al. Thyroglobulin measurement through fine-needle aspiration for optimizing neck node dissection in papillary thyroid cancer. *Ann Surg Oncol* (2022) 29(1):88–96. doi: 10.1245/s10434-021-10549-2

6. Haugen BR, Alexander EK, Bible KC, Doherty GM, Mandel SJ, Nikiforov YE, et al. 2015 American thyroid association management guidelines for adult patients with thyroid nodules and differentiated thyroid cancer: the American thyroid association guidelines task force on thyroid nodules and differentiated thyroid cancer. *Thyroid* (2016) 26(1):1–133. doi: 10.1089/thy.2015.0020

7. Ha EJ, Na DG, Moon W-J, Lee YH, Choi N. Diagnostic performance of ultrasound-based risk-stratification systems for thyroid nodules: comparison of the 2015 American thyroid association guidelines with the 2016 korean thyroid association/Korean society of thyroid radiology and 2017 American college of radiology guidelines. *Thyroid* (2018) 28(11):1532–7. doi: 10.1089/thy.2018.0094

8. Zhu Y, Song Y, Xu G, Fan Z, Ren W. Causes of misdiagnoses by thyroid fine-needle aspiration cytology (FNAC): our experience and a systematic review. *Diagn Pathol* (2020) 15(1):1–8. doi: 10.1186/s13000-019-0924-z

9. Jeon MJ, Chung MS, Kwon H, Kim M, Park S, Baek JH, et al. Features of papillary thyroid microcarcinoma associated with lateral cervical lymph node metastasis. *Clin Endocrinol (Oxf)* (2017) 86(6):845–51. doi: 10.1111/cen.13322

10. Raffaelli M, De Crea C, Sessa L, Tempera SE, Belluzzi A, Lombardi CP, et al. Risk factors for local recurrence following lateral neck dissection for papillary thyroid carcinoma. *Endocrine* (2019) 63(2):310–5. doi: 10.1007/s12020-018-1788-9

11. Zhang M, Tufano RP, Russell JO, Zhang Y, Zhang Y, Qiao Z, et al. Ultrasound-guided radiofrequency ablation versus surgery for low-risk papillary thyroid microcarcinoma: results of over 5 years' Follow-up. *Thyroid* (2020) 30(3):408–17. doi: 10.1089/thy.2019.0147

12. Back K, Kim JS, Kim J-H, Choe J-H. Superior located papillary thyroid microcarcinoma is a risk factor for lateral lymph node metastasis. *Ann Surg Oncol* (2019) 26(12):3992–4001. doi: 10.1245/s10434-019-07587-2

13. Wolinski K, Stangierski A, Ruchala M. Comparison of diagnostic yield of core-needle and fine-needle aspiration biopsies of thyroid lesions: Systematic review and meta-analysis. *Eur Radiol* (2017) 27(1):431–36. doi: 10.1007/s00330-016-4356-9

14. Zhai X, Zhang L, Chen L, Lian X, Liu C, Shi B, et al. An age-specific serum thyrotropin reference range for the diagnosis of thyroid diseases in older adults: A cross-sectional survey in China. *Thyroid* (2018) 28(12):1571–9. doi: 10.1089/thy.2017.0715

15. Barres B, Kelly A, Kwiatkowski F, Batisse-Lignier M, Fouilhoux Geneviève, Aubert B, et al. Stimulated thyroglobulin and thyroglobulin reduction index predict excellent response in differentiated thyroid cancers. *J Clin Endocrinol Metab* (2019) 104 (8):3462–72. doi: 10.1210/jc.2018-02680

16. Zheng WH, Wang KJ, Wu JZ, Wang WD, Shang JB. Multifocality is associated with central neck lymph node metastases in papillary thyroid microcarcinoma. *Cancer Manag Res* (2018) 10:1527–33. doi: 10.2147/CMAR.S163263

17. Wu X, Li BL, Zheng CJ, He XD. Predicting factors of central lymph node metastases in patients with unilateral multifocal papillary thyroid microcarcinoma. *Gland Surg* (2020) 9(3):695–701. doi: 10.21037/gs.2020.03.27

18. Xue S, Wang P, Liu J, Li R, Zhang L, Chen G. Prophylactic central lymph node dissection in cN0 patients with papillary thyroid carcinoma: A retrospective study in China. *Asian J Surg* (2016) 39(3):131–6. doi: 10.1016/j.asjsur.2015.03.015

19. Gong Y, Yang J, Yan S, Su A, Liu F, Gong R, et al. Pattern of and clinicopathologic risk factors for lateral lymph node metastases in papillary thyroid carcinoma patients with lateral cervical lymphadenopathy. *Med (Abingdon)* (2018) 97: e12263. doi: 10.1097/MD.0000000000012263

20. Ito Y, Tomoda C, Uruno T, Takamura Y, Miya A, Kobayashi K, et al. Papillary microcarcinoma of the thyroid: how should it be treated. *World J Surg* (2004) 28:1115–21. doi: 10.1007/s00268-004-7644-5

21. Lu KN, Zhang Y, Da JY, Zhou TH, Zhao LQ, Peng Y, et al. A novel scoring system for predicting the metastases of posterior right recurrent laryngeal nerve lymph node involvement in patients with papillary thyroid carcinoma by preoperative ultrasound. *Front Endocrinol* (2021) 12:738138. doi: 10.3389/fendo.2021.738138

22. Chang Q, Zhang J, Wang Y, Li H, Du X, Zuo D, et al. Nomogram model based on preoperative serum thyroglobulin and clinical characteristics of papillary thyroid carcinoma to predict cervical lymph node metastasis. *Front Endocrinol (Lausanne)* (2022) 13:937049. doi: 10.3389/fendo.2022.937049

23. Uruno T, Miyauchi A, Shimizu K, Tomoda C, Takamura Y, Ito Y, et al. Usefulness of thyroglobulin measurement in fine-needle aspiration biopsy specimens for diagnosing cervical lymph node metastasis in patients with papillary thyroid cancer. *World J Surg* (2005) 29(4):483–5. doi: 10.1007/s00268-004-7701-0

24. Kim MJ, Kim EK, Kim BM, Kwak JY, Lee EG, Park CS, et al. Thyroglobulin measurement in fine-needle aspirate washouts: the criteria for neck node dissection for patients with thyroid cancer. *Clin Endocrinol (Oxf)* (2009) 70:145–51. doi: 10.1111/j.1365-2265.2008.03297.x

25. Johnson NA, Tublin ME. Postoperative surveillance of differentiated thyroid carcinoma: rationale, techniques, and controversies. *Radiology* (2008) 249:429–44. doi: 10.1148/radiol.2492071313

26. Cooper DS, Doherty GM, Haugen BR, Hauger BR, Kloos RT, Lee SL, et al. Revised American Thyroid Association management guidelines for patients with thyroid nodules and differentiated thyroid cancer. *Thyroid* (2009) 19:1167–214. doi: 10.1089/thy.2009.0110

27. Leenhardt L, Erdogan MF, Hegedus L, Mandel SJ, Paschke R, Rago T, et al. 2013 European thyroid association guidelines for cervical ultrasound scan and ultrasound-guided techniques in the postoperative management of patients with thyroid cancer. *Eur Thyroid J* (2013) 2:147–59. doi: 10.1159/000354537

28. Campennì A, Barbaro D, Guzzo M, Capoccetti F, Giovanella L. Personalized management of differentiated thyroid cancer in real life - practical guidance from a multidisciplinary panel of experts. *Endocrine* (2020) 70(2):280–91. doi: 10.1007/s12020-020-02418-x

29. Piotrkowski-Viale F, Reyes A, Dios A, Pitoia F, Lowenstein A, Glikman P. Effects of sample storage and diluents in the reliability of thyroglobulin measurement in the washout of fine needle aspirates. *Endocrine* (2017) 56(3):504–8. doi: 10.1007/s12020-017-1294-5

30. Kahramangil B, Kose E, Donmez M, Aydin H, Reynolds JP, Krishnamurthy V. Thyroglobulin washout from cervical lymph node fine needle aspiration biopsies in patients with differentiated thyroid cancer: an analysis of different expressions to use in post-total. *Surgery* (2020) 167(1):34–9. doi: 10.1016/j.surg.2019.05.083

31. Wang J, Jiang X, Xiao G, Zhou W, Hu Y. Excellent diagnostic performance of Tg in detecting lymph nodes metastases from papillary thyroid cancer. *Future Oncol* (2020) 16(33):2735–46. doi: 10.2217/fon-2020-0213

32. Zhai L, Jiang W, Zang Y, Gao Y, Jiang D, Tian Q, et al. Impact of thyroid tissue status on the cutoff value of lymph node fine-needle aspiration thyroglobulin measurements in papillary thyroid cancer. *Br J BioMed Sci* (2022) 79:10210. doi: 10.3389/bjbs.2021.10210

33. Frasoldati A, Pesenti M, Gallo M, Caroggio A, Salvo D, Valcavi R, et al. Diagnosis of neck recurrences in patients with differentiated thyroid carcinoma. *Cancer* (2003) 97 (1):90–6. doi: 10.1002/cncr.11031

34. Baskin HJ. Detection of recurrent papillary thyroid carcinoma by thyroglobulin assessment in the needle washout after fine-needle aspiration of suspicious lymph nodes. *Thyroid* (2004) 14(11):959–63. doi: 10.1089/thy.2004.14.959

35. Boi F, Baghino G, Atzeni F, Lai ML, Faa G, Mariotti S. The diagnostic value for differentiated thyroid carcinoma metastases of thyroglobulin (Tg) measurement in washout fluid from fine-needle aspiration biopsy of neck lymph nodes is maintained in the presence of circulating anti-Tg antibodies. *J ClinEndocrinol Metab* (2006) 91 (4):1364–9. doi: 10.1210/jc.2005-1705

frontiers | Frontiers in Endocrinology

TYPE Original Research
PUBLISHED 07 December 2023
DOI 10.3389/fendo.2023.1303159

OPEN ACCESS

EDITED BY
I-Cheng Lu,
Kaohsiung Medical University, Taiwan

REVIEWED BY
Annamaria D'Amore,
Agostino Gemelli University Polyclinic (IRCCS), Italy
Kyriakos Vamvakidis,
Henry Dunant Hospital, Greece

*CORRESPONDENCE
Nurcihan Aygun
nurcihanaygun@hotmail.com

RECEIVED 27 September 2023
ACCEPTED 20 November 2023
PUBLISHED 07 December 2023

CITATION
Aygun N, Unlu MT, Kostek M, Caliskan O, Isgor A and Uludag M (2023) Intraoperative cricothyroid muscle electromyography may contribute to the monitorization of the external branch of the superior laryngeal nerve during thyroidectomy. *Front. Endocrinol.* 14:1303159. doi: 10.3389/fendo.2023.1303159

Intraoperative cricothyroid muscle electromyography may contribute to the monitorization of the external branch of the superior laryngeal nerve during thyroidectomy

Nurcihan Aygun[1]*, Mehmet Taner Unlu[1], Mehmet Kostek[1], Ozan Caliskan[1], Adnan Isgor[2] and Mehmet Uludag[1]

[1]General Surgery Department, Sisli Hamidiye Etfal Training and Research Hospital, Istanbul, Türkiye, [2]General Surgery Department, Memorial Sisli Hospital, Sisli, Istanbul, Türkiye

Background: In thyroid surgery, both the recurrent laryngeal nerve (RLN) and external branch of the superior laryngeal nerve (EBSLN) should be preserved for maintaining the vocal cord functions. We aimed to evaluate whether EMG of the CTM applied after the superior pole dissection provided additional informative data to the IONM via ETT or not, regarding the EBSLN function.

Methods: The prospectively collected data of the patients, who have undergone thyroidectomy with the use of IONM for the exploration of both the RLN and EBSLN between October 2016 and March 2017, were evaluated retrospectively. Patients over 18 years of age with primary thyroid surgery for malignant or benign thyroid disease, and whom were applied CTM EMG with a needle electrode after the completion of thyroidectomy were included in the study. In the study, each neck side was evaluated as a separate entity considering the EBSLN at risk.

Results: The data of 41 patients (32 female, 9 male) (mean age, 46.7 + 9.1; range, 22-71) were evaluated. Sixty seven EBSLNs out of 26 bilateral and 15 unilateral interventions were evaluated. With EBSLN stimulation after the superior pole dissection, positive glottic EMG waveforms via ETT were obtained in 45 (67.2%) out of 67, and the mean glottic amplitude value was 261 + 191 µV (min-max: 116-1086 µV). Positive EMG responses via the CTM EMG were achieved from all of the 67 EBSLNs (100%) with stimulation using a monopolar probe at the most cranial portion above the area of divided superior pole vessels. The mean value of CTM amplitudes via CTM EMG obtained with EBSLN stimulation was 5268 + 3916 µV (min-max:1215 -19726 µV). With EBSLN stimulation, the mean CTM EMG amplitude was detected significantly higher than the mean vocal cord amplitude ($p<0.0001$). The CTM EMG provided more objective quantifiable data regarding the EBSLN function (100% vs 67,2%, $p<0.001$).

Conclusion: In addition to the IONM via ETT, intraoperative post-dissection CTM EMG via needle electrode is a safe, simple and applicable method that may provide significant additional informative data to IONM with ETT by obtaining and recording objective quantitative data related to the EBSLN function.

KEYWORDS

cricothyroid muscle, electromyogarphy, intraoperative neural monitoring (IONM), external branch of the superior laryngeal nerve (EBSLN), thyroidectomy

Introduction

In thyroid surgery, both the recurrent laryngeal nerve (RLN) and external branch of the superior laryngeal nerve (EBSLN) should be preserved to maintain vocal cord functions (1). The adductor muscles (thyroarytenoid muscle (TAM) (main adductor muscle), lateral cricoarytenoid muscle, and interarytenoideus muscle) and abductor muscle (posterior cricoarytenoid muscle) of the larynx are supplied by the motor fibers of the RLN, while the tensor muscle of the vocal cords, cricoarytenoid muscle (CTM), is innervated by the EBSLN (2).

After innervating the CTM, the EBSLN enters the larynx extending through the cricothyroid membrane and makes anastomosis with the RLN in one-third anterior part of the TAM in the larynx, hence contributing to its motor innervation. This anastomosis is called the "human communicating nerve" (3). This nerve has been reported in up to 85% of anatomical dissection studies (3, 4).

The EBSLN has a highly variable course toward the CTM and is in a close anatomical relationship with the superior thyroid vessels. Therefore, it is a potential risk during superior pole dissection during thyroid surgery. Different classifications have been defined regarding EBSLN anatomy, and the Cernea classification is the most widely used classification system. The Cernea classification, based on the risk of EBSLN injury in thyroidectomy, categorizes the nerve according to its relation to the superior thyroid vessels and the upper edge of the superior thyroid pole. In the Cernea classification, the EBSLN crosses with the superior thyroid vessels at a distance more than 1 cm cranially from the upper edge of the superior pole in type I, less than 1 cm from the upper edge of the superior pole in type IIa, and below the upper edge of the superior pole in type IIb (5). Although both type IIa and type IIb nerves have a risk of injury during dissection and ligation of the superior thyroid vessels due to their close course to the superior pole, type IIb has the highest risk. In the last meta-analysis, the prevalences of type I, type IIa, and type IIb in intraoperative studies were reported as 35.23 (95% CI 26.07–42.57), 44.27% (95% CI 34.34–51.55), and 20.50% (95% CI 13.32–27.25), respectively (6).

Recently, the usage of intraoperative neuromonitorization (IONM) during thyroid surgery has increased considerably (7). IONM via endotracheal tube (ETT) with surface electrodes is a widely accepted technique as an aid to the gold standard of visual identification, which can be used for both the identification and assessment of the functions of the RLN and EBSLN (8, 9). In order to minimize the potential risk of EBSLN injury, three basic techniques have been described during superior pole dissection, including division of the superior pole vessels on the thyroid capsule without exploring the EBSLN, visual identification of the EBSLN before the division of the vessels, or mapping of the nerve using IONM or a stimulator probe during superior pole dissection (9–11). Although there is no consensus about which of these methods is the best method for the protection of the EBSLN, it has been reported that the use of IONM improves the visual and functional identification of the EBSLN and may reduce the risk of EBSLN injury (12–14).

The true positivity of EBSLN stimulation with IONM is defined as contraction in the CTM, which is the target organ of the EBSLN, and/or recording of endotracheal glottic electromyography (EMG) waveform obtained via ETT (9). The main target organ of the EBSLN is the CTM, and the CTM twitch with EBSLN stimulation is not a recordable quantitative data. Although it was reported in a study that positive EMG response (positive threshold value >50 μV) with EBSLN stimulation was recordable in 100% via the reinforced endotracheal tube with surface electrodes, in other studies, 68%–80% positive response (positive threshold value >100 μV) was obtained with EBSLN stimulation using standard ETT with surface electrodes (13–16).

Although the glottic EMG response is quantitative data, this finding is not related to the CTM motor function, which is mainly innervated by the EBSLN. This EMG activity is related to the adductor function of the vocal cord and motor innervation provided by the connection between the RLN and the EBSLN in the anterior third of the TAM described above as a "human communicating nerve". Although the rate of positive glottic EMG response has been found similar to that of human communicating nerve reported in human anatomical studies, the relationship of the magnitude of the EMG amplitude with the function of the EBSLN is yet to be clarified (9). In addition, there is no quantitative glottic EMG response in at least 20% of nerves.

Traditionally, RLN and EBSLN injuries, well-known complications of thyroidectomy, have been considered the main cause of postoperative voice problems. However, voice disorders are common after thyroidectomy, many of which are not associated with laryngeal nerve injuries and are multifactorial. More recently, many factors have been suggested such as arytenoid cartilage problems due to intubation, changes in laryngeal vascularization

and lymphatic drainage due to surgery, cricothyroid and strap muscle injuries, injury to the anastomotic branches in the perithyroidal neural plexus, laryngotracheal fixation causing deficiency in vertical movement of the larynx, local pain in the neck, and development of psychological reaction (1).

Voice disorders after thyroidectomy might be a great concern for patients as well as complications such as hypocalcemia and cervical scarring (17). Postthyroidectomy vocal disorders can negatively affect the work performance of professionals such as singers, announcers, lawyers, and teachers, who use their voices. However, with the increasing awareness of the quality of life recently, the importance of postthyroidectomy voice disorders in terms of quality of life is increasing for all patients (18).

Quantitative recording of intraoperative nerve functions may be important in the differential diagnosis of postoperative voice disorders as well as the preservation of laryngeal nerves in thyroidectomy. In addition, recording may provide more protection against unfounded claims related to sound problems in malpractice cases (19).

Intraoperative CTM EMG via a needle electrode may provide additional quantitative data regarding the EBSLN function. We aimed to evaluate whether the EMG of the CTM applied after superior pole dissection provided additional informative data to the IONM via ETT or not regarding the EBSLN function.

Materials and methods

The prospectively collected data of the patients who have undergone thyroidectomy with the use of IONM for the exploration of both the RLN and EBSLN between October 2016 and March 2017 were evaluated retrospectively. Patients over 18 years of age with primary thyroid surgery for malignant or benign thyroid disease and who underwent CTM EMG with a needle electrode after the completion of thyroidectomy were included in the study.

In the study, each neck side was evaluated as a separate entity due to the EBSLN at risk. Patients with secondary thyroidectomy, with preoperative vocal cord paralysis (VCP), with lateral neck dissection, with divided cricothyroid muscle or EBSLN due to extrathyroidal extension, who were operated on without IONM due to technical problems, and who were under the age of 18 years were excluded.

Surgical technique

The patients underwent thyroidectomy with the use of IONM. Thus, general anesthesia was applied using a low-dose short-acting neuromuscular blocking agent (rocuronium 0.3 mg/kg) only for the induction. They were intubated with a Nerve Integrity Monitor Standard Reinforced Electromyography Endotracheal Tube (size 6.0, 7.0, or 8.0) (Medtronic Xomed, Jacksonville, FL, USA). The surgical technique and the neuromonitoring method of the RLN and EBSLN have been described in detail in our previous studies (14, 20, 21).

Intraoperative neuromonitorization

IONM of the RLN and EBSLN and intraoperative EMG of the CTM were performed using a four-channel NIM 3.0 Nerve Monitoring System (Medtronic Xomed, Jacksonville, FL, USA). A monopolar stimulator probe (Medtronic Xomed) was used for the nerve stimulation at a current of 1.0 mA with a duration time of 100 µs, a frequency of 4 Hz, and an event threshold of 100 µV. The setup, application, data collection, and interpretation of IONM were carried out in accordance with the International Neural Monitoring Study Group guidelines (8, 9). A standard four-step procedure (V1, R1, R2, and V2) was performed for the RLN. The EMG waveform amplitude achieved via RLN stimulation defined the motor function of the thyroarytenoid muscle, which is the main adductor muscle of the vocal cords. For the RLN and vagus, audible alarm of the system combined with an EMG amplitude of ≥100 µV was defined as positive stimulation (8).

The function of the EBSLN via IONM was evaluated with visual CTM twitch and positive glottic EMG response in case of its presence. Positive stimulation for the EBSLN was also defined as the EMG response of >100 µV and the auditory signal of the monitoring system. S1 was defined as the first response achieved with EBSLN stimulation at identification, and S2 was the final response achieved at the most proximal point of the EBSLN located above the ligated superior pole vessels (22).

Superior pole dissection

After the vagus nerve was identified in the carotid sheath and initial vagal nerve stimulation (V1) was achieved, the superior pole was retracted inferolaterally for the dissection of the avascular plane and exposure of sternothyroid-laryngeal triangle (SLT), which harbors the EBSLN. The EBSLN was searched visually, and the fibrillar structure presumed to be the EBSLN was confirmed using a monopolar stimulator probe via CTM twitch evaluation. Additionally, if a positive glottic EMG response was achieved, it was recorded (S1) (Figure 1). If the EBSLN was not able to be identified visually and no CTM twitch was obtained with stimulation of any fibrillar structure using a probe, the CTM was directly stimulated using a probe, and the twitch was observed. Afterward, the EBSLN was searched using a probe in the area under the laryngeal insertion of the sternothyroid muscle and followed over the inferior pharyngeal constrictor (IPC) muscle toward the CTM. The fibers of the IPC muscle were not dissected thoroughly if the EBSLN was not able to be detected using the probe. Whether or not the EBSLN was identified, any of the dissected structures were not divided without stimulating it using a probe to confirm the absence of CTM twitch (21). The EBSLN was stimulated using a probe at the most cranial portion above the ligated superior thyroid vessels to confirm its integrity considering the CTM twitch and if there was also a positive glottic EMG response (S2) (Figure 2).

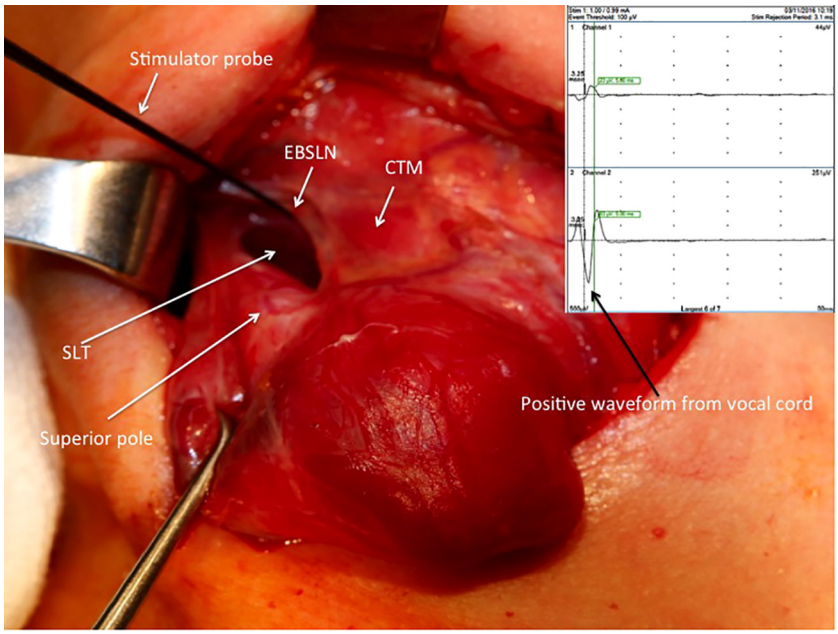

FIGURE 1
Positive EMG waveform achieved from the vocal cords with external branch of the superior laryngeal nerve stimulation using a stimulator probe during right superior pole dissection after the exposure of the sternothyroid-laryngeal triangle. SLT, sternothyroid-laryngeal triangle; EBSLN, external branch of the superior laryngeal nerve; CTM, cricothyroid muscle; EMG, electromyography.

Intraoperative cricothyroid muscle electromyography

A pair of needle electrodes was inserted through the CTM, and it was plugged into the third channel of the interface connector box of the NIM 3.0 nerve monitoring system. The EBSLN was stimulated using a monopolar stimulator probe with a current of 1 mA at the most cranial portion above the divided superior thyroid vessels, and the EMG response was recorded (14) (Figure 3). As Martin-Oviedo et al. suggested in their study, positive CTM EMG response was accepted

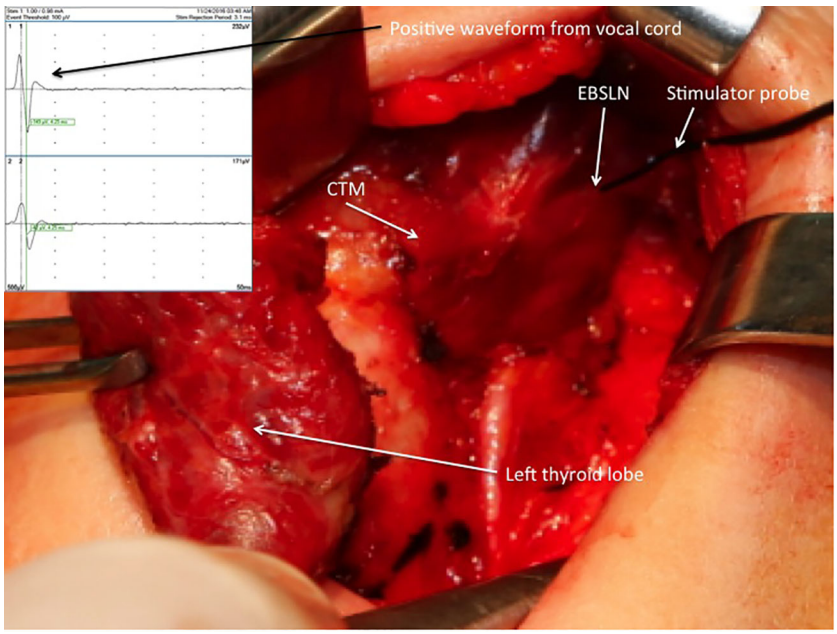

FIGURE 2
Positive EMG waveform achieved from the vocal cords with external branch of the superior laryngeal nerve stimulation using a stimulator probe at the most cranial portion above the ligated superior thyroid vessels after left superior pole dissection. EBSLN, external branch of the superior laryngeal nerve; CTM, cricothyroid muscle; EMG, electromyography.

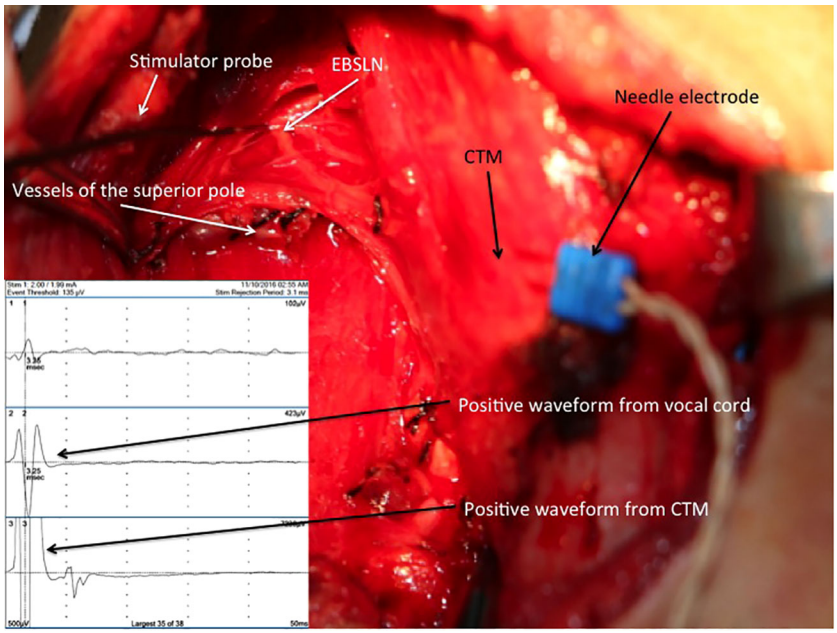

FIGURE 3
Positive EMG waveforms recorded from the vocal cords (channel 2) and CTM (channel 3) with external branch of the superior laryngeal nerve stimulation via a needle electrode inserted into the right CTM after the completion of thyroid resection. EBSLN, external branch of the superior laryngeal nerve; CTM, cricothyroid muscle; EMG, electromyography.

to be the amplitude achieved with EBSLN stimulation, which was at least four times greater than that of the uninnervated muscle (23). In our previous study, with EBSLN stimulation, we obtained a mean response value of 19.1 µV from the contralateral CPM and accepted the positive EMG response value as ≥100 µV (24).

Routinely, patients underwent pre- and postoperative (within 2 days) direct laryngoscopy, conducted by an independent laryngologist. Patients who had VCP postoperatively underwent vocal cord examination periodically in the first, second, fourth, and sixth months. RLN palsy was defined as permanent when there was no evidence of recovery within 6 months postoperatively. Since the study was retrospective, postoperative voice quality was not evaluated with either subjective or objective tests.

Statistical analyses

The incidence of nerve events was calculated based on the number of nerves at risk. All amplitude data are presented as mean and standard deviation (min–max). Positive EMG response values are expressed as frequency and percentage. Differences between continuous and categorical variables were assessed using the Mann–Whitney U test and Fisher's exact test or chi-square test, respectively. The Wilcoxon signed-rank test was applied for the analysis of the parameters of the two dependent groups.

A value of $p < 0.05$ was considered to be statistically significant.

Results

The data of 41 patients (32 female and three male) (mean age, 46.7 ± 9.1; range, 22–71) meeting the inclusion criteria were evaluated in the present study. A total of 67 EBSLNs out of 26 bilateral and 15 unilateral interventions were evaluated (Table 1). Three patients (4.5%; due to the number of nerves at risk) had unilateral transient VCP. Sixty out of 67 EBSLNs (89.5%) were identified before superior pole dissection using IONM, and the remaining seven (10.5%) were able to be detected using a stimulator probe after the completion of superior pole dissection. CTM twitch combined with positive glottic EMG waveform was achieved in 39 (65%) of 60 EBSLNs, which were detected before superior pole

TABLE 1 Demographic profile, surgical indications, and interventions.

	n = 41
Age (mean ± SD) year, (min–max)	46.7 ± 9.1 (22–71)
Gender (female/male) n (%)	32/9 (78/22)
Preoperative diagnosis	
MNG, n (%)	26 (63.4)
Toxic MNG, n (%)	3 (7.3)
Graves, n (%)	2 (4.9)
Suspicious for malignancy or malignant, n (%)	10 (24.4)
Surgical intervention, n (%)	26 (63.4)/15 (36.6)
TT (n)	23
TT+CND (n)	3
Lobectomy (right/left) (n)	7/8
EBSLN at risk (n)	67

MNG, multinodular goiter; TT, total thyroidectomy; CND, central neck dissection; EBSLN, external branch of the superior laryngeal nerve.

dissection (S1). In six (15.4%) out of 39 EBSLNs, CTM twitch was detected, but no positive glottic EMG response was achieved with EBSLN stimulation after superior pole dissection (S2). After completing superior pole dissection, the positive glottic EMG waveforms were achieved from seven (33.3%) out of 21 EBSLNs, which have been detected before superior pole dissection with CTM twitch but not positive glottic EMG response. Out of the remaining seven EBSLNs identified using a probe after superior pole dissection, five had positive glottic EMG response in addition to the CTM twitch. In two out of three patients with VCP, positive glottic responses were detected with S2 stimulation on the same side as the VCP after achieving S1 and detecting RLN paralysis. Only CTM twitch was observed in one patient with both S1 and S2 stimulation, but no positive response from the vocal cords. With EBSLN stimulation after superior pole dissection, positive glottic EMG waveforms via an endotracheal tube (ETT) were obtained in 45 (67.2%) out of 67 (Figure 4), and the mean glottic amplitude value was 261 ± 191 µV (min–max, 116–1,086 µV).

Positive EMG responses via the CTM EMG were achieved from all of the 67 EBSLNs with stimulation using a monopolar probe at the most cranial portion above the area of divided superior pole vessels. The mean value of CTM amplitudes via CTM EMG obtained with EBSLN stimulation was (mean ± SD) 5,268 ± 3,916 µV (min–max, 1,215–19,726 µV). With EBSLN stimulation, the mean CTM EMG amplitude was detected significantly higher than the mean vocal cord amplitude ($p < 0.0001$). The CTM EMG provided more objective quantifiable data regarding the EBSLN function (100% *vs.* 67.2%, $p < 0.001$). While applying CTM EMG, no trauma of the muscle such as bleeding or hematoma occurred due to the needle electrode inserted into the muscle.

Discussion

Recently, postoperative voice quality related to thyroid surgery has been an important issue for both surgeon and patient; hence, awareness of the consequences of EBSLN injury is increasing (18). Although the use of IONM in thyroidectomy is gradually increasing, the routine use of IONM for the EBSLN is not as common as it is for the RLN (25). The proofs regarding the contribution of IONM to the identification and preservation of the EBSLN are gradually increasing (18). Intraoperative EMG of the CTM is an effective method to determine the EBSLN injury and the etiology of the injury (14). Additionally, there are a limited number of studies regarding the intraoperative CTM EMG during thyroidectomy in the literature (14, 26–29).

In this study, we aimed to evaluate whether intraoperative CTM EMG with a needle electrode after thyroidectomy has an informative contribution to the IONM data or not.

In the present study, with the EBSLN stimulation, a positive EMG waveform response was achieved from all the EBSLNs via CTM EMG, and no loss of signal was detected.

Post-dissection positive CTM EMG response provided additional quantitative data in one-third of the nerves with a significant difference compared to the positive glottic response obtained via ETT (100% *vs.* 67.2%, respectively, $p < 0.001$). The mean amplitude obtained with EBSLN stimulation via CTM EMG was 5,268 ± 3,916 µV (min–max, 1,215–19,726 µV), which was significantly higher than the vocal cord amplitude via ETT (5,268 ± 3,916 µV *vs.* 261 ± 191 µV, $p < 0.001$). The higher amplitudes may provide more adequate information in evaluating the function of the EBSLN and predicting its prognosis. The higher amplitudes with CTM EMG compared to the amplitudes with ETT are related to the CTM being the target organ of the EBSLN. The TAM is supplied by the RLN, not the EBSLN, and the EBSLN alone may contribute to the anterior third of the TAM via the human communicating nerve.

The main principle of surgery is the identification of an anatomical structure with meticulous dissection so as not to injure it. This rule also applies to the EBSLN because of its variable anatomical course and close relation with the superior thyroid pole (30). However, the EBSLN can be detected functionally using IONM, but the nerve may not be visualized due to its course under the fascia or through the fibers of the IPC muscle (9, 13, 14).

Before superior pole dissection, 89.5% of the EBSLNs were able to be identified due to the CTM twitch assessment. The remaining

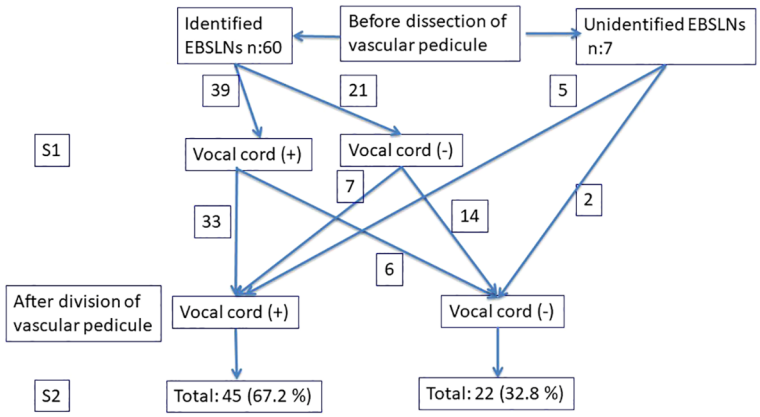

FIGURE 4
Evaluation of the EBSLNs before and after dividing the vascular pedicle using IONM. EBSLNs, external branch of the superior laryngeal nerves.

EBSLNs (10.5%) were able to be identified using IONM after superior pole dissection. During the vessel ligation, the dissected structure was stimulated using a probe and divided in the absence of CTM twitch (negative IONM signal). If the EBSLN cannot be identified during superior pole dissection, a negative IONM signal may be reliable for the surgeon to believe that the dissected structure is not the EBSLN.

With the stimulation of 39 (65%) out of 60 EBSLNs identified before superior pole dissection (S1), the positive glottic response was achieved secondary to the vocal cord innervation of the human communicating nerve in addition to the CTM twitch.

Positive glottic response was achieved with S1 stimulation in two out of three neck sides with postoperative VCP. Although these patients had a loss of signal (LOS) in the RLN, a positive IONM signal similar to the amplitude value of S1 stimulation was achieved with S2 stimulation, which was an important functional indicator for the contribution of the human communicating nerve to the vocal cord innervation.

With S2 stimulation after superior pole dissection, positive glottic response via ETT was achieved from 45 EBSLNs (67.2%) out of 67 including 33 (84.6%) of 39 nerves having positive glottic response with S1 stimulation, seven (33.3%) of 21 nerves having negative glottic response with S1 stimulation, and five of seven nerves detected after superior pole dissection. In 33% of the EBSLNs, with S2 stimulation, quantitative EMG responses were not able to be obtained via ETT regarding the EBSLN function.

The glottic response obtained in addition to the CTM twitch may change before and after superior pole dissection. In six out of 39 EBSLNs with positive EMG glottic response via S1, despite the positive CTM twitch via S2 stimulation, there was a negative glottic EMG response. Although this is primarily thought to be resulting from ETT malpositioning due to the tracheal displacement after tracheal traction and thyroidectomy, the possibility of injury to the human communicating nerve or its intralaryngeal anastomoses or partial injury of the EBSLN cannot be ignored.

Despite the presence of CTM twitch, negative S2 glottic response should not be considered an EBSLN injury. Although CTM twitch is the main positive finding in the EBSLN neuromonitoring via ETT, false-positive CTM twitch can be observed in partial EBSLN injury due to non-neural shunt stimulation via collateral stimulation using a probe within a 2-cm area of the CTM.

Sung et al. (31) prospectively evaluated the diagnostic value of the CTM twitch inspection via postoperative CTM EMG to determine EBSLN integrity in 712 EBSLNs at risk. They found high diagnostic values regarding the CTM inspection for sensitivity and positive predictive value (97.7% and 92.5%, respectively). Despite the low false-negative rate (2.3%), the false-positive rate was high (94.5%), and low specificity (5.5%) and negative predictive value (16.7%) were observed. The authors concluded that CTM twitch observation could be used in determining the EBSLN integrity, but it may not replace EMG considering the low specificity and negative predictive value. The results of this extensive and prospective study are important.

We think that intraoperative CTM EMG can provide important additional informative data on this subject.

There are some limitations of our study. First, it is a retrospective study Although the EBSLN is stimulated at the most cranial portion above the area of the divided superior pole vessels, it cannot be 100% guaranteed whether the nerve is injured more proximally or not. The weak point of this study is that postoperative objective and subjective voice tests have not been performed. To eliminate this, a study should be conducted to prospectively evaluate postoperative voice quality to confirm the anatomical and functional integrity of the EBSLN proved by the use of CTM EMG in the present study. Second, CTM EMG was performed intraoperatively after the thyroidectomy and was not compared with either CTM EMG performed before upper pole dissection or postoperative CTM EMG, which is accepted as a gold standard method. However, as far as we know, this study is the first to evaluate the contribution of intraoperative CTM EMG to the quantitative data obtained via IONM with ETT. It is important to obtain quantitative positive EMG recordings from the CTM in all of the EBSLNs, to be able to store them, and to have high EMG amplitude values in terms of the EBSLN function. CTM EMG is a simple, safe, and applicable method for surgeons using IONM.

In conclusion, in addition to the IONM via ETT, intraoperative post-dissection CTM EMG via a needle electrode is a safe, simple, and applicable method. It is a method that may provide significant additional informative data to IONM with ETT by obtaining and recording objective quantitative data related to the EBSLN function.

Data availability statement

The original contributions presented in the study are included in the article/supplementary material. Further inquiries can be directed to the corresponding author.

Author contributions

NA: Conceptualization, Investigation, Writing – original draft, Writing – review & editing. MU: Conceptualization, Data curation, Investigation, Methodology, Writing – review & editing. MK: Data curation, Investigation, Methodology, Writing – review & editing. OC: Data curation, Investigation, Methodology, Writing – review & editing. AI: Supervision, Writing – review & editing. MU: Conceptualization, Investigation, Supervision, Writing – review & editing.

Funding

The author(s) declare that no financial support was received for the research, authorship, and/or publication of this article.

Conflict of interest

The authors declare that the research was conducted in the absence of any commercial or financial relationships that could be construed as a potential conflict of interest.

Publisher's note

References

1. Nam IC, Park YH. Pharyngolaryngeal symptoms associated with thyroid disease. *Curr Opin Otolaryngol Head Neck Surg* (2017) 25:469–74. doi: 10.1097/MOO.0000000000000404

2. Zealear DL, Billante CR. Neurophysiology of vocal fold paralysis. *Otolaryngol Clin N Am* (2004) 37:1–23. doi: 10.1016/S0030-6665(03)00165-8

3. Wu BL, Sanders I, Mu L, Biller HF. The human communicating nerve. An extension of the external superior laryngeal nerve that innervates the vocal cord. *Arch Otolaryngol Head Neck Surg* (1994) 120:1321–8. doi: 10.1001/archotol.1994.01880360019004

4. Maranillo E, Leon X, Quer M, Orus C, Sanudo JR. Is the external laryngeal nerve an exclusively motor nerve? The cricothyroid connection branch. *Laryngoscope* (2003) 113:525–9. doi: 10.1097/00005537-200303000-00024

5. Cernea CR, AR F, Nishio S, Dutra AJr, FC H, dos Santos LR. Surgical anatomy of the external branch of the superior laryngeal nerve. *Head Neck* (1992) 14(5):380–3. doi: 10.1002/hed.2880140507

6. Cheruiyot I, Kipkorir V, Henry BM, Munguti J, Cirocchi R, Odula P, et al. Surgical anatomy of the external branch of the superior laryngeal nerve: a systematic review and meta-analysis. *Langenbecks Arch Surg* (2018) 403(7):811–23. doi: 10.1007/s00423-018-1723-9

7. Feng AL, Puram SV, Singer MC, Modi R, Kamani D, Randolph GW. Increased prevalence of neural monitoring during thyroidectomy: global surgical survey. *Laryngoscope* (2020) 130:1097–104. doi: 10.1002/lary.28210

8. Randolph GW, Dralle HInternational Intraoperative Monitoring Study Group, , Abdullah H, Barczynski M, Bellantone R, et al. Electrophysiologic recurrent laryngeal nerve monitoring during thyroid and parathyroid surgery: international standards guideline statement. *Laryngoscope* (2011) 121:S1–16. doi: 10.1002/lary.21119

9. Barczyński M, Randolph GW, Cernea CR, Dralle H, Dionigi G, Alesina PF, et al. External branch of the superior laryngeal nerve monitoring during thyroid and parathyroid surgery: International Neural Monitoring Study Group standards guideline statement. *Laryngoscope* (2013) 123:S1–14. doi: 10.1002/lary.24301

10. Bellantone R, Boscherini M, Lombardi CP, Bossola M, Rubino F, De Crea C, et al. Is the identification of the external branch of the superior laryngeal nerve mandatory in thyroid operation? Results of a prospective randomized study. *Surgery* (2001) 130:1055–9. doi: 10.1067/msy.2001.118375

11. Lennquist S, Cahlin C, Smeds S. The superior laryngeal nerve in thyroid surgery. *Surgery* (1987) 102:999–1008.

12. Cernea CR, Ferraz AR, Furlani J, Monteiro S, Nishio S, Hojaij FC, et al. Identification of the external branch of the superior laryngeal nerve during thyroidectomy. *Am J Surg* (1992) 164:634–9. doi: 10.1016/S0002-9610(05)80723-8

13. Uludag M, Aygun N, Kartal K, Besler E, Isgor A. Is intraoperative neural monitoring necessary for exploration of the superior laryngeal nerve? *Surgery* (2017) 161:1129–38. doi: 10.1016/j.surg.2016.10.026

14. Uludag M, Aygun N, Kartal K, Çitgez B, Besler E, Yetkin G, et al. Contribution of intraoperative neural monitoring to preservation of the external branch of the superior laryngeal nerve: A randomized prospective clinical trial langenbecks arch surg. *Langenbeck's Archives of Surgery* (2017) 402:965–76. doi: 10.1007/s00423-016-1544-7

15. Barczyński M, Konturek A, Stopa M, Honowska A, Nowak W. Randomized controlled trial of visualization versus neuromonitoring of the external branch of the superior laryngeal nerve during thyroidectomy. *World J Surg* (2012) 36:1340–7. doi: 10.1007/s00268-012-1547-7

16. Potenza AS, Phelan EA, Cernea CR, Slough CM, Kamani DV, Darr A, et al. Normative intra-operative electrophysiologic waveform analysis of superior laryngeal nerve external branch and recurrent laryngeal nerve in patients undergoing thyroid surgery. *World J Surg* (2013) 37:2336–42. doi: 10.1007/s00268-013-2148-9

17. Grover G, Sadler GP, Mihai R. Morbidity after thyroid surgery: patient perspective. *Laryngoscope* (2013) 123:2319–23. doi: 10.1002/lary.23850

18. Potenza AS, Araujo Filho VJF, Cernea CR. Injury of the external branch of the superior laryngeal nerve in thyroid surgery. *Gland Surg* (2017) 6:552–62. doi: 10.21037/gs.2017.06.15

19. Dralle H, Lorenz K, Machens A. Verdicts on malpractice claims after thyroid surgery: emerging trends and future directions. *Head Neck* (2012) 34:1591–6. doi: 10.1002/hed.21970

20. Uludag M, Aygun N, Isgor A. Motor function of the recurrent laryngeal nerve: sometimes motor fibers are also located in the posterior branch. *Surgery* (2016) 160:153–60. doi: 10.1016/j.surg.2016.02.003

21. Aygün N, Uludağ M, İşgör A. Contribution of intraoperative neuromonitoring to the identification of the external branch of superior laryngeal nerve. *Turk J Surg* (2017) 33:169–74. doi: 10.5152/turkjsurg.2017.3645

22. Dionigi G, Kim HY, Randolph GW, Wu CW, Sun H, Liu X, et al. Prospective validation study of Cernea classification for predicting EMG alterations of the external branch of the superior laryngeal nerve. *Surg Today* (2016) 46:785–91. doi: 10.1007/s00595-015-1245-9

23. Martin-Oviedo C, Maranillo E, Lowy-Benoliel A, Pascual-Font A, Martinez-Guirado T, Rodriguez-Niedenführ M, et al. Functional role of human laryngeal nerve connections. *Laryngoscope* (2011) 21:2338–43. doi: 10.1002/lary.22340

24. Uludag M, Aygun N, Isgor A. Innervation of the human cricopharyngeal muscle by the recurrent laryngeal nerve and external branch of the superior laryngeal nerve. *Langenbeck's Arch Surg* (2017) 402:683–90. doi: 10.1007/s00423-016-1376-5

25. Barczyński M, Randolph GW, Cernea C. International Neural Monitoring Study Group in Thyroid and Parathyroid Surgery. International survey on the identification and neural monitoring of the EBSLN during thyroidectomy. *Laryngoscope* (2016) 126:285–91. doi: 10.1002/lary.25548

26. Liddy W, Barber SR, Cinquepalmi M, Lin BM, Patricio S, Kyriazidis N, et al. The electrophysiology of thyroid surgery: electrophysiologic and muscular responses with stimulation of the vagus nerve, recurrent laryngeal nerve, and external branch of the superior laryngeal nerve. *Laryngoscope* (2017) 127:764–71. doi: 10.1002/lary.26147

27. Selvan B, Babu S, Paul MJ, Abraham D, Samuel P, Nair A. Mapping the compound muscle action potentials of cricothyroid muscle using electromyography in thyroid operations: a novel method to clinically type the external branch of the superior laryngeal nerve. *Ann Surg* (2009) 250:293–300. doi: 10.1097/SLA.0b013e3181b17342

28. Gavid M, Dubois MD, Larivé E, Prades JM. Superior laryngeal nerve in thyroid surgery: anatomical identification and monitoring. *Eur Arch Otorhinolaryngol* (2017) 274:3519–26. doi: 10.1007/s00405-017-4666-9

29. Iwata AJ, Liddy W, Barczyński M, Wu CW, Huang TY, Van Slycke S, et al. Superior laryngeal nerve signal attenuation influences voice outcomes in thyroid surgery laryngoscope. *Laryngoscope* (2021) 131:1436–42. doi: 10.1002/lary.29413

30. Patnaik U, Nilakantan A, Shrivastava T. Anatomical variations of the external branch of the superior laryngeal nerve in relation to the inferior constrictor muscle: cadaveric dissection study. *J Laryngol Otol* (2012) 126:907–12. doi: 10.1017/S0022215112001454

31. Sung ES, Chang JH, Kim J, Cha W. Is cricothyroid muscle twitch predictive of the integrity of the EBSLN in Thyroid Surgery? *Laryngoscope* (2018) 128:2654–61. doi: 10.1002/lary.27158

frontiers | Frontiers in Endocrinology

TYPE Clinical Trial
PUBLISHED 08 January 2024
DOI 10.3389/fendo.2023.1251820

Check for updates

OPEN ACCESS

EDITED BY
Gianlorenzo Dionigi,
University of Milan, Italy

REVIEWED BY
Ahmet Cem Dural,
Istinye University, Türkiye
Loris Bertazza,
University of Padua, Italy

*CORRESPONDENCE
Ming Gao
gaoming68@aliyun.com
Xiangqian Zheng
anlozxq@126.com

RECEIVED 02 July 2023
ACCEPTED 11 December 2023
PUBLISHED 08 January 2024

CITATION
Zhao J, Wang J, Cheng R, Qin J, Ai Z, Sun H, Guo Z, Zhang X, Zheng X and Gao M (2024) Safety and effectiveness of carbon nanoparticles suspension-guided lymph node dissection during thyroidectomy in patients with thyroid papillary cancer: a prospective, multicenter, randomized, blank-controlled trial.
Front. Endocrinol. 14:1251820.
doi: 10.3389/fendo.2023.1251820

Safety and effectiveness of carbon nanoparticles suspension-guided lymph node dissection during thyroidectomy in patients with thyroid papillary cancer: a prospective, multicenter, randomized, blank-controlled trial

Jingzhu Zhao[1], Junyi Wang[1], Ruochuan Cheng[2], Jianwu Qin[3], Zhilong Ai[4], Hui Sun[5], Zhuming Guo[6], Xiaohua Zhang[7], Xiangqian Zheng[1]* and Ming Gao[1,8]*

[1]Department of Thyroid and Neck Tumor, Tianjin Medical University Cancer Institute and Hospital, National Clinical Research Center for Cancer, Tianjin's Clinical Research Center for Cancer, Key Laboratory of Cancer Prevention and Therapy, Tianjin, China, [2]Department of Thyroid Disease Diagnosis and Treatment Center, First Affiliated Hospital of Kunming Medical University, Yunnan, China, [3]Department of Thyroid & Neck Surgery, Henan Cancer Hospital, Affiliated Cancer Hospital of Zhengzhou University, Zhengzhou, China, [4]General Surgery, Zhongshan Hospital Fudan University, Shanghai, China, [5]Department of Thyroid Surgery, China Japan Union Hospital of Jilin University, Jilin, China, [6]State Key Laboratory of Oncology in South China, Collaborative Innovation Center for Cancer Medicine, Sun Yat-sen University Cancer Center, Guangzhou, China, [7]Department of Thyroid & Breast Surgery, The First Affiliated Hospital of Wenzhou Medical University, Wenzhou, China, [8]Department of Breast and Thyroid Diseases, Tianjin Union Medical Center, Tianjin, China

Objective: This study aimed to evaluate the effectiveness and safety of carbon nanoparticles-guided lymph node dissection during thyroidectomy in patients with papillary thyroid cancer(PTC).

Methods: Clinical trials consisted of two subgroups: unilateral lobectomy (UL; n=283) and total thyroidectomy (TT; n=286). From each subgroup, the patients were randomly assigned to two groups: the carbon nanoparticle group and control group. Primary endpoints included parathyroid hormone (PTH) levels, number of lymph nodes (LNs) detected, number of tiny lymph nodes detected, and recognition and retention of the parathyroid glands. Secondary endpoint was recognition and protection of the recurrent laryngeal nerve.

Results: A total of 569 patients with PTC were recruited. There were no statistically significant differences in demographics between the carbon nanoparticles and control groups ($P > 0.05$). In the UL subgroup, there were no significant differences in PTH levels between the two groups at preoperative, intraoperative, and postoperative day one, and postoperative

month one (P>0.05). There was no significant difference in the serum Ca^{2+} levels between the two groups preoperatively and at postoperative month one (P>0.05). The number of lymph nodes dissected in the carbon nanoparticles group was significantly higher than that in the control group (P<0.0001). The detection rate of tiny lymph nodes in the carbon nanoparticles group was higher than that in the control group (P=0.0268). In the TT subgroup, there was no significant difference in PTH levels between the two groups at preoperative, intraoperative, and postoperative day one (P>0.05). However, the mean PTH level in the carbon nanoparticles group was significantly higher than that of the control group at postoperative month one (P=0.0368). There was no significant difference in the serum Ca^{2+} levels between the two groups preoperatively and at postoperative month one (P>0.05). There were no significant differences between the two groups in the number of dissected LNs (P>0.05) or the detection rate of tiny lymph nodes (P>0.05). No drug-related AE and complications due to the injection of carbon nanoparticles were recorded in this study. There were no significant differences between the two groups in terms of parathyroid preserved *in situ* and recurrent laryngeal nerve injury in the UL and TT subgroups.

Conclusions: Carbon nanoparticles demonstrated efficacy and safety in thyroidectomy. The application of carbon nanoparticles could significantly facilitate the identification and clearance of LNs and the optimum preservation of parathyroid function.

Clinical trial registration: https://www.chictr.org.cn/, identifier ChiCTR2300068502.

KEYWORDS

clinical trial, papillary thyroid cancer, carbon nanoparticles, parathyroid hormone, lymph node, thyroidectomy

1 Background

Papillary thyroid cancer (PTC) is a common endocrine malignancy, and its incidence has increased substantially in recent decades (1). The most effective treatment for PTC is complete removal of the primary tumor and metastatic regional lymph nodes. Complete lymph node dissection is key to reducing recurrence and improving prognosis. However, the patient's quality of life needs to be considered (2). Hypoparathyroidism and voice disorders are the two most common complications that can considerably affect the quality of life of patients (3). Effective protection of the parathyroid gland and recurrent laryngeal nerve is the best way to improve a patient's quality of life.

Carbon nanoparticles (CNs) are novel lymphatic tracers that have been successfully used for lymph node tracing in colorectal, breast, and gastric cancers (4–6). CNs have the advantages of a high specificity in the lymphatic system and low toxicity. Recently, carbon nanoparticles have been used to detect lymph nodes in PTC (7, 8). However, they were all monocentric studies with limited sample sizes. We conducted this prospective multicenter randomized controlled trial to evaluate the safety and effectiveness of carbon nanoparticles in thyroidectomy for PTC.

2 Patients and methods

2.1 Study design

This was a multicenter, randomized, blank-controlled study (ChiCTR2300068502 Http://www.chictr.org.cn/). This study was conducted in accordance with the Declaration of Helsinki and approved by the institutional review board. Written informed consent was obtained from all patients.

Based on the different resection ranges of the primary lesions, the clinical trials were divided into two subgroups: unilateral lobectomy and total thyroidectomy.

Patients satisfying the following criteria were recruited in the unilateral lobectomy group: (1) preoperative and intraoperative

diagnosis of untreated, unilateral, and single-focal papillary thyroid carcinoma; (2) no cervical lymph node metastasis on imaging examination, and no indication of lateral neck lymph node dissection; (3) unilateral lobectomy plus isthmectomy with ipsilateral central lymph node dissection; (4) age 18–70 years; (5) results of preoperative laboratory blood test–neutrophils (ANC) $\geq 1.5\times10^9$/L, platelets (PLT) $\geq 100\times10^9$/L, total bilirubin (TBI) ≤2 times the upper limit of normal (ULN) (2 mg/dL), alanine aminotransferase (ALT) ≤2 times the ULN, and aspartate aminotransferase (AST) ≤2 times the ULN; and (6) signed informed consent.

Patients who met the following criteria were recruited into the total thyroidectomy group: (1) preoperatively and intraoperatively diagnosed with untreated, unilateral, and single-focal papillary thyroid carcinoma; (2) no enlarged lymph nodes on physical examination; and lateral cervical lymph node metastasis on imaging examination; (3) total/near total thyroidectomy, ipsilateral central and lateral lymph node dissection; (4) age 18–70 years; (5) preoperative laboratory blood test results (ANC$\geq 1.5\times10^9$/L, PLT$\geq 100\times10^9$/L, TBI ≤ 2 times ULN (2 mg/dL), ALT ≤ 2 times ULN, AST ≤ 2 times ULN; and (6) signed informed consent.

Patients were excluded if they met one or more of the following criteria: (1) concomitant Hashimoto's thyroiditis; (2) active stage of liver disease or abnormal liver function, with ALT, AST, and TBIL≥2 times the ULN; (3) renal function impairment, Cr≥2 times the ULN or BUN≥2 times the ULN; (4) a history of alcohol, drug, or substance abuse and disturbance of blood coagulation; and (5) a history of serious uncontrolled medical disease, recent myocardial infarction, or acute infection.

2.2 Outcome

The primary endpoints included parathyroid hormone (PTH) levels, number of lymph nodes detected, number of tiny lymph nodes detected, and recognition and retention of the parathyroid glands. The secondary endpoint was recognition and protection of the recurrent laryngeal nerve. PTH levels were measured preoperatively, intraoperatively, and on postoperative days 1 and 1 month.

2.3 Statistical methods

All statistical analyses were performed using SAS version 9.4 statistical professional analysis software. Measurements were reported as the mean standard deviation. Continuous measurements were compared using the t-test, and count data were analyzed using the chi-squared test. The Wilcoxon rank-sum test was used for intergroup comparisons. The safety analysis was based on descriptive analytics. The adverse events and the incidence in each group were listed in the table and compared using the chi-square test or Fisher's exact test. Statistical significance was set at P value < 0.05.

3 Results

3.1 Patients' characteristics

A total of 569 patients with PTC from seven hospitals across China were enrolled. According to the different resection ranges of the primary lesion, they were assigned to two subgroups: the unilateral lobectomy group (UL, 283 patients) and total thyroidectomy group (TT, 286 patients), who were randomly assigned to the carbon nanoparticles group (A group) or control group (B group), respectively (Figure 1). The LNs in the A group were stained black by nanoparticles (Figure 2). As shown in Table 1, no significant differences were detected between the two groups regarding baseline characteristics.

3.2 Changes and comparison of PTH level

In the UL group, there were no significant differences between the carbon nanoparticles and control groups in terms of preoperative (P=0.1582), intraoperative (P=0.9048), and postoperative day one (P=0.7747) and first month (P=0.3840) serum PTH levels, Table 2.

In the TT group, there was no significant difference between the carbon nanoparticles and control groups in terms of preoperative (P=0.6870), intraoperative (P=0.6719), and postoperative day one (P=0.4255) serum PTH levels. However, the mean serum PTH in carbon nanoparticles group was significantly higher than that of the control group (25.92 ± 19.76 mmol/L *vs.* 21.29 ± 19.68 mmol/L, P=0.0368) on first month post-operation, Table 2.

3.3 Comparison of serum Ca^{2+} level

In the UL group, there was no significant difference between the carbon nanoparticles and control groups in terms of preoperative (P=0.4237) and first month post-operation (P=0.428) serum Ca^{2+} levels. While, there was no significant difference between the carbon nanoparticle and control groups in terms of preoperative (P=0.6148) and first month post-operation (P=0.99) serum Ca^{2+} levels in the TT group, Table 3.

3.4 Comparison of the number of LNs dissected

In UL group, the number of LNs dissected from the carbon nanoparticles group was significantly higher than that of the control group (8.02 ± 7.70 vs 5.37 ± 5.63, P< 0.0001). The detection rate of tiny lymph nodes in the carbon nanoparticles group was higher than that in the control group (P=0.0268). The number of tiny lymph nodes was also higher in the carbon nanoparticles group; however, the difference was not statistically significant (4.99 ± 3.80 vs. 3.93 ± 3.23, P=0.0823). Furthermore, significantly more ≤2 mm lymph

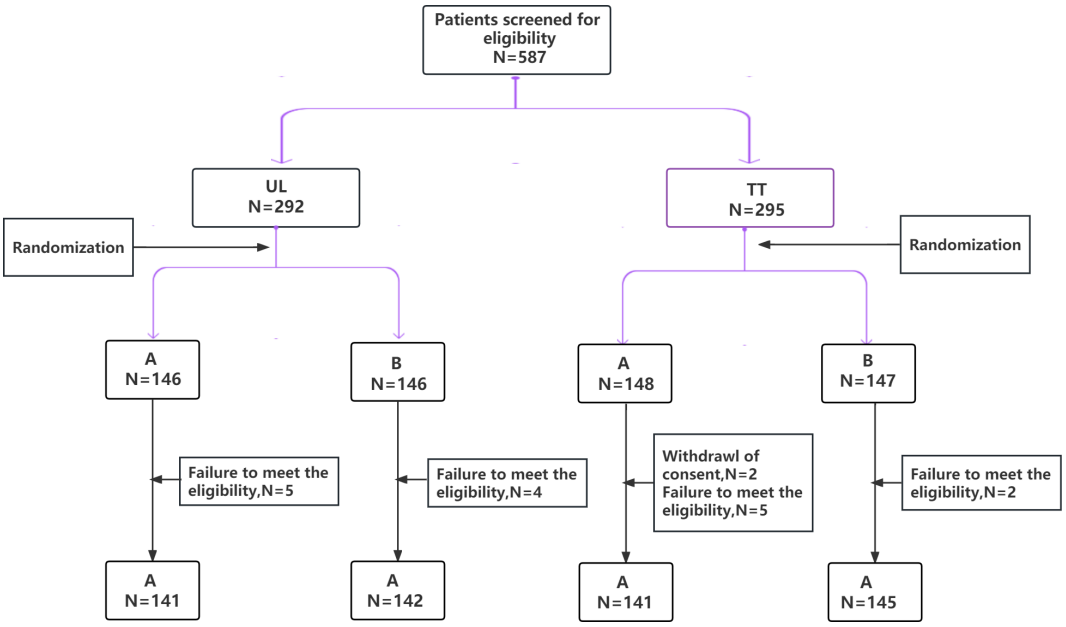

FIGURE 1
CONSORT diagram of patients randomized to used carbon nanoparticles group (A group) or control group (B group). According to the different resection ranges of the primary lesion, they were assigned to two subgroups: the unilateral lobectomy group (UL) and total thyroidectomy group (TT).

nodes were detected in the carbon nanoparticles group than that of the control group (2.45 ± 3.14 vs. 1.45 ± 2.55, P=0.0034), Table 4.

In the TT group, the number of dissected LNs was higher in the carbon nanoparticles group; however, the difference was not statistically significant (40.82 ± 21.61 vs. 38.20 ± 19.14, P=0.4346). In addition, the numbers and detection rate of tiny lymph nodes was also higher in the carbon nanoparticles group; however, the difference was not statistically significant (80.15% vs. 78.47%, P=0.7296;12.15 ± 8.96 vs 10.45 ± 7.73, P=0.1750). Furthermore, the number of ≤2 mm lymph nodes was also higher in the carbon nanoparticles group, and

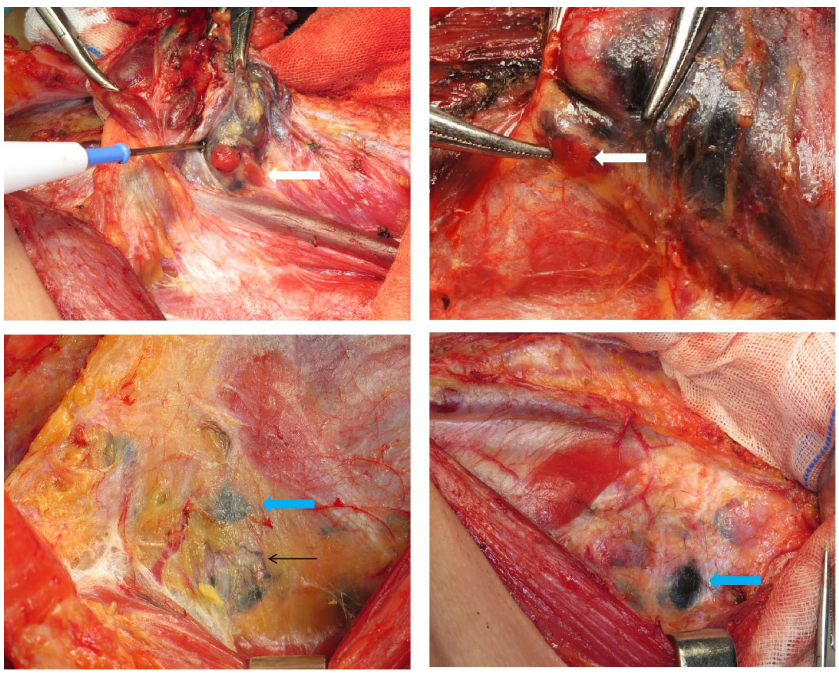

FIGURE 2
Carbon nanoparticles were injected into the thyroid around the tumour; the white arrow shows the parathyroid gland(negative staining); the green arrows show the lymph nodes coloured black; the black arrows show the lymph ducts coloured black.

10.3389/fendo.2023.1251820

TABLE 1 Comparison of baseline characteristics between carbon nanoparticles group and control group in UL and TT subgroup.

		UL		TT	
		A(N=141)	B(N=142)	A(N=141)	B(N=145)
Gender					
	Female	93(65.96)	100(70.42)	90(63.83)	95(65.52)
	Male	48(34.04)	42(29.58)	51(36.17)	50(34.48)
	χ^2	0.65		0.09	
	P	0.4200		0.7653	
Ages(Y)					
	Mean ± SD	41.17 ± 9.96	42.50 ± 10.66	40.16 ± 10.57	37.80 ± 10.48
	Median	42.00	42.00	40.00	37.00
	Min~Max	21.00~66.00	21.00~69.00	17.00~68.00	14.00~65.00
	t	1.084		1.90	
	P	0.2794		0.0586	
BMI(kg/m2)					
	Mean ± SD	23.70 ± 3.56	23.65 ± 3.36	23.78 ± 3.42	25.11 ± 4.12
	Median	23.2	23.43	23.50	24.60
	Min~Max	16.20~34.60	16.53~31.20	17.57~33.00	17.58~41.50
	t	0.136		2.31	
	P	0.8917		0.0208	
Allergic history					
	No	123(87.23)	120(84.51)	126(89.36)	12(86.21)
	Yes	18(12.77)	22(15.49)	15(10.64)	20(13.79)
	χ^2	0.43		0.66	
	P	0.5103		0.4157	
Stage T	N(missing)	132(9)	133(9)	132(9)	142(3)
	T1+T2	111(84.09)	111(83.46)	105(79.55)	105(73.94)
	T3+T4	21(15.91)	22(16.54)	27(20.45)	37(26.06)
	χ^2	0.02		1.20	
	P	0.8890		0.2735	
Stage N	N(missing)	131(10)	133(9)	132(9)	142(3)
	NX	0(0.00)	4(3.01)	0(0.00)	0(0.00)
	N0	81(61.83)	82(61.65)	4(3.03)	8(5.63)
	N1	50(38.17)	47(35.34)	128(96.97)	134(94.37)
	CMH-χ^2	4.07		1.11	
	P	0.1308		0.2927	

BMI, Body mass index; A, carbon nanoparticles group; B, Control group.

10.3389/fendo.2023.1251820

TABLE 2 Changes and comparison of parathyroid hormone at different time points in UL and TT subgroup.

		UL			TT	
		A(N=141)	B(N=142)		A(N=141)	B(N=145)
Preoperative	N(missing)	135(6)	137(5)	N	134(7)	142(3)
	Mean(sd)	37.91(21.99)	34.52(17.23)	Mean(sd)	29.51(23.26)	28.60(24.28)
	Median	36.09	34.6	Median	28.32	29.80
	Min~max	2.18~164.41	2.30~81.90	Min~max	1.02~123.60	1.20~114.80
	t	1.42		Wilcoxon Z	0.40	
	P	0.1582		*P*	0.6870	
Intraoperative	N(missing)	140(1)	137(5)	N	140(1)	143(2)
	Mean(sd)	32.65(19.92)	32.95(20.97)	Mean(sd)	11.97(14.48)	13.41(19.46)
	Median	28.92	31.4	Median	6.04	5.82
	Min~max	2.50~97.40	2.10~120.00	Min~max	0.38~76.46	0.29~115.50
	t	0.12		Wilcoxon Z	0.42	
	P	0.9048		*P*	0.6719	
Postoperative days 1	N(missing)	138(3)	135(7)	N	137(4)	143(2)
	Mean(sd)	25.94(15.63)	25.40(15.04)	Mean(sd)	8.79(9.82)	8.76(11.24)
	Median	27.13	25.9	Median	5.39	3.93
	Min~max	0.90~71.30	1.70~64.40	Min~max	0.01~53.40	0.10~61.44
	t	0.29		Wilcoxon Z	0.80	
	P	0.7747		*P*	0.4255	
Postoperative 1 month	N(missing)	125(16)	130(12)	N	121(20)	133(12)
	Mean(sd)	35.08(16.23)	37.07(20.01)	Mean(sd)	25.73(19.80)	21.09(19.55)
	Median	34.5	34.43	Median	24.88	17.16
	Min~max	1.31~79.70	2.50~132.70	Min~max	1.29~82.20	0.60~80.17
	t	0.87		Wilcoxon Z	2.09	
	P	0.3840		*P*	0.0368	

A: Carbon nanoparticles group; B: Control group.

TABLE 3 Comparison of serum Ca^{2+} level between carbon nanoparticles group and control group in UL and TT subgroup.

		UL			TT	
		A(N=141)	B(N=142)		A(N=141)	B(N=145)
Preoperative	Mean(sd)	2.33(0.11)	2.32(0.12)	Mean(sd)	2.35(0.11)	2.36(0.20)
	t	0.8		t	0.50	
	P	0.4237		*P*	0.6148	
Postoperative 1 month	Mean(sd)	2.36(0.12)	2.40(0.48)	Mean(sd)	2.36(0.16)	2.35(0.18)
	K-W	0.63		Wilcoxon Z	0.00	
	P	0.428		*P*	0.99	

A: Carbon nanoparticles group; B: Control group.

10.3389/fendo.2023.1251820

TABLE 4 Comparion of the number of LNs dissected between carbon nanoparticles group and control group in UL and TT subgroup.

		UL		TT	
		A(N=141)	B(N=142)	A(N=141)	B(N=145)
Number of LNs dissected	N(missing)	139(2)	142(0)	136(5)	144(1)
	Mean(sd)	8.02(7.70)	5.37(5.63)	40.82(21.61)	38.20(19.14)
	Median	6	4	36.00	35.00
	Min~max	0.00~70.00	0.00~35.00	9.00~139.00	6.00~152.00
	Wilcoxon Z	4.71		0.78	
	P	<0.0001		0.4346	
Tiny LNs	N(missing)	139(2)	140(2)	136(5)	144(1)
	Yes(%)	76(54.68)	58(41.43)	109(80.15)	113(78.47)
	No(%)	63(45.32)	82(58.57)	27(19.85)	31(21.53)
	χ^2	4.9		0.12	
	P	0.0268		0.7296	
Number of tiny LNs	N(missing)	76(0)	58(0)	109(0)	113(0)
	Mean(sd)	4.99(3.80)	3.93(3.23)	12.15(8.96)	10.45(7.73)
	Median	4	3	9.00	9.00
	Min~max	1.00~17.00	1.00~20.00	1.00~44.00	1.00~34.00
	Wilcoxon Z	1.74		1.36	
	P	0.0823		0.1750	
Number of ≤2mm LNs	N(missing)	138(3)	138(4)	141(7)	144(3)
	Mean(sd)	2.45(3.14)	1.45(2.55)	9.77(9.34)	8.24(7.96)
	Median	1	0	1	0
	Min~max	0.00~16.00	0.00~20.00	0.00~44.00	0.00~34.00
	Wilcoxon Z	2.93		1.16	
	P	0.0034		0.2449	

LNs: lymph nodes; A: Carbon nanoparticles group; B: Control group.

the difference was not statistically significant (9.77 ± 9.34 vs 8.24 ± 7.96, P=0.2449), Table 4.

3.5 Safety outcomes and operative complications

No drug-related AE or complications due to the injection of carbon nanoparticles were recorded in this study. There were no significant differences between the two groups in recurrent laryngeal nerve injury (three cases *vs.* one case) in the UL group. There were no significant differences between the two groups in recurrent laryngeal nerve injury (five *vs.* four cases) in the TT group. There were no significant differences between the carbon nanoparticles group and control groups regarding the parathyroid gland preserved *in situ* in the UL and TT groups, Table 5.

4 Discussion

This is the first prospective multicenter randomized blank-controlled trial. The study met its primary endpoint and carbon nanoparticles were proven to be safe.

The most effective treatment for PTC is complete removal of the primary and metastatic lymph nodes. However, the insensitivity of preoperative imaging may lead to an incomplete lymph node dissection. Although not usually fatal, it can lead to repeated surgeries and more damage to patients. Previous sample- or single-center studies have shown that carbon nanoparticles can effectively detect more lymph nodes in colorectal cancer (6, 9) and papillary thyroid cancer (7, 8, 10). In contrast, another study showed that carbon nanoparticles did not generate significant benefits in lymph node dissection (11). However, this study shows that CNs may help detect more lymph nodes and tiny

10.3389/fendo.2023.1251820

TABLE 5 Comparion of parathyroid preserved *in situ* between carbon nanoparticles and control groups in UL and TT subgroup.

	UL		TT	
	A(N=124)	B(N=125)	A(N=124)	B(N=133)
Upper-left				
N(missing)	53(71)	61(64)	123(1)	127(6)
Yes	49(92.45)	61(100.00)	119(96.75)	123(96.85)
No	4(7.55)	0(0.00)	4(3.25)	4(3.15)
*P**	0.0439		1.0000	
Upper-right				
N(missing)	71(53)	65(60)	123(1)	132(1)
Yes	67(94.37)	62(95.38)	120(97.56)	126(95.45)
No	4(5.63)	3(4.62)	3(2.44)	6(4.55)
*P**	1.0000		0.5025	
Lower-left				
N(missing)	53(71)	61(64)	112(12)	126(7)
Yes	42(79.25)	52(85.25)	99(88.39)	105(83.33)
No	11(20.75)	9(14.75)	13(11.61)	21(16.67)
χ^2	0.71		1.24	
P	0.4008		0.2656	
Lower-right				
N(missing)	71(53)	65(60)	117(7)	129(4)
Yes	65(91.55)	51(78.46)	105(89.74)	104(80.62)
No	6(8.45)	14(21.54)	12(10.26)	25(19.38)
χ^2	4.63		4.00	
P	0.0313		0.0456	

*Fisher exact test; A: Carbon nanoparticles group; B: Control group.

lymph nodes in papillary thyroid cancer, which may allow for more radical dissection. But, in terms of the number of lymph nodes removed, the trend between the UL groups and TT groups was inconsistent, which may be due to the following reasons: 1. Due to dynamic reasons, carbon nanoparticles are more likely to distribute in the central lymph nodes, and the distribution is limited in the whole region of the lateral neck, and the number of lymph nodes in the lateral neck region is much more than that in the central region. 2. In the TT group, patients with lateral cervical metastasis had a high probability of lymphatic blockage, and carbon nanoparticles were not easily distributed in lymphatic vessels.

Post-thyroidectomy hypocalcemia is the most common complication that seriously affects patients' quality of life. In a few cases, hypocalcemia can be severe and lead to acute life-threatening conditions, such as tetany, laryngospasm, arrhythmias, and heart failure (12). Effective preservation of the parathyroid gland is the best method to prevent hypocalcemia.

Clinically, parathyroid glands may be accidentally removed as LNs owing to variations in position. CNs have high specificity for the lymphatic system as lymph tracers. CNs have been successfully applied in gastric (13) and breast cancers (14). Once entering the lymphatic system, CNs can cause black-stained of the LNs but not neighboring tissues, especially the parathyroid gland, so-called "negative staining". This allows for the identification and clearance of LNs and the optimum preservation of parathyroid function. In our study, although there was no significant difference in the number of preserved parathyroid glands between the carbon nanoparticles and control groups, the parathyroid hormone level recovered more quickly in the carbon nanoparticles group than in the control group within the postoperative one month, indicating that carbon nanoparticles are essential for the protection of parathyroid function. This apparent protection by CNs staining may help surgeons preserve the parathyroid glands *in situ* during the operation with maximum retention of the blood supply, including tiny blood vessels around the parathyroid gland. Therefore, carbon nanoparticles are recommended for patients undergoing thyroidectomy, particularly for total thyroidectomy.

Although there was a significant difference in the parathyroid hormone level between the carbon nanoparticles and control groups at postoperative one month in the TT subgroup, there was

no significant difference in serum Ca^{2+} levels, possibly because patients were given regular calcium supplements.

No drug-related AE or complications due to the injection of carbon nanoparticles were recorded in this study. There were no significant differences between the two groups with respect to recurrent laryngeal nerve injury in the UL and TT subgroups. None of the patients experienced any discomfort during the study period. The clinical application of CNs has shown no toxicity (6, 13, 15).

This study had several limitations. First, this study could not be double-blind and may be biased when clinicians perform surgery. More, this study adopted competitive enrollment, and experienced surgical centers have more participants, which may lead to selection bias. Experienced surgeons, whether using carbon nanoparticles or not, have less impact on parathyroid blood flow and are less likely to miscut.

5 Conclusion

In conclusion, this prospective, multicenter, randomized, blank-controlled study confirmed that CNs are effective and safe for papillary thyroid cancer. More importantly, the application of carbon nanoparticles could significantly facilitate the identification and clearance of LNs and optimum preservation of parathyroid function.

Data availability statement

The original contributions presented in the study are included in the article/supplementary material. Further inquiries can be directed to the corresponding authors.

Ethics statement

This study was conducted in accordance with the Declaration of Helsinki and approved by the institutional review board. Written informed consent was obtained from all patients. The studies were conducted in accordance with the local legislation and institutional requirements. Written informed consent for participation in this study was provided by the participants' legal guardians/next of kin.

Author contributions

Literature research and article preparation by JZ. Data collection and statistical analysis by JW. Clinical studies, study concepts, and design by RC, JQ, ZA, HS, ZG, XZha, XZhe and MG. The corresponding author had full access to the data and took final responsibility for the decision to submit for publication. All authors contributed to the article and approved the submitted version.

Funding

The author(s) declare that no financial support was received for the research, authorship, and/or publication of this article.

Acknowledgments

We thank the patients and the investigators who participated in this study. This study was sponsored by the Chongqing Lummy Pharmaceutical Co. Ltd. The funders had no role in study design, data collection, or analysis. The corresponding author had full access to the data and took final responsibility for the decision to submit for publication.

Conflict of interest

The authors declare that the research was conducted in the absence of any commercial or financial relationships that could be construed as a potential conflict of interest.

Publisher's note

All claims expressed in this article are solely those of the authors and do not necessarily represent those of their affiliated organizations, or those of the publisher, the editors and the reviewers. Any product that may be evaluated in this article, or claim that may be made by its manufacturer, is not guaranteed or endorsed by the publisher.

References

1. Lim H, Devesa SS, Sosa JA, Check D, Kitahara CM. Trends in thyroid cancer incidence and mortality in the United States, (2017) 1974-2013. *JAMA* (2017) 317:1338–48. doi: 10.1001/jama.2017.2719

2. Wang TS, Sosa JA. Thyroid surgery for differentiated thyroid cancer - recent advances and future directions. *Nat Rev Endocrinol* (2018) 14:670–83. doi: 10.1038/s41574-018-0080-7

3. Mirallié E, Borel F, Tresallet C, Hamy A, Mathonnet M, Lifante JC, et al. Impact of total thyroidectomy on quality of life at 6 months: the prospective ThyrQoL multicentre trial. *Eur J Endocrinol* (2020) 182:195–205. doi: 10.1530/EJE-19-0587

4. Li Z, Ao S, Bu Z, Wu A, Wu X, Shan FJ, et al. Clinical study of harvesting lymph nodes with carbon nanoparticles in advanced gastric cancer: a prospective randomized trial. *World J Surg Oncol* (2016) 24(14):88. doi: 10.1186/s12957-016-0835-3

5. Liu CL, Yang TB. Sentinel lymph node mapping with emulsion of activated carbon particles in patients with pre-mastectomy diagnosis of intraductal carcinoma of the breast. *J Chin Med Assoc* (2003) 66:406–10.

6. Wang R, Mo S, Liu Q, Zhang W, Zhang Z, He Y, et al. The safety and effectiveness of carbon nanoparticles suspension in tracking lymph node metastases of colorectal

cancer: a prospective randomized controlled trial. *Jpn J Clin Oncol* (2020) 50:535–42. doi: 10.1093/jjco/hyaa011

7. Yu W, Cao X, Xu G, Song Y, Li G, Zheng H, et al. Potential role for carbon nanoparticles to guide central neck dissection in patients with papillary thyroid cancer. *Surgery* (2016) 160:755–561. doi: 10.1016/j.surg.2016.04.017

8. Xu XF, Gu J. The application of carbon nanoparticles in the lymph node biopsy of cN0 papillary thyroid carcinoma: A randomized controlled clinical trial. *Asian J Surg* (2017) 40:345–9. doi: 10.1016/j.asjsur.2015.11.004

9. Tang L, Sun L, Zhao P, Kong D. Effect of activated carbon nanoparticles on lymph node harvest in patients with colorectal cancer. *Colorectal Dis* (2019) 21:427–31. doi: 10.1111/codi.14538

10. Wang B, Qiu NC, Zhang W, Shan CX, Jiang ZG, Liu S, et al. The role of carbon nanoparticles in identifying lymph nodes and preserving parathyroid in total endoscopic surgery of thyroid carcinoma. *Surg Endosc* (2015) 29:2914–20. doi: 10.1007/s00464-014-4020-x

11. Liu J, Xu C, Wang R, Han P, Zhao Q, Li H, et al. Do carbon nanoparticles really improve thyroid cancer surgery? A retrospective analysis of real-world data. *World J Surg Oncol* (2020) 18:84. doi: 10.1186/s12957-020-01852-5

12. Shoback D. Clinical practice. Hypoparathyroidism. *N Engl J Med* (2008) 359 (4):391–403. doi: 10.1056/NEJMcp0803050

13. Yan J, Zheng X, Liu Z, Yu J, Deng Z, Xue F, et al. A multicenter study of using carbon nanoparticles to show sentinel lymph nodes in early gastric cancer. *Surg Endosc* (2016) 30:1294–300. doi: 10.1007/s00464-015-4358-8

14. Zhang L, Huang Y, Yang C, Zhu T, Lin Y, Gao H, et al. Application of a carbon nanoparticle suspension for sentinel lymph node mapping in patients with early breast cancer: a retrospective cohort study. *World J Surg Oncol* (2018) 16:112. doi: 10.1186/s12957-018-1414-6

15. Yan J, Xue F, Chen H, Wu X, Zhang H, Chen G, et al. A multi-center study of using carbon nanoparticles to track lymph node metastasis in T1-2 colorectal cancer. *Surg Endosc* (2014) 28:3315–21. doi: 10.1007/s00464-014-3608-5

frontiers | Frontiers in Endocrinology

TYPE Original Research
PUBLISHED 12 January 2024
DOI 10.3389/fendo.2023.1301191

OPEN ACCESS

EDITED BY
I-Cheng Lu,
Kaohsiung Medical University, Taiwan

REVIEWED BY
Gerdi Tuli,
Regina Margherita Hospital, Italy
Magdalena Stasiak,
Polish Mother's Memorial Hospital Research Institute, Poland
Jazmin Calyeca,
Nationwide Children's Hospital, United States

*CORRESPONDENCE
Patrycja Sosnowska-Sienkiewicz
patrycja.sosnowska@outlook.com

RECEIVED 24 September 2023
ACCEPTED 19 December 2023
PUBLISHED 12 January 2024

CITATION
Sosnowska-Sienkiewicz P, Danielewicz D, Januszkiewicz-Lewandowska D, Rusak P, Anderko I, Rzepecki M, Niedziela M, Harasymczuk J and Mańkowski P (2024) Thyroid diseases in children and adolescents requiring surgical treatment—indications, techniques, results, and complications based on 10 years of the single center's own experience.
Front. Endocrinol. 14:1301191.
doi: 10.3389/fendo.2023.1301191

Thyroid diseases in children and adolescents requiring surgical treatment—indications, techniques, results, and complications based on 10 years of the single center's own experience

Patrycja Sosnowska-Sienkiewicz[1]*, Dajana Danielewicz[1], Danuta Januszkiewicz-Lewandowska[2], Paulina Rusak[3], Iwona Anderko[3], Maciej Rzepecki[3], Marek Niedziela[4], Jerzy Harasymczuk[1] and Przemysław Mańkowski[1]

[1]Department of Pediatric Surgery, Traumatology and Urology, Poznan University of Medical Sciences, Poznań, Poland, [2]Department of Pediatric Oncology, Hematology and Transplantology, Poznan University of Medical Sciences, Poznań, Poland, [3]Student Research Group of Pediatric Surgery, Poznan University of Medical Sciences, Poznań, Poland, [4]Department of Pediatric Endocrinology and Rheumatology, Poznan University of Medical Sciences, Poznań, Poland

Introduction: Although thyroid abnormalities are observed less frequently in children than in adults, the increased incidence of thyroid cancer makes it mandatory for all pediatric surgeons to be knowledgeable about the disorders of this gland. Thyroid abnormalities can be associated with hyperthyroidism or hypothyroidism and euthyroidism and/or symmetric or asymmetric enlargement of the gland.

Aim: The present study was undertaken to retrospectively analyze the indications, surgical techniques used, results obtained, and complications found in the surgical treatment of thyroid diseases in children and adolescents in a surgical center for the macro-region of western Poland.

Methods: The data of 148 patients undergoing total or partial thyroidectomy between 2013 and 2022 were analyzed from the medical records of the Department of Pediatric Surgery, Traumatology, and Urology of the Medical University of Poznan, Poland.

Results: A total of 95 children underwent subtotal thyroidectomy and 64 underwent total thyroidectomy, of which the procedure was widened to include prophylactic removal of neck lymph nodes in 45 patients. There were 113 girls (76%) in the analyzed group, and the average age of the patients at the time of surgical treatment was 15 years. The average time from the diagnosis of thyroid disease to surgery was 4 months, ranging from 2 weeks to 3 years. Of the 64 patients undergoing total thyroid resection, 35 (54.69%) were diagnosed with thyroid cancer.

Conclusions: Collaboration within a multidisciplinary team ensures optimal surgical outcomes in children and adolescents with thyroid disease. With extreme caution, thyroid removal is a safe procedure with few complications, but the experience of the surgeon performing thyroid surgery in children remains crucial. Despite the absence of such a diagnosis in the first fine-needle aspiration biopsy, the high percentage of thyroid carcinomas in the analyzed group may be because the initial biopsy was performed in a less experienced center, also in terms of histopathological laboratory. Hence, we point out the necessity of performing a repeat fine-needle aspiration biopsy (according to the Bethesda classification) in a more experienced center before the final decision of thyroidectomy.

KEYWORDS

child, complications, outcomes, thyroid gland, thyroidectomy

Introduction

Thyroid diseases are an increasing problem in children, adolescents, and adults, affecting a growing group of patients. Although thyroid diseases are relatively infrequently described in children, compared to adult patients, the increased incidence in the pediatric group should contribute to increased awareness among pediatric surgeons, resulting in proper qualification for surgical treatment and improved prognosis (1–3). The basis for the diagnosis of thyroid disease is a physical examination, including consideration of family history of the disease. Thyroid hormone tests—TSH, FT3, FT4, anti-TSHR, anti-TPO, anti-TG antibodies, thyroglobulin, and calcitonin—are also important (1). The imaging studies include thyroid ultrasound and thyroid scintigraphy (2, 4). Fine-needle aspiration biopsy (FNAB), performed under ultrasound guidance, plays an important role (2–5). Table 1 shows the Bethesda system with diagnostic thyroid cytopathology and clinical recommendations.

Surgical treatment and the extent of resection of the thyroid gland depend on the diagnosis, accompanying clinical manifestations, and the involved area(s) of the thyroid gland. Owing to symptomatic compression of surrounding structures such as the trachea or esophagus, a colloid, nodular, or multinodular thyroid goiter may require surgery to reduce symptoms and improve the patient's quality of life (1). In addition, surgery may also be recommended for nodular goiter when imaging studies such as ultrasonography or the result of a fine-needle biopsy suggest the presence of malignant lesions (1, 2). Thyroidectomy may be necessary in autoimmune and functional thyroid diseases involving the entire thyroid gland. These include hyperthyroidism, unresponsive to treatment, or advanced autoimmune disorders in which the thyroid gland is significantly damaged and nodularly altered (1, 3). The thyroid gland can also become hyperactive due to the presence of autonomous adenomas. Thyrotoxicosis can also result from the use of amiodarone, an iodine-containing drug (6).

Surgical treatment is the treatment of choice for patients with precancerous lesions and confirmed thyroid cancer (2, 4, 7, 8). In children and adolescents, papillary and follicular thyroid carcinomas account for approximately 90% of all malignant thyroid tumors (4). Thyroid cancer staging is performed using the TNM (Tumor-Node-Metastasis) classification according to the 8th edition of the UICC (Union for International Cancer Control). There are two stages of papillary and follicular thyroid cancer (stage I includes each T, each N with M0, and stage II includes every T, every N of M1) (2). Tumor grade and histologic type are considered in determining the extent of surgery. However, the method of

TABLE 1 The Bethesda system with diagnostic thyroid cytopathology and clinical recommendations.

Diagnostic Category	Risk of Malignancy (%)	Usual Management
Nondiagnostic or unsatisfactory	5–10	Repeat FNA with ultrasound guidance
Benign	0–3	Clinical follow-up
Atypia of undetermined significance or follicular lesion of undetermined significance	6–18	Repeat FNA, molecular testing, or lobectomy
Follicular neoplasm or suspicious for a follicular neoplasm	10–40	Molecular testing, lobectomy
Suspicious for malignancy	45–60	Near total thyroidectomy or lobectomy
Malignant	94–96	Near total thyroidectomy or lobectomy

choice is total thyroidectomy, often in addition to the removal of regional neck lymph nodes (2). Prophylactic total thyroidectomy is performed when there is an increased risk of genetically based cancer, such as that caused by germline mutations of the RET protooncogene (5).

Long-term complications of total and partial thyroidectomy are not common, and perioperative mortality is very low (4, 9–12). The most often observed postoperative complication is hypoparathyroidism with associated hypocalcemia (8–11). A higher incidence of hypoparathyroidism has been described after total thyroidectomy with simultaneous removal of regional lymph nodes (9, 10). Other complications include bleeding, wound infection, and injury of the posterior laryngeal nerves and the vocal cords (9).

Aim of the study

The present study was undertaken to retrospectively analyze the indications for thyroidectomy, surgical techniques used, results obtained, and complications observed after surgical treatment of thyroid diseases in children and adolescents in a surgical center for the macro-region of western Poland.

Materials and methods

Data were collected from the medical records of patients treated in the Department of Pediatric Surgery, Traumatology, and Urology at the Poznan University of Medical Sciences from 2013 to 2022. A total of 148 patients underwent surgical treatment—total or subtotal thyroidectomy. A total of 11 children required reoperation, including 3 cases due to recurrence of disease, and in 8 patients, the initial histopathological result indicated the need for extended resection. Based on laboratory tests performed, patients were defined as having hyperthyroidism, euthyroidism, or pharmacologically controlled hypothyroidism. According to published recommendations, patients were qualified based on ultrasound and laboratory tests for thin-needle biopsy, subtotal, or total thyroidectomy with or without lymph node excision (13–18). Analysis included age, gender, comorbidities, laboratory tests, indications for surgery, preoperative period (need for pharmacotherapy before surgery and other treatments from history), type of surgery (primary surgery, reoperation, duration of surgery, need for blood transfusion, occurrence of complication, and type of complication), postoperative period (complications, need for additional therapy, duration of hospitalization, reported pain on a scale of 1–10, pain medications used resulting in relief of pain, and blood transfusion during hospitalization after surgery), and histopathological diagnosis.

Each patient underwent surgical evaluation 7–10 days and 2 months after surgery. Patients remained under constant follow-up by an endocrinologist or an oncologist and had regular laboratory tests and ultrasound examinations until they were 18 years old.

Surgery technique

The types of thyroid surgery used included subtotal thyroidectomy, which was the removal of one lobe of the thyroid gland, including the isthmus, and total thyroidectomy, which was the removal of both lobes of the thyroid gland, including the isthmus.

Subtotal thyroidectomy

At the base of the neck, approximately 2 cm above the cervical notch of the sternum, an incision of approximately 4 cm is made. The length of the incision depends on the size of the thyroid gland to be operated on. Such an incision provides adequate access to the organ, vascular course, and adjacent structures necessary for visualization. The next step is to release—to detach the thyroid gland from the surrounding tissues—muscles and other soft tissues. The vessels (the superior and inferior thyroid arteries) should be carefully worked out. They could be secured by coagulating or puncturing, depending on the diameter of the vessel and the operator's beliefs. Critical to the operation is the correct identification of the recurrent laryngeal nerve. According to the latest standards, the recurrent laryngeal nerve and the superior laryngeal nerve must be identified by neuromonitoring. With special care, the first lobe of the gland is dissected, reaching the expected location of the recurrent laryngeal nerve. The recurrent laryngeal nerves lie on both sides of the trachea; they then reach the posterior surface of the thyroid gland in the groove between the trachea and the esophagus. The recurrent laryngeal nerve is dissected, remembering not to coagulate near it and to stop the bleeding by ligating or puncturing the bleeding vessel. During the operation, we identified the parathyroid glands. After excision of the gland lobe, the isthmus of the thyroid gland should be exposed and dissected. The procedure is completed by checking for hemostasis. Tranexamic acid is used in infiltrative form after removal of the thyroid lobe, including the isthmus. Layered tissue reconstruction completes the operation.

Total thyroidectomy

Depending on the size of the thyroid gland, the surgical incision must be extended by approximately 1–2 cm. The steps described above are repeated on the side of the second operated lobe, constantly with due care, remembering intraoperative neuromonitoring. Drains are currently used sporadically.

Statistical analysis

Calculations were made using Statistica 13 by TIBCO and PQStat by PQStat Software. The significance level was $\alpha = 0.05$. The result was considered statistically significant when $p < \alpha$. The

normality of the distribution of variables was tested with the Shapiro–Wilk test. The Mann–Whitney test was calculated to compare the variables between the 2 groups. Spearman's rank correlation coefficient (*Rs*) was calculated to examine the relationship between the variables. The χ^2 test of independence, Fisher's exact test, or Fisher–Freeman–Halton test was calculated to investigate the relationship between categorical variables. The odds ratio was calculated with a 95% confidence interval if there was a relationship. Cohen's kappa concordance coefficient was calculated to assess the concordance of the initial and final diagnosis.

The study was approved by the Bioethics Committee of the Poznan University of Medical Sciences (Resolution no. KB-752/23, 22 September 2023).

Results

In the group of 148 operated patients, 95 subtotal thyroidectomies and 64 total thyroidectomies were performed. In 45 patients, the procedure was extended with prophylactic removal of the neck lymph nodes at the same time as total or subtotal thyroidectomy. Reoperation was necessary in 11 children due to the recurrence of the disease or diagnosis of malignant lesions on histopathological examination. In two patients, a biopsy of the second lobe of the thyroid gland was performed due to the abnormality of the lesions found macroscopically. The final histopathological examination showed a benign lesion in the first operated lobe and no pathology in the second lobe in both children (Figure 1).

There were 113 (76%) girls with a median age at the time of surgery of 14.95 years. In the boy group, the median age at surgery was 14.86 years. The average time from diagnosis to surgery was 4 months, ranging from 2 weeks to 3 years. The prolonged time from diagnosis to surgery was due to attempts to treat the disease conservatively. Among the operated girls, 80 (70.80%) were euthyroid, 8 (7.80%) presented hyperthyroidism, and 25 (22.12%) were hypothyroid. Among the boys, 26 (74.29%) had euthyroidism, 3 (8.57%) had hyperthyroidism, and 6 (17.14%) had hypothyroidism.

Among 64 children undergoing total thyroidectomy, 26 (40.62%) had indications other than cancer. Detailed indications for thyroid removal and final histopathological results in girls and boys are shown in Table 2.

Of the five children with Hashimoto's goiter, two had symptoms of tracheal compression as an indication for surgery; in another two, the FNAB result indicated the malignant nature of the lesion, and in one, the ultrasound result suggested a malignant process. Of the 100 children with nodular goiter, the indication for thyroidectomy was the cytologic result of FNAB according to the Bethesda classification in 56 patients, which suggested atypia of undetermined significance. In 15 cases, the result indicated suspected follicular neoplasm; in another 19 cases, the huge size of the nodular goiter was the reason for the indication for surgery, and in the remaining 5 children, the worrisome ultrasound image was the indication for surgery. In four patients, thyrotoxicosis was caused by amiodarone treatment.

The initial (preoperative) diagnosis corresponded to the final diagnosis in 68 (42.77%) girls and 22 (13.84%) boys. The malignant lesions in girls on final histopathological examination were diagnosed more often than in the initial diagnosis based on ultrasound imaging and FNAB biopsy (27.43% vs. 38.93%, respectively). A similar situation was also observed in boys (22.86% vs. 37.14%, respectively). Among the 45 neck lymphadenectomies performed, histopathological examination confirmed the involvement of the lymph nodes of the third region in 8 patients and the sixth region in 23 patients. In children with a malignant thyroid lesion, lymph node involvement was demonstrated in 68.9%. In all 54 children with papillary and follicular carcinoma, the stage was defined as I (T1 in 40 patients, T2 in 10 patients, and T3 in 4 patients).

Additional health problems were observed in 30.41% of the operated patients. Figure 2 shows the percentage distribution of comorbidities in the study group of children.

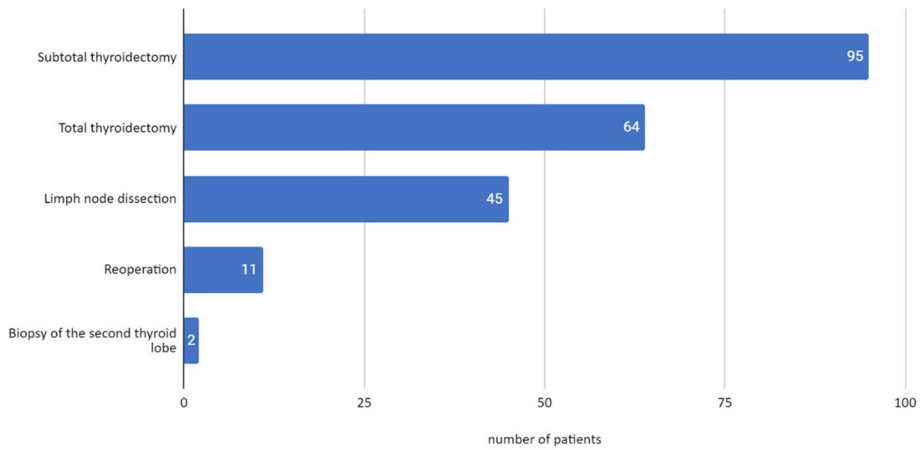

FIGURE 1
Types of surgical procedures performed in the analyzed patients.

TABLE 2 Comparison of accuracy of initial and final diagnoses in a group of girls and boys.

Gender						
	Girls			Boys		
Diagnosis	Initial number of patients	Final number of patients	Concordance factor	Initial number of patients	Final number of patients	Concordance factor
Goiter	76	42	0.87	24	14	0.292
Graves' disease	3	3	0.0008	0	0	*
Hashimoto's disease	4	10	0.01	1	3	0.0009
Thyrotoxicosis	3	0	*	1	0	*
Benign thyroid neoplasms, undefined	7	0	0.222[+]	1	0	0.463[+]
Malignant thyroid neoplasms, undefined	25	0	0.66[+]	5	0	0.552[+]
Papillary thyroid carcinoma	5	38	0.14	3	10	0.126
Follicular thyroid carcinoma	1	4	0.05	0	2	*
Medullary thyroid carcinoma	0	2	*	0	0	*
Lymphoepithelial cyst	0	1	*	0	0	*
Sinus histiocytosis	0	2	*	0	0	*
Hyalinizing trabecular adenoma	0	0	*	0	1	*
Burkitt's lymphoma	0	0	*	0	1	*
Mature teratoma	0	1	*	0	0	*
Thyroid tissue	0	5	*	0	0	*
Thyroid adenoma	0	16	*	0	4	*

*Cannot be counted because there was a value of "0" in the initial/final diagnosis.
[+]When the initial diagnosis was "Malignant thyroid neoplasms, undefined," and the final diagnosis was a detailed specification of the type of malignant neoplasm, a concordance factor was calculated for the given value. A similar principle was applied for the diagnosis of "Benign thyroid neoplasms, undefined".

Six children had prior therapy for the oncological disease before thyroid surgery. Because of hyperthyroidism, 11 children required pharmacological preparation for surgery with Lugol's iodine for 7 days.

The average duration of surgery was 71 min, from 40 to 120 min in the subtotal thyroidectomy group, and 100 min, from 40 to 270 min in the total thyroidectomy group. The prolongation of surgery was related to the advancement of the disease, difficult surgical access, and the lack of experience of the surgical team.

None of the children required blood transfusion during surgery. A blood transfusion was needed on day 4 after surgery in only one child. The patient rated pain on the first postoperative day on a scale of 1 to 10. Most patients rated pain at 1 (107 patients); the maximum value of 5 occurred only in 1 child. The mean value of reported pain was 1.68. Standard pain medications after surgery were paracetamol and metamizole. All children who underwent total thyroidectomy required an intravenous calcium supply for the first 48 h, followed by an oral calcium supply in a dose that depended on the total and ionized calcium level in the body. Two of 54 children diagnosed with malignant neoplasm required subsequent radioiodine therapy. One child diagnosed with Burkitt's lymphoma required further chemotherapy. Early complications after thyroid surgery were observed in 43 patients (39.05%). Six children had symptoms of transient retrograde laryngeal nerve palsy, which completely resolved in all of them 7–10 days after surgery. Thirty-seven patients developed transient hypoparathyroidism, which resolved completely 2 months after thyroidectomy. Late complications after thyroid surgery were observed in three patients (2.03%). One child developed vocal cord paralysis and required a tracheostomy. Two patients developed hypoparathyroidism and required regular oral calcium supplementation (500 mg three times a day).

The duration of hospitalization after surgery ranged from 2 to 23 days, with an average of 6 days. A significant correlation was found between the time of surgery and the rate of complications (Spearman's rank correlation coefficient = 0.419965) (Figure 3). A significant correlation was also found between the duration of surgery and the length of hospitalization (Spearman's rank correlation coefficient = 0.425831) (Figure 4). A significant correlation was also found between thyroidectomy with lymph

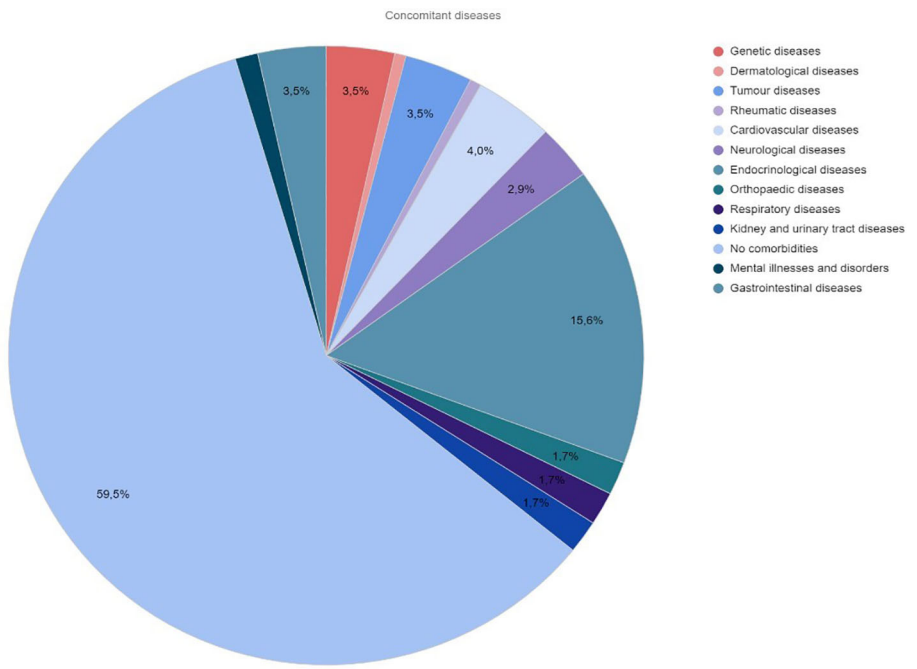

FIGURE 2
Percentage distribution of comorbidities in children who have undergone thyroidectomy.

node resection and duration of surgery, as well as the length of hospitalization (Spearman's rank correlation coefficient = 0.772595 and 0.675662, respectively) (Figures 5, 6).

Discussion

Thyroid diseases in children and adolescents are a growing problem that affects an increasing number of patients. Many factors can influence this. Increased awareness and better diagnostics can lead to more appropriate diagnosis and detection of thyroid diseases in children, and increased awareness among doctors and the public about the symptoms and risks of thyroid diseases can result in earlier diagnoses. Increased exposure to various environmental factors, such as air pollution, chemicals, and hormonal substances, can affect thyroid health in children and adults. Dietary changes, such as low intake of iodine, essential for proper thyroid function, can also contribute to thyroid disorders in children. Modern lifestyles, including the pace and level of stress, can affect thyroid health. Stress can affect hormonal regulation, which, in turn, can lead to thyroid disorders (19).

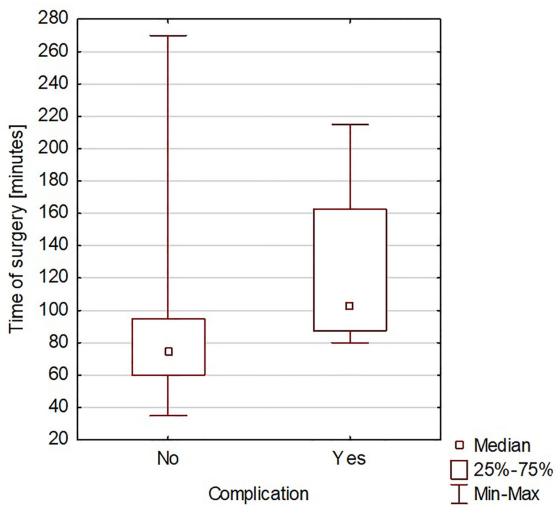

FIGURE 3
The duration of surgery and the rate of complications.

A characteristic feature of thyroid diseases is that they occur mainly in women. The female-to-male ratio is 4–6:1 for autoimmune thyroid diseases and approximately 3–4:1 for thyroid nodules (20). In our group, the number of girls operated on for thyroid diseases was three times higher than for boys. The standard management of thyroid diseases in their early stages is observing the nodules' growth rate and possible drug treatment (19). Surgery is indicated in selected situations (21). Until qualification for surgery, patients remain under the constant supervision of an endocrinologist. In analyzed patients, the time interval from the diagnosis of thyroid disease to surgical treatment ranged from 2 weeks to 3 years. Operative treatment after such a long time was due to ineffective conservative treatment. An alarming ultrasound image, suggestive of a malignant process, resulted in urgent biopsy and, if the malignant nature of the lesion was confirmed, urgent surgical treatment. Ultrasound parameters such as microcalcifications, hypoechogenicity, lack of halo, increased intratumoral vascularization, nodule shape, or irregular margins have traditionally been associated with an increased risk of malignancy. However, none of these features

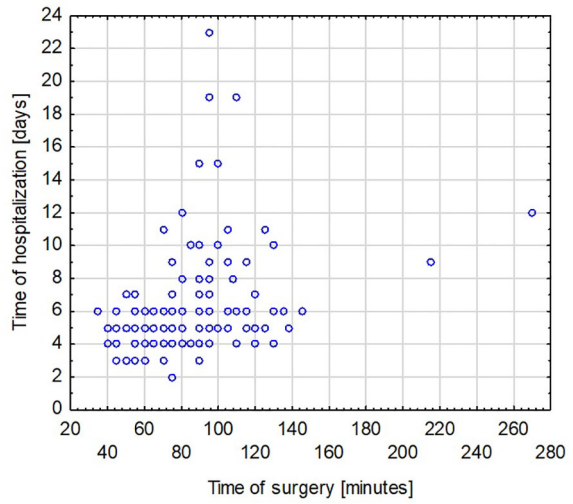

FIGURE 4
The duration of surgery and the length of hospitalization.

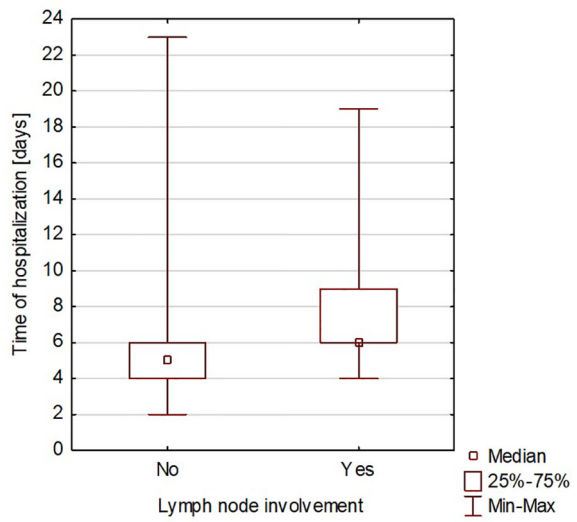

FIGURE 6
Thyroidectomy with lymph node resection and length of hospitalization.

appear to be reliable enough to diagnose malignancy based on ultrasound alone (22, 23).

It is estimated that approximately 60% of surgeries are for removing nodular goiter, and approximately 20% of procedures are performed for oncological reasons (3, 24). In our material, the most common indications for surgery were goiter (28% of patients) and papillary thyroid carcinoma (26% of children). In 56.61% of all patients, the preoperative diagnosis matched the final histopathological diagnosis. The initial benign recognition based on FNAB may differ from the final diagnosis of the removed thyroid. In the study group, we observed a relatively high malignancy rate of the thyroid gland operated due to multinodular goiter. Similar observations were found by Jenica Su-Ern Yong et al., where the incidence of malignancies in surgically treated multinodular goiter was 14.3% (32 of 223 patients) (25). Such discrepancies between the cytologic result from the biopsy and the histopathological final result from surgery can be explained by the different experiences of the centers in performing FNAB. The children analyzed in the study overwhelmingly had FNAB performed outside our center, which may account for the differences between the initial and final diagnoses. The impact of the centralization of treatment of the patients we operated on the frequency of histopathological results is also worth noting. Our clinic is one of the three higher referral centers for thyroid surgery in children and adolescents; thus, we have many problematic patients. This makes the analyzed group of patients somewhat selective. In the group we studied, the diagnosis of Burkitt's lymphoma and teratoma in the operated thyroid was surprising.

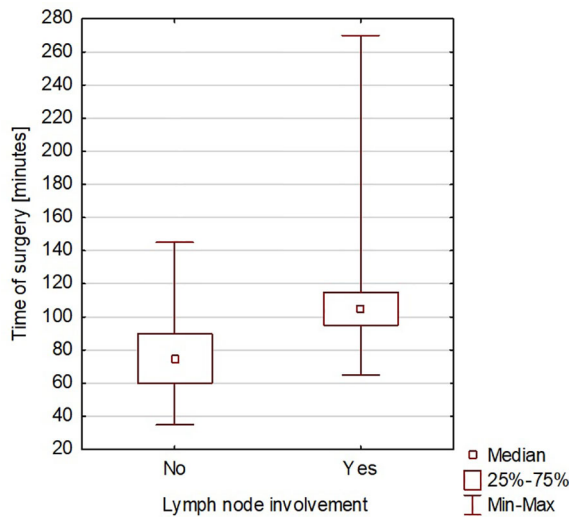

FIGURE 5
Thyroidectomy with lymph node resection and duration of surgery.

Current surgical techniques include classic approaches such as subtotal or total thyroidectomy with or without lymph node removal. Videoscopic and endoscopic procedures are also available (26–28). These two methods are not used in our center. The available literature rarely describes them in children (29).

As described in the literature, complications associated with retrobulbar nerve injury have decreased due to the greater availability of intraoperative neuromonitoring (30). In our center, every thyroid surgery is performed with neuromonitoring as standard. According to Motos-Micó et al., the availability of neuromonitoring reduced the number of described complications in his study group to zero (31). In our group, transient symptoms of laryngeal nerve palsy occurred in six children (4% of patients) despite using neuromonitoring. Unilateral vocal cord paralysis manifested by dysphonia, dysphonia, and difficulty swallowing was observed in only one child. The other most frequently observed complication was transient hypoparathyroidism, which occurred in 37% of children. Compared to the literature data, these are comparable in the incidence of retrobulbar laryngeal nerve injury and hypoparathyroidism in the pediatric group, depending

on the center performing the study (32, 33). Willobee et al. showed that the most common complications were hypocalcemia and laryngeal nerve injury, with rates of 9% and 3%, respectively (3). Hanba et al. described that vocal cord paralysis was found in 1.7% of children after thyroidectomy. Postoperative hypocalcemia occurred in almost 20% of children undergoing total thyroidectomy (33).

The correlation we observed between the duration of surgery and the presence of intra- or postoperative complications is worth noting. This can be explained by the more difficult course of the surgical procedure. Hanba et al. reported that children under 1 year of age stayed in the hospital significantly longer, and patients aged 1 to 5 years stayed much longer than those aged 6 to 20 years (33). In our study, we did not observe a similar relationship. Willobee et al. showed that compared with partial thyroidectomy, total thyroidectomy was associated with an increased rate of postoperative complications. Moreover, the median length of hospital stay was significantly higher in patients after total thyroidectomy (32). In our observations, prolonged surgery time was also associated with more extended hospital stays. This was also confirmed in the study by Willobee et al. (32). We showed a correlation between lymphadenectomy and more extensive surgery with longer hospitalization time. Martucci et al. presented that according to international guidelines, prophylactic central and lateral neck excision is not recommended (34). They stated that it should only be performed in patients with malignant cytology (grade 4, 5, or 6 on the Bethesda scale) or when there is clear clinical evidence of extrathyroidal node involvement or locoregional metastasis based on preoperative staging or intraoperative findings. In the study by Martucia et al., 153 children (60%) underwent lymphadenectomy, and 85.6% had lymph node metastases (34). In the material we analyzed, 45 patients (30.41% of all patients) underwent lymphadenectomy, and metastasis was confirmed in 31 children (68.9%).

Thyroid surgeries in our center are performed by teams led by three experienced surgeons. The experience of the operating team and its impact on the number of complications during thyroidectomy are widely emphasized in the available literature (35, 36).

Conclusion

Cooperation in a multidisciplinary team ensures optimal treatment results for patients. With special care, removal of the thyroid gland is a safe procedure with few complications, but the surgeon's experience in performing thyroid surgery in children is crucial. Cytologic result and final histopathological verification, especially in the case of the slightest suspicion of thyroid cancer, are crucial. Qualification for surgery should adhere to the Bethesda classification. For thyroid conditions warranting surgical intervention, a follow-up fine-needle biopsy with cytologic evaluation should be conducted before reaching a final decision on thyroidectomy. As per the Bethesda classification, a cytologic reassessment should be carried out at a specialized referral center for thyroidectomy.

Data availability statement

The raw data supporting the conclusions of this article will be made available by the authors, without undue reservation.

Ethics statement

The studies involving humans were approved by the Bioethics Committee of the Poznan University of Medical Sciences (Resolution no. KB-752/23, 22 September 2023). The studies were conducted in accordance with the local legislation and institutional requirements. Written informed consent for participation in this study was provided by the participants' legal guardians/next of kin.

Author contributions

PS-S: Conceptualization, Data curation, Formal analysis, Investigation, Methodology, Project administration, Software, Visualization, Writing – original draft. DD: Data curation, Methodology, Software, Visualization, Writing – original draft, Formal analysis, Funding acquisition. PR: Data curation, Investigation, Software, Writing – original draft, Funding acquisition. IA: Data curation, Methodology, Software, Writing – original draft, Funding acquisition, Investigation. MR: Data curation, Methodology, Software, Writing – original draft, Funding acquisition, Investigation. DJ-L: Conceptualization, Formal analysis, Funding acquisition, Methodology, Supervision, Writing – review & editing. MN: Conceptualization, Funding acquisition, Investigation, Supervision, Writing – review & editing. JH: Data curation, Funding acquisition, Investigation, Supervision, Writing – review & editing. PM: Conceptualization, Formal analysis, Funding acquisition, Investigation, Supervision, Writing – review & editing.

Funding

The author(s) declare that no financial support was received for the research, authorship, and/or publication of this article.

Conflict of interest

The authors declare that the research was conducted in the absence of any commercial or financial relationships that could be construed as a potential conflict of interest.

Publisher's note

References

1. Zobel MJ, Padilla BE. Surgical management of benign thyroid disease in children. *Semin Pediatr Surg* (2020) 29(3):150922. doi: 10.1016/j.sempedsurg.2020.150922

2. Francis GL, Waguespack SG, Bauer AJ, Angelos P, Benvenga S, Cerutti JM, et al. Management guidelines for children with thyroid nodules and differentiated thyroid cancer. *Thyroid.* (2015) 25(7):716–59. doi: 10.1089/thy.2014.0460

3. Ledbetter DJ. Thyroid surgery in children. *Semin Pediatr Surg* (2014) 23(2):60–5. doi: 10.1053/j.sempedsurg.2014.03.002

4. Stefan AI, Piciu A, Mester A, Apostu D, Badan M, Badulescu CI. Pediatric thyroid cancer in europe: an overdiagnosed condition? A literature review. *Diagnostics (Basel).* (2020) 10(2):112. doi: 10.3390/diagnostics10020112

5. Jasim S, Dean DS, Gharib H. Fine-needle aspiration of the thyroid gland. In: Feingold KR, Anawalt B, Blackman MR, Boyce A, Chrousos G, Corpas E, et al, editors. *Endotext*. South Dartmouth (MA: MDText.com, Inc (2000). Available at: https://www.ncbi.nlm.nih.gov/books/NBK285544/.

6. Siccama R, Balk AH, de Herder WW, van Domburg R, Vantrimpont P, van Gelder T. Amiodarone therapy before heart transplantation as a predictor of thyroid dysfunction after transplantation. *J Heart Lung Transplant.* (2003) 22(8):857–61. doi: 10.1016/s1053-2498(02)01149-x

7. Diesen DL, Skinner MA. Pediatric thyroid cancer. *Semin Pediatr Surg* (2012) 21 (1):44–50. doi: 10.1053/j.sempedsurg.2011.10.004

8. Scholz S, Smith JR, Chaignaud B, Shamberger RC, Huang SA. Thyroid surgery at Children's Hospital Boston: a 35-year single-institution experience. *J Pediatr Surg* (2011) 46(3):437–42. doi: 10.1016/j.jpedsurg.2010.09.009

9. van Rooijen JJ, van Trotsenburg ASP, van de Berg DJ, Zwaveling-Soonawala Dijkum N, Nieveen van Dijkum EJM, Engelsman AF, et al. Complications after thyroidectomy in children: lymph node dissection is a risk factor for permanent hypocalcemia. *Front Endocrinol (Lausanne).* (2021) 12:717769. doi: 10.3389/fendo.2021.717769

10. Chen Y, Masiakos PT, Gaz RD, Hodin RA, Parangi S, Randolph GW, et al. Pediatric thyroidectomy in a high volume thyroid surgery center: Risk factors for postoperative hypocalcemia. *J Pediatr Surg* (2015) 50(8):1316–9. doi: 10.1016/j.jpedsurg.2014.10.056

11. de Jong M, Nounou H, Rozalén García V, Christakis I, Brain C, Abdel-Aziz TE, et al. Children are at a high risk of hypocalcaemia and hypoparathyroidism after total thyroidectomy. *J Pediatr Surg* (2020) 55(7):1260–4. doi: 10.1016/j.jpedsurg.2019.06.027

12. Bellantone R, Lombardi CP, Bossola M, Boscherini M, De Crea C, Alesina PF, et al. Video-assisted vs conventional thyroid lobectomy: a randomized trial. *Arch Surg* (2002) 137(3):301–5. doi: 10.1001/archsurg.137.3.301

13. Francis GL, Waguespack SG, Bauer AJ, Angelos P, Benvenga S, Cerutti JM, et al. American thyroid association guidelines task force. Management guidelines for children with thyroid nodules and differentiated thyroid cancer. . *Thyroid* (2015) 25 (7):716–59. doi: 10.1089/thy.2014.0460

14. Musholt TJ, Bockisch A, Clerici T, Dotzenrath C, Dralle H, Goretzki PE, et al. Aktualisierung der S2k-Leitlinie : Operative Therapie benigner Schilddrüsenerkrankungen [Update of the S2k guidelines : Surgical treatment of benign thyroid diseases]. *Chirurg.* (2018) 89(9):699–709. doi: 10.1007/s00104-018-0653-y

15. Dralle H, Musholt TJ, Schabram J, Steinmüller T, Frilling A, Simon D, et al. German Societies of General and Visceral Surgery; Endocrinology; Nuclear Medicine; Pathology; Radiooncology; Oncological Hematology; and the German Thyroid Cancer Patient Support Organization Ohne Schilddrüse leben e.V. German Association of Endocrine Surgeons practice guideline for the surgical management of Malignant thyroid tumors. *Langenbecks Arch Surg* (2013) 398(3):347–75. doi: 10.1007/s00423-013-1057-6

16. Paschke R, Cantara S, Crescenzi A, Jarzab B, Musholt TJ, Sobrinho Simoes M. European thyroid association guidelines regarding thyroid nodule molecular fine-needle aspiration cytology diagnostics. *Eur Thyroid J* (2017) 6(3):115–29. doi: 10.1159/000468519

17. Russ G, Bonnema SJ, Erdogan MF, Durante C, Ngu R, Leenhardt L. European thyroid association guidelines for ultrasound Malignancy risk stratification of thyroid nodules in adults: the EU-TIRADS. *Eur Thyroid J* (2017) 6(5):225–37. doi: 10.1159/000478927

18. Lim-Dunham JE, Toslak IE, Reiter MP, Martin B. Assessment of the american college of radiology thyroid imaging reporting and data system for thyroid nodule Malignancy risk stratification in a pediatric population. *AJR Am J Roentgenol.* (2019) 212(1):188–94. doi: 10.2214/AJR.18.20099

19. Hanley P, Lord K, Bauer AJ. Thyroid disorders in children and adolescents: A review. *JAMA Pediatr* (2016) 170(10):1008–19. doi: 10.1001/jamapediatrics.2016.0486

20. Li H, Li J. Thyroid disorders in women. *Minerva Med* (2015) 106(2):109–14.

21. Alyahya KA, Alarfaj AA, Alyahya AA, Alnaim AE. Indications and complications for surgical management of thyroid diseases: a single center experience. *Ann Med Surg (Lond).* (2022) 79:103980. doi: 10.1016/j.amsu.2022.103980

22. Remonti LR, Kramer CK, Leitão CB, Pinto LC, Gross JL. Thyroid ultrasound features and risk of carcinoma: a systematic review and meta-analysis of observational studies. *Thyroid.* (2015) 25(5):538–50. doi: 10.1089/thy.2014.0353

23. Frates MC, Benson CB, Charboneau JW, Cibas ES, Clark OH, Coleman BG, et al. Management of thyroid nodules detected at US: Society of Radiologists in Ultrasound consensus conference statement. *Radiology.* (2005) 237(3):794–800. doi: 10.1148/radiol.2373050220

24. Sandy JL, Titmuss A, Hameed S, Cho YH, Sandler G, Benitez-Aguirre P. Thyroid nodules in children and adolescents: Investigation and management. *J Paediatr Child Health* (2022) 58(12):2163–8. doi: 10.1111/jpc.16257

25. Yong JS, Loh KS, Petersson BF, Thong M. Multinodular goiter: A study of Malignancy risk in nondominant nodules. *Ear Nose Throat J* (2017) 96(8):336–42. doi: 10.1177/014556131709600821

26. Bliss RD, Gauger PG, Delbridge LW. Surgeon's approach to the thyroid gland: surgical anatomy and the importance of technique. *World J Surg* (2000) 24(8):891–7. doi: 10.1007/s002680010173

27. Byeon HK, Ban MJ, Lee JM, Ha JG, Kim ES, Koh YW, et al. Robot-assisted Sistrunk's operation, total thyroidectomy, and neck dissection *via* a transaxillary and retroauricular (TARA) approach in papillary carcinoma arising in thyroglossal duct cyst and thyroid gland. *Ann Surg Oncol* (2012) 19(13):4259–61. doi: 10.1245/s10434-012-2674-y

28. Zorron R, Bures C, Brandl A, Seika P, Müller V, Alkhazraji M, et al. Tipps und technische Aspekte zur Durchführung der transoralen endoskopischen Thyreoidektomie mit vestibulärem Zugang (TOETVA): eine neue narbenlose Technik für die Halschirurgie [Tips and technical issues for performing transoral endoscopic thyroidectomy with vestibular approach (TOETVA): a novel scarless technique for neck surgery]. *Chirurg.* (2018) 89(7):529–36. doi: 10.1007/s00104-018-0658-6

29. Ngo DQ, Le DT, Ngo QX, Van Le Q. Transoral endoscopic thyroidectomy vestibular approach as a novel technique for pediatric populations: Results from a single surgeon. *Front Endocrinol (Lausanne).* (2023) 14:1177633. doi: 10.3389/fendo.2023.1177633

30. Mathieson T, Jimaja W, Triponez F, Licker M, Karenovics W, Makovac P, et al. Safety of continuous intraoperative vagus nerve neuromonitoring during thyroid surgery. *BJS Open* (2023) 7(3):zrad039. doi: 10.1093/bjsopen/zrad039

31. Motos-Micó JJ, Felices-Montes M, Abad-Aguilar T. Neuromonitorización intraoperatoria en cirugía tiroidea [Intraoperative neuromonitoring in thyroid surgery]. *Cir.* (2017) 85(4):312–9. doi: 10.1016/j.circir.2016.10.016

32. Willobee BA, Huerta CT, Quiroz HJ, Mao ML, Ryon EL, Ferrantella A, et al. Higher complication rates for total versus partial thyroidectomy in the pediatric population. *J Surg Res* (2023) 283:449–58. doi: 10.1016/j.jss.2022.10.074

33. Hanba C, Svider PF, Siegel B, Sheyn A, Shkoukani M, Lin HS, et al. Pediatric thyroidectomy. *Otolaryngol Head Neck Surg* (2017) 156(2):360–7. doi: 10.1177/0194599816677527

34. Martucci C, Crocoli A, De Pasquale MD, Spinelli C, Strambi S, Brazzarola P, et al. Thyroid cancer in children: A multicenter international study highlighting clinical features and surgical outcomes of primary and secondary tumors. *Front Pediatr* (2022) 10:914942. doi: 10.3389/fped.2022.914942

35. Sosa JA, Bowman HM, Tielsch JM, Powe NR, Gordon TA, Udelsman R. The importance of surgeon experience for clinical and economic outcomes from thyroidectomy. *Ann Surg* (1998) 228(3):320–30. doi: 10.1097/00000658-199809000-00005

36. Al-Hakami HA, Al Garni MA, Malas M, Abughanim S, Alsuraihi A, Al Raddadi T. Surgical complications after thyroid surgery: a 10-year experience at Jeddah, Saudi Arabia. *Indian J Otolaryngol Head Neck Surg* (2019) 71(Suppl 1):1012–7. doi: 10.1007/s12070-019-01695-x

frontiers | Frontiers in Endocrinology

TYPE Original Research
PUBLISHED 16 January 2024
DOI 10.3389/fendo.2023.1305629

OPEN ACCESS

EDITED BY
Joseph V. Martin,
Rutgers University Camden, United States

REVIEWED BY
Ilker Sengul,
Giresun University, Türkiye
Ahmet Omer Ikiz,
Dokuz Eylül University, Türkiye

*CORRESPONDENCE
Tai-Hung Yeh
Peteryeh3112@gmail.com
Tzu-Yen Huang
tyhuang.ent@gmail.com

RECEIVED 02 October 2023
ACCEPTED 28 December 2023
PUBLISHED 16 January 2024

CITATION
Chiang F-Y, Shih Y-C, Lien C-F, Wang C-C, Wang C-C, Hwang T-Z, Huang Y-C, Wu C-W, Yeh T-H and Huang T-Y (2024) Comparison of EMG amplitudes recorded by ipsilateral and contralateral electrodes placement during using trans-thyroid cartilage recording method in thyroid surgery.
Front. Endocrinol. 14:1305629.
doi: 10.3389/fendo.2023.1305629

Comparison of EMG amplitudes recorded by ipsilateral and contralateral electrodes placement during using trans-thyroid cartilage recording method in thyroid surgery

Feng-Yu Chiang[1,2], Yu-Chen Shih[3], Ching-Feng Lien[1,2], Chih-Chun Wang[1,2], Chien-Chung Wang[1], Tzer-Zen Hwang[1,2], Yaw-Chang Huang[1], Che-Wei Wu[4], Tai-Hung Yeh[1]* and Tzu-Yen Huang[4,5]*

[1]Department of Otolaryngology-Head and Neck Surgery, E-Da Hospital, Kaohsiung, Taiwan, [2]School of Medicine, College of Medicine, I-Shou University, Kaohsiung, Taiwan, [3]Department of Otolaryngology, E-Da Cancer Hospital, Kaohsiung, Taiwan, [4]Department of Otorhinolaryngology-Head and Neck Surgery, International Thyroid Surgery Center, Kaohsiung Medical University Hospital, Kaohsiung Medical University, Kaohsiung, Taiwan, [5]Department of Otorhinolaryngology, School of Post-Baccalaureate Medicine and School of Medicine, College of Medicine, Kaohsiung Medical University, Kaohsiung, Taiwan

Objectives: The feasibility and reliability of trans-thyroid cartilage EMG recording method (TCERM) during intraoperative monitoring (IONM) of the recurrent laryngeal nerve (RLN) in thyroid surgery have been established. This study compared two different recording electrode placements on the ipsi-lateral and contra-lateral lamina of the thyroid cartilage (TC).

Methods: Fifty consecutive patients undergoing total thyroidectomy with 100 RLNs at risk were enrolled. Two paired subdermal needle electrodes were inserted into the subperichondrium of the bilateral TC lamina to record electromyography (EMG) signals. The channel leads from the TC electrodes were connected to the patient interface with two different modes. In A-mode, the electrode leads were placed ipsi-laterally, and channel 1 monitored the left RLN and channel 2 monitored the right RLN respectively. In B-mode, the electrode leads were placed contra-laterally, and channels 1 and 2 simultaneously monitored the same side of the RLN. The amplitudes of four EMG signals (V_1-R_1-R_2-V_2) recorded by A-mode and B-mode were compared.

Results: All EMG amplitudes of V_1-R_1-R_2-V_2 signals recorded with B-mode were all above 500μV and significantly higher than those with A-mode ($p<0.001$). No false loss of signal, electrode dislodgement, or needle-related complications were noted during IONM. Postoperatively, all patients had symmetrical vocal cord movement. Lower EMG amplitudes were observed in older and male patients. Histopathology and laterality showed no significant differences in EMG amplitude.

Conclusion: During using TCERM in thyroid surgery, the recording electrodes should be placed contra-laterally on the TC lamina. This approach ensures high and stable EMG signals, which are important for high-quality IONM of the RLN.

KEYWORDS

recurrent laryngeal nerve (RLN), intraoperative neuromonitoring (IONM), thyroid surgery, electromyography (EMG), recording method

Introduction

During the application of intraoperative neuromonitoring (IONM) in thyroid surgery, at least one pair of electrodes is required to record the electromyography (EMG) signal or potential difference from the intrinsic laryngeal muscle, a diagnostic procedure used to assess recurrent laryngeal nerve (RLN) function.

Surface electrode placement is preferred over intramuscular placement because of its non-invasive nature to the vocal cords (1, 2). Therefore, surface electrodes placed on the endotracheal tube (ETT electrodes) have been commonly used to monitor RLN function for decades. However, ETT electrodes often experience changes in electrode-vocal cord contact quality due to laryngeal edema or electrode displacement during surgical manipulation of the trachea. The inconsistent electrodes-vocal cord contact quality can lead to significant changes in the EMG amplitudes during surgery, making quantitative amplitude analysis and actual RLN function evaluation difficult (3–9).

In recent years, the trans-thyroid cartilage EMG recording method (TCERM) has been reported to provide higher quality and more stable EMG signals than the trans-ETT recording method (10–20). The one-channel recording method, in which two independent recording electrodes are placed on the contra-lateral TC lamina, was utilized in the studies by Chiang (10), Liddy (11), Van Slycke (12), Türk (13), and Jung (14). With this electrode placement, both sides of the RLN can be successfully monitored with the same channel electrodes, but it does not provide the lateral discrimination of nerve stimulation. Using the one-channel recording method, Lee et al. (15) placed the recording electrodes on the ipsilateral TC lamina during unilateral hemithyroidectomy. This approach successfully obtained EMG signals, but only one side of the RLN could be monitored.

During using TCERM, the EMG signals can be recorded by one- or two-channel methods, and the recording electrodes can be ipsi-laterally or contra-laterally placed on the TC lamina. When performing a two-channel recording method for TCERM, two pairs of recording electrodes are required to be placed on the bilateral TC lamina. The method is similar to the use of Medtronic standard EMG ETT (3), where the paired electrodes are placed on both sides of the ETT. With this type of electrode placement, the left paired electrodes monitor the left RLN and the right paired electrodes monitor the right RLN separately. However, in the reports of Chiang (16), Huang (17) and Chiu (18), the channel leads of the TC electrodes were inserted into the patient interface with a cross-connection. With this connection, the placement of the recording electrodes on the TC lamina changes from ipsi-lateral to contra-lateral position, and both channels will monitor the same RLN simultaneously. In order to understand the differences between the two EMG recording methods in which the electrodes are placed on the TC lamina ipsi-laterally and contra-laterally, further investigation is necessary.

Materials and methods

Patients

From August 2022 to November 2022, 50 consecutive patients undergoing nerve-monitored total thyroidectomy for various thyroid diseases were enrolled in this study. All surgical procedures were performed by the same surgeon (F.-Y.C.). This study was approved by the E-Da Hospital Institutional Review Board (EMRP-112-015/ed112358).

General anesthesia

General anesthesia was induced with 2% lidocaine (1 mg/kg), propofol (2-3 mg/kg), a single dose of rocuronium (0.6 mg/kg), and a bolus of fentanyl (2 μg/kg) as necessary. Regular oral endotracheal tubes were intubated and anesthesia was maintained with sevoflurane and propofol target-controlled infusion. Sugammadex (1 mg/kg) was administrated to reverse rocuronium-induced neuromuscular blockade at the time point of skin incision.

Abbreviations: EMG, Electromyography; ETT, Endotracheal tube; IONM, Intraoperative monitoring; LOS, Loss of signal; RLN, Recurrent laryngeal nerve; TC, Thyroid cartilage; TCERM, Trans-thyroid cartilage EMG recording method; VN, Vagus nerve.

IONM setup and recording electrodes placement

After resection of the pyramidal lobe and exposure of the TC, two paired subdermal needle electrodes (length, 12.0 mm; diameter, 0.4 mm; needle spacing, 2.5 mm, Medtronic, Jacksonville, FL) (Figure 1) were bilaterally inserted into the subperichondrium of the middle TC lamina from the anterior edge of the thyrohyoid muscle with a slope of 10° to 15° on each side (blue color electrodes on the left; red color electrodes on the right) (Figure 2). After the needle electrode was placed, it was confirmed that it was stable and not prone to dislodge. The electrode wires were then sutured to the anterior laryngeal soft tissue and the surgical sheet.

The channel leads from the TC electrodes were connected to the NIM 3.0 patient interface with A- and B-mode (Figures 3A, B). In A-mode, the two blue electrode leads were inserted into channel 1, and the two red electrode leads were inserted into channel 2. With A-mode TCERM, the recording electrodes are placed ipsi-laterally on the TC lamina, where the left paired electrodes monitor the left side nerves and the right paired electrodes monitor the right side nerves, respectively (Figures 4A, B). In B-mode, one of the blue electrode leads was inserted into channel 2 and one of the red electrode leads was inserted into channel 1. With B-mode TCERM, the recording electrodes were placed contra-laterally on each side of the TC lamina. The evoked EMG signals were recorded simultaneously by channels 1 and 2, and the signal with higher amplitude between the two channels was selected and registered (Figures 5A, B).

The monitoring system generated stimuli with a time window set to 50 ms and an amplitude scale set to 0.2 mV/division. The pulsed stimuli were 100 µs in duration and 4 Hz in frequency. The event threshold was initially set at 300 µV and was reduced to 100 µV or even 50 µV if no EMG signal could be elicited from electrical stimulation of the RLN or vagus nerve (VN).

IONM procedures and EMG signals

Standardized IONM procedures were followed routinely in all patients and V_1-R_1-R_2-V_2 signals were obtained from VN and RLN stimulation. At each step, EMG signals were first recorded by B-mode and then by A-mode. We used 5-10 mA of stimulus current for VN stimulation without VN exposure and 3-5 mA for RLN stimulation. The EMG amplitudes of V_1-R_1-R_2-V_2 signals recorded by A-mode and B-mode were compared, and the EMG amplitudes in the patients with different age, sex, and histopathology were also compared.

All patients underwent pre- and post-operative examination of vocal cord mobility using a flexible laryngofiberscope. All data are presented as mean and standard deviation. To analyze the variables, the paired t-test, independent t-test, and Mann-Whitney U test were performed using SPSS (Version 18.0 for Windows; SPSS Inc., Chicago, IL, USA). A two-tailed p value of less than 0.05 was considered statistically significant.

Results

A total of 50 consecutive patients with 100 RLNs at risk were evaluated in this study. The cohort consisted of 42 females and 8 males. The age of the patients ranged from 23 to 78 years with a mean age of 55.3 years. In the diagnosis, 23 patients were benign disease and 27 patients were malignant disease.

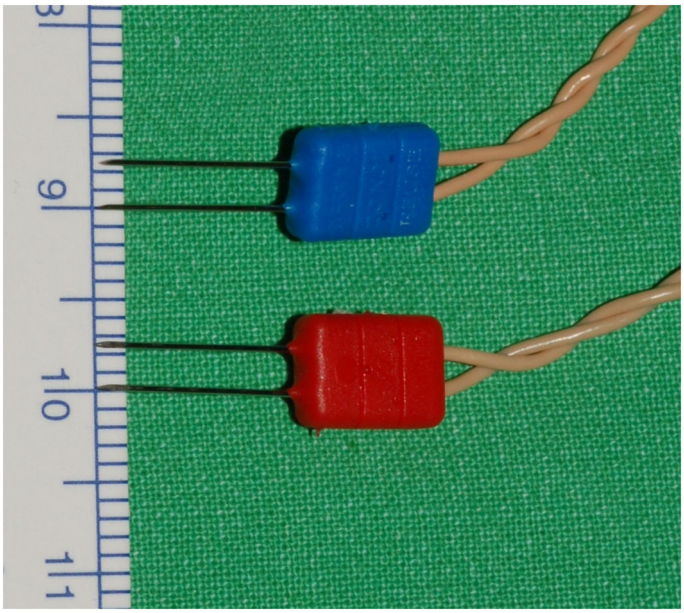

FIGURE 1
Medtronic paired subdermal needle electrodes: 12.0 mm length, 0.4 mm diameter, and 2.5 mm needle spacing.

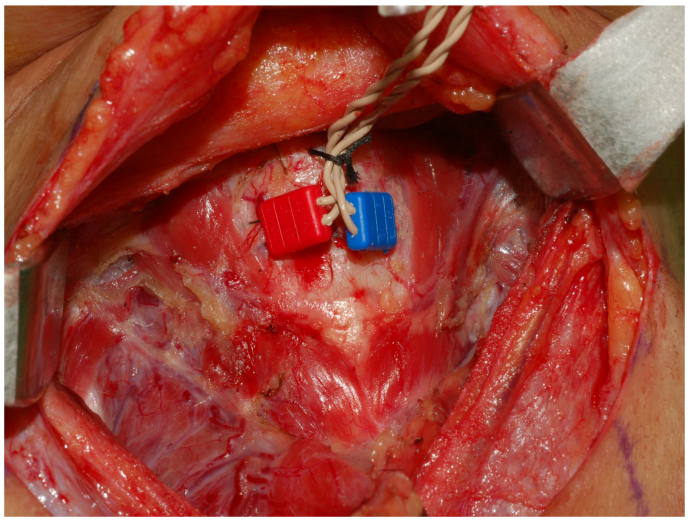

FIGURE 2
Insertion of paired needles into the subperichondrium of the middle TC lamina with a 10° to 15° angle on each side.

The results for the EMG amplitudes of V_1-R_1-R_2-V_2 signals recorded by A-mode and B-mode are presented in Table 1. Using A-mode, the mean amplitudes showed consistently lower values compared to B-mode across all signals. Statistically, there was a significant difference in the mean amplitudes between the two recording methods for all signals, with p-values less than 0.001. Lower amplitudes were also found with A-mode TCERM, in which 50%, 19%, and 3% of V_1 signals were less than 500μV, 300μV, and 100μV, respectively. In contrast, no (0%) B-mode V_1-R_1-R_2-V_2 signals were less than 500μV.

Table 2 compares the EMG amplitudes based on age, sex, and histopathology. In the age-based comparisons, patients aged ≥ 60 years had lower bilateral EMG amplitudes than those younger than 60 years. In sex-based comparisons, male patients had lower bilateral EMG amplitudes than female patients. This difference was significant ($p<0.05$) for all signals on the right side as well as for the left B-mode signals. In comparisons based on histopathology between patients with benign and malignant disease, the difference was not statistically significant.

When comparing the effect of laterality on EMG amplitude, there was no specific side that showed notably higher EMG amplitude in this comparison (Table 3).

Five RLNs experienced a significant decrease in amplitude intraoperatively due to traction distress. The amplitude recovered completely in 3 nerves and recovered more than 70% in another 2 nerves, and all 5 cases showed symmetric vocal cord movement postoperatively. In addition, no occurrence of false loss of signal (LOS), electrode dislodgement, or needle-related complications were observed.

Discussion

When IONM is applied in thyroid surgery, the 4-step IONM procedure to obtain V_1-R_1-R_2-V_2 signals has been generally accepted as standard (21). The EMG amplitude measured at each step can reflect the functional status of the RLN. Theoretically, a decrease in EMG amplitude during surgery

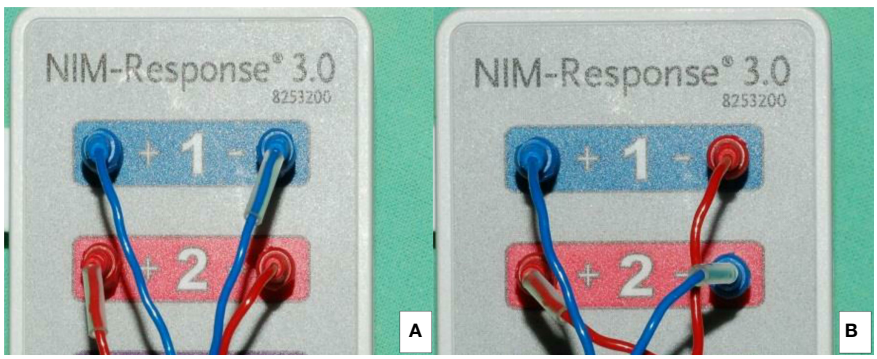

FIGURE 3
The channel leads from the TC electrodes are connected to the patient interface: ipsi-laterally in A-mode **(A)** and contra-laterally in B-mode **(B)**.

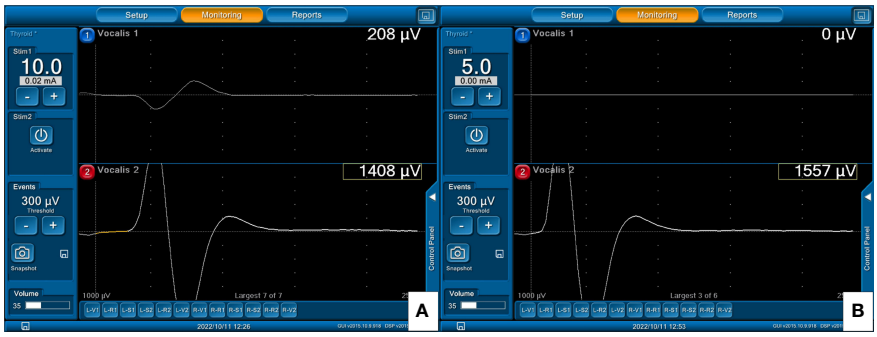

FIGURE 4
With A-mode TCERM, the left paired TC electrodes monitor the left side nerves and the right TC electrodes monitor the right side nerves, respectively. The EMG signals elicited by stimulation of the right VN **(A)** and right RLN **(B)** are shown on channel 2.

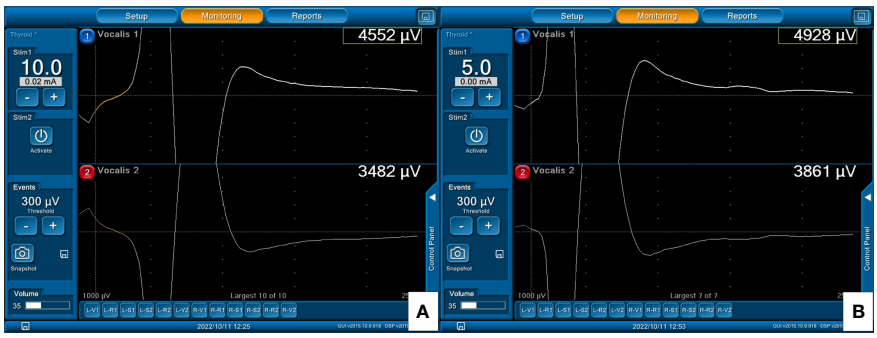

FIGURE 5
With B-mode TCERM, the EMG signal is recorded simultaneously by channels 1 and 2, and the higher amplitude is selected on channel 1 after stimulation of the right VN **(A)** and right RLN **(B)**.

TABLE 1 The EMG amplitudes of V1-R1-R2-V2 signals recorded by A-mode and B-mode TCERM.

Signal	Right					Left				
	A-mode (n=50)		B-mode (n=50)		p value	A-mode (n=50)		B-mode (n=50)		p value
	Mean ± SD (µV)	Range (µV)	Mean ± SD (µV)	Range (µV)		Mean ± SD (µV)	Range (µV)	Mean ± SD (µV)	Range (µV)	
V_1	593 ± 445	65 – 2122	2373 ± 988	595 – 5500	<0.001*	700 ± 529	83 – 2465	2051 ± 729	579 – 3833	<0.001*
R_1	724 ± 646	65 – 3579	2790 ± 1158	638 - 7251	<0.001*	974 ± 798	72 – 4335	3130 ± 1123	667 – 5876	<0.001*
R_2	725 ± 632	85 – 3607	2844 ± 1145	866 - 7395	<0.001*	1013 ± 839	106 – 4402	3148 ± 1117	863 – 5654	<0.001*
V_2	586 ± 470	69 – 2306	2305 ± 890	630 – 5157	<0.001*	734 ± 658	90 – 3337	2103 ± 799	625 – 4004	<0.001*

EMG, electromyography; TCERM, trans-thyroid cartilage EMG recording method; *p value < 0.05 showed significant difference.

indicates a decreased number of muscle fibers participating in the polarization or a deficit of RLN function (22, 23). Therefore, maintaining high and stable EMG amplitudes throughout the entire surgical procedure is important to help not only for RLN identification, but also for early detection of adverse EMG changes to prevent impending traction injury, quantitative analysis of amplitude change after RLN dissection, accurate prediction of vocal cord function outcome, avoidance of the occurrence of false LOS, and elucidation of the mechanism and severity of nerve injury.

TCERM provides a novel surgical application for IONM technology. The recording electrodes placed on the outer surface of the TC lamina can well receive the evoked EMG signals from the thyroarytenoid or vocalis muscles, since the thyroarytenoid muscle runs through the entire length of the vocal cords from the angle of the inner TC lamina to the vocal processes of arytenoid cartilage. In addition, the TC electrodes can be placed and fixed directly on the TC lamina by the surgeon and the EMG signals will not be affected by electrodes position change during surgical maneuvers.

10.3389/fendo.2023.1305629

TABLE 2 Comparison of EMG amplitudes in patients of different age, sex, and histopathology.

EMG signal	Age			Sex			Histopathology		
	<60 years (n=21) Mean ± SD (μV)	≥60 years (n=29) Mean ± SD (μV)	p value	Female (n=42) Mean ± SD (μV)	Male (n=8) Mean ± SD (μV)	p value	Benign (n=23) Mean ± SD (μV)	Malignant (n=27) Mean ± SD (μV)	p value
Right									
A-Mode V_1	702 ± 490	382 ± 190	0.002*	643 ± 456	334 ± 199	0.043*	678 ± 558	522 ± 287	0.245
A-Mode R_1	878 ± 717	427 ± 266	0.003*	799 ± 666	334 ± 210	0.014*	833 ± 850	632 ± 350	0.31
A-Mode R_2	864 ± 704	456 ± 286	0.007*	796 ± 654	354 ± 193	0.031*	829 ± 824	637 ± 361	0.317
A-Mode V_2	693 ± 521	377 ± 207	0.004*	640 ± 484	303 ± 155	0.024*	687 ± 601	500 ± 277	0.188
B-Mode V_1	2666 ± 956	1805 ± 743	0.001*	2563 ± 918	1376 ± 612	0.001*	2570 ± 975	2206 ± 950	0.199
B-Mode R_1	3048 ± 1163	2288 ± 925	0.018*	3019 ± 1074	1586 ± 657	<0.001*	3056 ± 1186	2563 ± 1059	0.139
B-Mode R_2	3107 ± 1167	2332 ± 859	0.013*	3060 ± 1078	1710 ± 636	<0.001*	3069 ± 1190	2652 ± 1046	0.208
B-Mode V_2	2509 ± 910	1909 ± 661	0.013*	2454 ± 845	1523 ± 612	0.005*	2543 ± 895	2102 ± 816	0.083
Left									
A-Mode V_1	737 ± 567	628 ± 417	0.457	740 ± 545	491 ± 319	0.201	733 ± 537	672 ± 510	0.692
A-Mode R_1	1043 ± 876	839 ± 564	0.336	1039 ± 831	630 ± 363	0.219	1094 ± 903	871 ± 662	0.342
A-Mode R_2	1067 ± 903	909 ± 655	0.492	1070 ± 879	716 ± 394	0.418	1093 ± 954	946 ± 702	0.553
A-Mode V_2	776 ± 742	652 ± 411	0.462	770 ± 694	545 ± 285	0.516	742 ± 673	727 ± 632	0.935
B-Mode V_1	2199 ± 600	1763 ± 841	0.076	2155 ± 652	1505 ± 817	0.014*	2210 ± 768	1916 ± 650	0.163
B-Mode R_1	3311 ± 997	2780 ± 1233	0.147	3351 ± 985	1972 ± 1022	0.003*	3228 ± 1124	3047 ± 1095	0.577
B-Mode R_2	3285 ± 989	2883 ± 1262	0.275	3359 ± 991	2042 ± 1016	0.006*	3230 ± 1137	3079 ± 1075	0.64
B-Mode V_2	2240 ± 758	1836 ± 786	0.099	2196 ± 751	1611 ± 816	0.059	2182 ± 833	2035 ± 748	0.526

EMG, electromyography; *p value < 0.05 showed significant difference.

In clinical studies, several types of TC electrode placement for TCERM have been reported. Liddy (11), and Van Slycke (12) reported two independent surface electrodes sutured contra-laterally on the perichondrium of the TC lamina. Both studies concluded that TC surface electrodes provide similar and stable EMG responses with equal sensitivity for recording evoked EMG responses compared to ETT electrodes and appear to be a feasible and reliable alternative. Besides, several commercialized single or paired needle electrodes for TCERM have also been reported, where the recording electrode can be conveniently fixed on the TC by inserting them into the TC lamina. Chiang (10), Türk (13), and Jung (14) used two single-needle electrodes that were inserted into the TC lamina contra-laterally. The results of these studies showed that the mean EMG amplitude of all four EMG signals (V_1-R_1-R_2-V_2) recorded by the TC needle electrodes were significantly higher. In addition, no false LOS occurred, and the positive predictive value of LOS was 100%.

TABLE 3 Comparison of laterality and EMG amplitudes.

EMG signals	Right vs. Left	
	Higher amplitude	p value
A-Mode V_1	Left	0.288
A-Mode R_1	Left	0.074
A-Mode R_2	Left	0.049*
A-Mode V_2	Left	0.202
B-Mode V_1	Right	0.016*
B-Mode R_1	Left	0.063
B-Mode R_2	Left	0.093
B-Mode V_2	Right	0.127

EMG, electromyography.
*p value < 0.05 showed significant difference.

The Medtronic paired subdermal needle electrodes (12.0 mm in length, 0.4 mm in diameter and 2.5 mm in electrode spacing, Figure 1) are commonly applied in facial nerve monitoring and are also suitable for TCERM of the RLN in thyroid surgery. Lee et al. (15) used one paired needle electrode inserted into one side of the TC lamina during unilateral hemithyroidectomy, where the paired recording electrodes were placed ipsi-laterally on TC lamina. The results showed that EMG amplitude was significantly lower when needle insertion was superficial (< 5 mm) and the amplitude was less than 500 μV in 23.5% of cases for V_1 signal. In this study,

two-channel recording method was used and two paired needle electrodes were inserted into the subperichondrium of the bilateral TC lamina. Lower amplitudes were also found with A-mode TCERM, in which 50%, 19%, and 3% of V_1 signals were less than 500μV, 300μV, and 100μV, respectively. Two possible reasons may explain why the A-mode TCERM has lower EMG amplitudes. One possibility is due to the increased impedance of calcified TC when the needles are inserted superficially. Another is that the spacing between the two recording needles is only 2.5 mm, so only a small part of the vacalis muscle can be monitored. However, with B-mode TCERM, where two pairs of recording electrodes are placed on the TC lamina contra-laterally, the two-channel recording needles allow monitoring of a larger area of the intrinsic laryngeal muscle. Figure 6 shows the significant difference between the right V_1 signals recorded by A-mode and B-mode TCERM when needle electrodes were inserted into the TC lamina superficially (269μV vs. 2173μV).

In this study, the B-mode TCERM provides high-quality IONM results: 1) the mean EMG amplitudes of V_1-R_1-R_2-V_2 signals showed significantly higher as compared with A-mode TCERM, 2) all V_1 signals were higher than 500μV that was recommended by international IONM guidelines as a satisfactory initial EMG signal for proper interpretation, diagnosis, and verification of RLN function, 3) the amplitudes of V_2 and R_2 signal showed close to or higher than those of V_1 and R_1 signals in 95 nerves and all showed normal vocal cords movement, 4) the amplitude decreased significantly due to traction distress during surgery in 5 nerves, 3 nerves recovered completely, 2 nerves recovered more than 70%, and all cases showed normal vocal cord movement postoperatively and 5) no occurrence of false LOS.

This study has several limitations similar to other studies when using needle electrodes for TCERM, including:

1). Adequate flap elevation is required to expose TC and limits its use in small neck incision wounds. Pyramidal lobe resection and pre-laryngeal lymph node dissection are routine procedures for our thyroid surgery. TC exposure is not an issue in this study.

2). Patients with calcified TC may have difficulty inserting needle electrodes into the TC lamina. In this study, when the electrodes were placed superficially on the TC, the EMG amplitude showed significantly lower with A-mode TCERM, but a satisfactory EMG signal was obtained with B-mode TCERM.

3). Penetration of the needle electrodes into the larynx may cause laryngeal hematoma, laceration, infection, or rupture of the endotracheal cuff. Although the needle electrodes are inserted into the TC lamina, the needle-related complications can be avoided by proper setup maneuvers, where the needles are inserted into the subperichondrium of the middle thyroid lamina from the anterior margin of the thyrohyoid muscle with a slope of 10° to 15° on each side.

4). Whether the TC thickness is affected by thyroiditis and whether this subsequently affects nerve signaling remains unknown, necessitating future research to confirm.

Conclusion

The paired subdermal needle electrodes used in this study provide a two-channel recording method for IONM of the RLN. From the results of this study, the B-mode TCERM with the recording electrodes placed contra-laterally on the TC lamina meets the requirements for high-quality IONM in thyroid surgery as compared with A-mode TCERM. The novel application of B-mode TCERM provides high and stable EMG amplitudes throughout the entire surgical procedure, which is useful for 1) detection of adverse EMG changes early to prevent impending traction injury, 2) quantifying the amplitude change before and after RLN dissection to elucidate the mechanism and severity of nerve injury, 3) accurately predicting the outcome of vocal cord function, 4) obtaining satisfactory EMG signals, even the needle electrodes placed superficially on the calcified TC lamina, and 5) avoid unnecessary staged thyroidectomy due to false LOS.

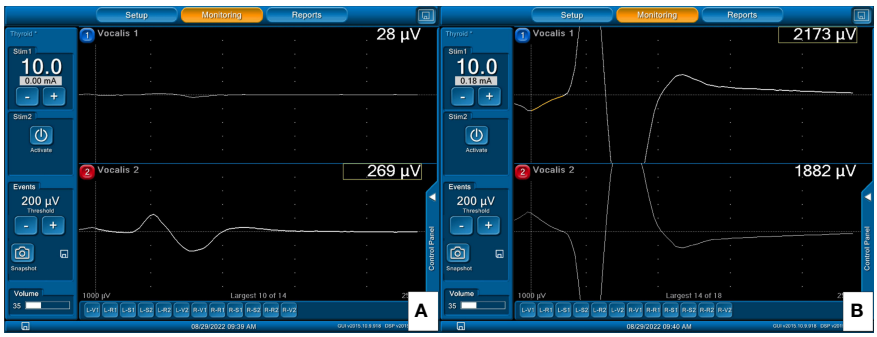

FIGURE 6
EMG signals from right VN stimulation: **(A)** 269μV with A-mode and **(B)** 2173μV with B-mode TCERM, in a patient in whom the needle electrodes were inserted superficially into the TC.

Data availability statement

The original contributions presented in the study are included in the article/supplementary material. Further inquiries can be directed to the corresponding authors.

Ethics statement

The studies involving humans were approved by E-Da Hospital Institutional Review Board (EMRP-112-015/ed112358). The studies were conducted in accordance with the local legislation and institutional requirements. The ethics committee/institutional review board waived the requirement of written informed consent for participation from the participants or the participants' legal guardians/next of kin because Retrospective chart review, informed consent was waived.

Author contributions

F-YC: Conceptualization, Data curation, Formal analysis, Investigation, Resources, Supervision, Visualization, Writing – original draft, Writing – review & editing. Y-CS: Data curation, Investigation, Resources, Writing – original draft, Writing – review & editing. C-FL: Formal analysis, Investigation, Writing – review & editing. CChun-W: Data curation, Resources, Writing – review & editing. CChung-W: Data curation, Resources, Writing – review & editing. T-ZH: Project administration, Supervision, Writing – review & editing. Y-CH: Formal analysis, Writing – review & editing. C-WW: Funding acquisition, Project administration, Supervision, Writing – review & editing. T-HY: Data curation, Resources, Supervision, Validation, Writing – original draft, Writing – review & editing. T-YH: Conceptualization, Data curation, Formal analysis, Funding acquisition, Investigation, Resources, Visualization, Writing – original draft, Writing – review & editing.

Funding

The author(s) declare financial support was received for the research, authorship, and/or publication of this article. This study was supported by grants from Kaohsiung Medical University Hospital, Kaohsiung Medical University (KMUH111-1R48, KMUH111-1R49), and National Science and Technology Council (NSTC112-2314-B-037-033, NSTC 112-2314-B-037-034), Taiwan.

Acknowledgments

The authors would like to thank all the patients included in this study.

Conflict of interest

The authors declare that the research was conducted in the absence of any commercial or financial relationships that could be construed as a potential conflict of interest.

Publisher's note

All claims expressed in this article are solely those of the authors and do not necessarily represent those of their affiliated organizations, or those of the publisher, the editors and the reviewers. Any product that may be evaluated in this article, or claim that may be made by its manufacturer, is not guaranteed or endorsed by the publisher.

References

1. Dralle H, Sekulla C, Lorenz K, Brauckhoff M, Machens A, Group GIS. Intraoperative monitoring of the recurrent laryngeal nerve in thyroid surgery. *World J Surg* (2008) 32:1358–66. doi: 10.1007/s00268-008-9483-2

2. Randolph GW, Dralle HGroup wtIIMS, , Abdullah H, Barczynski M, Bellantone R, et al. Electrophysiologic recurrent laryngeal nerve monitoring during thyroid and parathyroid surgery: international standards guideline statement. *Laryngoscope* (2011) 121(S1):S1–S16. doi: 10.1002/lary.21119

3. Lu I-C, Chu K-S, Tsai C-J, Wu C-W, Kuo W-R, Chen H-Y, et al. Optimal depth of NIM EMG endotracheal tube for intraoperative neuromonitoring of the recurrent laryngeal nerve during thyroidectomy. *World J Surg* (2008) 32:1935–9. doi: 10.1007/s00268-008-9549-1

4. Tsai C-J, Tseng K-Y, Wang F-Y, Lu I-C, Wang H-M, Wu C-W, et al. Electromyographic endotracheal tube placement during thyroid surgery in neuromonitoring of recurrent laryngeal nerve. *Kaohsiung J Med Sci* (2011) 27(3):96–101. doi: 10.1016/j.kjms.2010.08.002

5. Wu C-W, Wang M-H, Chen C-C, Chen H-C, Chen H-Y, Yu J-Y, et al. Loss of signal in recurrent nerve neuromonitoring: causes and management. *Gland Surg* (2015) 4(1):19. doi: 10.3978/j.issn.2227-684X.2014.12.03

6. Dionigi G, Bacuzzi A, Boni L, Rovera F, Dionigi R. What is the learning curve for intraoperative neuromonitoring in thyroid surgery? *Int J Surg* (2008) 6:S7–S12. doi: 10.1016/j.ijsu.2008.12.023

7. Kim HY, Tufano RP, Randolph G, Barczyński M, Wu CW, Chiang FY, et al. Impact of positional changes in neural monitoring endotracheal tube on amplitude and latency of electromyographic response in monitored thyroid surgery: results from the porcine experiment. *Head Neck* (2016) 38(S1):E1004–E8. doi: 10.1002/hed.24145

8. Snyder SK, Hendricks JC. Intraoperative neurophysiology testing of the recurrent laryngeal nerve: plaudits and pitfalls. *Surgery* (2005) 138(6):1183–92. doi: 10.1016/j.surg.2005.08.027

9. Chan W-F, Lo C-Y. Pitfalls of intraoperative neuromonitoring for predicting postoperative recurrent laryngeal nerve function during thyroidectomy. *World J Surg* (2006) 30:806–12. doi: 10.1007/s00268-005-0355-8

10. Chiang FY, Lu IC, Chang PY, Dionigi G, Randolph GW, Sun H, et al. Comparison of EMG signals recorded by surface electrodes on endotracheal tube and thyroid cartilage during monitored thyroidectomy. *Kaohsiung J Med Sci* (2017) 33(10):503–9. doi: 10.1016/j.kjms.2017.06.014

11. Liddy W, Lawson BR, Barber SR, Kamani D, Shama M, Soylu S, et al. Anterior laryngeal electrodes for recurrent laryngeal nerve monitoring during thyroid and parathyroid surgery: New expanded options for neural monitoring. *Laryngoscope* (2018) 128(12):2910–5. doi: 10.1002/lary.27362

12. Van Slycke S, Van Den Heede K, Magamadov K, Brusselaers N, Vermeersch H. New placement of recording electrodes on the thyroid cartilage in intra-operative neuromonitoring during thyroid surgery. *Langenbeck's Arch Surg* (2019) 404:703–9. doi: 10.1007/s00423-019-01825-7

13. Türk Y, Kıvratma G, Özdemir M, İçöz G, Makay Ö. The use of thyroid cartilage needle electrodes in intraoperative neuromonitoring during thyroidectomy: C ase–control study. *Head Neck* (2021) 43(11):3287–93. doi: 10.1002/hed.26810

14. Jung SM, Tae K, Song CM, Lee SH, Jeong JH, Ji YB. Efficacy of transcartilaginous electrodes for intraoperative neural monitoring during thyroid surgery. *Clin Exp Otorhinolaryngology* (2020) 13(4):422–8. doi: 10.21053/ceo.2019.01529

15. Lee HS, Seo SG, Kim DY, Kim SW, Choi Y, Lee KD. Intraoperative neuromonitoring using a single transcartilage needle electrode during thyroidectomy. *Laryngoscope* (2021) 131(2):448–52. doi: 10.1002/lary.28835

16. Chiang F-Y, Wu C-W, Chang P-Y, Wu S-H, Chen H-Y, Lin Y-C, et al. Trans-thyroid cartilage recording for neural monitoring of the recurrent laryngeal nerve in thyroid surgery. *Laryngoscope* (2020) 130(4):E280–E3. doi: 10.1002/lary.28049

17. Huang T-Y, Kim H-Y, Dionigi G, Lu I-C, Chang P-Y, Chiang F-Y, et al. Laryngeal neural monitoring during pediatric thyroid cancer surgery—Is transcartilage recording a preferable method? *Cancers* (2021) 13(16):4051. doi: 10.3390/cancers13164051

18. Chiu K-L, Lien C-F, Wang C-C, Wang C-C, Hwang T-Z, Shih Y-C, et al. Intraoperative EMG recovery patterns and outcomes after RLN traction-related amplitude decrease during monitored thyroidectomy. *Front Endocrinol* (2022) 13:888381. doi: 10.3389/fendo.2022.888381

19. Wu C-W, Chiang F-Y, Randolph GW, Dionigi G, Kim HY, Lin Y-C, et al. Feasibility of intraoperative neuromonitoring during thyroid surgery using transcartilage surface recording electrodes. *Thyroid* (2018) 28(11):1508–16. doi: 10.1089/thy.2017.0680

20. Zhao Y, Li C, Zhang D, Zhou L, Liu X, Li S, et al. Experimental study of needle recording electrodes placed on the thyroid cartilage for neuromonitoring during thyroid surgery. *J Br Surg* (2019) 106(3):245–54. doi: 10.1002/bjs.10994

21. Chiang F-Y, Lee K-W, Chen H-C, Chen H-Y, Lu I-C, Kuo W-R, et al. Standardization of intraoperative neuromonitoring of recurrent laryngeal nerve in thyroid operation. *World J Surg* (2010) 34:223–9. doi: 10.1007/s00268-009-0316-8

22. Huang H-Y, Lien C-F, Wang C-C, Wang C-C, Hwang T-Z, Shih Y-C, et al. Necessity of routinely testing the proximal and distal ends of exposed recurrent laryngeal nerve during monitored thyroidectomy. *Front Endocrinol* (2022) 13:923804. doi: 10.3389/fendo.2022.923804

23. Chiang F-Y, Lu I-C, Kuo W-R, Lee K-W, Chang N-C, Wu C-W. The mechanism of recurrent laryngeal nerve injury during thyroid surgery—the application of intraoperative neuromonitoring. *Surgery* (2008) 143(6):743–9. doi: 10.1016/j.surg.2008.02.006

frontiers | Frontiers in Endocrinology

TYPE Systematic Review
PUBLISHED 19 January 2024
DOI 10.3389/fendo.2023.1295548

OPEN ACCESS

EDITED BY
Tzu-Yen Huang,
Kaohsiung Medical University, Taiwan

REVIEWED BY
Alfred SImental,
Loma Linda University, United States
Maria Rosa Pelizzo,
University of Padua, Italy

*CORRESPONDENCE
Yantao Fu
fuyt@jlu.edu.cn

†These authors share first authorship

RECEIVED 16 September 2023
ACCEPTED 18 December 2023
PUBLISHED 19 January 2024

CITATION
Chen Y, Wang Y, Li C, Zhang X and Fu Y (2024) Meta-analysis of the effect and clinical significance of Delphian lymph node metastasis in papillary thyroid cancer. *Front. Endocrinol.* 14:1295548. doi: 10.3389/fendo.2023.1295548

Meta-analysis of the effect and clinical significance of Delphian lymph node metastasis in papillary thyroid cancer

Yan Chen†, YiHan Wang†, Changlin Li, XueYan Zhang and Yantao Fu*

Division of thyroid Surgery, China-Japan Union Hospital Of Jilin University, Jilin University, Changchun, China

Objective: To investigate the effect and clinical significance of Delphian lymph nodes (DLN) on the factors influencing papillary thyroid cancer (PTC) to provide individualized guidance for the surgical treatment of thyroid cancer.

Methods: Relevant studies from PubMed, Web of Science, the Cochrane Library, Embase, and China National Knowledge Infrastructure databases were searched until February 13, 2023. Stringent selection parameters were used to obtain included data and homogeneous articles. Analyses were performed using Revman 5.4 and SPSS software. A *P*-value of < 0.05 was considered statistically significant.

Results: Five studies were finally included in this study. The results revealed a higher risk of DLN metastasis (DLNM) in patients with tumor size >1cm, multifocality, and extrathyroidal extension (ETE) of the thyroid. The risk of central lymph node metastasis (CLNM) was 11.25 times higher in DLN-positive patients with PTC than in DLN-negative (OR = 11.25, 95% CI: 8.64–14.64, $P < 0.05$) patients. The risk of LLNM was 5.57 times higher in DLN-positive patients with PTC than in DLN-negative (OR = 5.57, 95% CI: 4.57–6.78, $P < 0.001$) patients. The risk of postoperative recurrence in DLN-positive patients with PTC was 3.49 times higher (OR = 3.49, 95% CI: 1.91–6.38, $P < 0.001$) than in DLN-negative patients with PTC.

Conclusion: Patients with tumor size >1 cm in diameter, multifocality, and ETE have an increased risk for DLN development. DLN-positive patients with central and lateral cervical lymph node metastasis and postoperative recurrence are at higher risk than DLN-negative patients.

KEYWORDS

Delphian lymph node, thyroid cancer, papillary thyroid carcinoma (PTC), surgical treatment, recurrence

1 Introduction

The global incidence of thyroid cancer has been rapidly increasing in recent times. The global cancer statistics of 2023 (1) reported that thyroid cancer is three times more prevalent in women than in men. Furthermore, papillary thyroid cancer (PTC) is the most prevalent pathological type of thyroid cancer, accounting for approximately 85% ~ 90% (2), which also has a good prognosis and a five-year survival rate of more than 95% (3). Nevertheless, PTC is prone to early regional lymph node metastasis. Previous studies have reported that the rate of lymph node metastasis in patients with PTC ranges from 30%–80% (3–5).

Central lymph nodes (CLN) serve as the primary site for lymph node metastasis of PTC. Within the CLN, the Delphian lymph nodes (DLN) play a crucial role and have the ability to predict the further development of thyroid cancer. The term Delphian was coined by Raymond B. Randall in 1948, a senior at Harvard Medical School. When Raymond B. Randall was an intern at Massachusetts General Hospital, he found that DLN nodules could predict the clinical progression of head and neck malignancies, similar to Delphi the prophet, a priestess of the Temple of Apollo, known for predicting the future (6). It is positioned between the thyroid cartilage and the cricoid cartilage and anterior to the cricothyroid membrane. DLN receives lymphatic drainage mainly from the epiglottis, subglottis, and the superior pole and isthmus of the thyroid gland. Despite its significance, DLN is often easily intraoperatively overlooked by the operator. Therefore, it is not routinely utilized as a central group clearance area.

Ultrasound (US) is the primary method for preoperative diagnosis of lymph node metastasis in thyroid cancer; however, its accuracy in determining central lymph node metastasis (CLNM) is only approximately 10%–63%. US is limited due to its subjectivity and is related to the standard of the operator, contributing to considerable differences in the study results across different institutions (7). Due to the concealed anatomical site of DLN, preoperative US examination is challenging. Hence, pathological evaluations are performed to determine the presence of DLN metastasis (5). Furthermore, lymphatic imaging using the US is a preoperative technique to determine CLN metastases, which can avoid excessive lymph node dissection compared with the intraoperative application of lymph node contrast agent (4); however, the value of its application warrants further investigation.

The postoperative recurrence of patients with PTC has been prevalently reported (8). The presence of lymph node metastasis is strongly associated with the risk of recurrence in patients with PTC (9, 10). Yang et al. (11) reported that the probability of recurrence in patients with PTC was 6.8% and their tumor size was >20 mm. Furthermore, multifocality and cervical lymph node metastasis are independent risk factors for recurrence. Papaleontiou et al. (12) investigated 2454 patients and reported that the probability of postoperative recurrence in patients with PTC was 4.1% and the probability of persistent disease was 5.8%. The differences in the results of the aforementioned studies can be due to the differences in sample size, geography, and other factors. Notably, no large sample study has investigated the relationship between DLN and postoperative recurrence in patients with PTC. To address this gap in literature, we performed a meta-analysis on five studies on influencing factors and clinical significance of DLN metastasis in PTC to investigate the correlation between DLN, lymph node metastasis, and prognosis in patients with PTC.

2 Materials and methods

2.1 Search strategy

A systematic literature search was conducted to retrieve relevant articles published up to February 13, 2023. We searched PubMed, Web of Science, The Cochrane Library, Embase database, and China National Knowledge Infrastructure (CNKI). The following English keywords were used: (((thyroid carcinoma OR thyroid cancer OR thyroid neoplasm) AND papillary) OR PTC) AND ((prelaryngeal lymph node) OR (Delphian node OR DN) OR (Delphian lymph node OR DLN)). The following Chinese keywords were used in CNKI: (Thyroid Cancer OR Papillary Thyroid Carcinoma) AND (Prelaryngeal Lymph Nodes OR Delphian). The literature selection process was monitored by two data retrievers, with any discrepancies resolved through discussion and consensus or a third author was consulted.

2.2 Inclusion and exclusion criteria and literature screening results

The inclusion criteria for this meta-analysis were as follows (1): articles published before March 7, 2023 (2); patients who underwent first thyroid surgery, with pathologically confirmed PTC for tumor and lymph node metastasis; and (3) studies comparing clinical case parameters between positive DLN and negative DLN in patients with PTC.

The exclusion criteria for this meta-analysis were as follows (1): reviews, conference abstracts, commentaries, commentaries, case reports, and (2) studies with insufficient data collection and overlapping clinical data.

The search results yielded a total of 332 articles, including 97 from PubMed, 97 from Web of Science, 3 from The Cochrane Library, 125 from Embase database, and 10 from CNKI. We excluded 165 duplicate articles. Based on primary screening, we excluded 111 articles, and based on conference abstracts, reviews, case reports, and commentaries, we excluded 24 articles. Full text was unavailable for 2 articles. All the articles included in this meta-analysis were not analyzed or grouped differently were 24 articles. One additional study (13) was excluded from this meta-analysis because it included undetected cases of DLN in the DLN-negative group, which is different from other study groups (Figure 1).

Finally, based on the Newcastle–Ottawa Scale (NOS) quality evaluation, 5 articles were included (Figure 1). Two DLN-related meta-analyses have been previously performed (14, 15). The difference between the two previous meta-analyses and our study is that we have included different indicators. The classification methods of influencing factors of the included articles are

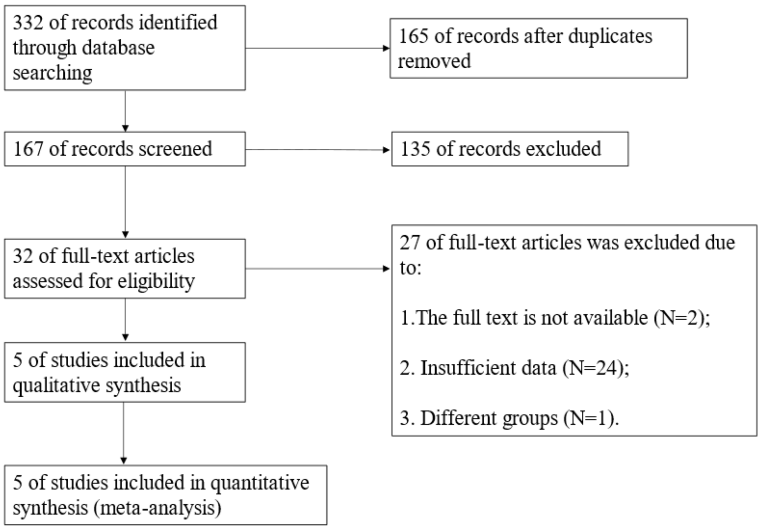

FIGURE 1
Flow chart of study selection.

different. and the correlation between DLN and recurrence has been investigated. Furthermore, we did not deliberately screen the number and geography of cases.

2.3 Data extraction

Two investigators independently evaluated the literature and extracted valid data. Basic information included first author, year of publication, sample size, age (<55 years and ≥55 years), gender, tumor diameter (≤1cm and >1cm), the number of DLN detection and DLN-positive cases, the number of CLNM and LLNM in the subgroup, and the number of recurrences.

2.4 Assessment of literature quality

In this meta-analysis, the NOS quality assessment scale was utilized to evaluate the following three aspects: the study population selection, comparability between groups, and outcome indicators. This assessment uses the semi-quantitative principle of the star system, with the exception of comparability, which can be rated up to 2 stars. The rest of the entries can be rated up to 1 star of 9 stars, where higher scores indicate higher study quality. Of note, scores ranging from 0 to 4 were considered as low-quality research, and scores ranging from 5 to 9 were considered as high-quality research (Table 1).

2.5 Statistical analysis

The odds ratio (OR) and 95% confidence interval (CI) were calculated using a fixed effects model. Heterogeneity was statistically quantified by performing the I^2 test. A heterogeneity of $I^2 \geq 50\%$ was considered significantly different, which was analyzed using a random effects model along with sensitivity analysis. The Revman 5.4 and SPSS software were used to perform statistical analysis. A *P*-value of < 0.05 was considered statistically significant.

3 Results

3.1 Basic information

Table 2 presents the basic information. Based on DLN detection, DLN was categorized into negative and positive groups to compare the difference in DLN metastasis rates between the included studies. The results revealed $P < 0.05$, suggesting that the DLN metastasis rates in the five included papers were unequal (Table 3).

3.2 Influencing factors

Several original studies have investigated the correlation between age, gender, tumor size, multifocality, extrathyroidal extension (ETE), and DLN metastasis (19, 20). Therefore, this meta-analysis obtained the data to further confirm the correlation between DLN lymph node metastasis and these factors.

3.2.1 Age

Three of the five included articles reported age-related data. The ages included <55 years (OR = 1.08, 95% CI: 0.56–2.10, $P = 0.81$, Figure 2A) and ≥55 years (OR = 0.92, 95% CI: 0.48–1.79, $P = 0.81$, Figure 2B) for patients with DLNM transfer, and the results were not statistically significant.

3.2.2 Gender

The results showed that the rate of DLN positivity was 1.39 times higher than DLN negativity in male patients (OR = 1.39, 95% CI: 0.68–2.84, $P = 0.37$, Figure 2C). However, with $P > 0.01$, the study did not

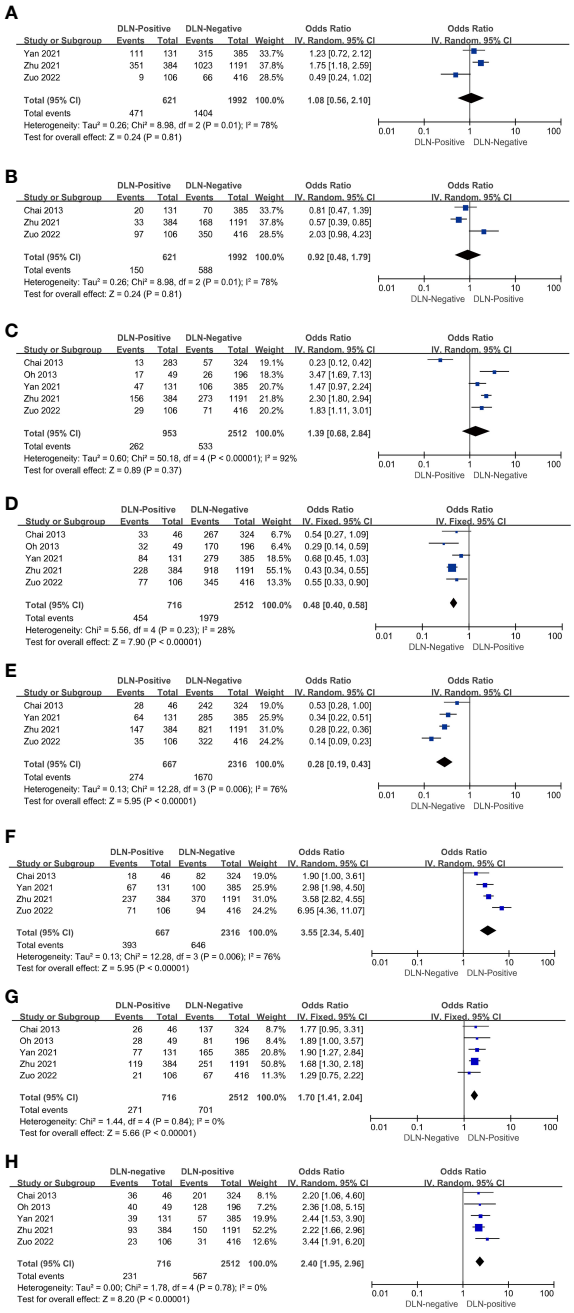

FIGURE 2
Characteristics with regard to age < 55 **(A)**, age ≥ 55 **(B)**, male **(C)**, female **(D)**, cancer lesion diameter ≤ 1 cm **(E)**, cancer lesion diameter > 1cm **(F)**, multifocality **(G)**, ETE **(H)** of patients with PTC with and without DLNM.

reach statistical significance. On the other hand, the rate of DLN positivity was 0.48 times higher than DLN negativity in female patients (OR = 0.48, 95% CI: 0.40–0.58, $P < 0.01$, Figure 2D). Hence, it can be assumed that DLNM in female patients is less likely to occur.

3.2.3 Tumor size

Four of the five included articles reported tumor size-associated data. The results showed that the DLN-positive rate in patients with tumor size ≤1 cm was 0.28 times higher than DLN-negative (OR = 0.28, 95% CI: 0.19–0.43, $P < 0.01$, Figure 2E) patients. Conversely, the DLN-positive rate in patients with tumor size >1 cm was 3.55 times higher than DLN-negative (OR = 3.55, 95% CI: 2.34–5.40, $P < 0.01$, Figure 2F). Thus, it can be assumed that DLNM is correlated with the size of the cancer lesion. Furthermore, the risk of DLNM is higher in patients with a cancer lesion diameter >1 cm.

3.2.4 Multifocality

The results showed that the rate of DLN positivity in patients with PTC having multifocal tumors was 1.70 times higher than that of DLN-negative (OR = 1.70, 95% CI: 1.41–2.04, $P < 0.01$, Figure 2G). It can be inferred that patients with PTC having multifocal tumors are at a higher risk of DLN positivity.

3.2.5 ETE

The results showed that the rate of DLN positivity in patients with PTC having multifocal tumors was 1.70 times higher than that of DLN-negative (OR=1.70, 95% CI: 1.41-2.04, $P < 0.01$, Figure 2H). It can be inferred that patients with PTC having multifocal tumors are at a higher risk of DLN positivity.

3.3 Lymph node metastasis

Four of the five articles included relevant data on CLNM and DLN. The results showed that the risk of CLNM in DLN-positive patients with PTC was 11.25 times higher than in DLN-negative patients (OR = 11.25, 95%: 8.64–14.64, $P < 0.01$, Figure 3A). The risk of LLNM in DLN positive patients with PTC is 5.57 times higher than DLN negative (OR = 5.57, 95% CI: 4.57–6.78, $P < 0.01$, Figure 3B) and it can be assumed that DLNM positive patients are at higher risk of CLNM and LLNM.

3.4 Recurrence

Postoperative recurrence occurred in 22 of 716 DLN-positive patients and 22 of 2512 DLN-negative patients. The risk of postoperative recurrence was 3.49 times higher in DLN-positive patients with PTC than in DLN-negative patients (OR = 3.4 9, 95% CI: 1.91–6.83, $P < 0. 01$, Figure 3C). It can be reported that DLN-positive patients with PTC have a higher risk of postoperative recurrence.

3.5 Heterogeneity analysis

Significant heterogeneity was observed in the forest plots of CLNM ($I^2 = 12\%$, $P = 0.34$, Figure 4A) and LLNM ($I^2 = 94\%$, $P < 0.01$, Figure 4B). Both statistics were analyzed by excluding one study at a time for sensitivity analysis to observe changes in heterogeneity, with no significant changes in heterogeneity in the final results and stable results. Four original studies on CLNM were included, which performed prophylactic clearance of central group

TABLE 1 Quality evaluation of the eligible studies with Newcastle–Ottawa scale.

		Chai 2013	Oh 2013	Yan 2021	Zhu 2021	Zuo 2022
Selection	Representativeness	*	*	*	*	*
	Selection of non-exposed	*	*	*	*	*
	Ascertainment of exposure	*	*	*	*	*
	Outcome not present at start	–	–	–	–	–
Comparability	Comparability on most important factors	*	*	*	*	*
	Comparability on other risk factors	*	*	*	*	*
Outcome	Assessment of outcome	*	*	*	*	*
	Long enough follow-up (median≥6 months)	–	–	–	–	–
	Adequacy (completeness) of follow-up	*	–	*	*	–
Quality score		7	6	7	7	6

*indicates criterion met; - indicates significant of criterion not met.

TABLE 2 Basic information of the 5 included studies.

	Chai 2013	Oh 2013	Yan 2021	Zhu 2021	Zuo 2022
Country	Korea	Korea	China	China	China
Type of study	Retrospective	Retrospective	Retrospective	Retrospective	Retrospective
Institute	Seoul National University Hospital	Gachon University Gil Hospital	Tianjin Medical University Cancer Institute and Hospital	The First Affiliated Hospital of Chongqing Medical University	First People's Hospital of Yunnan Province
Study period	Jan. 2011 - May 2013	Jul. 2009 - Dec. 2011	Aug. 2017 - Jun. 2020	Jul. 2013 - Dec. 2018	Jan. 2017 - May 2021
Case number (n)	1436	898	516	2271	969
Surgical intervention	TT/LI +CLND±LLND	TT +CLND±LLND	TT/LI+CLND±LLND	TT/LI+CLND±LLND	TT/LI+CLND±LLND
Delphian detection n(%)	370(25.8)	245(27.3)	516 (–)	1575(69.4)	522(53.9)
Delphian Positive n(%)	46(12.4)	49(20.0)	131(25.39)	384(24.4)	106(20.3)

LT, lobe thyroidectomy; TT, total thyroidectomy; CLND, central lymph node dissection; LLND, lateral lymph node dissection.

lymph nodes. Furthermore, the heterogeneity in the final results may be due to differences in sample size. Heterogeneity in the results of the meta-analysis of LLNM may be due to the different conditions of performing lateral cervical zone clearance. In some studies (13, 16–18), ipsilateral lateral cervical zone lymph node dissection was performed only when preoperative evaluation (US, CT, MRI, or FNA) or intraoperative LLNM was suspected. Additionally, the accuracy of preoperative diagnosis is unknown due to the presence of occult lymph node metastases in patients with PTC. Zhu et al. (14) performed lymph node dissection in the lateral cervical region when all of the following four conditions were simultaneously fulfilled in addition to preoperative diagnosis: intraoperative frozen section finding CLNM ≥ 3, positive DLN metastasis, ETE, and cancer foci located in the upper pole of the thyroid. This led to the heterogeneity in the results of the analysis of the included studies.

4 Discussion

No large-sample study has reported the relationship between DLN and postoperative recurrence in patients with PTC. In the present meta-analysis, we examined factors influencing DLN in patients with PTC and performed prognostic analysis by obtaining data from 5 related papers. The results revealed that the risk of DLN metastasis was higher in patients with a cancer diameter >1 cm, multifocality, and ETE. Furthermore, the rate of the central group and lateral cervical lymph node metastasis, along with the risk of postoperative recurrence, were increased in DLNM-positive patients with PTC compared with that in DLNM-negative patients. Therefore, based on this meta-analysis, we believe that when relevant risk factors are identified during the preoperative evaluation of patients with PTC, DLN can be dissected and used for intraoperative rapid pathology analysis. Due to their superficial

TABLE 3 Basic information and chi-square tests of DLNM.

Study * DLN Crosstabulation				
Count				
		DLN		
		Positive	Negative	Total
Study	Chai 2013 (37)	46	324	370
	Oh 2013 (16)	106	522	628
	Yan 2021 (17)	131	385	516
	Zhu 2021 (14)	384	1191	1575
	Zuo 2022 (18)	49	196	245
Total		716	2618	3334
Chi-Square Tests				
		Value	df	Asymptotic Significance (2-sided)
Pearson Chi-Square		38.694[a]	4	.000
Likelihood Ratio		41.136	4	.000
Linear-by-Linear Association		23.675	1	.000
N of Valid Cases		3334		

[a]0 cells (0.0%) have expected count less than 5. The minimum expected count is 52.62.

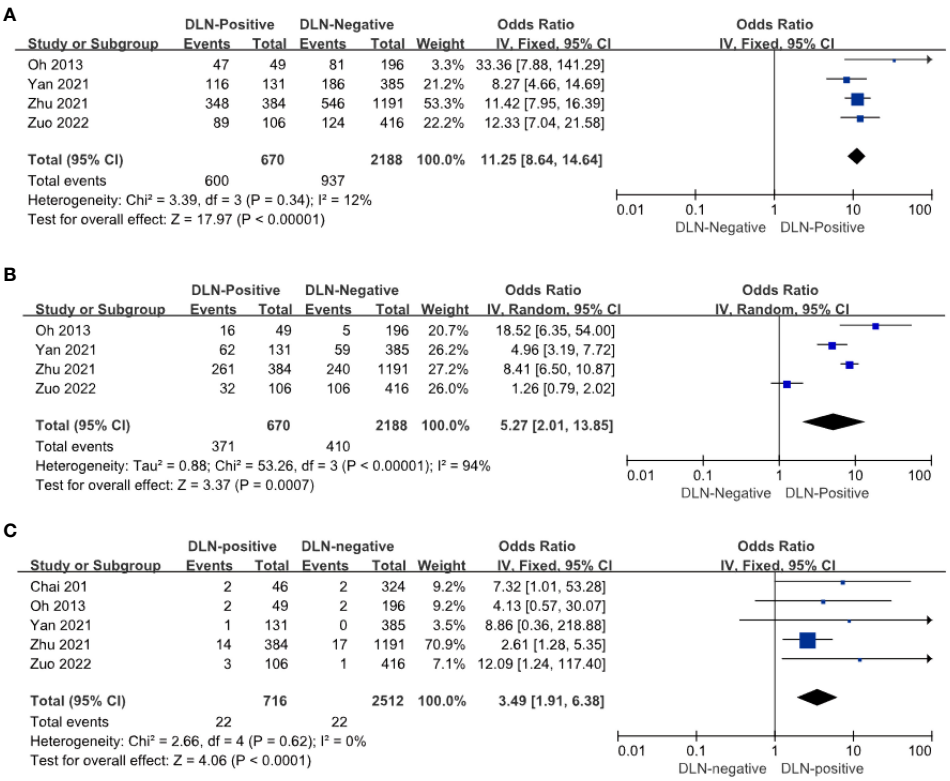

FIGURE 3
Other compartments regarding CLNM **(A)**, LLNM **(B)**, and recurrence **(C)** of patients with PTC with and without DLNM.

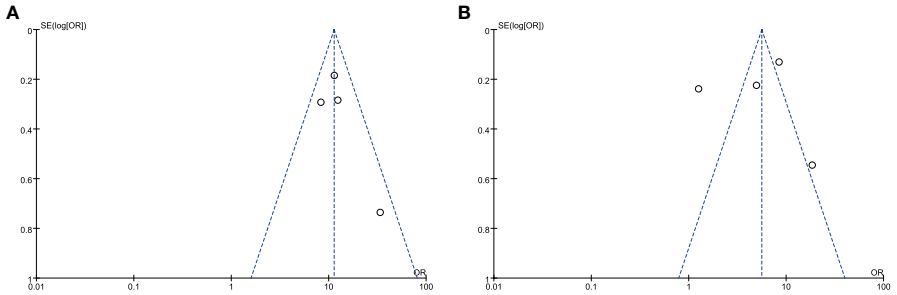

FIGURE 4
Funnel plot of standard error by log relative risks. **(A)**The CLNM group and **(B)** the LLNM group.

anatomical position, this neither prolongs the operation time nor increases the risk of nerve or parathyroid injury. When DLN metastases are diagnosed, indicating disease progression, the surgeon should consider the possibility of malignancy in the contralateral lobe or metastasis in the lateral cervical lymph nodes. DLNM-positive patients have a higher rate of postoperative recurrence, suggesting that for patients with intraoperative pathology suggestive of positive DLN metastases, surgery should be more thorough, and these patients should be closely monitored during follow-up. We believe that DLN can have guidance significance for the personalized surgical treatment of patients with PTC.

4.1 The special role of DLN

Unlike other CLN, DLNM cannot be diagnosed preoperatively because of some anatomical factors and can only be diagnosed intraoperatively using rapid pathological analysis. Zhao et al. (21) reported that the diagnostic rate of CLNM in the US was 48.0%, and the diagnosis of LLNM was 59.2%. Compared with LLN, CLN is not rapidly diagnosed due to various factors such as sternum occlusion and occult lymph node metastasis. Therefore, prophylactic central group lymph node dissection should be considered in patients with PTC, especially for those with cancer lesions of size > 1cm, multifocal, and ETE. Furthermore, the best treatment plan should be selected after weighing the benefits for patients and the risk of surgical complications. Generally, the lymphatic drainage pattern of thyroid cancer is considered to initially metastasize to the central group and then to the lymph nodes in the lateral cervical region. Nevertheless, Kim et al. (22) reported that male patients, patients with DLN-positive, and patients with CLNM-positive unilateral invasive PTC are at a higher risk of bilateral cervical lymph node metastases. Zuo et al. (18) reported that approximately 10% (4/40) of DLN-positive patients had skipping metastases (only DLNM and LLNM positive and CLNM negative). Liu et al. (23) reported that the incidence of LLNM and skipping metastasis was highest in tumors situated on the glandular lobe, giving a fresh understanding of the nature of lymph node metastasis. We suspected that jumpy metastases are associated with DLNM positivity due to DLN drainage of lymph from bilateral upper thyroid poles and isthmus. Furthermore, the role of DLN in the process of lymph node metastasis in patients with PTC and the mechanism underlying nodal jumping metastasis are unclear and warrant further investigation.

4.2 Prognosis and DLN

Patients with PTC tend to experience recurrence after surgery. Postoperative relapses include biochemical recurrence and structural recurrence. The main test for biochemical relapse is serum thyroglobulin (sTg). sTg is presently used to detect persistent disease and recurrent disease (24, 25), with postoperative eugenol suppression treatment sTg < 0.2 ng/mL or TSH-stimulated Tg < 1 ng/mL as the best indicator with the lowest risk of postoperative relapse of 1%–4% (26). In postoperative patients, regular review of Tg helps with the timely detection of recurrence trends and avoids excessive adjuvant testing (27). The following indicators are found to be closely associated with postoperative recurrence: TNM stage, $BRAF^{V600E}$ mutation, postoperative Tg levels, and tumors not completely removed (28, 29). Structural recurrence is a primary recurrence detected in imaging examinations. The US is mainly used for imaging examination of thyroid cancer. FNA, CT, MRI, and 18F-FDG PET can be performed for patients who require further confirmation or for patients with suspected distant metastasis (30). The risk of postoperative recurrence is currently judged postoperatively based on indicators, such as TNM staging. Studies are exploring new potential biomarkers that can be used as prognostic markers in the future. These biomarkers can reveal if preoperative examinations can predict the risk of recurrence among patients, which include investigations on mRNA, microRNA, FN1, ITGα3, MET, miR486, miR-1179, and other genes (31, 32). However, this needs further investigation. Yu Heng et al. (33) reported that patients with PTC situated in the upper portion are more likely to develop LLNM and recurrence. As a part of the central group lymph nodes, the value of DLN in predicting contralateral lobe recurrence or lymph node recurrence in patients with PTC has not been investigated individually. Based on the results of this meta-analysis, we conclude that the risk of postoperative recurrence in DLN-positive patients with PTC is 3.49 times higher than that in DLN-negative patients. Therefore, when combined with the evaluation of preoperative risk factors and

intraoperative rapid pathology, if DLN metastasis is detected, lymph nodes should be meticulously dissected. Attention should be focused on re-evaluating whether there is metastasis in the lateral cervical lymph nodes, providing a foundation for individualized intraoperative treatment. There is a notable association between mortality and postoperative recurrence in patients with PTC. Additionally, the probability of surgical complications is significantly increased with secondary surgery in patients (34). Thorough removal of lesions and lymph nodes during the initial surgery, coupled with regular follow-up post-surgery, proves beneficial for patients with PTC. The surgeon must enhance surgical skills and collaborate actively with the patient to achieve the best therapeutic outcomes. Unfortunately, there is a paucity of articles exploring the relationship between DLN and biochemical recurrence or structural recurrence. Due to the lack of more specific data, we anticipate and welcome further prospective studies in the future to contribute to a more comprehensive understanding of this relationship.

4.3 Influencing factors of DLN

In present studies on laryngeal and hypopharyngeal cancers, DLNM positivity is considered a risk factor for poor prognosis, indicating an unfavorable outcome for patients (35). Nevertheless, in thyroid cancer, the clinical significance of DLN is not known. Previous studies have reported that anterior laryngeal lymph nodes are the sentinel lymph nodes of thyroid cancer and have a predictive effect on cervical lymph node metastasis. Furthermore, DLNM-positive patients have a higher rate of central group lymph nodes and lymph nodes in the lateral cervical region compared with that in DLNM-negative patients (15, 19, 36). Some original studies have reported that the detection rate of DLN is approximately 25.8%–76% (13, 16, 18, 37) and the metastasis rate is approximately 12.4%–25.4% (13, 14, 16–18, 37). Metastasis in the anterior laryngeal lymph nodes correlated with age, gender, multifocality, metastatic site of paratracheal lymph nodes, and location of cancer foci. These can be considered as risk factors. However, the findings of Gong et al. do not support these findings (20). The results of this meta-analysis confirmed that the factors, namely cancer foci >1 cm in diameter, multifocality, and ETE, can be considered risk factors.

To summarize, the presence of positive DLNM indicates a more extensive lymph node metastasis and a higher risk of recurrence in patients. In clinical practice, operators should prioritize DLN and strive for complete clearance when DLNM is present. Clinically, physicians should be attentive to DLN by evaluating preoperative risk factors and relying on intraoperative DLN analysis for rapid pathology. In the presence of positive DLNM, achieving complete lymph node dissection and maintaining close follow-up should be crucial. DLNM has a guiding significance for the personalized surgical treatment of patients with PTC.

The present study also has some limitations that should be addressed. Based on stringent parameters for data screening, only 5 articles were finally included, of which 3 are from China and 2 are from South Korea. Therefore, the results of this meta-analysis are limited due to lesser geographical coverage. However, it is important to note that the number of cases and geographical location were not deliberately screened in the data screening process. Therefore, DLN in this global region may garner more attention and may benefit from routine testing during surgery to establish individualized treatment. Future studies are expected to encompass a broader range of regions to study DLN, allowing in-depth exploration. Furthermore, even regions with a higher DLN rate can be screened in the future.

Data availability statement

The original contributions presented in the study are included in the article/supplementary material. Further inquiries can be directed to the corresponding author.

Author contributions

YC: Writing – original draft. YW: Writing – original draft. CL: Writing – review & editing. XZ: Writing – review & editing. YF: Writing – review & editing.

Funding

The author(s) declare that no financial support was received for the research, authorship, and/or publication of this article.

Conflict of interest

The authors declare that the research was conducted in the absence of any commercial or financial relationships that could be construed as a potential conflict of interest.

Publisher's note

References

1. Siegel RL, Miller KD, Wagle NS, Jemal A. Cancer statistics, 2023. *CA Cancer J Clin* (2023) 73:17–48. doi: 10.3322/caac.21763

2. Megwalu UC, Moon PK. Thyroid cancer incidence and mortality trends in the United States: 2000-2018. *Thyroid* (2022) 32:560–70. doi: 10.1089/thy.2021.0662

3. National Health Commission of the People's Republic of China Medical Administration and Hospital Administration. Guidelines for the diagnosis and treatment of thyroid carcinoma. *Natl Health Commission People's Republic China Med Administration Hosp Administration* (2022) 42:1343–57+63. doi: 10.19538/j.cjps.issn1005-2208.2022.12.02

4. Liu Z, Wang R, Zhou J, Zheng Y, Dong Y, Luo T, et al. Ultrasound lymphatic imaging for the diagnosis of metastatic central lymph nodes in papillary thyroid cancer. *Eur Radiol* (2021) 31:8458–67. doi: 10.1007/s00330-021-07958-y

5. Qi Q, Xu P, Zhang C, Guo S, Huang X, Chen S, et al. Nomograms combining ultrasonic features with clinical and pathological features for estimation of delphian lymph node metastasis risk in papillary thyroid carcinoma. *Front Oncol* (2021) 11:792347. doi: 10.3389/fonc.2021.792347

6. Olsen KD, DeSanto LW, Pearson BW. Positive Delphian lymph node: clinical significance in laryngeal cancer. *Laryngoscope* (1987) 97:1033–7. doi: 10.1288/00005537-198709000-00007

7. Yao F, Yang Z, Li Y, Chen W, Wu T, Peng J, et al. Real-world evidence on the sensitivity of preoperative ultrasound in evaluating central lymph node metastasis of papillary thyroid carcinoma. *Front Endocrinol (Lausanne)* (2022) 13:865911. doi: 10.3389/fendo.2022.865911

8. Hughes C, Shaha A, Shah J, Loree T. Impact of lymph node metastasis in differentiated carcinoma of the thyroid: a matched-pair analysis. *Head Neck* (1996) 18:127–32. doi: 10.1002/(SICI)1097-0347(199603/04)18:2<127::AID-HED3>3.0.CO;2-3

9. Sun JH, Li YR, Chang KH, Liou M.J, Lin SF, Tsai SS, et al. Evaluation of recurrence risk in patients with papillary thyroid cancer through tumor-node-metastasis staging: A single-center observational study in Taiwan. *BioMed J* (2022) 45:923–30. doi: 10.1016/j.bj.2021.11.009

10. Nam SH, Roh JL, Gong G, Cho KJ, Choi SH, Nam SY, et al. Nodal factors predictive of recurrence after thyroidectomy and neck dissection for papillary thyroid carcinoma. *Thyroid* (2018) 28:88–95. doi: 10.1089/thy.2017.0334

11. Yang J, Zhao C, Niu X, Wu S, Li X, Li P, et al. Predictive value of ultrasonic features and microscopic extrathyroidal extension in the recurrence of PTC. *Eur J Radiol* (2022) 157:110518. doi: 10.1016/j.ejrad.2022.110518

12. Papaleontiou M, Evron JM, Esfandiari NH, Reyes-Gastelum D, Ward KC, Hamilton AS, et al. Patient report of recurrent and persistent thyroid cancer. *Thyroid* (2020) 30:1297–305. doi: 10.1089/thy.2019.0652

13. Zhu Y, Lin J, Yan Y, Zheng K, Zhang H, Wu K, et al. Delphian lymph node metastasis is a novel indicator of tumor aggressiveness and poor prognosis in papillary thyroid cancer. *J Surg Oncol* (2021) 123:1521–8. doi: 10.1002/jso.26380

14. Zhu J, Huang R, Yu P, Hu D, Ren H, Huang C, et al. Clinical implications of Delphian lymph node metastasis in papillary thyroid carcinoma. *Gland Surg* (2021) 10:73–82. doi: 10.21037/gs-20-521

15. Huang J, Sun W, Zhang H, Zhang P, Wang Z, Dong W, et al. Use of Delphian lymph node metastasis to predict central and lateral involvement in papillary thyroid carcinoma: A systematic review and meta-analysis. *Clin Endocrinol* (2019) 91:170–8. doi: 10.1111/cen.13965

16. Oh EM, Chung YS, Lee YD. Clinical significance of Delphian lymph node metastasis in papillary thyroid carcinoma. *World J Surg* (2013) 37:2594–9. doi: 10.1186/s40463-019-0362-7

17. Yan Y, Wang Y, Liu N, Duan Y, Chen X, Ye B, et al. Predictive value of the Delphian lymph node in cervical lymph node metastasis of papillary thyroid carcinoma. *Eur J Surg Oncol* (2021) 47:1727–33. doi: 10.2147/CMAR.S232884

18. Zuo Q, Chen X, Yang J, Qiu S, Zhao Y, Sun J. Analysis of the clinical value of delphian lymph node metastasis in papillary thyroid carcinoma. *J Oncol* (2022) 2022:8108256–8108256. doi: 10.1155/2022/8108256

19. Wang B, Wen XZ, Zhang W, Qiu M. Clinical implications of Delphian lymph node metastasis in papillary thyroid carcinoma: a single-institution study, systemic review and meta-analysis. *J Otolaryngol Head Neck Surg* (2019) 48:42. doi: 10.1007/s00268-013-2157-8

20. Gong JX, Gu JW, Ji F, Li K, Zhu Q, Gu FY, et al. Clinical study on prelaryngeal lymph node metastasis in papillary thyroid carcinoma. *Cancer Manag Res* (2020) 12:1323–7. doi: 10.1016/j.ejso.2021.02.010

21. Zhao H, Li H. Meta-analysis of ultrasound for cervical lymph nodes in papillary thyroid cancer: Diagnosis of central and lateral compartment nodal metastases. *Eur J Radiol* (2019) 112:14–21. doi: 10.1016/j.ejrad.2019.01.006

22. Kim SY, Kim SM, Chang H, Kim BW, Lee YS, Chang HS, et al. Lateral neck metastases in the ipsilateral and contralateral compartments of papillary thyroid carcinoma located in one lobe. *ANZ J Surg* (2019) 89:E498–501. doi: 10.1111/ans.15458

23. Liu C, Xiao C, Chen J, Li X, Feng Z, Gao Q, et al. Risk factor analysis for predicting cervical lymph node metastasis in papillary thyroid carcinoma: a study of 966 patients. *BMC Cancer* (2019) 19:622. doi: 10.1186/s12885-019-5835-6

24. Chou R, Dana T, Brent GA, Goldner W, Haymart M, Leung AM, et al. Serum thyroglobulin measurement following surgery without radioactive iodine for differentiated thyroid cancer: A systematic review. *Thyroid* (2022) 32:613–39. doi: 10.1089/thy.2021.0666

25. Jayasekara J, Jonker P, Lin JF, Engelsman AF, Wong MS, Kruijff S, et al. Early postoperative stimulated serum thyroglobulin quantifies risk of recurrence in papillary thyroid cancer. *Surgery* (2020) 167:40–5. doi: 10.1016/j.surg.2019.06.048

26. Haugen BR, Alexander EK, Bible KC, Doherty GM, Mandel SJ, Nikiforov YE, et al. 2015 American thyroid association management guidelines for adult patients with thyroid nodules and differentiated thyroid cancer: the american thyroid association guidelines task force on thyroid nodules and differentiated thyroid cancer. *Thyroid* (2016) 26:1–133. doi: 10.1089/thy.2015.0020

27. Saravana-Bawan B, Bajwa A, Paterson J, McMullen T. Active surveillance of low-risk papillary thyroid cancer: A meta-analysis. *Surgery* (2020) 167:46–55. doi: 10.1016/j.surg.2019.03.040

28. Cho JS, Kim HK. Thyroglobulin levels as a predictor of papillary cancer recurrence after thyroid lobectomy. *Anticancer Res* (2022) 42:5619–27. doi: 10.21873/anticanres.16070

29. Kim SY, Kim YI, Kim HJ, Chang H, Kim SM, Lee YS, et al. New approach of prediction of recurrence in thyroid cancer patients using machine learning. *Med (Baltimore)* (2021) 100:e27493. doi: 10.1097/MD.0000000000027493

30. Santhanam P, Ladenson PW. Surveillance for differentiated thyroid cancer recurrence. *Endocrinol Metab Clin North Am* (2019) 48:239–52. doi: 10.1016/j.ecl.2018.11.008

31. Nieto HR, Thornton CEM, Brookes K, Nobre de Menezes A, Fletcher A, Alshahrani M, et al. Recurrence of papillary thyroid cancer: A systematic appraisal of risk factors. *J Clin Endocrinol Metab* (2022) 107:1392–406. doi: 10.1210/clinem/dgab836

32. Ruiz EML, Niu T, Zerfaoui M, Kunnimalaiyaan M, Friedlander PL, Abdel-Mageed AB, et al. A novel gene panel for prediction of lymph-node metastasis and recurrence in patients with thyroid cancer. *Surgery* (2020) 167:73–9. doi: 10.1016/j.surg.2019.06.058

33. Heng Y, Feng S, Yang Z, Cai W, Qiu W, Tao L. Features of lymph node metastasis and structural recurrence in papillary thyroid carcinoma located in the upper portion of the thyroid: A retrospective cohort study. *Front Endocrinol (Lausanne)* (2021) 12:793997. doi: 10.3389/fendo.2021.793997

34. Otsuki N, Shimoda H, Morita N, Furukawa T, Teshima M, Shinomiya H, et al. Salvage surgery for structural local recurrence of papillary thyroid cancer: recurrence patterns and surgical outcome. *Endocr J* (2020) 67:949–56. doi: 10.1507/endocrj.EJ20-0152

35. Iyer NG, Shaha AR, Ferlito A, Thomas Robbins K, Medina JE, Silver CE, et al. Delphian node metastasis in head and neck cancers–oracle or myth? *J Surg Oncol* (2010) 102:354–8. doi: 10.1002/jso.21640

36. Wang B, Zhu CR, Liu H, Yao XM, Wu J. Relationship between pretracheal and/or prelaryngeal lymph node metastasis and paratracheal and lateral lymph node metastasis of papillary thyroid carcinoma: A meta-analysis. *Front Oncol* (2022) 12. doi: 10.3389/fonc.2022.950047

37. Chai YJ, Kim SJ, Choi JY, Koo H, Lee KE, Youn YK. Papillary thyroid carcinoma located in the isthmus or upper third is associated with Delphian lymph node metastasis. *World J Surg* (2013) 38:1306–11. doi: 10.1007/s00268-013-2406-x

frontiers | Frontiers in Endocrinology

TYPE Systematic Review
PUBLISHED 12 July 2024
DOI 10.3389/fendo.2024.1352503

OPEN ACCESS

EDITED BY
Maaike van Gerwen,
Icahn School of Medicine at Mount Sinai,
United States

REVIEWED BY
Adnan Işgör,
Memorial Sisli Hospital, Türkiye
Akira Sugawara,
Tohoku University, Japan

*CORRESPONDENCE
Di Zhu
judy3481@163.com
Caizhe Yang
yangcaizhe2008@163.com

RECEIVED 08 December 2023
ACCEPTED 24 June 2024
PUBLISHED 12 July 2024

CITATION
Kong X, Wang L, Sun Y, Zhu D and Yang C (2024) Comparison of radiofrequency ablation and surgery for thyroid papillary microcarcinoma: efficacy, safety and life quality.
Front. Endocrinol. 15:1352503.
doi: 10.3389/fendo.2024.1352503

Comparison of radiofrequency ablation and surgery for thyroid papillary microcarcinoma: efficacy, safety and life quality

Xiaoyan Kong[1,2], Liangchen Wang[1,2], Yuchen Sun[1,2], Di Zhu[1,2]* and Caizhe Yang[1,2]*

[1]Department of Endocrinology, Air Force Medical Center, Beijing, China, [2]Department of Graduate School, China Medical University, Shenyang, China

Objective: To compare the efficacy, safety and patients' quality of life of radiofrequency ablation (RFA) and surgery in the treatment of papillary thyroid microcarcinoma (PTMC).

Methods: MEDLINE, EMBASE, Cochrane, CNKI and other databases were searched for studies on radiofrequency ablation versus traditional surgery for PTMC up to October 2022. RevMan5.4 software was used for Meta-analysis.

Results: 10 articles were selected from 392 articles, including 873 cases of radiofrequency ablation and 781 cases of open surgery. After meta-analysis, the incidence of postoperative complications in the radiofrequency ablation group was lower than that in the surgery group, and the difference was statistically significant [OR=0.24, 95%CI (0.14,0.41), P<0.001]. There were no significant differences in lymph node metastasis rate, local recurrence rate, and new tumor rate between the two groups [OR=1.6, 95%CI (0.21, 12.41), P>0.05; OR=0.85, 95% CI (0.05, 13.8), P>0.05; OR=0.12, 95%CI (0.01, 0.98), P>0.05]. The treatment time and hospital stay in the radiofrequency ablation group were shorter than those in the open surgery group [MD=-49.99, 95%CI (-62.02, -37.97), P<0.001; MD=-5.21, 95%CI(-7.19,-3.23),P<0.001], and the cost was significantly lower than that of the traditional surgery group [SMD=-14.97, 95%CI (-19.14, -10.81), P<0.001]. The quality of life of patients in the radiofrequency ablation group was higher than that in the surgery group [MD=-1.61, 95%CI (-2.06, -1.17), P<0.001].

Conclusion: Compared with traditional open surgery, radiofrequency ablation for papillary thyroid microcarcinoma has the advantages of less trauma, fewer complications, faster recovery and higher quality of life. The indications need to be strictly controlled in the treatment.

Systematic review registration: https://www.crd.york.ac.uk/PROSPERO/, identifier (CRD42022374987).

KEYWORDS

papillary thyroid microcarcinoma, radiofrequency ablation, surgery, meta-analysis, life quality

1 Introduction

In recent years, the incidence of thyroid cancer has increased dramatically, among which the main type is papillary thyroid microcarcinoma (PTMC) with a diameter of ≤10mm. The situation in China is similar to that abroad (1). According to the Guidelines for the Diagnosis and Treatment of Thyroid Cancer (2022 Edition) (2), surgery is the preferred treatment for thyroid cancer in China, but not all patients are candidates for surgery or choose to undergo surgery. Therefore, minimally invasive treatment of thyroid microcarcinoma has attracted much attention. In this paper, the efficacy, safety and quality of life satisfaction of radiofrequency ablation and surgery were comprehensively evaluated.

2 Materials and methods

2.1 Search strategy

The study was registered in the International Prospective Register of Systematic Reviews (PROSPERO) (registration number CRD42022374987). This study searched MEDLINE, EMBASE, Cochrane, CNKI and other databases by subject headings + free words. The English search term is Thyroid Cancer, Papillary thyroid microcarcinoma, Papillary Thyroid Carcinoma, Papillary Thyroid Cancers, Radiofrequency ablation, surgery, etc. The Chinese search terms were papillary thyroid carcinoma, thyroid microcarcinoma, radiofrequency ablation, surgery, etc. The search time was up to October 2022.

2.2 Inclusion and exclusion criteria

Inclusion criteria: 1) studies on low-risk PTMC patients and 2) studies comparing treatment outcomes between thermal ablation and surgery.

Exclusion criteria: 1) case report or case series included <20 patients; 2) Letters, editorials, conference abstracts, consensus statements, guidelines, and review articles; 3) articles that do not focus on specific topics.

2.3 Data extraction and quality assessment

Two reviewers used a standard data extraction form to extract the following data from the included studies (1): study characteristics: first author's name, publication year, study design, sample size (2); Demographic and clinical characteristics of patients: mean age, sex distribution, tumor diameter (3); Postoperative characteristics: volume reduction rate, tumor complete disappearance rate, postoperative hospital stay, perioperative cost, complication rate, operation time, recurrence rate and Thyroid Health-related Quality of Life (THYCA-QOL) (4). Postoperative complications.

Two reviewers independently assessed the methodological quality of the included studies using the Newcastle-Ottawa Scale (NOS), and disagreements were resolved with a third reviewer. The NOS scale is suitable for evaluating case-control studies and cohort studies. It has 8 items in 3 parts to evaluate cohort studies and case-control studies. These include:

Selection:

1) Representative of exposed group (1 point)

2) Representative of the non-exposed group (1 point)

3) Identification of exposure factors (1 point)

4) Confirm the outcome indicators not to be observed at the beginning of the study (1 point)

Comparability:

1) The comparability of exposed group and non-exposed group was considered in design and statistical analysis (2 points)

Outcome:

1) Evaluation of outcome indicators (1 point)

2) Long enough follow-up time (1 point)

3) Integrity of exposed group and non-exposed group (1 point)

2.4 Statistical analysis

RevMan 5.4 software was used to analyze the indicators, and chi-square test was used to test the heterogeneity of the indicators included in the study. If the heterogeneity test was not statistically significant ($I2<50\%$, $P\geq0.05$), the fixed effect model was used. The count data were analyzed by Odds Ratio (OR) (95% confidence interval), and the measurement data were analyzed by Mean Difference (MD) (95% confidence interval). If the heterogeneity test showed significant heterogeneity ($I2\geq50\%$, $P<0.05$), then sensitivity analysis was used to find the source of heterogeneity and Meta-analysis was performed using the random effect model. $P<0.05$ was considered statistically significant.

3 Outcome

3.1 Results of literature search

A total of 392 literatures were retrieved from the database by means of subject headings + free words, and 88 duplicate literatures were screened out. By reading titles and abstracts, 178 unrelated studies were removed, and articles such as meta-analysis, case report and guidelines were removed. Twenty-one articles were read in full, and 10 articles were finally included according to the inclusion and exclusion criteria (3–12), The screening flow chart is shown Figure 1. The basic characteristics of each included article are shown in Table 1. According to the criteria of the NOS scale, the quality of the studies was within the acceptable range, as shown in Table 2.

The surgery group included lobectomy or total thyroidectomy combined with lymph node dissection. Among them, Du Ke-feng,

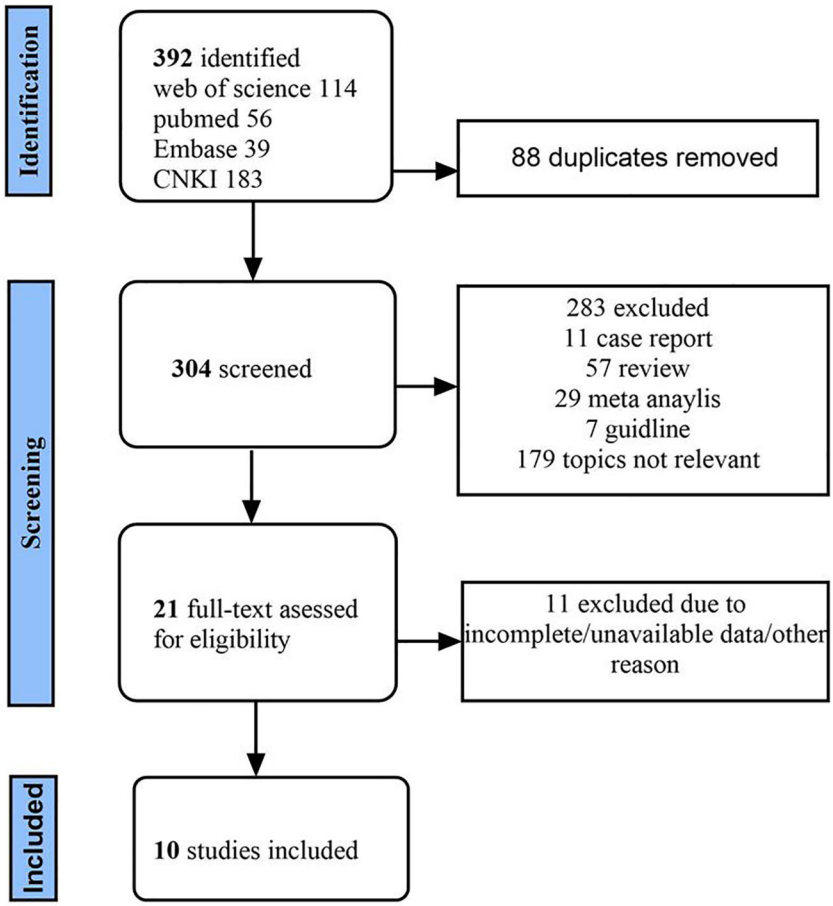

FIGURE 1
The screening flow chart.

Feng Na and Zhao Xiao-li studied thyroid lobectomy combined with central cervical lymph node dissection (TL+CLD), and Song et al. performed total thyroidectomy combined with central cervical lymph node dissection (TT+CLD). The surgical methods of Yu Lan, Zhang2021, Zhang2020, Zhang Guangxu were determined according to ATA guidelines. The surgical group of LAN Yu et al. was divided into lobectomy group and total resection group, without mention of lymph node dissection. Gong Hai et al. did

TABLE 1 Basic characteristics of the included studies.

Included Literature	Year	Radiofrequency Ablation Group			Surgical Group		
		Number	Mean age	Sex Men/ women	Number	Mean age	Sex Men/ women
Gong,Hai (3)	2019	75	49.7 ± 7.4	23/52	73	48.9 ± 7.4	20/53
Lan (8)	2020	54	41.9 ± 10.2	12/42	34	42.4 ± 9.9	3/31
Zhang (5)	2020	94	45.4 ± 10.8	24/70	80	44.1 ± 9.6	20/60
Du,Kefeng (6)	2021	37	45.4 ± 6.1	13/24	37	44.6 ± 7.0	11/26
Feng,Na (7)	2021	102	47.4 ± 11.2	26/76	115	43.9 ± 10.7	23/92
Yu, Lan (8)	2021	80	42.6 ± 10.2	17/63	69	43.2 ± 10.4	5/64
Zhang,Guangxu (9)	2021	132	41.6 ± 8.9	33/99	118	43.6 ± 9.2	21/97
Zhang (9)	2021	133	45.8 ± 9.9	0/97	101	45.7 ± 10.8	0/101
Song (11)	2021	115	44.9 ± 10.4	18/97	103	45.4 ± 9.9	19/84
Zhao,Xiaoli (12)	2022	51	46.1 ± 7.4	10/41	51	47.4 ± 7.7	11/40

10.3389/fendo.2024.1352503

TABLE 2 Quality scores of the included literature.

First author,year	1	2	3	4	5	6	7	8	9	NOS
Gong,Hai,2019 (3)	1	1	1	1	0	1	1	0	0	7
Yu,2020 (4)	1	1	1	1	0	1	1	1	0	8
Zhang,2020 (5)	1	1	1	1	0	1	1	1	1	9
Du,Kefeng,2021 (6)	1	1	1	1	1	1	1	1	0	9
Feng,Na,2021 (7)	1	1	1	1	0	1	1	1	1	9
Lan,Yu,2021 (8)	1	1	1	1	1	1	1	0	0	8
Zhang, Guangxu,2021 (9)	1	1	1	1	0	1	1	1	1	9
Zhang,2021 (9)	1	1	1	1	1	0	1	1	0	8
Song,2021 (11)	1	1	1	1	0	1	1	1	1	9
Zhao,Xiaoli,2022 (12)	1	1	1	1	1	1	1	0	0	8

not mention the extent of surgery and the presence or absence of lymph node dissection.

3.2 Results of meta-analysis

3.2.1 Efficacy of radiofrequency ablation and tumor progression

A total of four articles reported the efficacy of radiofrequency ablation for thyroid microcarcinoma. The efficacy was evaluated by the volume reduction rate. The patients were followed up at 1, 3, 6, 12 months and every 6 months thereafter. Feng Na (7) followed up 102 patients in the radiofrequency ablation group for 12 months, and evaluated that 100% of the nodules were completely ablated without signs of recurrence or metastasis. The effective rate of the same group was 100%, and the difference was not statistically significant. Similarly, Zhang Guangxu (9) followed up 121 of 132 patients in the ablation group, and the volume of the thyroid ablation area increased significantly on the first day and 1 month after surgery, and gradually decreased in the subsequent process. At 6 months, the ablation zone had disappeared in 37 patients (30.6%). At 12 months, the ablation zone had disappeared in 75 patients (62.0%). At the latest follow-up, the ablation area of 121 patients disappeared, and the volume reduction rate was 100%. Du Kefeng (6) et al., 37 patients in the observation group, had a preoperative tumor volume of (0. 14 ± 0. 04) mm3, the tumor volume at 1 month and 3 months after surgery was (0. 27 ± 0. 13) mm3, (0. 11 ± 0. 05) mm3. The tumor volume at 6 months after operation was (0. 07 ± 0. 04) mm3, the tumor volume at 12 months after operation was (0. 01 ± 0. 01) mm3, the tumor volume before and after operation was statistically significant (F = 74. 472, P < 0. 001). The final tumor volume reduction rate in the observation group was (93. 05 ± 3. 27) %. Zhang (10) observed the volume of ablation zone in 133 cases of ablation group at each follow-up time point, and calculated the volume reduction rate. At 18 months after the last follow-up time point, the volume reduction rate was 99.98%. A number of studies and a large number of data show that radiofrequency ablation is effective in the treatment of papillary thyroid microcarcinoma, and the tumor nodules that reach or close to the surgical group disappear completely.

A total of 6 studies reported the local recurrence rate of tumors. A total of 1167 patients were included in the literature, including 613 patients in the radiofrequency ablation group and 554 patients in the traditional thyroid surgery group. There was no heterogeneity in the indicators of the included studies (P=0.65, I2 = 0.0%), and the fixed effect model was used for analysis. Meta-analysis showed that there was no significant difference in local recurrence rate between the radiofrequency ablation group and the traditional surgery group [OR=1.6, 95%CI (0.21, 12.41), P > 0.05]. The forest plot is shown in Figure 2.

A total of 4 studies reported the incidence of new cancer. A total of 908 patients were included in the literature, including 461 patients in the radiofrequency ablation group and 447 patients in the traditional thyroid surgery group. There was no heterogeneity in the indicators of the included studies (P=0.91, I2 = 0.0%), and the fixed effect model was used for analysis. Meta-analysis showed that there was no significant difference in the incidence of new tumors between the thermal ablation group and the conventional surgery group. [OR=0.85, 95%CI (0.05, 13.8), P > 0.05].

A total of 5 studies reported the lymph node metastasis rate. They indicated that the mode of follow-up and lymph node metastasis was 1, 3, 6, 9, and 12 months after surgery, with reexamination of thyroid ultrasound, and patients after 12 months after surgery were followed up every 6 to 12 months

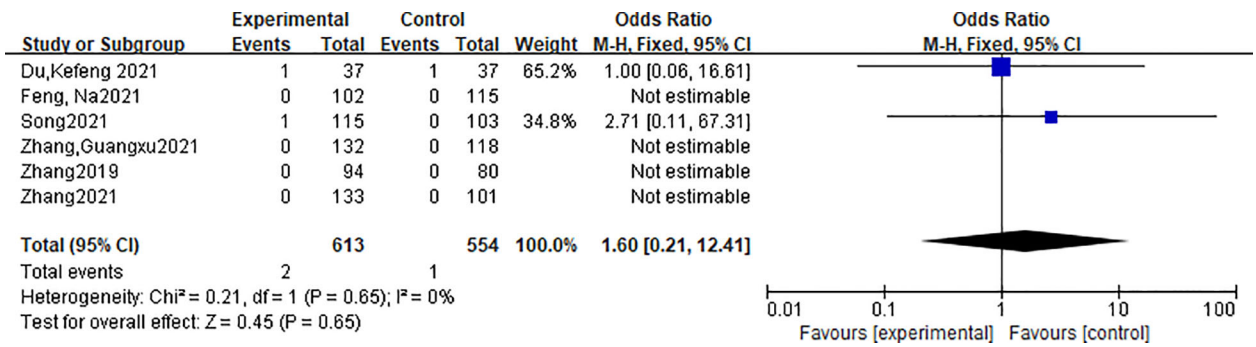

FIGURE 2
Forest plot of local recurrence rate.

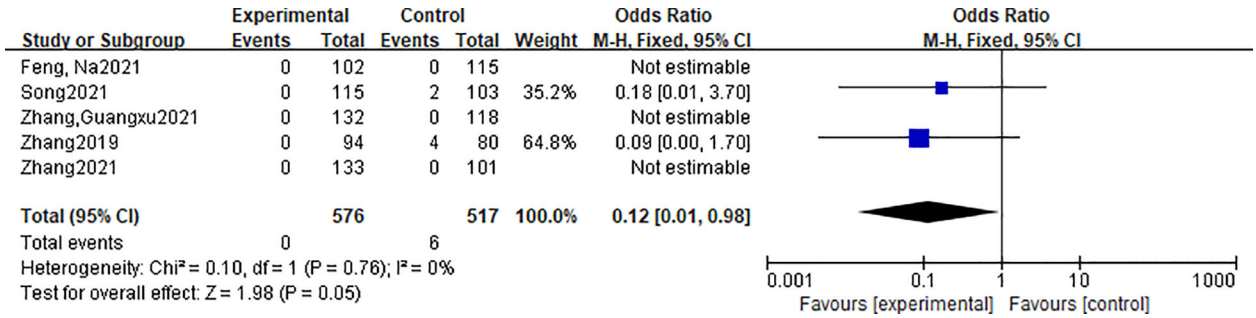

FIGURE 3
Forest plot of lymph node metastasis rate.

according to the patient's condition. If suspicious nodules or lymph nodes were detected by ultrasound, aspiration cytology and thyroglobulin in the eluate were performed if necessary. A total of 1093 patients were included in the literature, including 576 patients in the radiofrequency ablation group and 517 patients in the traditional thyroid surgery group. There was no heterogeneity in the indicators of the included studies (P=0.05, I2 = 0.0%), and the fixed effect model was used for analysis. Meta-analysis showed that there was no significant difference in local recurrence rate between the thermal ablation group and the traditional surgery group [OR=0.12, 95%CI (0.01, 0.98), P > 0.05]. The forest plot is shown in Figure 3.

3.2.2 Safety comparison

A total of 8 articles reported the postoperative complications of radiofrequency ablation and surgery group, including hoarseness, drinking cough, permanent recurrent laryngeal nerve damage, peripheral tissue damage, convulsions, incision bleeding, pain, incision infection, anesthesia vomiting, hypothyroidism, hyperthyroidism, etc. Severe complications included recurrent laryngeal nerve injury, tracheal injury, and hypoparathyroidism, while minor complications included pain, transient hoarseness, and wound infection. The impact on thyroid function was not included in the comparison, because all patients in the surgical group had permanent hypothyroidism and scar after surgery. In a study by Zhang Guangxu (9) et al., the number of patients with complications such as pain and hoarseness in the two groups was not listed. It was only reported that 1 of 132 patients in the ablation group had hypothyroidism and 3 had hyperthyroidism due to the use of Euthyroxine, while all 118 patients in the surgery group had hypothyroidism. After its removal, the heterogeneity is less than 50%, and the funnel plot is shown in Figure 4, with approximate symmetry on both sides indicating that the synthesized results are robust. The incidence of postoperative complications in the radiofrequency ablation group was lower than that in the surgery group, and the difference was statistically significant [OR=0.24,95% CI(0.14,0.41),P < 0.001].The forest plot is shown in Figure 5.

3.2.3 Comparison of time and economic benefits

A total of 5 studies reported the treatment time and postoperative hospital stay. A total of 1291 patients were included in the literature, including 481 patients in the radiofrequency

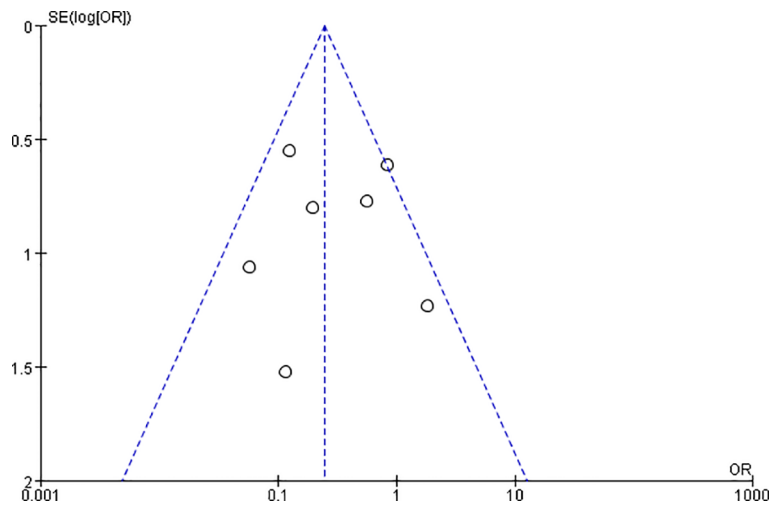

FIGURE 4
Plot of postoperative complication rates.

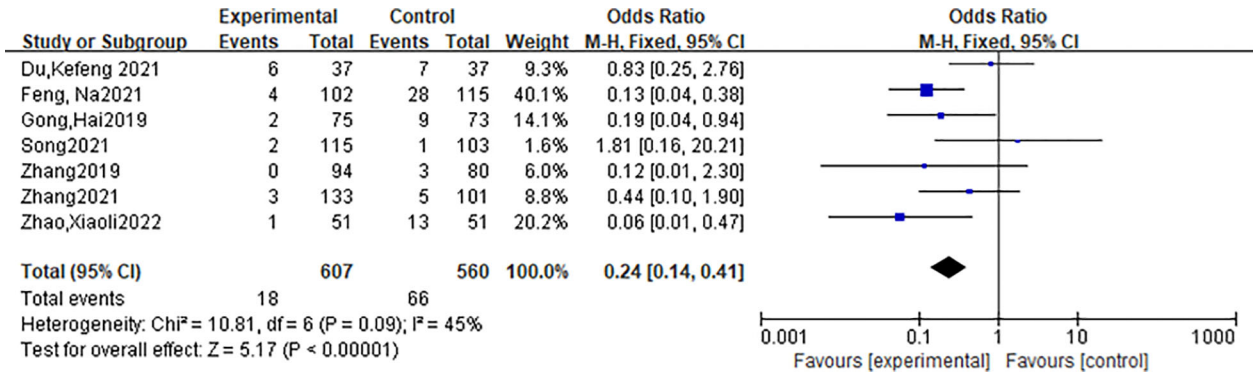

FIGURE 5
Forest plot of postoperative complication rates.

ablation group and 436 patients in the traditional thyroid surgery group. There was heterogeneity in the indicators of the included studies (P < 0.001, I2 > 50%), and the random effect model was used for analysis. Meta-analysis showed that the treatment time and postoperative hospital stay in the thermal ablation group were less than those in the traditional surgery group, and the difference was statistically significant [MD=-49.99, 95%CI(-62.02, -37.97), P<0.001; MD=-5.21, 95%CI(-7.19,-3.23),P<0.001]. Four studies reported the cost of treatment. There was heterogeneity in the indicators of the included studies, and the random effect model was used for analysis. Meta-analysis showed that the treatment cost of the thermal ablation group was lower than that of the traditional surgery group, and the difference was statistically significant [SMD=-14.97, 95%CI (-19.14, -10.81), P < 0.001]. The greater heterogeneity may be related to the different hospitals and geographic locations in which treatment was performed, but the results consistently showed that radiofrequency ablation was associated with shorter hospital stay, shorter treatment duration, and lower costs than surgery.

3.2.4 Comparison of quality of life scores

A total of 4 studies reported the thyroid-specific quality of life score of tumors. The indicators of the included studies were heterogeneous (I2 = 99%). Sensitivity analysis excluded the literature with large heterogeneity of Song2021, and no heterogeneity was found. The THYQOL score of the RFA group was lower than that of the traditional surgery group, that is, the quality of life of the RFA group was higher than that of the surgery group, and the difference was statistically significant [MD=-1.61, 95%CI (-2.06, -1.17), P < 0.001]. The forest plot is shown in Figure 6.

4 Discussion

Due to the widespread use of ultrasound-guided fine needle aspiration cytology, the detection rate of primary papillary thyroid carcinoma (PTMC) is increasing, accounting for 50% of papillary thyroid carcinoma (13, 14). The World Health Organization (WHO) defines PTMC as thyroid microcarcinoma or less than 10 mm in diameter (1). The American Joint Committee on Cancer (AJCC) TNM system classifies T1 category (T; 1: ≤2 cm) were divided into T1a: ≤1 cm and T1b: ≤2 cm (15). There are three treatments for papillary thyroid microcarcinoma: follow-up, surgery, or minimally invasive thyroid surgery. Although several landmark studies have suggested that the prognosis of papillary thyroid microcarcinoma is good, even if the long-term survival rate of patients without intervention is not statistically different from that of patients with immediate surgery (13, 16, 17), the diagnosis of cancer may affect the quality of life of patients, and the majority of patients will choose intervention. Chinese guidelines for primary thyroid cancer (2)recommend surgery as the first-line treatment, and RFA can be applied as the preferred alternative for patients who are not suitable for surgery or refuse surgery. Although the curative

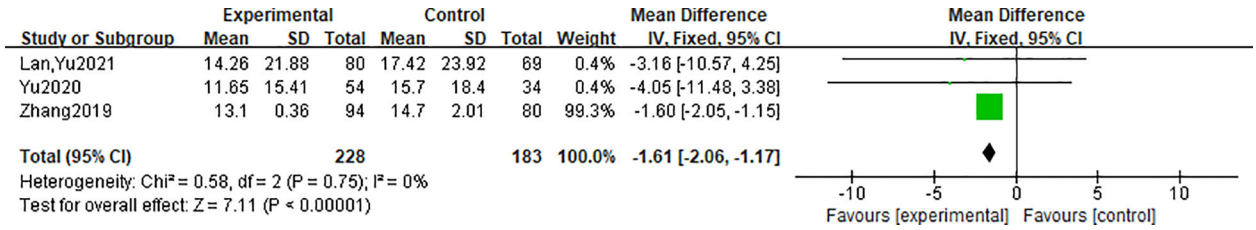

FIGURE 6
Forest plot of THYQOL score comparison.

effect of RFA is very good, it will lead to a variety of postoperative complications such as permanent hypothyroidism, recurrent laryngeal nerve injury, surgical scar and other shortcomings, as well as aesthetic impact. More and more studies have proved the safety and efficacy of RFA in PTMC (18–22). For example, One of the largest cohort studies to date found that Yan et al. followed 414 patients with single-focus PTMC for long-term tumor efficacy after RFA treatment after 42.15 ± 11.88 months (range, 24–69 months) (10). After RFA, 366 of 414 tumors (88.41%) completely disappeared, with a volume reduction rate of 98.81 ± 6.41%, indicating long-term efficacy in this large cohort (22).What's more, a meta-analysis of three 5-year follow-up PTMC patients who underwent RFA involved 207 patients and 219 PTMCS, none of whom had local tumor recurrence, lymph node metastasis, or distant metastasis, or underwent delayed surgery during a mean follow-up of 67.8 months. Five new tumors developed in the remaining thyroid in four patients, four of which were successfully treated by repeated thermal ablation. The mean combined major complication rate was 1.2%, and no patient had life-threatening or delayed complications. The long-term safety of RFA has been demonstrated (20).

Therefore, ten studies were included in this study, and the radiofrequency ablation group was compared with the surgery group. In terms of efficacy, the tumor volume reduction rate of the radiofrequency ablation group was close to or reached 100% after a long enough follow-up, which was close to the efficacy of the surgery group. However, the concern that RFA treatment may affect tumor progression, such as lymph node metastasis, local recurrence, and increase in new tumors, occurred in a small number of cases among the thousands of cases in the literature, and the difference between the radiofrequency ablation group and the surgery group was not statistically significant. In terms of safety, the incidence of postoperative complications in the radiofrequency ablation group was lower than that in the surgery group, and the difference was statistically significant. The efficacy of radiofrequency ablation in the treatment of papillary thyroid microcarcinoma is similar to that of surgery, with low incidence of complications and good safety.

The study found that the treatment time and length of hospital stay in the radiofrequency ablation group were less than those in the surgery group, and the cost was lower, which was helpful to reduce the economic burden of disease. In terms of quality of life, this paper uses the thyroid specific Quality of Life scale score, which is an internationally used quality of life scale for thyroid cancer (23, 24). It was sinicized by Liu Jie et al., a Chinese expert (25) in 2019. It has been confirmed that it has good reliability and validity, and can be used as an assessment tool for the quality of life of Chinese thyroid cancer patients. It includes 24 questions summarized into seven symptom domains (neuromuscular, voice, attention, sympathetic symptoms, throat or mouth, psychological, and sensory problems) and six single items (scarring, feeling cold, tingling in hands or feet, weight gain, headache, and decreased libido). All items were scored on a 4-point scale (none, somewhat, fairly, very good). A higher score indicates that the patient complains more about the symptom. The results of meta-analysis showed that the THYQOL score of the RFA group was lower than that of the traditional surgery group, that is, the quality of life was higher than that of the surgery group, and the difference was statistically significant.

Our meta-analysis also has shortcomings, for example, there are few studies included in the quality of life score. In the future, we hope that more studies will focus on the quality of life of patients, rather than only the efficacy and safety of treatment, especially the proportion of women in patients with thyroid cancer is high, and the scar caused by surgery will affect the quality of life of patients. In addition, the surgical methods of the included studies were different, which would affect the study results. However, study heterogeneity is acceptable in the comparison of outcome measures. If there are more studies on the comparison of radiofrequency ablation and surgery in the treatment of PTMC in the future, the surgery group can be further divided into TT group and TL group for comparison.

In conclusion, RFA can fill the gap between surgery and follow-up in a minimally invasive manner. Radiofrequency ablation is the first choice for patients who are not suitable for surgery or refuse surgery. In addition, if more studies support the efficacy and safety of radiofrequency ablation, radiofrequency ablation may become the preferred treatment for patients with thyroid microcarcinoma in the future.

Data availability statement

The original contributions presented in the study are included in the article/supplementary material. Further inquiries can be directed to the corresponding authors.

Author contributions

XK: Writing – original draft. CY: Writing – review & editing. DZ: Writing – review & editing. LW: Writing – review & editing. YS: Data curation, Writing – original draft.

Funding

The author(s) declare financial support was received for the research, authorship, and/or publication of this article. This work was supported by Clinical Research Program of Air Force Medical Center (Grant No. 2021LC016) and Chuying Project of Air Force Medical University (Grant No.KT2021DX005).

Conflict of interest

The authors declare that the research was conducted in the absence of any commercial or financial relationships that could be construed as a potential conflict of interest.

Publisher's note

References

1. Tufano RP, Pace-Asciak P, Russell JO, Suárez C, Randolph GW, López F, et al. Update of radiofrequency ablation for treating benign and Malignant thyroid nodules. The future is now. *Front Endocrinol (Lausanne)*. (2021) 12:698689. doi: 10.3389/fendo.2021.698689

2. People HCOT, #39, National sROC. National guidelines for diagnosis and treatment of thyroid cancer (2022 edition). *Chin J Pract Surg*. (2022) 42:1343–57+63. doi: 10.21147/J.ISSN.1000-9604.2022.03.01

3. Gong H, Liu W, Yao Z. Efficacy of ultrasound-guided microwave ablation, radiofrequency ablation and surgical resection in the treatment of papillary thyroid microcarcinoma. *Chin J Cancer Clinic Rehabil*. (2019) 26:781–4. doi: 10.13455/j.cnki.cjcor.2019.07.04

4. Yu L, Yukun L, Mingbo Z, Zhuang J, Jing X, Lin Y, et al. Quality of life in papillary thyroid microcarcinoma patients undergoing radiofrequency ablation or surgery: A comparative study. *Front Endocrinol*. (2020) 11. doi: 103389/fendo.2020.00249

5. Zhang M, Tufano RP, Russell JO, Zhang Y, Zhang Y, Qiao Z, et al. Ultrasound-guided radiofrequency ablation versus surgery for low-risk papillary thyroid microcarcinoma: results of over 5 years' Follow-up. *Thyroid*. (2020) 30:408–17. doi: 10.1089/thy.2019.0147

6. Du KF, Dong G. Clinical efficacy and safety of ultrasound-guided radiofrequency ablation in the treatment of papillary thyroid microcarcinoma. *Cancer Basic Clinic*. (2021) 34:378–81.

7. Feng N, Huang PT, Xu D, Liping W. Comparison of radiofrequency ablation and surgery for papillary thyroid microcarcinoma. *J Intervent Radiol*. (2021) 30:356–60. doi: 10.21147/J.ISSN.1000-9604.2022.03.01

8. Lan Y, Zhang MB, Zhang Y, Qing S, Lin Y, Jing X, et al. Comparison of quality of life in patients with papillary thyroid microcarcinoma treated with different methods. *J Chin Acad Med Sci*. (2021) 43:328–37. doi: 10.3881/J.ISSN.1000-503X.1334

9. Zhang G. *Efficacy comparison of ablation and surgery in the treatment of low-risk papillary thyroid microcarcinoma*. Changchun: Jilin University (2021).

10. Chao Z, Jing Y, Chenlu H, Qin Y, Ping W, Pintong H. Comparison of ultrasound guided percutaneous radiofrequency ablation and open thyroidectomy in the treatment of low-risk papillary thyroid microcarcinoma: A propensity score matching study. *Clin Hemorheol Microcirc*. (2021) 80(20). doi: 10.3233/CH-201087

11. Song Q, Gao H, Ren L, Tian X, Lan Y, Yan L, et al. Radiofrequency ablation versus total thyroidectomy in patients with papillary thyroid microcarcinoma located in the isthmus: a retrospective cohort study. *Int J Hyperthermia*. (2021) 38(1). doi: 10.1080/02656736.2021.1916625

12. Zhao X, Song M. Efficacy of ultrasound-guided radiofrequency ablation and surgical resection in the treatment of papillary thyroid microcarcinoma and its influence on complications. *Clin Med Res Pract*. (2022) 7(17):105–7. doi: 10.19347/j.cnki.2096-1413.202217028

13. Bernardi S, Giudici F, Cesareo R, Antonelli G, Cavallaro M, Deandrea M, et al. Five-year results of radiofrequency and laser ablation of benign thyroid nodules: A multicenter study from the Italian minimally invasive treatments of the thyroid group. *Thyroid*. (2020) 30:1759–70. doi: 10.1089/thy.2020.0202

14. Tumino D, Grani G, Di Stefano M, Di Mauro M, Scutari M, Rago T, et al. Nodular thyroid disease in the era of precision medicine. *Front Endocrinol (Lausanne)*. (2019) 10:907. doi: 10.3389/fendo.2019.00907

15. Perrier ND, Brierley JD, Tuttle RM. Differentiated and anaplastic thyroid carcinoma: Major changes in the American Joint Committee on Cancer eighth edition cancer staging manual. *CA Cancer J Clin*. (2018) 68:55–63. doi: 10.3322/caac.21439

16. Wells SA Jr., Asa SL, Dralle H, Elisei R, Evans DB, Gagel RF, et al. Revised American Thyroid Association guidelines for the management of medullary thyroid carcinoma. *Thyroid*. (2015) 25:567–610. doi: 10.1089/thy.2014.0335

17. Oda H, Miyauchi A, Ito Y, Yoshioka K, Nakayama A, Sasai H, et al. Incidences of unfavorable events in the management of low-risk papillary microcarcinoma of the thyroid by active surveillance versus immediate surgery. *Thyroid*. (2016) 26:150–5. doi: 10.1089/thy.2015.0313

18. Bernardi S, Palermo A, Grasso RF, Fabris B, Stacul F, Cesareo R. Current status and challenges of US-guided radiofrequency ablation of thyroid nodules in the long term: A systematic review. *Cancers (Basel)*. (2021) 13. doi: 10.3390/cancers13112746

19. Ding M, Tang X, Cui D, et al. Clinical outcomes of ultrasound-guided radiofrequency ablation for the treatment of primary papillary thyroid microcarcinoma. *Clin Radiol*. (2019) 74:712–7. doi: 10.1016/j.crad.2019.05.012

20. Cho SJ, Baek SM, Na DG, et al. Five-year follow-up results of thermal ablation for low-risk papillary thyroid microcarcinomas: systematic review and meta-analysis. *Eur Radiol*. (2021) 31:6446–56. doi: 10.1007/s00330-021-07808-x

21. Van Dijk SPJ, Coerts HI, Gunput STG, et al. Assessment of radiofrequency ablation for papillary microcarcinoma of the thyroid: A systematic review and meta-analysis. *JAMA Otolaryngol Head Neck Surg*. (2022) 148:317–25. doi: 10.1001/jamaoto.2021.4381

22. Yan L, Lan Y, Xiao J, et al. Long-term outcomes of radiofrequency ablation for unifocal low-risk papillary thyroid microcarcinoma: a large cohort study of 414 patients. *Eur Radiol*. (2021) 31:685–94. doi: 10.1007/s00330-020-07128-6

23. Husson O, Haak HR, Buffart LM, et al. Health-related quality of life and disease specific symptoms in long-term thyroid cancer survivors: a study from the population-based PROFILES registry. *Acta Oncol*. (2013) 52:249–58. doi: 10.3109/0284186X.2012.741326

24. Rogers SN, Mepani V, Jackson S, et al. Health-related quality of life, fear of recurrence, and emotional distress in patients treated for thyroid cancer. *Br J Oral Maxillofac Surg*. (2017) 55:666–73. doi: 10.1016/j.bjoms.2016.09.001

25. Liu J, Gao J, Tang Y, et al. Evaluation of the reliability and validity of the Chinese version of the thyroid cancer specific quality of life Scale. *Cancer*. (2019) 39:178–87.

frontiers | Frontiers in Endocrinology

TYPE Original Research
PUBLISHED 26 November 2024
DOI 10.3389/fendo.2024.1361736

OPEN ACCESS

EDITED BY
Tzu-Yen Huang,
Kaohsiung Medical University, Taiwan

REVIEWED BY
Hanwei Peng,
Shantou University, China
Jilai Tian,
Nanjing University of Chinese Medicine, China

*CORRESPONDENCE
Kunxiu Ming
kwsjyzw@126.com

RECEIVED 26 December 2023
ACCEPTED 12 November 2024
PUBLISHED 26 November 2024

CITATION
Wang Y, Li Q, Fan M and Ming K (2024) The parathyroid glands identification of carbon nanoparticles via preoperative injection in reoperation of recurrent benign multinodular goiter.
Front. Endocrinol. 15:1361736.
doi: 10.3389/fendo.2024.1361736

The parathyroid glands identification of carbon nanoparticles via preoperative injection in reoperation of recurrent benign multinodular goiter

Yonghui Wang[1], Quancai Li[2], Mingxiu Fan[1] and Kunxiu Ming[3]*

[1]Department of Thyroid and Breast Surgery, Weifang People's Hospital, Weifang, Shandong, China, [2]Department of Neurosurgery, Weifang People's Hospital, Weifang, Shandong, China, [3]Department of Central Sterile Supply, Weifang People's Hospital, Weifang, Shandong, China

Introduction: Benign multinodular goiter (BMNG) can grow very large and cause compression symptoms, making the operation procedure difficult. However, the recurrence rate of BMNG ranges from 3% to 43%. Reoperative thyroid surgery for BMNG is uncommon and can result in a high rate of complications, including hypoparathyroidism and recurrent laryngeal nerve palsy. Carbon nanoparticles (CNs) have been widely used as a protective agent for the parathyroid gland and as a tracer agent in central lymph node dissection. However, the protection effect of CNs in redoing BMNG has not been well illustrated. This study investigates whether CNs could protect parathyroid glands (PGs) during reoperation for patients with BMNG.

Methods: BMNG patients who previously underwent thyroidectomy and received reoperation between January 2019 and January 2022 were retrospectively recruited. The Dunhill approach was employed for all patients. The patients were divided into two groups: the CNs group, who received injection CNs injection 1 hour before the operation (n = 24), and the control group, who underwent thyroid surgery without CNs injection (control group, n = 25). The numbers of PGs preserved *in situ*, autotransplantation, the accidental removal of the PGs, and the parathyroid hormone level were recorded and analyzed.

Results: The results revealed that more PGs were preserved *in situ* in the CNs group compared to the control group (3.25±0.15 *vs* 2.60±0.16, P=.007). Moreover, fewer PGs were subjected to autotransplantation and were accidentally discovered in the specimen in the CNs group compared to the control group. Patients who had CNs injection exhibited a lower rate of transient (5/24 *vs.* 13/25, P=.024) and permanent hypoparathyroidism (2/24 *vs.* 9/25, P=.020) compared to the control group.

KEYWORDS

reoperation, thyroid, benign multinodular goiter, carbon nanoparticles, hypoparathyroidism

Introduction

Benign multinodular goiter (BMNG) is the most popular endocrine disease, especially in the iodine-deficiency areas (1). Generally, BMNG is not treated if the patient has normal thyroid function and no compressive symptoms (2). Surgery for BMNG is necessary for those with compressive symptoms, large substernal goiter, suspected malignancy, and cosmetic concerns (2). The extent of resection for BMNG has varied over the years but focused on removing all involved diseases (1). However, the surgery complication rate has significantly increased with the extent of resection (1). L-thyroxin therapy has been advocated to decrease the recurrence rate but with minimal efficiency (3, 4). The recurrence rate of BMNG ranges from 3% to 43% (5–7).

Reoperative thyroid surgery has dramatically increased the incidence of complications, particularly hypoparathyroidism and recurrent laryngeal nerve (RLN) palsy (8). The intraoperation monitoring of RLN has significantly reduced RLN injury (9, 10). Fine dissection operation to protect the parathyroid in the thyroid operation has been recommended (8, 11). However, scar formation, landmark distortion, and tissue friability complicated efforts to identify and protect the parathyroid (8). Carbon nanoparticles (CNs) as lymph node tracers have been widely used in stomach, breast, and thyroid cancers (12–14). Given that the space between capillary endothelial cells is between 20 and 50 nm, smaller than the CN diameter (150 nm), CNs could not transport via the capillary. Therefore, the thyroid and lymph node were stained black, while the parathyroid was still in its original color if CNs were injected into the thyroid (15). Recent studies have shown that applying CNs in thyroid surgery has significantly decreased the rate of hypoparathyroidism and increased the number of dissection lymph nodes (15). However, the leakage of CNs may drain the tissue, including the parathyroid around the thyroid, making identifying the parathyroid more difficult (15). The purpose of this study was to investigate whether CNs via preoperative injection could identify and protect the parathyroid during reoperation for recurrent BMNG.

Materials and methods

Patients

From January 2019 to January 2022, 49 consecutive patients who performed reoperative thyroid surgery at the Department of Thyroid and Breast Surgery, Weifang People Hospital, were retrospectively enrolled. Patients were divided into the CNs injection group (CNs group, n=24) and the control group (n=25).

Inclusion criterion: Patient have a history of thyroid surgery, with pathology indicating BMNG. The patient presents compression symptoms and a tumor whose longest diameter exceeds 40 mm with postoperative pathology confirmation of BMNG.

Exclusion criterion: The patient has a history of neck radiotherapy. The patient also has RLN palsy or hypoparathyroidism before the secondary thyroid surgery with postoperative pathology confirmation of a malignant tumor.

All the redoing thyroid surgery was performed by the same professional thyroid surgeon (Yonghui Wang).

CNs injection before the operation

Ultrasound-guided injection of CNs was performed 1 hour before the surgery in the CNs group. Carbon nanoparticles (0.5 mL per ampoule, Chongqing LaiMei Pharmaceutical Co., Ltd., Chongqing, China) were used. The special procedures were as follows: 0.6 mL of CNs was extracted with a 1 mL syringe, and the air in the needle was expelled (Figure 1A). Under the ultrasound guide, CNs were slowly

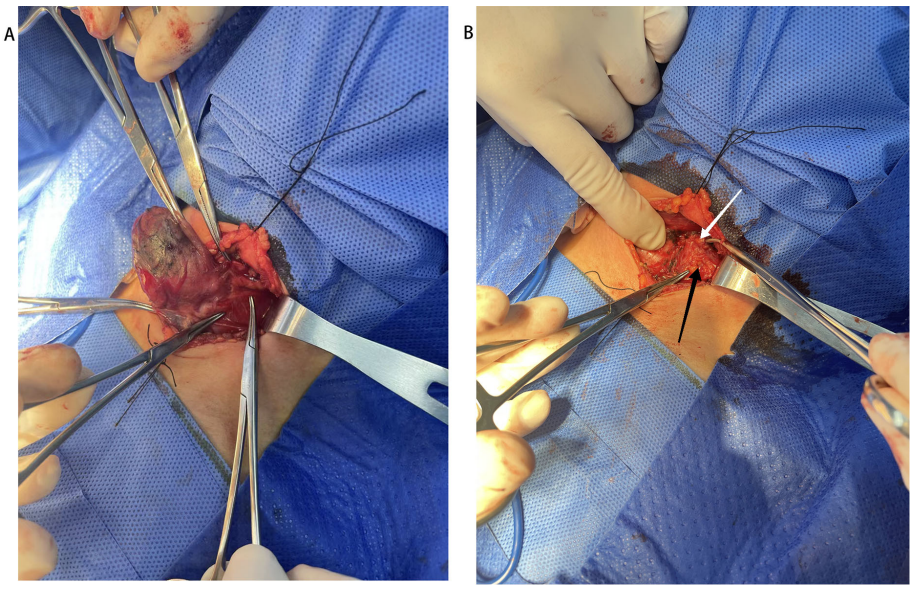

FIGURE 1
Injection of Carbon nanoparticles. **(A)** Preparation of Carbon nanoparticles. **(B)** The Carbon nanoparticles injection under the guiding of ultrasound.

injected into the gland at the superior, middle, and inferior parts of every thyroid lobe (0.1 mL at each point). The needle should be gently withdrawn with negative pressure after injection (Figure 1B) and immediately pressed for 3 min with gauze. To avoid the skin staining by CNs, we firstly changed a new needle, then expelled the air from the needle as much as possible. In addition, after the injection, the needle gently withdrawn with negative pressure. Preoperative injection of CNs was performed by an experienced surgeon (Yonghui Wang) 1 hour before the operation.

Surgical procedure

All the patients underwent the Dunhill approach (hemithyroidectomy with counterlateral subtotal resection). After general anesthesia with tracheal intubation was administered, patients were placed supine with cervical hyperextension. The reoperation approach was through the scar of the previous Kocher's incision, with the linea alba cervicalis split, exposing the thyroid. The isthmus of thyroid was break along the trachea. Then total right lobectomy and subtotal left lobectomy were performed. The first step was ligation of the inferior thyroid vessels. Then, the RLN was identified in the tracheoesophageal groove and traced very carefully along its cervical course. Thirdly, the superior thyroid vessels were ligated. At last, the right thyroid lobe was total removed. While for the left lobe, the superior pole of the thyroid turned up and discovered the superior parathyroid gland, then preserved the back of the superior pole of thyroid and removed the most of the left thyroid lobe. A nerve stimulator was used to monitor the effect of RLN in all cases. All the patients were performed indirect laryngoscopy three days post-surgery. If RLN palsy was observed, indirect laryngoscopy was performed 6 months post-surgery to confirm persistent RLN palsy, indicated by the vocal cord remaining in the middle position.

Monitoring indicators

Parathyroid (PG) related parameters (number of PGs preserved *in situ*), number of PGs autotransplantation, number of PG accidentally removed, and postoperative parathyroid hormone level (PTH) were collected and analyzed.

The level of PTH would be tested at three time points: preoperation, 1 day, and 3 months after the operation. Hypoparathyroidism is defined as a decline in serum PTH below 15 pg/mL. The patient was considered to have permanent hypoparathyroidism when the serum PTH level at 3 months after surgery was below 15 pg/mL.

Statistical analysis

Continuous variables were presented as mean ± standard deviation and compared using independent samples t-tests. Chi-square tests were performed to analyze categorical data. Statistical analysis was performed by SPSS 17.0, and $p < 0.05$ was considered statistically significant.

Results

Patients' characteristics

The process of patient selection based on the inclusion and exclusion criteria is shown in Figure 2. No death was noted in both groups, and no toxic side effect due to CNs was observed in the CNs group. As summarized in Table 1, no significant difference was noted in clinical characteristics, including age, sex, and Hashimoto's thyroiditis, between the two groups. No significant difference was observed between them regarding the first surgical approach, the PTH level before the reoperation, the interval between the first surgery and reoperation, and the nodule size.

PG identification and protection

During the operation, the residual thyroid gland was stained black, whereas the PGs and surrounding adipose tissues were not (Figures 3A, B). Table 2 shows that more PGs in the CNs group were preserved *in situ* compared to the control group. Out of the studied cases, four patients in the CNs group and eleven cases in the control group underwent PGs autotransplantation. The difference between the two groups was statistically significant. Three cases in the CNs group and fourteen cases in the control group had PGs detected in the specimen after the surgery, with a significant difference between the two groups. Twenty-four hours after the surgery, the PTH level in 5 patients of the CNs group and 13 patients of the control group was lower than the normal state, with a statistical difference between the two groups (Table 3). Six months after the surgery, two patients in the CNs group and nine patients of the control group were diagnosed with persistent hypoparathyroidism.

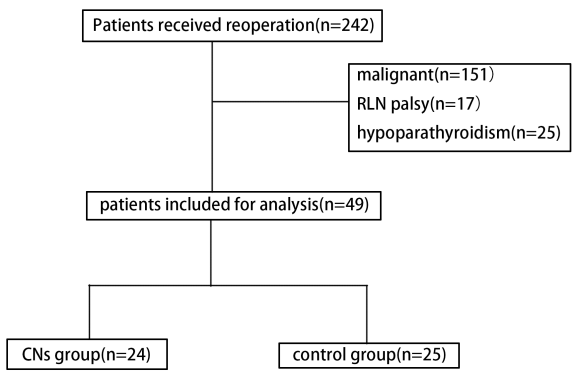

FIGURE 2
Diagram showing the patient inclusion and exclusion criteria. (CNs, carbon nanoparticles).

10.3389/fendo.2024.1361736

TABLE 1 The clinical characteristics of the patients in the CNs group and control group.

characteristics	CNs group	control group	P value
Age	59.63±7.87	61.12±4.67	0.426
Sex			0.950
Male	20	21	
Female	4	4	
Hashimoto's thyroiditis			0.138
Yes	2	6	
No	22	19	
First surgical approach			0.588
Partial hemithyroidectomy	18	17	
Bilateral partial hemithyroidectomy	6	8	
Interval (Y)	34.25±9.42	38.92±10.30	0.105
nodule size (cm)			0.897
< 5 cm	13	14	
≥5 cm	11	11	

CNs, Carbon nanoparticles.

Postoperative complications

No postoperative deaths were reported. The other complications of thyroid reoperation were RLN injury, bleeding, and wound infection (Table 4). All the patients completed 6 months of follow-up. Transient RLN injury was found in two patients with two RLNs in the CNs group and three patients with three RLNs in the control group. No statistically significant difference was found between the two groups. After 6 months, the function of RLN of the five patients returned to normal. Three patients (two in CNs group and one in the control group) had reoperation for the bleeding. Three patients (one in CNs group and two in the control group) had wound infection. Both bleeding and wound infection occurrences in the two groups have no significance.

Discussion

Scar formation, landmark distortion, and tissue friability made reoperative thyroid surgery difficult (8). Thus, advanced experience and skills are required to perform reoperative thyroid surgery. However, reoperative thyroid surgery remains a dangerous procedure because of the relatively high rates of complication including permanent RLN palsy and hypoparathyroidism compared to primary thyroid surgery (8). Both complications can decrease the quality of patients' life. Therefore, protecting RLN and parathyroid is important (16). CNs were used to identify and protect the parathyroid during the reoperative BMNG procedure.

BMNG is the most common endocrine disease requiring surgery (1). In our series, the most common benign reoperative thyroid surgery is BMNG. Two main reasons for the recurrence of BMNG are as follows: First, the hospital is located in an iodine-deficiency region with high rates of multinodular goiter and autoimmune thyroiditis. Second, most patients with thyroid disease underwent partial thyroidectomy during the initial surgery due to surgeons with limited thyroid surgery experience. For the reoperation of BMNG, three popular surgical approaches were included in our choice: the Dunhill procedure, total thyroidectomy, and bilateral subtotal resection (1). Recurrence was observed in 0.5% of patients treated with total thyroidectomy, 5% were treated with the Dunhill procedure, and 12% underwent bilateral subtotal resection at the 5-year follow-up after the surgery (1). In our series, we mainly chose the Dunhill procedure because of the relatively low recurrence rate compared to the bilateral subtotal resection and low complications compared to the total thyroidectomy.

Hypoparathyroidism is one of the major complications of reoperation (17). Hypocalcemia induced by hypoparathyroidism could lead to a series of problems (17). The incidence of transient

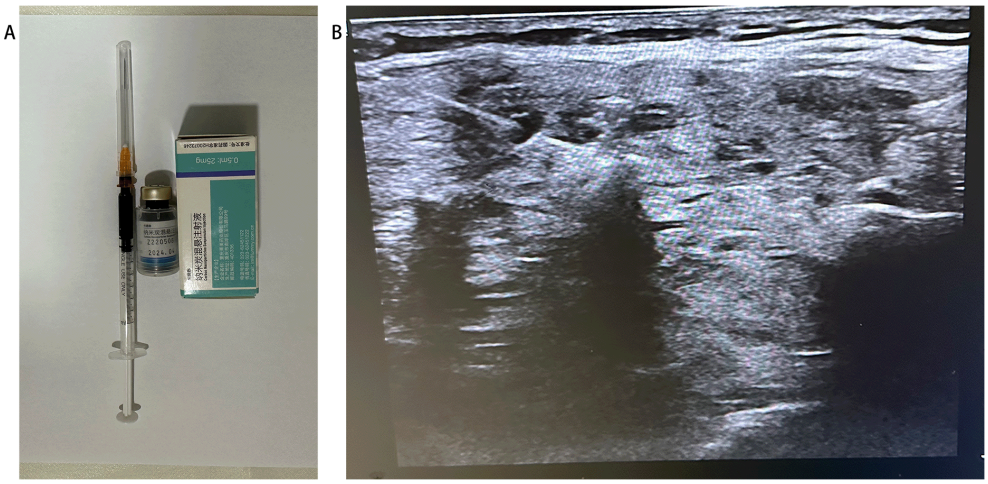

FIGURE 3
(A) residual thyroid gland (black arrow). **(B)**. left superior (black arrow) and inferior (white arrow) parathyroid gland (white arrow).

10.3389/fendo.2024.1361736

TABLE 2 PGs preserved in situ, PGs autotransplanted, PGs accidentally discovered in the CNs group and control group.

	CNs group	control group	P value
PGs preserved in situ	3.25±0.15	2.60±0.16	0.007
PGs autotransplanted			0.038
No	20	14	
Yes	4	11	
PGs accidentally discovered			0.001
No	21	11	
Yes	3	14	

PG, parathyroid; CNs, Carbon nanoparticles.

TABLE 3 Hypoparathyroidism after the surgery.

	CNs group	control group	P value
Transient hypoparathyroidism			0.024
No	5	12	
Yes	19	13	
Persistent hypoparathyroidism			0.020
No	2	9	
Yes	22	16	

CNs, Carbon nanoparticles.

hypoparathyroidism is 10.9% for total thyroidectomy and 4.2% and 2.1% for Dunhill procedure and subtotal bilateral resection, respectively, during primary thyroid surgery (18–20). However, the incidence of transient hypoparathyroidism after reoperation is 0% to 47.3%, while that of permanent hypoparathyroidism is 0% to 7.6% (21, 22). Temporary hypoparathyroidism manifested in fingers and toes numbness. Hypocalcemic tetany might happen in some severe cases. These symptoms immediately disappear after intravenous or oral administration of calcium. The features of permanent hypoparathyroidism include temporary hypoparathyroidism and induced anxiety and depression. Therefore, these patients need long-term oral supplements of calcium. However, the additional calcium supplement could induce bone and joint injury. Therefore, permanent hypoparathyroidism needs more medical therapy to maintain physical and psychological health. The extent of resection, surgical technique, and recurrent goiter were the risk factors for hypoparathyroidism in thyroid surgery. Concerning the protection of parathyroid, we used a relatively lower complication approach of the Dunhill procedure (21, 22). Several strategies have been applied to visualize PGs intraoperatively. The fine dissection operation to protect the parathyroid in the thyroid operation has been advocated recently. However, the parathyroid glands are often difficult to identify because of the parathyroid ectopia or sanguine in the operative field. Meanwhile, identifying the parathyroid for the reoperation thyroid is challenging due to the adhesion and scar formation in the operative area, which dramatically changed the anatomical structure. Nuclide was used as a radiotracer for intraoperative localization of adenomatous PGs via gamma probe identification. However, it has not been widely used because of the special expensive equipment and radioactive contamination (23, 24). Methylene blue is the most widely used staining agent, which has the advantage of identifying enlarged PGs such as parathyroidoma. However, it can also falsely stain the thyroid, lymph nodes, and normal PGs (25). Recent studies have shown that applying CNs in thyroid surgery has significantly decreased the rate of hypoparathyroidism and increased the number of dissection lymph nodes. However, the leakage of CNs might contaminate the tissue, including the parathyroid around the thyroid, which made identifying the parathyroid more difficult. Moreover, the effect of CNs in the reoperative BMNG has not been well illustrated. This study has applied the preoperative injection of CNs to avoid leakage and identify the parathyroid. Through applying CNs and protective measures for the parathyroid in the reopreative BMNG, we have gained valuable clinical experience. (a) Administering under ultrasound guidance, a 1 ml syringe was selected for the injection before the surgery. (b) Injection was administered at three points (superior, immediate, and inferior poles) with 0.1 ml of CNs injection at each point. (c) The tip of the syringe was located in the middle of normal thyroid tissue. (d) The tip of the syringe in the vessel was avoided by withdrawal before injection. (e) Negative pressure should be adopted to withdraw the needles, and the injection sites should be immediately pressed for 3 min with the gauze. However, in this series, with the assistance of the negative tracing, most of the parathyroid have been discovered, persistent hypoparathyroidism has been happened for 2 patients. The main reason might be that the capillaries around the parathyroid have been destroyed if the parathyroid was discovered. Therefore, in order to protect the capillaries around the parathyroid, we have selected the Dunhill procedure although the recurrence of total thyroidectomy was lower compared to the Dunhill procedure.

TABLE 4 The other postoperative complications.

	CNs group	control group	P value
RLN injury			
Transient	2	3	1.000
Permanent	–	–	–
Postoperative bleeding	2	1	0.609
Would infection	1	2	1.000

RLN, recurrent laryngeal nerve; CNs, Carbon nanoparticles.

Another dangerous complication of thyroid surgery is RLN injury. The incidence of transient RLN palsy for total thyroidectomy was 5.5% higher compared to 4% and 2% for the Dunhill procedure and subtotal bilateral resections, respectively (18–20). The risk factors of RLN injury included the surgery approach, the surgeon's experience, and the type of surgery (reoperation or primary surgery) (18–20). Intraoperative monitoring of RLN has been used in thyroid surgery and

significantly decreased RLN injury (9, 10). In this study, transient RLN palsy occurred in five patients with no permanent RLN injury.

This study has some limitations. First, it is a retrospective study with a relatively limited number of cases, thus carrying the possibility of selection bias. Second, the number of parathyroid before the surgery could not be confirmed, potentially impacting the conclusion of this study. Future prospective studies or randomized controlled trials should be performed to ensure the protection effect of CNs' reoperative thyroid surgery.

The Dunhill procedure seems to be a good choice for the reoperation BMNG. The application of CNs via preoperative injection in reoperation BMNG could significantly decrease the occurrence of transient and permanent hypoparathyroidism.

Data availability statement

The original contributions presented in the study are included in the article/supplementary material. Further inquiries can be directed to the corresponding author.

Ethics statement

The studies involving humans were approved by ethics committee of Weifang People's Hospital. The studies were conducted in accordance with the local legislation and institutional requirements. Written informed consent for participation in this study was provided by the participants' legal guardians/next of kin.

Author contributions

YW: Funding acquisition, Writing – original draft. QL: Investigation, Writing – review & editing. MF: Investigation, Methodology, Writing – review & editing. KM: Formal analysis, Funding acquisition, Investigation, Methodology, Supervision, Visualization, Writing – original draft, Writing – review & editing.

Funding

The author(s) declare that no financial support was received for the research, authorship, and/or publication of this article.

Conflict of interest

The authors declare that the research was conducted in the absence of any commercial or financial relationships that could be construed as a potential conflict of interest.

Publisher's note

References

1. Mauriello C, Marte G, Canfora A, Napolitano S, Pezzolla A, Gambardella C, et al. Bilateral benign multinodular goiter: What is the adequate surgical therapy? A review of literature. *Int J Surg*. (2016) 28 Suppl 1:S7–12. doi: 10.1016/j.ijsu.2015.12.041

2. Wong R, Farrell SG, Grossmann M. Thyroid nodules: diagnosis and management. *Med J Aust*. (2018) 209:92–8. doi: 10.5694/mja17.01204

3. Bellantone R, Lombardi CP, Boscherini M, Raffaelli M, Tondolo V, Alesina PF, et al. Predictive factors for recurrence after thyroid lobectomy for unilateral non-toxic goiter in an endemic area: results of a multivariate analysis. *Surgery*. (2004) 136:1247–51. doi: 10.1016/j.surg.2004.06.054

4. Moalem J, Suh I, Duh QY. Treatment and prevention of recurrence of multinodular goiter: an evidence-based review of the literature. *World J Surg*. (2008) 32:1301–12. doi: 10.1007/s00268-008-9477-0

5. Reeve TS, Delbridge L, Brady P, Crummer P, Smyth C. Secondary thyroidectomy: a twenty-year experience. *World J Surg*. (1988) 12:449–53. doi: 10.1007/bf01655417

6. Colak T, Akca T, Kanik A, Yapici D, Aydin S. Total versus subtotal thyroidectomy for the management of benign multinodular goiter in an endemic region. *ANZ J Surg*. (2004) 74:974–8. doi: 10.1111/j.1445-1433.2004.03139.x

7. Terris DJ, Khichi S, Anderson SK, Seybt MW. Reoperative thyroidectomy for benign thyroid disease. *Head Neck*. (2010) 32:285–9. doi: 10.1002/hed.21196

8. Medas F, Tuveri M, Canu GL, Erdas E, Calò PG. Complications after reoperative thyroid surgery: retrospective evaluation of 152 consecutive cases. *Updates Surg*. (2019) 71:705–10. doi: 10.1007/s13304-019-00647-y

9. Nagaty M, Shehata MS, Elkady AS, Eid M, Nady M, Youssef A, et al. An assessment of the role of surgical loupe technique in prevention of postthyroidectomy complications: a comparative prospective study. *Ann Med Surg (Lond)*. (2023) 85:446–52. doi: 10.1097/MS9.0000000000000271

10. Zhu Y, Gao DS, Lin J, Wang Y, Yu L. Intraoperative neuromonitoring in thyroid and parathyroid surgery. *J Laparoendosc Adv Surg Tech A*. (2021) 31:18–23. doi: 10.1089/lap.2020.0293

11. Lefevre JH, Tresallet C, Leenhardt L, Jublanc C, Chigot JP, Menegaux F. Reoperative surgery for thyroid disease. *Langenbecks Arch Surg*. (2007) 392:685–91. doi: 10.1007/s00423-007-0201-6

12. Liu P, Tan J, Tan Q, Xu L, He T, Lv Q. Application of carbon nanoparticles in tracing lymph nodes and locating tumors in colorectal cancer: A concise review. *Int J Nanomed*. (2020) 15:9671–81. doi: 10.2147/ijn.S281914

13. Li J, Jia S, Wang Y, Zhang Y, Kong L, Cao Y, et al. Long-term tracing and staining of carbon nanoparticles for axillary lymph nodes in patients with locally advanced breast cancer treated with neoadjuvant chemotherapy. *Asian J Surg*. (2022) 45:89–96. doi: 10.1016/j.asjsur.2021.03.020

14. Wang H, Chen MM, Zhu GS, Ma MG, Du HS, Long YP. Lymph node mapping with carbon nanoparticles and the risk factors of lymph node metastasis in gastric cancer. *J Huazhong Univ Sci Technol Med Sci*. (2016) 36:865–70. doi: 10.1007/s11596-016-1676-6

15. Wang Y, Zhang L, Huang J, Wang L. Preoperative application of carbon nanoparticles in transoral endoscopic thyroidectomy vestibular approach for papillary thyroid cancer. *Front Oncol*. (2023) 13:1120411. doi: 10.3389/fonc.2023.1120411

16. Su AP, Wang B, Gong YP, Wu WS, Gong RX, Li ZH, et al. Carbon nanoparticles facilitate lymph nodes dissection and parathyroid glands identification in reoperation of papillary thyroid cancer. *Med (Baltimore)*. (2017) 96:e8380. doi: 10.1097/md.0000000000008380

17. Benkhadoura M, Taktuk S, Alobedi R. Recurrent laryngeal nerve injury and hypoparathyroidism rates in reoperative thyroid surgery. *Turk J Surg*. (2017) 33:14–7. doi: 10.5152/ucd.2017.3369

18. Barczyński M, Konturek A, Hubalewska-Dydejczyk A, Gołkowski F, Cichoń S, Nowak W. Five-year follow-up of a randomized clinical trial of total thyroidectomy versus Dunhill operation versus bilateral subtotal thyroidectomy for multinodular nontoxic goiter. *World J Surg*. (2010) 34:1203–13. doi: 10.1007/s00268-010-0491-7

19. Thomusch O, Machens A, Sekulla C, Ukkat J, Brauckhoff M, Dralle H. The impact of surgical technique on postoperative hypoparathyroidism in bilateral thyroid surgery: a multivariate analysis of 5846 consecutive patients. *Surgery*. (2003) 133:180–5. doi: 10.1067/msy.2003.61

20. Rayes N, Steinmüller T, Schröder S, Klötzler A, Bertram H, Denecke T, et al. Bilateral subtotal thyroidectomy versus hemithyroidectomy plus subtotal resection (Dunhill procedure) for benign goiter: long-term results of a prospective, randomized study. *World J Surg*. (2013) 37:84–90. doi: 10.1007/s00268-012-1793-8

21. Seiler CA, Vorburger SA, Bürgi U, Candinas D, Schmid SW. Extended resection for thyroid disease has less operative morbidity than limited resection. *World J Surg*. (2007) 31:1005–13. doi: 10.1007/s00268-006-0054-0

22. Pelizzo MR, Variolo M, Bernardi C, Izuzquiza M, Piotto A, Grassetto G, et al. Complications in thyroid resurgery: a single institutional experience on 233 patients from a whole series of 4,752 homogeneously treated patients. *Endocrine*. (2014) 47:100–6. doi: 10.1007/s12020-014-0225-y

23. Pasta V, Monteleone F, Del Vecchio L, Iacobelli S, Urciuoli P, D'Orazi V. Original technique for preoperative preparation of patients and intraoperative localization of parathyroid adenomas. *G Chir*. (2015) 36:97–100. doi: 10.11138/gchir/2015.36.3.097

24. Grubbs EG, Mittendorf EA, Perrier ND, Lee JE. Gamma probe identification of normal parathyroid glands during central neck surgery can facilitate parathyroid preservation. *Am J Surg*. (2008) 196:931–5. doi: 10.1016/j.amjsurg.2008.07.026

25. Patel HP, Chadwick DR, Harrison BJ, Balasubramanian SP. Systematic review of intravenous methylene blue in parathyroid surgery. *Br J Surg*. (2012) 99:1345–51. doi: 10.1002/bjs.8814

Frontiers in Endocrinology

Explores the endocrine system to find new therapies for key health issues

The second most-cited endocrinology and metabolism journal, which advances our understanding of the endocrine system. It uncovers new therapies for prevalent health issues such as obesity, diabetes, reproduction, and aging.

Discover the latest Research Topics

See more →

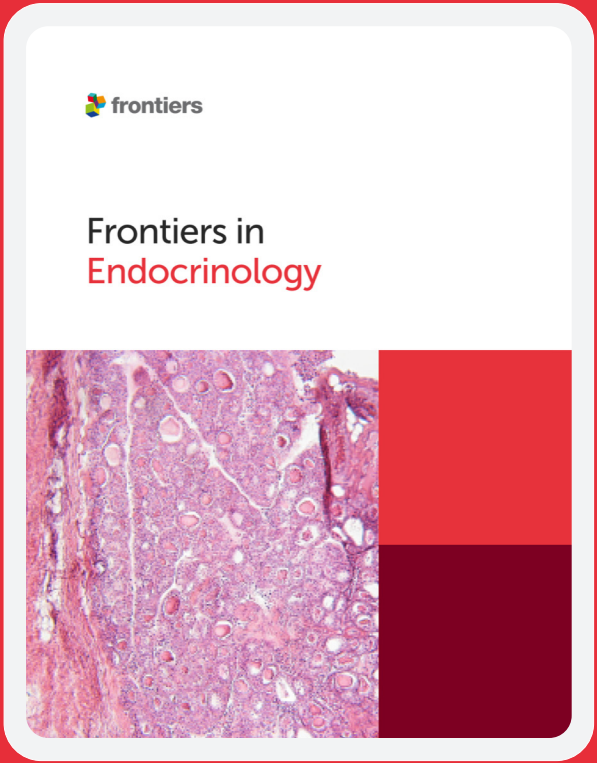

Frontiers

Avenue du Tribunal-Fédéral 34
1005 Lausanne, Switzerland
frontiersin.org

Contact us

+41 (0)21 510 17 00
frontiersin.org/about/contact